

A STUDY OF NOISE IN MISSILE CONTROL SYSTEMS

by

WILLIAM WALTHER SEIFERT

B.E.E., Rensselaer Polytechnic Institute  
(1941)

S.M., Massachusetts Institute of Technology  
(1947)

SUBMITTED IN PARTIAL FULFILLMENT OF THE  
REQUIREMENTS FOR THE DEGREE OF  
DOCTOR OF SCIENCE

at the

MASSACHUSETTS INSTITUTE OF TECHNOLOGY  
(1951)

*Declassified per letter  
dated 2 July 1965  
per BuWeps.  
A.C. Quiselle by direction  
of Ed. Barrett*

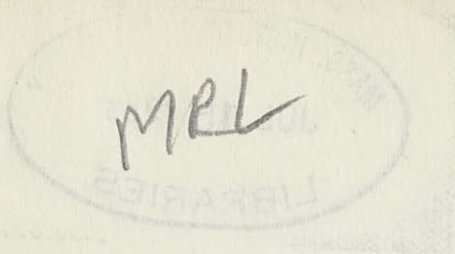
**Signature redacted**

Signature of Author.....  
Department of Electrical Engineering, May 11, 1951

**Signature redacted**

Certified by.....  
Thesis Supervisor

.....  
Chairman, Departmental Committee on Graduate Students



A STUDY OF NOISE IN MISSILE CONTROL SYSTEMS

*Handwritten notes:*  
MPL  
1951  
1951  
1951

Thesis

WILLIAM WALTER SEIBERT

1951  
S. M. Massachusetts Institute of Technology  
(1951)

S. M., Massachusetts Institute of Technology  
(1951)

SUBMITTED IN PARTIAL FULFILLMENT OF THE  
REQUIREMENTS FOR THE DEGREE OF  
DOCTOR OF PHILOSOPHY

at the

MASSACHUSETTS INSTITUTE OF TECHNOLOGY  
(1951)

.....  
Signature of Author: *William Walter Seibert*  
Department of Electrical Engineering, May 11, 1951

.....  
Certified by: *A. J. Gammeter*  
Thesis Supervisor

.....  
Chairman, Departmental Committee on Graduate Students



██████████

"A STUDY OF NOISE IN MISSILE CONTROL SYSTEMS"

by

W. W. SEIFERT

P. 16

$$\left. \begin{aligned} \frac{M_T}{A^2 a_T \cos \alpha_0} &= \frac{e^{-\ell_1}}{2!} \ell_1^2 && \text{for } N = 3 \\ &= -\frac{e^{-\ell_1}}{3!} (\ell_1^3 - 3\ell_1^2) && \text{for } N = 4 \\ &= \frac{e^{-\ell_1}}{4!} (\ell_1^4 - 8\ell_1^3 + 12\ell_1^2) && \text{for } N = 5 \end{aligned} \right\} (1.4-25)$$

P. 32

X channel - 0.5v F.S.

P. 68

Add N = 4 to the caption.

P. 70

Add N = 4 to the caption.

P. 139

Add - b+1 = 6

A = 0.5 SEC to the caption.

Note: The curve of "Miss as a function of Range" should start from 0 range with the form  $1/2 a_T t^2$ . The miss should be approximately 26.5 feet for an initial range of 2000 feet. The value given for 4000 feet is essentially correct.

P. 146

Figure 5.5-1 -  $\frac{1}{d_2}$  should be  $\frac{1}{d_1}$ .

P. 149

Figure 5.5-3 - Add to the caption: 4g turn beginning at  $r_1$   
 $a_{M,\max} = 10g$ .

P. 152

Delete - A = 0.5 SEC from caption.

P. 192

$$\phi = \tan^{-1} \left[ \frac{2\mu}{v} \left( \frac{1}{\mu} - \frac{v^2}{4\mu^2} \right) \right]^{1/2} .$$

P. 209

$m_2$  of  $I_5$  should read " $m_1 = -d_0 d_3 + d_1 d_2$ ."

P. 210

$m_1$  of  $I_6$  should read " $m_1 = -d_0 d_1 d_5$  (etc.)."

P. 211

$m_3$  of  $I_7$  should read " $m_3 = -(d_0 d_7 - d_1 d_6)^2$  (etc.)."

[REDACTED]

A STUDY OF NOISE IN MISSILE CONTROL SYSTEMS

by

William Walther Seifert

Submitted for the degree of Doctor of Science in the  
Department of Electrical Engineering on June 8, 1951.

ABSTRACT

The homing-missile problem is defined by the kinematic equations necessary to describe the target-missile geometry plus the equations to specify the control system of the missile. One of the important questions that have arisen in the design of control systems for guided missiles concerns the selection of the control-system function which optimizes the probability that a radar-controlled missile kill its target. The optimization problem is complicated by the fact that the description of the over-all system requires a set of nonlinear differential equations with time-varying coefficients. Furthermore, the radar signals returned from the target to the receiver in the missile are corrupted by random noise, with the result that the values of the miss distances can be determined only statistically. Because of the small probability that an analytic solution can be found to the problem, the utilization of some of the large-scale computing facilities now being developed appears to offer the only practical means for obtaining answers concerning the optimum form of the control system and the

[REDACTED]

probable values of miss distances which can be achieved.

This thesis concerns an application of the Massachusetts Institute of Technology Flight Simulator to a study of a two-dimensional version of the general homing problem. With the linearized analytic solution obtained by R. C. Booton, Jr., and a brief description of the Flight Simulator as starting points, the problems of simulating radar noise and introducing it into the computer are discussed at some length. Difficulties arose because of the requirement that servos in the computer faithfully transmit random signals. As a result, an analysis of the ability of servos to pass random signals was undertaken and some results of interest in the field of servo analysis are obtained. The measures taken to evaluate the ability of the computer to handle this class of problems are discussed and considerable data on the general proportional-navigation homing-missile problem are presented. The results obtained are evaluated and a number of fundamental questions are answered concerning the type of control system which should be built into a missile.

[REDACTED]

## PREFACE

The author of this thesis began his work in the guided-missile field in 1944. This early work was concerned primarily with the missiles Bat and Pelican that were launched from airplanes and, guided by a radar homing system, glided to their ship targets. While the initial difficulties with these early missiles were being overcome, the importance of the effects of radar scintillation noise in the system became apparent. Before much was learned about these effects World War II ended. The Dynamic Analysis and Control Laboratory at M.I.T., with which the author then became associated, had as its first major undertaking the design and construction of a Flight Simulator for testing missile control systems. As work on the Simulator progressed, some of the effort was diverted to build a generalized analog computer which would be capable of solving missile trajectory problems without actually involving any of the physical equipment used in the missile.

During the spring and summer of 1948 the generalized computer was nearing the point where simple trajectory problems could be set up on it. At this time Dr. A. C. Hall, who was then director of the laboratory, suggested that the author investigate the problem of simulating the effects of radar noise in order that the computer could be used to study the influence of this phenomenon in determining the miss distances of radar-controlled homing missiles. Thereupon, the author conducted a preliminary study of the problem and built a model of a random-noise source.

[REDACTED]

Some noise-free trajectory studies were made during December 1948 and January 1949 but the first studies involving noise were made in January and early February 1949. A paper\* covering the results of these early studies was presented at a "Noise Symposium" held at the University of California at Los Angeles in February 1949. For the greater part of 1949 the computer was employed on trajectory studies. Equipment break-downs and modifications, however, retarded this work. During the summer and autumn of 1949, R. C. Booton, Jr., also of the D.A.C.L., succeeded in solving analytically the trajectory problem for the case of a missile capable of unlimited acceleration. This work, together with a considerable group of hand solutions which were worked out as check problems, served as a guide for evaluating the operation of the machine and pointed out the fact that unless every possible precaution is exercised in setting up and in operating the machine the results obtained, even in the noise-free cases, are apt to be worthless. The inclusion of radar noise increases the complications and still further reduces the chances of correct machine operation.

A truly satisfactory method of shaping and monitoring the radar noise injected into the computer was not developed until the end of May 1950. During July 1950 a series of tests was begun to evaluate the ability of the D.A.C.L. electromechanical integrators to pass random signals when operated as position servos. These tests demonstrated that appreciable errors were being introduced by the arc-tangent servo used in trajectory problems. For the studies which were made during August and September 1950, computation of x/y was

\* Hall, A.C., and W. W. Seifert, "Noise in Nonlinear Servo Systems," Symposium on Noise Reduction, February 10, 11 and 12, 1949, Report AL-930, Part I. Los Angeles, Calif.: North American Aviation, Inc., November, 1949 (Confidential).

substituted for the arc tangent of  $x/y$ . The results obtained at this time were the first trustworthy data from trajectory studies involving noise. Because so much time was spent in analyzing the operation of the computer, only a limited amount of data on the homing-missile problem could be obtained. This study, however, furnished the answers to a number of significant questions concerning the operation of homing missiles. In addition, a number of equally important results were obtained in the fields of servo analysis and analog-computer operation.

The author expresses his appreciation to his associates at the D.A.C.L. for the excellent cooperation which they gave him during the entire course of this investigation. He wishes to give special thanks to Dr. A. C. Hall, who served as director of the D.A.C.L. until July 1950, and who suggested that the author undertake this study for a thesis. Dr. Hall also supervised the thesis until he left M.I.T. and was most helpful in offering encouragement when it was most needed and in making available for this work the facilities of the D.A.C.L. The author is particularly indebted to R. C. Booton, Jr., who was also studying trajectory problems and who, during the course of this thesis, succeeded in obtaining an analytic solution for the unlimited-acceleration problem. Booton contributed many helpful suggestions concerning both the work itself and the form of the final manuscript. Gratitude is extended to Dr. J. A. Hrones, who succeeded Dr. Hall as director of the D.A.C.L., and who continued to make every facility of the laboratory available for completing this study. Appreciation is also expressed to H. Jacobs, Jr., and C. M. Edwards for the splendid cooperation

[REDACTED]

which they afforded during the actual operation of the computer, to Misses B. L. White and V. D. Lee for reading data and making numerical calculations, to Miss C. D. Boyd for her painstaking editorial efforts, to Miss M. T. Kerwin, who typed the final manuscript, and to Mr. J. M. Aitken for his assistance in the preparation of the illustrations.

The author also wishes to express thanks to Prof. H. J. Zimmerman who succeeded Dr. Hall as thesis supervisor and to Prof. R. H. Frazier, Dr. J. A. Hrones and Dr. Y. W. Lee who acted as thesis readers.

This work was conducted at the Massachusetts Institute of Technology under the Guided Missiles Program which operates under Bureau of Ordnance Contract NOrd 9661 with the Division of Industrial Cooperation on technical tasks for the Bureau of Ordnance of the Navy Department.

[REDACTED]



TABLE OF CONTENTS

TITLE PAGE . . . . . 1

ABSTRACT . . . . . ii

PREFACE . . . . . iv

TABLE OF CONTENTS . . . . . viii

LIST OF ILLUSTRATIONS . . . . . xii

CHAP. 1. THE HOMING-MISSILE PROBLEM . . . . . 1

    1.1. Introduction . . . . . 1

    1.2. Statement of the Specific Homing Problem  
         Considered . . . . . 4

    1.3. Analytic Statement of the Problem . . . . . 4

    1.4. Booton's Solution of the Linearized Unlimited Case . . . . . 8

    1.5. Need for a Simulator Study of the Effects of  
         Limiting . . . . . 18

    1.6. Contributions Made in This Study . . . . . 18

CHAP. 2. SETUP OF THE M.I.T. FLIGHT SIMULATOR FOR PROPORTIONAL-  
 NAVIGATION STUDIES . . . . . 20

    2.1. Introduction . . . . . 20

    2.2. Computer Setup for Studying the Proportional-  
         navigation Problem . . . . . 21

    2.3. Basic Checking Procedures . . . . . 29



CHAP. 3. RADAR NOISE AND ITS SIMULATION . . . . .	34
3.1. Introduction . . . . .	34
3.2. Possible Sources of Noise . . . . .	37
3.3. Glint Noise . . . . .	40
3.4. Generation of Glint Noise for Use in the Computer .	45
3.41. Type of Signal Required . . . . .	45
3.42. Possible Methods of Generating the Desired Noise Spectrum . . . . .	46
3.43. Method Adopted for Generating Noise Signals	48
3.44. Random-square-wave Generator . . . . .	56
3.45. Method of Injecting Glint Noise into the Computer . . . . .	59
3.46. Method of Monitoring the Noise . . . . .	61
3.5. Effect of Using Nonwhite Noise in the Computer . . .	65
 CHAP. 4. ANALYSIS OF COMPUTER OPERATION FOR PROPORTIONAL- NAVIGATION PROBLEMS INVOLVING NOISE . . . . .	 71
4.1. Introduction . . . . .	71
4.2. Analysis of $\alpha$ -servo Operation . . . . .	72
4.21. Basis of Analysis . . . . .	72
4.22. Rms Error and Acceleration Calculations for the $\alpha$ Servo . . . . .	80
4.23. Procedures for Improving the $\alpha$ Servo . . .	98
4.3. Computer Checking When Noise is Inserted . . . . .	105
4.4. Effect of Time Lag in the $\alpha$ Servo. . . . .	114

CHAP. 5. PRESENTATION AND INTERPRETATION OF EXPERIMENTAL RESULTS	119
5.1. Probable Error Imposed by the Statistical Nature of the Problem . . . . .	119
5.2. Comparison between Experimental and Analytic Results for the Case of Linear Operation . . . . .	121
5.3. Methods of Introducing Limiting . . . . .	128
5.4. Results Obtained with Noise, Target Maneuver, and Limiting for the Proportional-navigation Problem Involving a Simple-lag Filter . . . . .	134
5.5. Proportional-navigation System with Quadratic Filter	145
5.6. Proportional-navigation System with Cubic Filter . .	154
5.7. Calculation of Mean-square Miss Distance for a Missile Subject to Random-square-wave Acceleration	160
5.8. Effect of Changes in the Amplitude Probability Distribution of the Noise . . . . .	166
5.9. Use of Nonlinear Filter Systems in Missiles . . . .	168
5.10. Some Comments on the Study of Homing-missile Systems	174
CHAP. 6. CONCLUSIONS . . . . .	179
6.1. Evaluation of the Ability of the D.A.C.L. Computer to Handle Trajectory Problems . . . . .	179
6.2. Evaluation of the Probable Effectiveness of Missiles with Proportional-navigation Control Systems . . . . .	181
6.3. Comments on Oil Consumption and Drag . . . . .	184

## CHAP. 6. (Continued)

6.4. General Conclusions Concerning Nonlinear Problems of the Type Studied . . . . .	185
APPENDIXES . . . . .	187
A. Glossary of Terms . . . . .	187
B. Description of the Variable-time-scale Section of the M.I.T. Flight Simulator . . . . .	193
C. Table of Integrals . . . . .	207
D. Accuracy Considerations in Statistical Studies . . . . .	214
E. Solution Coding and Data Recording Techniques . . . . .	222
F. Bibliography . . . . .	227
G. Biographical Note on the Author . . . . .	231

[REDACTED]

LIST OF ILLUSTRATIONS

1.3-1.	Geometry of the homing-missile problem . . . . .	5
2.2-1.	Geometry of the homing-missile problem . . . . .	21
2.2-2.	Block diagram of the setup of the computer for studying the proportional-navigation problem with a simple-time-lag filter, no limiting, and no radar noise . . . . .	23
2.3-1.	Typical recording of the important variables in a proportional-navigation trajectory problem with simple-lag filter, no radar noise, and no limit- ing. (Hand solution.) . . . . .	32
3.3-1.	Variation of tracking deviations with range for targets flying radial courses. . . . .	42
3.43-1.	Schematic of noise generator, type N-1. . . . .	49
3.43-2.	Block diagram of noise-generating and filtering equipment. . . . .	54
3.44-1.	Schematic of suppressed-carrier square-wave generator. . . . .	58
3.46-1.	Noise-monitoring equipment . . . . .	63
3.5-1.	Simple-lag-noise-bandwidth effect on miss for a missile with a simple-lag control system . . . . .	68
3.5-2.	Quadratic-noise-bandwidth effect on miss for a missile with a simple-lag control system . . . . .	70



4.21-1.	Coordinate system of the $\alpha$ servo . . . . .	73
4.21-2.	Simplified diagram of arc-tangent solver . . . . .	74
4.21-3.	Representation of Fig. 4.21-2, valid when $\alpha_c$ is small and $y$ is constant . . . . .	75
4.22-1.	Representation of input signal and servo system studied analytically . . . . .	82
4.22-2.	Normalized error for position servo following quadratic noise. . . . .	85
4.22-3.	$a/\Phi_N^{1/2}$ versus $K$ , for servo following quadratic noise. . . . .	87
4.22-4.	Arrangement of $\alpha$ servo studied experimentally. . . . .	88
4.22-5.	Equivalent form of Fig. 4.22-4 for small-angle operation. . . . .	90
4.22-6.	Curves of error versus gain. . . . .	93
4.22-7.	Minimum error as a function of the frequency of the input signal and the factor $a_{\max}/(\Phi_N')^{1/2}$ . . . . .	95
4.22-8.	Optimum gain as a function of the frequency of the input signal and the factor $a_{\max}/(\Phi_N')^{1/2}$ . . . . .	96
4.23-1.	Normalized error for position servo following quadratic noise. . . . .	104
4.3-1.	Geometry of target and missile . . . . .	106
4.3-2.	Quadratic noise into $y$ -locked system . . . . .	109
4.4-1.	Effect of limited $\alpha$ -servo gain in a study of the $y$ -locked problem . . . . .	117

5.2-1.	Basic computer setup diagram for codes AA, AB, AC, and AD . . . . .	122
5.2-2.	Typical solutions with simple-lag filter, noise, and no limiting. . . . .	123
5.2-3.	Computer setup with a divider servo for the noise and an $\alpha$ servo for the signal. . . . .	126
5.2-4.	Computer setup with divider servo replacing $\alpha$ servo. . . . .	127
5.2-5.	Comparison between analytic and machine results of miss vs. noise bandwidth in unlimited accel- eration case . . . . .	129
5.2-6.	Histogram of miss distances in unlimited accel- eration case . . . . .	130
5.3-1.	Two means of introducing limiting. a. Open-loop limiting. b. Closed-loop limiting. . . . .	131
5.3-2.	Energy storage possibilities in a system with limiting . . . . .	133
5.4-1.	Typical solutions with simple-lag filter, noise, and limiting . . . . .	135
5.4-2.	Rms miss distance vs. noise bandwidth for simple-lag control systems . . . . .	136
5.4-3.	Histogram of miss distances for a typical simple-lag control system. . . . .	137

██████████

5.4-4.	Target maneuver, miss distance, and average missile acceleration vs. range. . . . .	139
5.4-5.	Rms miss distance vs. navigation constant. . . . .	143
5.5-1.	Block diagram of quadratic filter. . . . .	146
5.5-2.	Miss distances obtained with missiles using quadratic control systems and operating in the absence of radar noise . . . . .	148
5.5-3.	Miss distance caused by target maneuver. No launching error. No noise . . . . .	149
5.5-4.	Miss distances obtained with missiles using quadratic control systems and operating in the presence of radar noise. . . . .	150
5.5-5.	Typical solution involving noise, target maneuver, limiting, and a quadratic control system . .	151
5.5-6.	Histogram of miss distances for missile with a quadratic control system . . . . .	152
5.6-1.	Miss distances obtained with cubic control systems. . . . .	155
5.6-2.	Step responses of cubic and quadratic systems. . . . .	159
5.7-1.	Rms miss distance as a function of the limiting value of the missile acceleration for the case of a random-square-wave acceleration program . . . .	165
5.9-1.	Input signal plus noise. . . . .	170
5.9-2.	Nonlinear filter system. . . . .	171

██████████

5.9-3.	Form of signals appearing at various points in the nonlinear filter system of Fig. 5.9-2.	
	a. Input signal plus noise.	
	b. Output of auxiliary limiter.	
	c. Output of dead-space simulator.	
	d. Output of summing circuit for gain of 2 in dead-space channel . . . . .	173
B-1.	Over-all view of the generalized computer . . . . .	194
B-2.	View of the d-c portion of the computer. . . . .	195
B-3.	View of rack containing high-speed multiplier units. . . . .	203
D-1.	Probability of achieving an accuracy $\rho$ (per unit) as a function of the number of solutions . . . . .	215
D-2.	Almost-certain and expected accuracy from n solutions. . . . .	217
E-1.	AC code sheet. . . . .	224
E-2.	List of parameters held constant for all code AC studies. . . . .	225
E-3.	Typical data sheet . . . . .	226

  
CHAPTER 1

## THE HOMING-MISSILE PROBLEM

1.1. Introduction.

Guided missiles recently have assumed considerable importance in storybook warfare. Nevertheless, if these weapons are to emerge from the realm of science fiction and achieve real tactical significance, their "probability of kill" must be made sufficiently greater than that achieved with unguided missiles, such as shells or rockets, to offset the enormously greater cost of firing a guided missile. A number of missiles have been designed for various tactical applications, but this thesis concerns homing missiles that derive their intelligence from a radar receiver in the missile. The transmitter which illuminates the target may be carried in the missile or may be mounted elsewhere. The specific missiles considered are designed to destroy airborne targets, particularly of the heavy-bomber class. Since only the terminal phase of the flight (the last 20,000 feet or less) is considered in this study, the manner in which the missile arrives at the beginning of this phase is of no consequence. The Meteor missile is designed to be launched from an airplane and to fly at a speed of approximately 2000 feet per second but the results presented here are equally applicable to missiles launched from a ground station.

Among the numerous problems arising in the design of homing missiles, this thesis focuses attention on the specific problem of



[REDACTED]

determining the optimum control system to be used in a missile. The design of a suitable system would be relatively simple if information were available concerning the exact location of the target and if the missile were always able to develop the lateral acceleration called for by the control system. Unfortunately, the guidance information used to control the missile becomes unavoidably corrupted with noise and the lateral acceleration that the missile can develop is limited by structural considerations.

If noise were not present, and if the initial range is made sufficiently large to permit removal of the launching error, the parameters in the missile control system could be so selected that a hit would be assured for any target capable of less than half the lateral acceleration of the missile. Nevertheless, noise is present and as the speed of response of the control system is increased to allow the missile to follow possible target maneuvers, the noise accepted by the system is increased, with the result that a miss occurs, even if the target does not maneuver. The difficulty of achieving a hit becomes very pronounced when the three factors, target maneuver, noise, and limited missile-acceleration capabilities must all be dealt with simultaneously. The choice of a missile response function which can best accommodate target maneuvers while rejecting noise thus presents a basic problem.

Since this optimization problem involves the study of a system characterized by a set of nonlinear differential equations with time-varying coefficients, a complete analytic solution is impossible with

[REDACTED]

[REDACTED]

the mathematical techniques at present available. Hence machine methods of solution must be employed to obtain a large quantity of data.

The object of this thesis is to bring to bear on a study of the homing-missile problem the computing facilities of the generalized analog computer which has been developed in the Dynamic Analysis and Control Laboratory at the Massachusetts Institute of Technology. This computer has been termed the Variable-Time-Scale Section of the M.I.T. Flight Simulator. The study was begun very soon after the preliminary testing of the computer was completed, but a number of difficulties arose. Problems involving noise impose a considerably greater burden on the servos in the computer than similar problems without noise. An evaluation of the ability of the servos to transmit random signals was, therefore, necessary before meaningful data could be obtained on the homing-missile problem. As a result, this thesis breaks into several natural divisions.

The basic proportional-navigation missile problem is discussed in Chap. 1 and some of the fundamentals involved in setting up the computer for this study are outlined in Chap. 2. Chapter 3 discusses the ways in which noise can enter a radar-controlled homing-missile system and considers means for simulating radar noise and injecting noise into the computer. Chapter 4 investigates servos operating with random input signals. It constitutes a complete unit and may be read separately by those interested in the general servo problem or may be omitted by those interested in the homing-missile problem but not in

[REDACTED]

[REDACTED]

the servo problem. In Chap. 5 the experimental results obtained in this study of the homing-missile problem are presented and interpreted. Some general conclusions and recommendations for further study are considered in Chap. 6 and several bits of isolated data which are important to the over-all study are included as appendixes.

### 1.2. Statement of the Specific Homing Problem Considered.

Particular attention is given to the phase of the flight during which the missile depends upon line-of-sight measurements for its guidance information. Specifically, the quantities measured at the missile are its own heading relative to some fixed reference and the apparent relative bearing of the target, or derivatives of these quantities. Range or range-rate measurements also can be used, but these quantities are often omitted because they are unnecessary in the basic control systems.

The present study is restricted to a consideration of the case where the target and missile move with constant speed in a plane, not because this situation would generally arise in the tactical use of a missile but because much is to be learned from a study of this relatively simple case of the general three-dimensional problem. The results obtained are, nevertheless, of immediate interest to the missile designer and the experience gained in operating the computer forms a necessary background for further more elaborate studies.

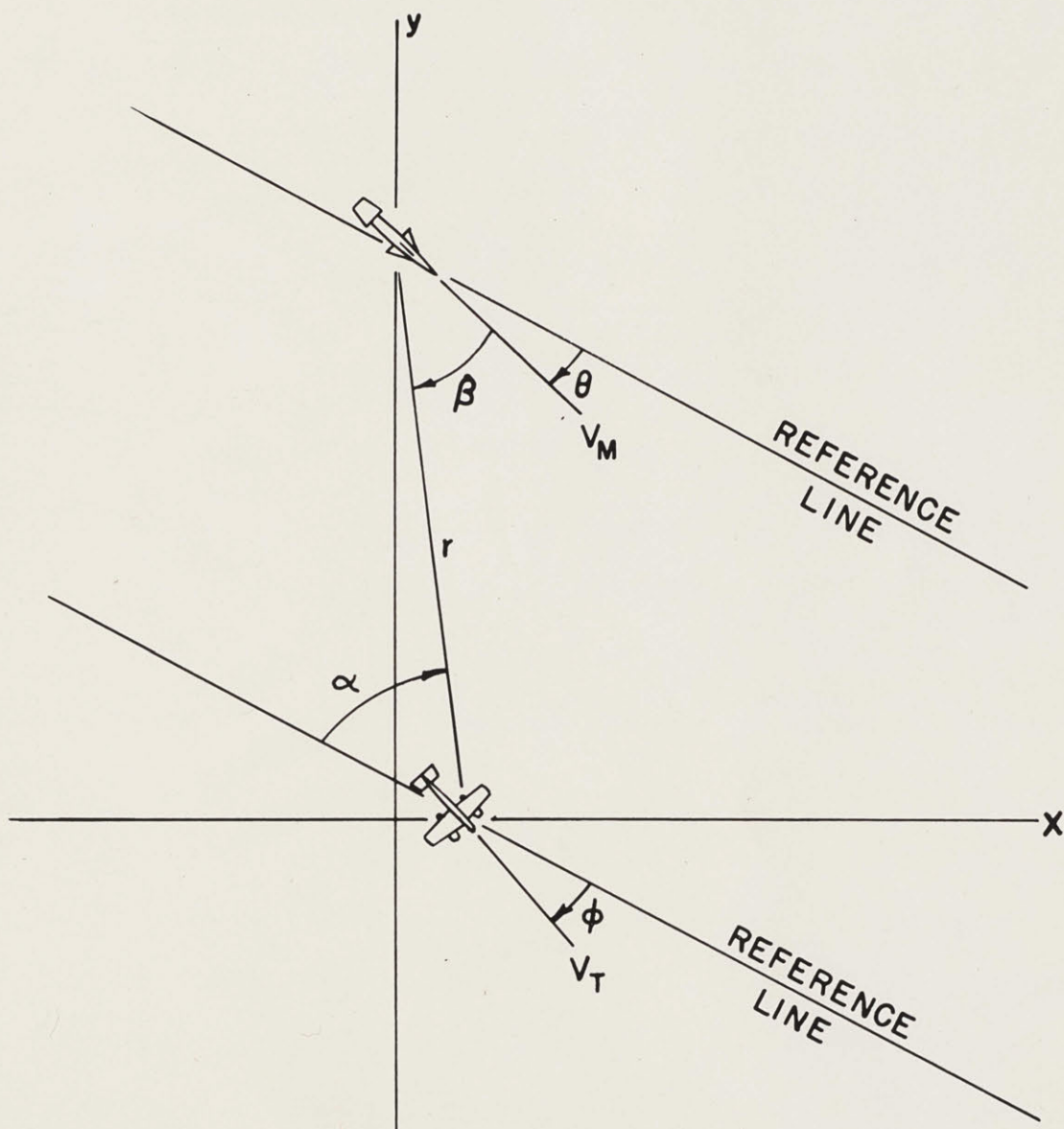
### 1.3. Analytic Statement of the Problem.

The geometry of the problem to be considered is shown in Fig. 1.3-1. The velocities of the missile and the target,  $V_M^*$  and  $V_T$ ,

---

\* All the symbols used in this thesis are defined in the glossary, Appendix A.

[REDACTED]



NOTE: Y AXIS IS ALWAYS PARALLEL TO INITIAL LINE OF SIGHT.

FIG. I.3-1. GEOMETRY OF THE HOMING-MISSILE PROBLEM.

respectively, are here considered constants. The angle  $\theta$  defines the heading vector of the missile with respect to a fixed but arbitrary reference line, while  $\alpha$  defines the angle of the line of sight and  $\phi$  the target-heading angle with respect to this same reference. Since motion of the target and the missile are to be confined to a single plane, the kinematics of the problem are completely defined by a pair of differential equations. In polar form these equations are

$$\dot{r} = V_T \cos(\alpha - \phi) - V_M \cos(\alpha - \theta) \quad (1.3-1)$$

and

$$r\dot{\alpha} = -V_T \sin(\alpha - \phi) + V_M \sin(\alpha - \theta). \quad (1.3-2)$$

The representation of the system is completed by a control equation, the exact form of which varies somewhat with the quantities which are measured by the radar system and with the control system used, including the airframe response. In general, this control equation is of the form

$$\dots + A_2 \ddot{\theta} + A_1 \dot{\theta} = B_1 \dot{\alpha} + B_2 \ddot{\alpha} + \dots \quad (1.3-3)$$

The coefficients in Eq. (1.3-3) are determined by the gains and the time lags in the over-all system and may be functions of range or time. In a widely used simplification of the preceding equation, the rate of change of the missile heading is considered proportional to the rate of change of the line-of-sight bearing. This type of control is called proportional navigation and follows the basic control equation<sup>1,2,\*</sup>

$$\dot{\theta} = (b+1)\dot{\alpha} \quad (1.3-4)$$

An actual missile control system must, however, include time lags and, for the sake of filtering noise, additional lags may be inserted.

\* Numbers refer to the bibliography in Appendix F.

Therefore, more terms are added to the left-hand side of Eq. (1.3-4). Furthermore, terms may be added to the right-hand side of the equation or the coefficient of  $\dot{\alpha}$  may be made a function of range. The object is to adjust the response function of the missile system so that the miss is minimized when target maneuvers and noise appear simultaneously in the problem. The over-all response function actually results from the combined responses of the radar system, the antenna-training servo system, if one is used, the filters added in the radar and/or in the control system, the control system itself, and the airframe. The individual transfer functions involved may be cascaded in a simple arrangement or there may be complex feedback loops involving signals from rate gyros or accelerometers. The over-all transfer function, from the information received by the radar to the resulting change in missile heading, is therefore very complex. For the general case, this function can be represented as a ratio of polynomials

$$F(s) = \frac{a_n s^n + a_{n-1} s^{n-1} + \dots + a_1 s + a_0}{b_n s^n + b_{n-1} s^{n-1} + \dots + b_1 s + b_0} \quad (1.3-5)$$

In this basic study only simple forms of  $F(s)$  are considered and no attempt is made to specify the source of the terms in the over-all transfer function.

The simplest practical modification of Eq. (1.3-4) is obtained when  $F(s)$  assumes the form of a simple-lag term.<sup>3,4</sup> The equation then becomes

$$A\ddot{\theta} + \dot{\theta} = (b + 1) \dot{\alpha} \quad (1.3-6)$$

[REDACTED]

The problem defined by Eqs. (1.3-1), (1.3-2), and (1.3-6) leads to a nonlinear differential equation and, therefore, cannot be solved analytically. Nevertheless, if the initial heading of the missile is approximately on a collision course, and if the deviations of all angles from their initial values are small, the usual small-angle approximations can be used to linearize the problem. Since the coefficients appearing in the simplified equations vary with range (or time), the differential equation arrived at, although linear, still has time-varying coefficients.

By using the small-angle approximations and assuming that the available lateral acceleration of the missile is sufficient to insure that no acceleration limiting occurs, R. C. Booton, Jr.,<sup>5</sup> was able to solve the problem analytically while including the effects of initial heading errors, target maneuvers, and noise. The present investigation shows how, by employing the analog computer developed in the Dynamic Analysis and Control Laboratory, the work of Booton can be extended to include the case where acceleration limiting in the missile becomes an important factor in determining the miss distance.

Because of the close connection between Booton's analysis and the present study, and because of the importance of his results as a check point for experimental work, his method of attack and principal results are discussed briefly.

#### 1.4. Booton's Solution of the Linearized Unlimited Case.

If the small-angle approximations are valid, then the range rate is nearly constant and Eq. (1.3-1) becomes

[REDACTED]

$$\dot{r} = V_T \cos (\alpha_o - \phi_o) - V_M \cos (\alpha_o - \theta_o). \quad (1.4-1)$$

Furthermore, if  $\dot{r}$  is set equal to  $-V_R$ , then

$$r = r_o - V_R t. \quad (1.4-2)$$

By use of Eq. (1.4-1) and by writing each angle as the sum of the initial value and a small transient term, Eq. (1.3-2) may be reduced to

$$r \dot{\alpha}_t + \dot{r} \alpha_t = r_o \dot{\alpha}_o + \phi_t V_T \cos \alpha_o - \theta_t V_M \cos \beta_o \quad (1.4-3)$$

where the reference has been chosen so that  $\phi_o$  equals zero and  $\beta_o$  is defined as  $\alpha_o - \theta_o$ .

When the missile and target positions are referred to a rectangular coordinate system (Fig. 1.3-1) moving (without rotation and with the y axis always parallel to the initial line of sight) with a velocity equal to the initial velocity of the target, the lateral movement of the target position from the y axis may be written as

$$x_T = V_T \cos \alpha_o \int_0^t \phi_t(\tau) d\tau \quad (1.4-4a)$$

and the lateral movement of the missile position from the y axis as

$$x_M = V_M \cos \beta_o \int_0^t \theta_t(\tau) d\tau - r_o \dot{\alpha}_o t \quad (1.4-4b)$$

where  $\tau$  is a time variable of integration and  $\phi_t$  and  $\theta_t$  refer to the transient terms in  $\phi$  and  $\theta$ .

Then

$$r \alpha_t = x_T - x_M. \quad (1.4-5)$$

Since the y axis of the moving coordinate system is always parallel to the initial line of sight, the difference between missile-and target-y coordinates is approximately equal to the range, and the miss

distance is approximately given by  $x_T - x_M$  when  $t = t_f = r_0/V_R$ .

At this point, the effects of noise in the system must be considered. The intelligence system in the missile is not able to measure the actual range and the line-of-sight angle to the target but measures rather an apparent range  $r_A$  and an apparent line-of-sight angle  $\alpha_A$ . The effects of errors in the apparent range may be neglected ( $r_A = r$ ), since the primary guidance information comes from measurements of  $\alpha$ . As discussed in Chap. 3, the most serious source of error in  $\alpha_A$  for the type of radar-controlled missile considered here, originates from shifts in the radar center of gravity of the target. Errors in  $\alpha_A$  are equivalent to errors in the apparent value of  $x_T$  and are referred to as "noise" and denoted by  $x_N$ . When the noise effect is added, Eq. (1.4-5) becomes

$$r\alpha_{At} = x_T + x_N - x_M. \quad (1.4-6)$$

As was pointed out in reference to Eq. (1.3-5), the quantities  $\theta$ ,  $r$ , and  $\alpha_A$  are related by the missile-control equation. Missile-control equations which can be defined as differential equations linear in  $\theta$  and  $\alpha_A$  may be expressed in general form as

$$G(r,t,p)\theta = \alpha_A + f_1(r,t) \quad (1.4-7)$$

where  $f_1$  is an arbitrary function of  $r$  and  $t$ , and  $G(r,t,p)$  is a linear integrodifferential operator.

For the general proportional-navigation system Eq. (1.4-7) becomes

$$D(p)\dot{\theta} = \dot{\alpha}. \quad (1.4-8)$$

Substituting Eqs. (1.4-2), (1.4-4b), and (1.4-6) into Eq. (1.4-8)

yields a linear differential equation relating  $x_M$  and  $x_T + x_N$ .

$$\left[ \frac{r_0 - V_R t}{V_M \cos \beta_0} D(p)p + 1 \right] x_M = x_T + x_N + C(r_0 - V_R t) \quad (1.4-9)$$

where  $C$  is a constant depending upon the initial conditions ( $C = 0$  if the missile is initially on a straight-line collision course).

Since  $x_M$ ,  $x_T$ , and  $x_N$  are related by a linear equation, the response of the missile to any target motion and noise may be expressed in terms of a generalized step-response function by means of the superposition integral. To determine the entire trajectory, a function of two variables must usually be known, but to determine only the terminal value of  $x_M$ , a function of only one variable need be known.

If the step-response function of the missile is designated by  $a(\tau)$ , the miss distance is given by

$$x_T \left( \frac{r_0}{V_R} \right) - x_M \left( \frac{r_0}{V_R} \right) = M_T + M_N - \int_0^{r_0/V_R} a'(\tau) f_2 \left( \frac{r_0}{V_R} - \tau \right) d\tau. \quad (1.4-10)$$

where

$$M_T = x_T \left( \frac{r_0}{V_R} \right) - \int_0^{r_0/V_R} a'(\tau) x_T \left( \frac{r_0}{V_R} - \tau \right) d\tau \quad (1.4-11)$$

and

$$M_N = - \int_0^{r_0/V_R} a'(\tau) x_N \left( \frac{r_0}{V_R} - \tau \right) d\tau \quad (1.4-12)$$

denote, respectively, the component of the miss caused by target

maneuver and the component of the miss caused by noise. The third term of Eq. (1.4-10) is a function only of the control system and the initial conditions and is generally zero if the missile is initially on a straight-line collision course.

For the computer runs made in this study, of special interest is the case where the target is initially flying in a straight line but at time  $t_1 = (r_0 - r_1)/V_R$  makes a constant-lateral-acceleration turn.

Here

$$\left. \begin{aligned} x_T(t) &= 0 && \text{for } t < t_1 \\ x_T(t) &= \frac{1}{2} a_T (t-t_1)^2 \cos \alpha_0 && \text{for } t > t_1. \end{aligned} \right\} \quad (1.4-13)$$

Substitution of Eq. (1.4-13) into Eq. (1.4-11) yields

$$\frac{M_T}{a_T \cos \alpha_0} = \frac{1}{2} \left( \frac{r_1}{V_R} \right)^2 - \int_0^{r_1/V_R} a'(\tau) \frac{1}{2} \left( \frac{r_1}{V_R} - \tau \right)^2 d\tau. \quad (1.4-14)$$

To evaluate the miss caused by noise,  $x_N$  must be specified. For the present,  $x_N$  is considered a Gaussian random process, therefore,  $M_N$  is also Gaussian. All the information concerning  $M_N$  is then contained in its standard deviation  $\sigma_N$ . If the spectral density of the noise signal  $x_N(t)$  is designated as  $\Phi_N(\omega)$  (see Chap. 3), then use of Eq. (4.21-3) and the fact that the transfer function of a system (even though it contains time-varying coefficients) is the transform of its impulse response yield

$$\sigma_N^2 = \int_{-\infty}^{+\infty} \left| \int_0^{r_0/V_R} a'(\tau) e^{-i\omega\tau} d\tau \right|^2 \Phi_N(\omega) d\omega. \quad (1.4-15)$$

In the special case where  $\Phi_N(\omega)$  can be considered constant (white noise), Eq. (1.4-15) may be written in accord with Parseval's theorem as

$$\sigma_N^2 = 2\pi \Phi_N \int_0^{r_0/V_R} \left[ a'(\tau) \right]^2 d\tau. \quad (1.4-16)$$

For the proportional-navigation-with-simple-time-lag control system characterized by Eq. (1.3-8),  $D(p)$  of Eq. (1.4-8) becomes  $D(p) = (Ap+1)/(b+1)$ . If this expression for  $D(p)$  is substituted into Eq. (1.4-9), the resulting expression obtained for this case is

$$\frac{A}{N} \left( \frac{r_0}{V_R} - t \right) \ddot{x}_M + \frac{1}{N} \left( \frac{r_0}{V_R} - t \right) \dot{x}_M + x_M = x_T + x_N + C \left( r_0 - V_R t \right) \quad (1.4-17)$$

where

$$N = \frac{(b+1)(V_M \cos \beta_0)}{V_R} \quad (1.4-18)$$

and  $t$  is any general time.

The response of the missile to a step applied at time  $t_1$  is  $A(t_1, t)$ . For the determination of miss distance a knowledge of  $A(t_1, r_0/V_R)$  is sufficient. This will be designated as  $a(\tau)$  and may be obtained from Eq. (1.4-17) for the case where

$$x_M(t) = 0 \quad \text{for } t < t_1$$

and

$$x_T(t) + x_N(t) + C(r_0 - V_R t) = 1 \text{ for } t > t_1.$$

For these conditions if each side of Eq. (1.4-17) is multiplied by  $N$  and

then differentiated, the following expression is obtained relating the derivatives of  $x_M$ .

$$A \left( \frac{r_0}{V_R} - t \right) \ddot{x}_M + \left( \frac{r_0}{V_R} - A - t \right) \dot{x}_M + (N-1) \dot{x}_M = 0 . \quad (1.4-19a)$$

Repeated differentiation of Eq. (1.4-17) yields Eq. (1.4-19b) as the general expression relating the derivatives.

$$A \left( \frac{r_0}{V_R} - t \right) x_M^{(2+i)} + \left( \frac{r_0}{V_R} - iA - t \right) x_M^{(1+i)} + (N - i) x_M^{(i)} = 0 . \quad (1.4-19b)$$

If  $i$  is taken equal to  $N$  in Eq. (1.4-19b), a differential equation is obtained which may be solved for  $x_M^{(1+N)}$ . Repeated integration of this result and evaluation of the constant of integration yield the following expression for  $x_M(t)$ .

$$x_M(t) = x_M^{(1+N)}(t_1) \left( \frac{r_0}{V_R} - t_1 \right)^N e^{t_1/A} \frac{1}{N!} \int_{t_1}^t (t - \tau)^N \left( \frac{r_0}{V_R} - \tau \right)^{-N} e^{-\tau/A} d\tau \\ + \sum_{j=2}^N \frac{x_M^{(j)}(t_1)}{j!} (t - t_1)^j . \quad (1.4-20)$$

The step response  $a(\tau)$  is then the expression for  $x_M(t_f)$  of Eq. (1.4-20) obtained by substitution of  $t_f = r_0/V_R$  and  $t_1 = (r_0/V_R) - \tau$ , and by use of Eqs. (1.4-17) and (1.4-19b). The first nonzero derivative is obtained from Eq. (1.4-17) by again taking

$$x_M(t) = 0 \quad \text{for } t < t_1$$

and

$$x_M(t) + x_N(t) + C(r_0 - V_R t) = 1 \text{ for } t > t_1 .$$

If the missile is initially on a straight-line collision course  $x_M(t_1)$  and  $\dot{x}_M(t_1)$  are both zero. Then

$$\frac{A}{N} \tau \ddot{x}_M(t_1) = 1 \quad \text{or} \quad \ddot{x}_M(t_1) = \frac{N}{A\tau}.$$

The higher derivatives required for the solution of Eq. (1.4-20) may then be evaluated by repeated application of Eq. (1.4-19b). When the values of the derivatives are substituted in Eq. (1.4-20), the step response in the general case assumes the form

$$a(\tau) = 1 - e^{-l} \sum_{k=0}^{N-1} \frac{(N-1)! (-l)^k}{(N-1-k)! (k!)^2} \quad (1.4-21)$$

where

$$l = \frac{\tau}{A}.$$

The distance-to-distance transfer characteristic  $F(s)$ , associated with  $a(\tau)$ , can be obtained from the Laplace transform of  $a(\tau)$ .

$$\mathcal{L}[a(\tau)] = \frac{1}{s} F(s). \quad (1.4-22)$$

After substitution of the expression for  $a(\tau)$  from Eq. (1.4-21) the Laplace transform yields

$$\mathcal{L} \left[ 1 - e^{-l} \sum_{k=0}^{N-1} \frac{(N-1)! (-l)^k}{(N-1-k)! (k!)^2} \right] = \frac{1}{s} \left[ 1 - \frac{s^N}{\left(s + \frac{1}{A}\right)^N} \right], \quad (1.4-23)$$

or

$$F(s) = 1 - \frac{s^N}{\left(s + \frac{1}{A}\right)^N}. \quad (1.4-24)$$

The miss caused by target maneuver may also be obtained for this proportional-navigation-with-simple-time-lag control system by using the expression for  $a(\tau)$ . For the case where the target makes a constant-lateral-acceleration turn beginning at a range  $r_1$ , substitution of Eq. (1.4-21) into Eq. (1.4-14) yields

$$\left. \begin{aligned} \frac{M_T}{A^2 a_T \cos \alpha_0} &= \frac{e^{-l_1}}{2!} && \text{for } N = 3 \\ &= -\frac{e^{-l_1}}{3!} (l_1^3 - 3l_1^2) && \text{for } N = 4 \\ &= \frac{e^{-l_1}}{4} (l_1^4 - 8l_1^3 + 12l_1^2) && \text{for } N = 5 \end{aligned} \right\} \quad (1.4-25)$$

where

$$l_1 = \frac{r_1}{AV_R}.$$

The deviation of the miss caused by white noise was obtained for the proportional-navigation-with-simple-time-lag system in the case where the initial range is sufficiently large that the upper limit of the integral in Eq. (1.4-16) may be considered infinity. In this instance, the  $\int_0^\infty [a'(\tau)]^2 d\tau$  can be calculated for integral values of  $N$  with the expression given in Eq. (1.4-21) for the step-response function. When  $A \int_0^\infty [a'(\tau)]^2 d\tau$  is plotted as a function of  $N$ , for  $N = 1, 2, \dots, 6$ , the results are found to lie approximately on a straight line (on log-log paper) with a slope of 1.25. The integral may, therefore, be approximated as

$$\int_0^{\infty} [a'(\tau)]^2 d\tau = 0.5 N^{1.25} A^{-1} . \quad (1.4-26)$$

Substituting this expression for the integral and

$$N = \frac{(b+1)(V_M \cos \beta_o)}{V_R} \quad (1.4-18)$$

into Eq. (1.4-16) yields

$$\left. \begin{aligned} \sigma_N^2 &= K_N A^{-1} (b+1)^{1.25} , \\ K_N &= \pi \Phi_N \left( \frac{V_R}{V_M \cos \beta_o} \right)^{-1.25} . \end{aligned} \right\} \quad (1.4-27)$$

Booton also derived expressions for the miss caused by initial conditions (initial error in missile heading and initial-lateral-acceleration of the missile) but these are not considered here. In addition, he investigated the parameters required to give a minimum rms miss with a simple-lag control system. Since the effects of  $A$  and  $(b+1)$  on the miss cannot be separated, this optimization furnishes the optimum value for the product  $[A (b+1)^{-1.25}]_o$  but not for the individual factors. Thus

$$[A (b+1)^{-1.25}]_o = \frac{0.368 (2\pi \Phi_N)^{1/5} \left( \frac{V_R}{V_M \cos \beta_o} \right)^{-1.25}}{\left( a_T \cos \alpha_o \right)^{2/5}} . \quad (1.4-28)$$

He further found that, with the minimum rms miss distance as a criterion, the proportional-navigation-with-simple-time-lag system is as good as the best possible linear control system (including time-variant systems), within the accuracy of the approximations involved.

1.5. Need for a Simulator Study of the Effects of Limiting.

Booton's linear analysis summarized in the previous section is a valuable contribution to the investigation of the proportional-navigation problem. However, when a missile is following a maneuvering target, particularly in the presence of noise, at times the control system almost certainly calls for a greater lateral acceleration than the missile is capable of attaining. Accordingly, a nonlinearity is introduced into the problem, making the linear analysis inapplicable. In many of the problems of interest, the effects of acceleration limiting are too great to be considered merely as a slight modification of the linear case, and too small to wipe out completely the influence of other factors in the system and thereby allow an analysis in which the missile is always called upon to deliver its full acceleration. An analytic solution to this intermediate problem appears unlikely, but this is exactly the type of problem in which an accurate, high-speed analog computer should be able to provide the solutions desired. A study of this particular problem was therefore undertaken using the Variable-Time-Scale Section of the Generalized Flight Simulator which has been developed in the Dynamic Analysis and Control Laboratory at the Massachusetts Institute of Technology.

1.6. Contributions Made in This Study.

The contributions made in this thesis fall into three main categories. The first, reported in Chap. 3, includes an investigation of various means of generating a noise signal suitable for injection into the Variable-Time-Scale Section of the M.I.T. Flight Simulator and of

means of accurately monitoring this signal. The second phase of the work, Chaps. 2 and 4, is concerned with an analysis of the operation of the computer. Here a start is made toward evaluating the accuracy to be expected from the computer when handling problems involving noise signals. As this work progressed, its importance became more apparent and, although only a beginning in the field of computer evaluation was possible in this thesis, the techniques employed should play an important part in a future, more comprehensive, computer-evaluation program, as well as in the general field of servo analysis. As a third and primary phase of the work, a general study of the class of homing-missile control systems discussed in Sec. 1.3 was undertaken on the computer. The results obtained are presented and analyzed in Chap. 5 and some valuable conclusions are obtained concerning the type of missile control system required to minimize the miss distance.



## CHAPTER 2

### SETUP OF THE M.I.T. FLIGHT SIMULATOR FOR PROPORTIONAL- NAVIGATION STUDIES

#### 2.1. Introduction.

The experimental work conducted for this thesis made use of the analog computer which has been developed at the M.I.T. Dynamic Analysis and Control Laboratory.<sup>6</sup> Most of the equipment employed in this computer uses a 400-cps suppressed-carrier-modulated signal as the data carrier. An auxiliary set of equipment is available which employs direct current because some operations are more conveniently carried out on a d-c basis. In order to provide a background for a better understanding of the computer and of some of the problems encountered in its operation, a brief description of each of the principal components is given in Appendix B.

Since the initial operational use of the D.A.C.L. Computer was made during the course of the study herein described, numerous problems arose. The contributions made in this thesis concern as much the analysis of the ability of the computer to handle random signals, and the consideration of techniques for correcting deficiencies and improving operations, as the analysis of the particular homing-missile problem being studied. Consequently, procedures developed for setting up and checking the computer are discussed.



## 2.2. Computer Setup for Studying the Proportional-navigation Problem.

The first computer application considered here investigates a simple-time-lag filter in the missile control system. This setup includes the effects of target maneuvers and missile launching errors but does not make provision for the effects of radar noise. For the initial setup the assumption is made that the missile is capable of unlimited lateral acceleration.

The problem studied is defined in accord with the discussion of Sec. 1.3 by the kinematic equations

$$\dot{r} = V_T \cos(\alpha - \phi) - V_M \cos(\alpha - \theta) \quad (1.3-1)$$

$$r\dot{\alpha} = -V_T \sin(\alpha - \phi) + V_M \sin(\alpha - \theta) \quad (1.3-2)$$

and by the missile control equation

$$A\ddot{\theta} + \dot{\theta} = (b + 1)\dot{\alpha}. \quad (1.3-6)$$

Solution on the computer can be obtained more conveniently if the kinematic equations are written in rectangular form. For this purpose it is convenient to redraw Fig. 1.3-1 with the reference along the x axis and  $\alpha$  redefined as shown in Fig. 2.2-1. Again, the y axis is

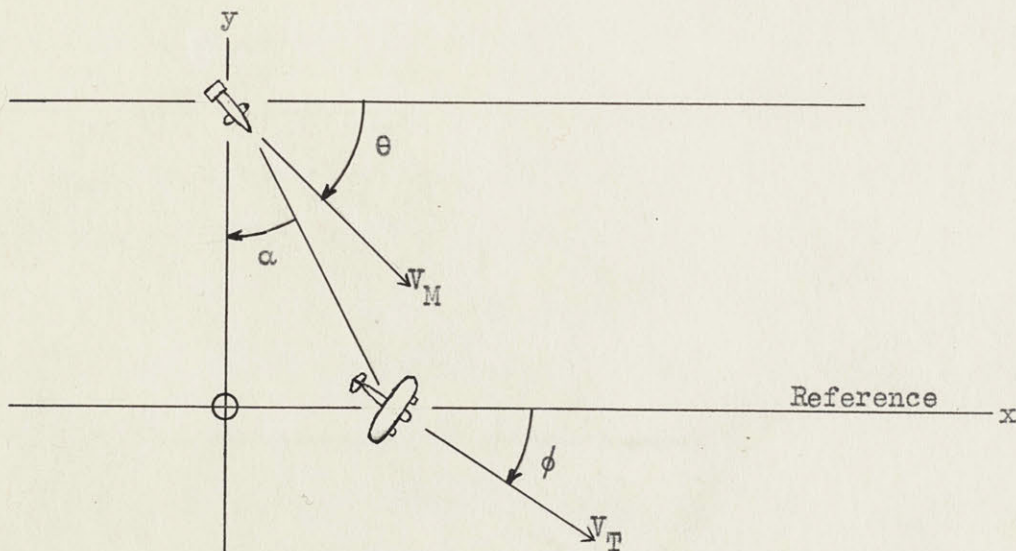


Fig. 2.2-1. Geometry of the Homing-missile Problem.

always parallel to the initial line of sight and the coordinate system moves (without rotation) with a velocity equal to the velocity of the target. Then

$$\dot{x} = V_T \cos \phi - V_M \cos \theta \quad (2.2-1)$$

$$\dot{y} = V_T \sin \phi - V_M \sin \theta \quad (2.2-2)$$

and

$$\alpha = \arctan \frac{x}{y} . \quad (2.2-3)$$

In order to simplify the machine setup, Eq. (1.3-6) is considered to have been integrated on paper before being used in the computer.

The equation actually simulated is, therefore,

$$A\dot{\theta} + \theta = (b+1)\alpha - \gamma \quad (2.2-4)$$

where  $-\gamma$  is the constant of integration.

Figure 2.2-2 shows a simplified block diagram of the computer setup. The operation of this arrangement is easily understood if the quantities  $\dot{\phi}$  and  $\dot{\theta}$  are taken as starting points. The target turning rate,  $\dot{\phi}$ , is one of the parameters of the study and may be considered known at this point. Furthermore, the missile turning rate is assumed to be available somewhere in the computer. The quantity  $\dot{\phi}$  is integrated<sup>7</sup> and voltages proportional to  $V_T \sin \phi$  and  $V_T \cos \phi$  are obtained from a resolver which is mounted on the output of the integrator and excited with a voltage proportional to the target velocity,  $V_T$ . Likewise,  $V_M \sin \theta$  and  $V_M \cos \theta$  are obtained from  $\dot{\theta}$  and  $V_M$ . These quantities are then summed according to Eqs. (2.2-1) and (2.2-2) and the quantities  $\dot{x}$  and  $\dot{y}$  are thus obtained.

Integrations of  $\dot{x}$  and  $\dot{y}$  yield, respectively,  $x$  and  $y$ . These quantities are then fed into a position servo which solves for the angle  $\alpha$

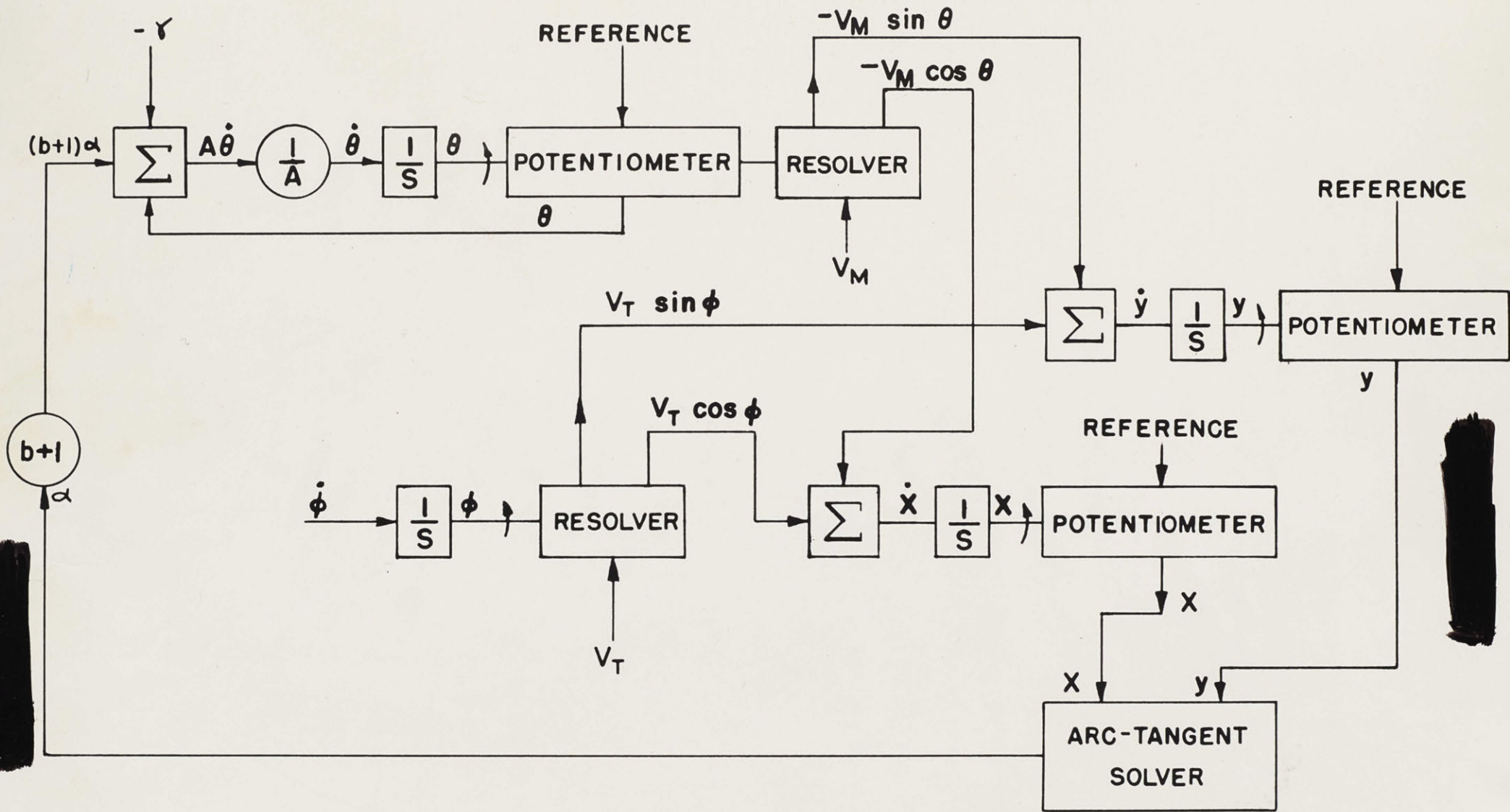


FIG. 2.2-2. BLOCK DIAGRAM OF THE SETUP OF THE COMPUTER FOR STUDYING THE PROPORTIONAL-NAVIGATION PROBLEM WITH A SIMPLE-TIME-LAG FILTER, NO LIMITING, AND NO RADAR NOISE.

according to Eq. (2.2-3). The operation of this arc-tangent servo is discussed in detail in Chap. 4. With the assumption that  $\dot{\theta}$  is available, then  $-\theta$  can be obtained by an integration. A summation of  $\alpha$  multiplied by  $(b+1)$ ,  $-\gamma$ , and  $-\theta$  then yields  $A\dot{\theta}$  which, when multiplied by  $1/A$ , gives  $\dot{\theta}$ . Since  $\dot{\theta}$  actually becomes available in this process, the original assumption is justified.

The preceding problem can be set up in ways other than shown in Fig. 2.2-2. As long as a completely linear system is being studied, the choice of the setup is dictated only by convenience and the accuracy to be expected. On the other hand, when the effects of limiting are studied, care must be exercised to simulate the limiting in exactly the manner in which it occurs in the system being studied. This point is discussed in more detail in Sec. 5.3.

After a block diagram for the computer setup has been established, the matter of selecting the voltage levels, time scale, mechanical scale factors, and gearboxes which enable the machine to operate to its best advantage must be considered. These are extremely important choices because upon their selection rests the difference between obtaining good data and completely worthless data. Unfortunately, the determination of the optimum factors to be used is not possible until a correct solution to the problem has been obtained either by point-by-point integration methods or by successive trials on the simulator. A tentative machine setup may be outlined on the basis of the following limitations.

1. The maximum permissible voltage at the output of an amplifier<sup>8,9</sup> is 50 volts.
2. The maximum allowable rotation of the potentiometers used on the electromechanical integrators<sup>7</sup> is 5 turns each side of the center (zero) position.
3. For the potentiometers used on the integrators there are approximately 200 turns of wire per radian. The resolution, due to finite wire size is, therefore, approximately 0.02 per cent of full scale (10 turns).
4. The maximum permissible velocity, at the motor shaft, for the integrators is 300 rad/sec, and the maximum available acceleration is approximately 3000 rad/sec<sup>2</sup>.
5. All circuits must be fed from the proper impedance sources and must feed into the proper loads. Furthermore, loops caused by multiple grounds must be avoided.

With these limitations as a basis, the scale factors to be used in setting up the problem outlined in Fig. 2.2-2 can be selected.

The y integrator is considered first. If ranges up to 20,000 feet are to be studied, then full scale (5 turns) of the potentiometer would be made to represent 20,000 feet. For a head-on approach,  $\dot{y}$  is  $V_M + V_T$  and equals 3000 ft/sec for the case to be studied here. Therefore, the 20,000 feet are traveled in approximately 7 seconds. If the problem is solved in real time, then the potentiometer on the y integrator must turn 5 revolutions in 7 seconds. The gear ratio between the motor shaft and the potentiometer may be represented as 30G where G is the ratio of the gearbox used with the built-in 30-to-1 ratio.

Then the motor must turn  $150G$  revolutions or  $300\pi G$  radians in 7 seconds. As a result, the angular velocity is  $135G$  rad/sec. If the motor is to run at approximately 80 per cent of full velocity ( $300$  rad/sec), then a 2:1 gearbox should be used. If, on the other hand, an 8-to-1 time scale extension is to be used, a 16:1 gearbox should be employed. Wherever possible, the motors should be run at a substantial fraction of full speed so that the tachometer will operate at a large fraction of its full-scale output and, therefore, provide the highest possible accuracy. The tachometer output at  $300$  rad/sec is 5 volts, but its zero-speed output may be as high as 5 millivolts. Since the  $y$  integrator runs at essentially constant speed in this application, very small acceleration demands are made upon it.

The  $\phi$  servo also operates with a fixed and known input, so the appropriate gearbox to be used in it can also be selected without difficulty. The demands on the  $x$  servo, the  $\theta$  servo, and the arc-tangent solver are, on the other hand, much more difficult to foresee, until at least a preliminary solution to the problem has been obtained. Probably the easiest approach to the problem is to guess a set of gearboxes, run the problem, and record the input and output of each integrator. The maximum velocity and acceleration called for in each integrator can then be estimated and the gearboxes changed accordingly. A few trials should lead quickly to the most suitable choices.

Where both potentiometers and resolvers must be used on the output of an integrator, an additional source of error arises. The resolvers provide a very high degree of resolution, whereas there are approximately

only 200 turns of wire per radian on the potentiometers. If the resolvers and potentiometers are both turned through the same angle, which may be only a few degrees, the low resolution of the potentiometer immediately presents a source of error. A partial remedy is obtained by gearing the potentiometer so that it turns further than the resolver, but at present only a 3-to-1 step-up is available, and because of added backlash, even this small improvement cannot be completely realized.

Before the final electrical and mechanical gains to be used with the integrators can be established, the signal voltage levels throughout the system should be checked and an attempt made to arrive at an advantageous set of scale factors. Signal levels should never be allowed to exceed 50 volts at the output of a repeater amplifier nor 10 volts into a resolver, but the operating levels should be as close to these limits as possible and convenient. The scale factors should be selected with a view toward simplifying the processes of reading data from the recorders and making calculations. For example, allowing 1 volt to represent 100 feet would be quite acceptable, provided that this choice did not lead to overloading, but allowing 1 volt to represent 65 feet in order to operate the equipment at a slightly higher voltage level would not be acceptable because of the resulting difficulties in data reduction. To insure that equipment is operated at nearly optimum accuracy, scale-factor choices must be reviewed as parameters in a study are changed.

Because no physical missile equipment is employed in the computer, the length of time required for a problem may be scaled so that the solution takes either a longer or a shorter time than the duration of the corresponding flight. The ratio of the time the computer requires to solve a problem to the interval the trajectory lasts in real time is termed the time-scale-extension factor. The choice of a proper time-scale-extension factor is another very important consideration in the operation of the computer. If the time scale is extended to the point where a single trajectory requires 2 minutes or more, drift occurring in the integrators during the course of a solution may cause serious errors. Furthermore, particularly in making statistical studies, the amount of data which can be collected per day is severely limited by using a longer time-scale extension than is necessary. On the other hand, if too short a time-scale extension is used, the acceleration and velocity demands made upon the servos become excessive, resulting in serious computing errors.

The 8-to-1 extension factor employed during this study represented approximately the best compromise which could be achieved with the existing equipment. In this setup, after careful adjustment, nearly perfect collision courses could be run for initial ranges up to 10,000 feet and yet no excessive errors were introduced due to the limited acceleration capabilities of the servos. With longer extension factors acceptable collision courses were obtained only with extreme difficulty, while for shorter factors the computing errors became excessive.

### 2.3. Basic Checking Procedures.

When setting up even as simple a problem as represented in Fig. 2.2-2, every available means for checking the machine should be employed to insure obtaining accurate results. A brief consideration of these checking procedures appears appropriate at this point.

The first test to be made after the cabling for the problem has been completed, consists in checking the zero setting and measuring the static gain through each potentiometer and resolver channel. In this process the 400-cps phase shift through the various channels is adjusted to essentially zero. This adjustment is necessary if the signal obtained after subtracting two fairly large voltages is to be relatively free of quadrature component. The integrators are most vulnerable to trouble from the 90-degree voltage components since the voltage fed back to their error point from the tachometer is essentially all "inphase" signal. The 90-degree components are, therefore, not canceled out and can cause overloading in the high-gain amplifier after the error point. Similar overload difficulties can result from the presence of harmonics in the 400-cps supply or from noise voltages picked up from the power supplies. This static gain checking can be extended to include larger blocks of the problem and is often useful in pointing out overloading difficulties.

Two static tests are made on the electromechanical integrators. First, the drift with no input signal is checked and adjusted to zero. Next, the input voltage required to turn the tachometer at a certain speed is checked. A magnetic pickup unit has been mounted on each

[REDACTED]

integrator motor and the speed is determined by comparing the output of the pickup with a signal from a standard frequency source. Thus both the tachometer calibration factor and the input attenuator unit are checked. In the newest section of the computer semiautomatic equipment has been installed for making these static tests.

If the problem includes the simulation of simple-lag or quadratic filters, a rough over-all check on this portion of the equipment may readily be obtained by applying a step input to the filter and observing the response on a recorder.

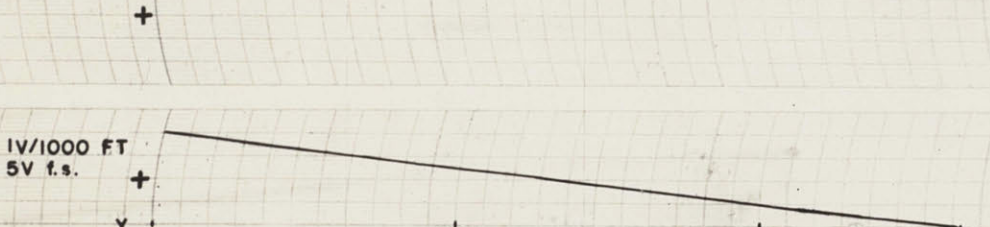
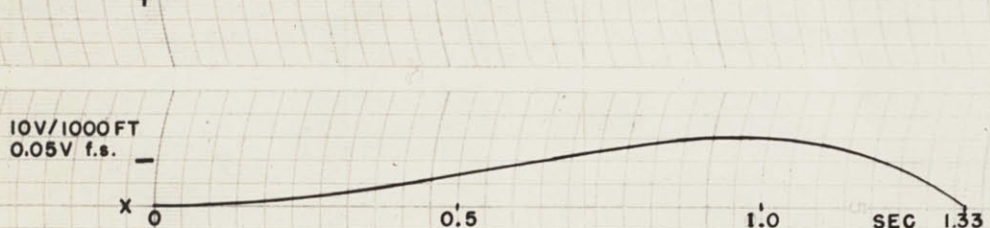
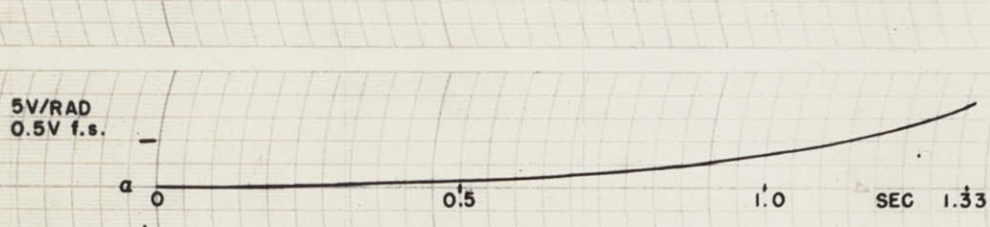
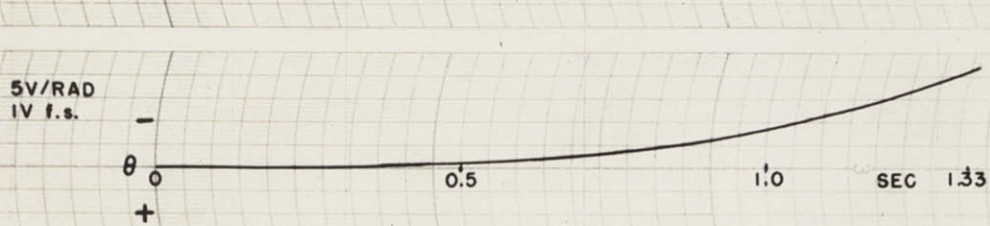
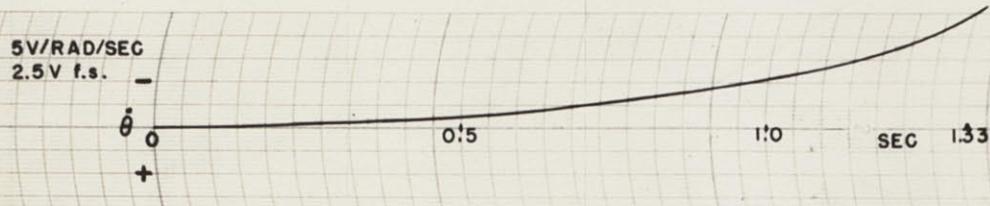
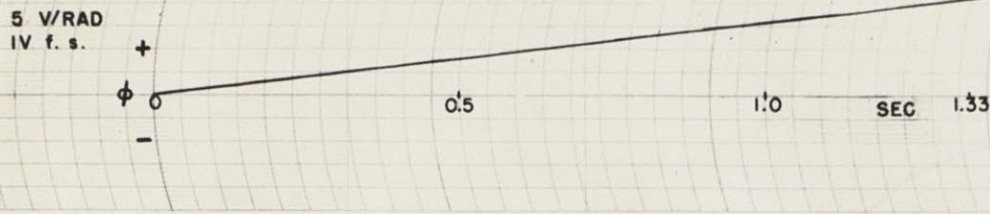
After the operation of the separate units in the computer has been checked, the procedure is extended to include the complete problem setup. The presence of drift in the  $\alpha$ ,  $\theta$ , or  $x$  integrator servos may be discovered by running a collision course, where  $x$  should remain zero throughout the flight. This test is considered satisfactory if the maximum excursion of  $x$  for a 4000-foot head-on attack is less than 0.5 foot. A check that the signals fed into the  $y$  integrator are correct is obtained by observing the length of time required to reach the collision point.

The final check on whether the machine is solving the desired problem can, unfortunately, be obtained only by comparing its solution with a solution of indisputable accuracy. Therefore, solutions to several typical problems of interest here were obtained by point-by-point integration methods using a hand calculator. The usual check solution used was the case where the missile and the target are initially flying a straight-line head-on collision course but, at a predetermined range, the target begins a constant-lateral-acceleration turn.

[REDACTED]

Figure 2.3-1 shows a typical set of recordings of the important variables in a noise-free proportional-navigation trajectory problem for a missile with a simple-lag control system and no acceleration limiting. Both the scale factor at which the quantity was recorded and the volts required to give full-scale (f.s.) deflection of the recorder are noted at the left end of each recording. The data used to plot Fig. 2.3-1 were obtained from a hand solution but, when sufficient care is taken, similar results can be obtained from the simulator.

Even after satisfactory agreement has been obtained between the machine solution and the hand solution to a specific problem, extreme care must be exercised when parameters are changed, since a situation may easily arise in which the scale factors are very unfavorable to good machine operation. The signals may be so small that no accuracy can be obtained, or they may be so large as to cause overloads. An overload system will be available soon, which will immediately indicate when the signal level becomes too high at a point in the computer or when the velocity or acceleration capabilities of the servos are being exceeded. Determining when signals are of too low a level for satisfactory computation will remain a problem which can be avoided only if the operators exercise extreme care. A proposal is, however, being considered for installing a system for roughly indicating and automatically recording the maximum voltage level reached at a large number of selected points throughout the computer.



CONDITIONS:  
 $\dot{\theta} = 2(6\alpha - \theta)$   
 $\dot{Y} = -1000 \cos kt - 2000 \cos \theta$   
 $\dot{X} = -1000 \sin kt - 2000 \sin \theta$   
 $\alpha = \text{TAN}^{-1} X/Y$

HEAD-ON ATTACK FROM AN INITIAL COLLISION COURSE WITH TARGET MAKING A CONSTANT 4g TURN BEGINNING AT A RANGE OF 4000 FEET.

A = 1/2 SEC  
 b + 1 = 6  
 $V_T = 1000 \text{ FT/SEC}$   
 $V_M = 2000 \text{ FT/SEC}$

MISS DISTANCE < 1 FT

FIG. 2.3-1. TYPICAL RECORDING OF THE IMPORTANT VARIABLES IN A PROPORTIONAL-NAVIGATION TRAJECTORY PROBLEM WITH SIMPLE-LAG FILTER, NO RADAR NOISE, AND NO LIMITING (HAND SOLUTION).

During the past two years operating techniques have been developed at the D.A.C.L. and a staff of operators has been trained to insure that, once the computer has been checked out, acceptable solutions are obtained.

[REDACTED]

## CHAPTER 3

### RADAR NOISE AND ITS SIMULATION

#### 3.1. Introduction.

The probability that a guided missile destroy its target depends considerably upon the characteristics of the noise in the system and upon the ability of the system to separate the true signal from the noise, where the term noise applies to any effect which contaminates the true signal. The information used to control a guided missile may be corrupted before it reaches the missile or within the missile. Since this investigation is concerned with a study of radar-controlled missiles, the characteristics of radar noise and of the various types of noise occurring in the radar receiver and in the missile control system must be considered.

The characteristics of noise will, in the general case, be very difficult to define. Noise signals may be divided into two broad classes; one has characteristics invariant with time and the other requires time-varying parameters for its description. It may be possible theoretically to give an analytic description of noise signals possessing characteristics which are variant with time. The experimental measurement of such signals is, however, extremely difficult and the mathematical techniques for dealing with such signals have not yet been developed. Consequently, the treatment of noise will be limited to the case in which the noise can be described in terms of such a variable that its characteristics are invariant with time. Even in

[REDACTED]

[REDACTED]

this case, the description can be made only on a statistical basis. No attempt is made to describe a noise signal as a function of time but rather in terms of its average characteristics. One description is made in terms of the average noise power and the distribution of this power in the frequency spectrum (i.e., in terms of the power density spectrum). An alternate description gives the average power and the average correlation between the amplitude of noise voltage existing at one time and that at some later time when this correlation is considered as a function of the time between the points being correlated (i.e., the autocorrelation function). In this discussion only the power spectrum representation will be employed.

Considerable difficulty arises in obtaining a reliable description of a noise signal from experimental data. Each of the means discussed for describing the noise requires theoretically that the sample of noise data being examined have an infinite length, and furthermore that the characteristics of the noise be invariant with time. Experimentally, only finite sections of noise data can be obtained and in many cases these sections are not portions of a stationary series. Nevertheless, by employing the proper techniques in collecting and analyzing the data, it is possible to specify the limitation imposed by using a finite section of data and to determine whether the sample obtained belongs to a stationary time series. In this regard, considerable attention should be given to the choice of the variable in terms of which the noise is described, since noise functions may have time-varying components when referred to one variable but be constant when

[REDACTED]

referred to some other variable. For example, noise described in terms of an angle may be variable with time, whereas the same noise given in terms of a distance may be invariant with respect to time and may therefore be described on the basis of belonging to a stationary time series.

Since noise functions are not periodic and do not approach zero as  $t \rightarrow \infty$ , they cannot be represented either by Fourier coefficients or by a Fourier transform. As shown by Wiener,<sup>10</sup> the noise can be represented by an "averaged" Fourier transform,  $F(i\omega)$ , given by

$$F(i\omega) = \lim_{T \rightarrow \infty} \frac{1}{2T} \int_{-T}^T f(t) e^{-i\omega t} dt. \quad (3.1-1)$$

The power density spectrum  $\Phi(\omega)$  is then given as

$$\Phi(\omega) = |F(i\omega)|^2. \quad (3.1-2)$$

Alternately,  $\Phi(\omega)$  can be expressed directly in terms of  $f(t)$ , as

$$2\pi\Phi(\omega) = \lim_{T \rightarrow \infty} \frac{1}{2T} \left| \int_{-T}^T f(t) e^{-i\omega t} dt \right|^2. \quad (3.1-3)$$

Furthermore, the mean-square value of  $f(t)$  is given by the integral of  $\Phi(\omega)$  from minus infinity to plus infinity. That is,

$$\overline{f^2} = \int_{-\infty}^{\infty} \Phi(\omega) d\omega. \quad (3.1-4)$$

For signals which may be classed as stationary time series,  $\Phi(\omega)$  can be determined without undue difficulty, once a sufficiently long sample of the signal as a function of time is available. The function  $\Phi(\omega)$  may then be presented graphically or it may often be approximated by a relatively simple analytic function.

██████████

The specification of  $\Phi(\omega)$  does not define a unique amplitude-versus-time relation. This ambiguity causes no trouble in the analysis of completely linear systems, if the interest is only in the mean-square-value description of the quantities. Even for linear systems, however, if descriptions other than the mean-square values are considered, as in calculations of amplitude-probability distributions, it is conceivable that this ambiguity may lead to considerable error. Moreover, in systems where limiting or other nonlinear effects occur, and superposition is, therefore, not applicable, the calculation of even the mean-square values may depend upon the particular amplitude-versus-time relation of the signal.

A Gaussian amplitude distribution is usually the easiest to handle because, if the input to a linear system is Gaussian (i.e., each frequency component is Gaussian), the distributions occurring at all other points in the system are also Gaussian. In this situation, a determination of the power at various points in the system is all that is required for a complete description of the signals.

### 3.2. Possible Sources of Noise.

A number of different sources of noise appear or may appear in a homing-missile system. Their importance depends to a large degree on the conditions under which the missile is being used and on the characteristics of the missile itself. Furthermore, the relative significance of the different components may change considerably as a missile approaches its target. The major sources of noise are:

1. "Glint" or "angular scintillation" effects.
- ██████████

- 
2. Signal fading (amplitude fluctuations).
  3. Thermal and shot-effect noise.
  4. Backlash in gearing or linkages in the control system.
  5. Wind gusts.
  6. Enemy countermeasures.
  7. Multiple-target noise.

Since the primary interest in this investigation lies in the glint type of noise, the discussion of this effect will be reserved for the last.

Signal fading,\* which is generally caused by changes in the apparent radar cross section of the target with changes in target aspect, can be a very important source of noise in some types of radar equipment. The most serious difficulties from this source arise when a conical-scan system is being used to track a target and the spectrum of signal modulation caused by fading contains appreciable components near the scan frequency. This condition will usually be serious only with radars using low scanning rates but may be very serious if a large periodic component of fading (such as caused by propeller modulation) should occur at the scan rate of the radar system. The effects of this type of noise can, however, be made practically negligible<sup>11</sup> by the use of high scanning rates or instantaneous automatic gain control systems (IAGC), by the use of monopulse or simultaneous lobe-switching systems, or by the use of an interferometer type of radar system such

---

\* It should be noted that signal fading and glint noise are related since both are generated by essentially the same mechanism. The two types of noise, however, have a very different effect in the receiver.



██████████

as used in the Meteor missile. For the purpose of this investigation, it will be assumed that the missile is equipped with one of these systems which are insensitive to the effects of signal fading.

Noise troubles, associated with the Johnson noise of resistances in the input stages of a radar receiver or with the shot-effect noise of the first tubes in the receiver, will also be considered negligible. These noise sources are significant mainly in determining the maximum range at which the missile radar is able to detect an echo from a target.\* It is assumed that, once the missile has started to track the target properly, the echo-return signal level overrides this type of noise. This assumption is particularly justified in the terminal phase of guidance.

It is further assumed that sufficient care has been taken in the design and construction of the control system to eliminate any serious sources of backlash.

The effects of wind gusts and enemy countermeasures, such as using "window," towing reflectors behind their planes, or transmitting jamming signals, are admittedly important in some situations, but will not be considered in this investigation. When they are tactically important, they could form the basis of a complete separate study. In many other cases they may be completely disregarded. An additional effect giving rise to large signals, which may be classed as noise, occurs when a missile attempts to track two or more targets flying close together. The radar is then unable to track any one of the targets

---

\* Thermal noise influences the accuracy of measurements made with a receiver until the signal-to-noise ratio is about 3. For higher ratios the effect quickly becomes negligible.

██████████

continuously until the range becomes very small, but rather wanders from one to the other, and most of the time may indicate a virtual target quite far removed from any of the actual targets. The multiple target problem is serious, but for this study isolated targets will be assumed.

### 3.3. Glint Noise.

The glint type of noise arises from changes in the reflecting properties of the target with changes in the angle from which the target is viewed. Since targets such as airplanes are complex structures, the radar echo becomes the sum of the returns from different parts of the target, proper regard being taken of the phases in which the returns combine. The high-frequency radar signals used cause the relative phases of signals from various parts of the target to change considerably with only small changes in path lengths from the receiver to various points on the target. For a geometrically complex target this effect causes the apparent center of gravity of the target, as seen by the radar, to shift considerably from the physical center of gravity, with practically no correlation between the position of the virtual center of gravity and the target aspect, or between the frequency with which the center of gravity appears to shift and the turning rates of the target. Although there is no absolute restriction, it seems from a study of simplified cases<sup>12</sup> that the apparent center of gravity will, most of the time, lie within the limits of the actual target. Glint is of basic importance, since it is always present and

cannot be avoided by modifications in the missile radar. Furthermore, the effects of glint noise become significant at approximately the range at which the effects of target maneuvers become important. Unfortunately, it is difficult to obtain measurements of either the amplitude or the power spectrum of this type of noise as divorced from other types. Since collecting such experimental data is beyond the scope of this thesis, the best available data<sup>13, 14, 15, 16</sup> have been examined and typical values selected for this investigation. In addition, the specification of the noise has been taken as one of the chief parameters in the study.

The results of one set of data collected at the Bell Telephone Laboratories are reproduced in Fig. 3.3-1. This figure shows how the noise, measured as a distance at the target, varies as a function of range, when observed by two different X-band radars feeding a servo with a 1/2-cycle pass band.\*

For large ranges where the radar receiver operates at full gain, the standard deviation of the tracking, expressed in angular mils, tends to be proportional to the square of the range. Expressed in yards at the target, the standard deviation of the component of noise due to thermal agitation,  $\sigma_t$ , is proportional to the cube of the range. This effect is expected for a transmit-receiver radar in which the power returned from the target varies inversely with the fourth power of the range, while the noise power generated in the receiver remains constant. Since thermal agitation is not the only source of noise present, the

\* Since glint noise includes components at frequencies very much higher than 1/2 cycle very little of the character of the power spectrum can be learned from measurements involving such a servo.

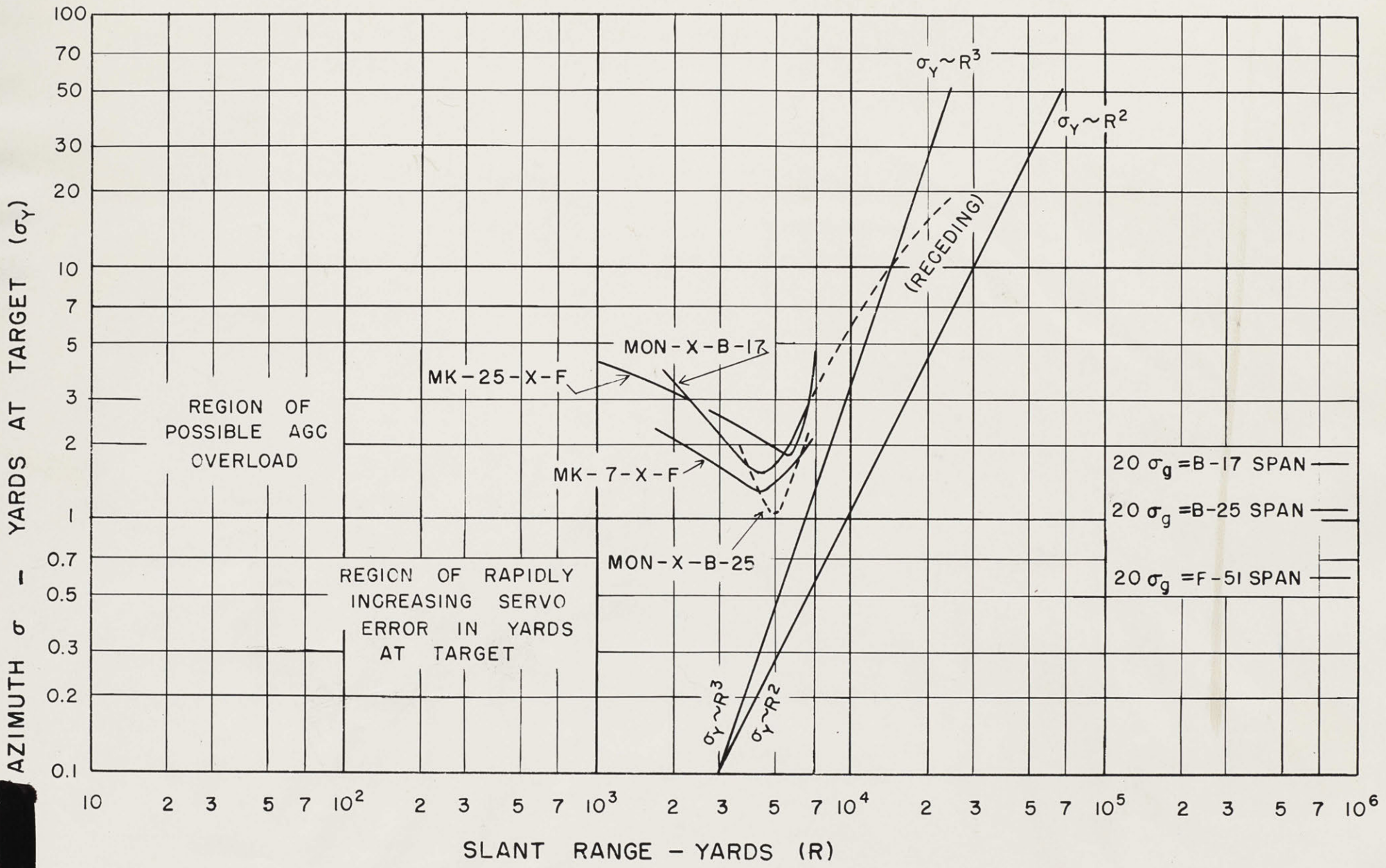


FIG. 3.3-1. VARIATION OF TRACKING DEVIATIONS WITH RANGE FOR TARGETS FLYING RADIAL COURSES.

██████████

standard deviation of the tracking does not continue to decrease with a decrease in the range but passes through a minimum. The increase in apparent noise at low ranges is attributed to rapidly increasing servo error, as measured in yards at the target, and to possible AGC-system overload, as the target nears the radar. The value of the minimum observed has been interpreted as representing the glint component of the noise which, when measured as a distance at the target, should be independent of range.

Because the minima of the curves in Fig. 3.3-1 are sharp it appears very possible that the regions where thermal noise and servo errors are important have overlapped. If this condition occurred the values assigned to glint noise may be slightly high.

The data of Fig. 3.3-1 were collected using a servo with a 1/2-cycle pass band and observing radial target-plane courses. These data indicate that the glint noise, expressed as a linear distance measured at the target, has an rms value which, for the average of the planes on which data were collected, can be expressed as 1/20 the wing span of the plane for head-on or tail aspects. Other data collected for planes flying arc courses indicate that, for the beam approach, the glint noise may be approximated as 1/6 of the length of the fuselage of the target plane.

Data recently collected at the Naval Research Laboratory<sup>15</sup> by a somewhat different method than used in the Bell Laboratories indicate that, for a 1/2-cycle bandwidth, the glint noise can be approximated as 1/4 the length of the plane for beam approaches or 1/12 the wing span

██████████

for head-on approaches. These data, furthermore, indicate that the glint-noise power density is relatively constant to at least 6 cps, and above that value falls off slowly.

If the power density of the noise is assumed to have a constant value  $\Phi_N$ , over an equivalent bandwidth  $\omega_{ss}$ , then, from Eq. (3.1-4),  $\Phi_N$  is given as

$$\Phi_N = \frac{\overline{f^2}}{2\omega_{ss}} \quad (3.3-1)$$

where  $\Phi_N(\omega)$  is defined symmetrically about zero, whereas the filter system is defined only for positive values of  $\omega$ .

With the use of Eq. (3.3-1) and the Bell Laboratories' description of the glint phenomenon, the spectral power density of the glint noise can be calculated for the head-on approach as

$$\Phi_{N,HO} = \frac{\left[\frac{1}{20} (S)\right]^2}{(2)(2\pi \frac{1}{2})} = \frac{(S)^2}{800\pi} \text{ ft}^2/\text{rad}/\text{sec} \quad (3.3-2)$$

or for a beam approach as

$$\Phi_{N,B} = \frac{\left[\frac{1}{6} (L_a)\right]^2}{(2)(2\pi \frac{1}{2})} = \frac{(L_a)^2}{72\pi} \text{ ft}^2/\text{rad}/\text{sec} \quad (3.3-3)$$

where  $S$  and  $L_a$  are, respectively, the wing span and length of the target plane. As an example, in a B-29 the 141-foot wing span and the 96-foot length give, respectively,  $\Phi_N = 7.9 \text{ ft}^2/\text{rad}/\text{sec}$  for head-on or tail approaches and  $46 \text{ ft}^2/\text{rad}/\text{sec}$  for a beam approach.

Recently some additional experimental data on glint-noise power spectra have been obtained<sup>16,\*</sup> at the M.I.T. Research Laboratory for

\* This work is being conducted under the supervision of Prof. H. J. Zimmermann and will be reported in a forthcoming doctoral thesis by J. B. Angell.

██████████

Electronics. Preliminary examination of the data obtained for a broadside aspect of a B-29 bomber shows a noise spectrum with a power density of approximately  $0.6 \text{ ft}^2/\text{rad}/\text{sec}$  from  $-20 \text{ cps}$  to  $20 \text{ cps}$  and a slow cutoff outside  $20 \text{ cps}$ .\* The value of  $\Phi_N$  obtained from this set of data is considerably lower than that obtained from data collected elsewhere. The M.I.T. data cover a relatively broad band of frequencies ( $0-60 \text{ cps}$ ) but, so far, only analysis with a coarse frequency resolution has been completed. Data collected elsewhere, in general, cover one cycle or less. Possibly, when the M.I.T. data are reexamined, a rather high peak will be found in the region from  $0$  to  $0.5 \text{ cps}$  with a broad plateau extending from  $0.5$  to  $20 \text{ cps}$ .

A noise power density  $\Phi_N$  of  $10 \text{ ft}^2/\text{rad}/\text{sec}$  was used for most of the tests made in this study. This value was based on the Bell Laboratories' data, which appeared to be the most reliable information available at the time these tests were made. The value of  $10 \text{ ft}^2/\text{rad}/\text{sec}$  was used merely for convenience and was intended to be representative for a B-29 or a slightly larger bomber. Additional tests should be made if further analysis of the M.I.T. data indicates that a lower value of  $\Phi_N$  is more realistic.

### 3.4. Generation of Glint Noise for Use in the Computer.

#### 3.41. Type of Signal Required.

Neither the characteristics of glint-noise spectra nor the effects on the missile problem of changes in the noise spectrum were known at the beginning of this study. Therefore, the criterion governing the choice of the power spectrum used in the first simulator studies was

---

\* To conform with the mathematical convention used elsewhere in this thesis the noise power is divided equally between positive and negative frequencies.

██████████

[REDACTED]

that the noise should approximate white noise in the problem being studied but should not overload the computing elements with unnecessary high-frequency signals. Bandwidths of the order of 8 to 80 cps (real time) were first employed but an analysis of servo operation when following such signals indicated serious overload difficulties. Calculations of the effect of the noise bandwidth on the miss distance were made, therefore, for problems involving missiles capable of unlimited acceleration, and noise bandwidths as narrow as 50 rad/sec were found to give essentially the same miss distances as white noise (Sec. 3.5). Consequently, the noise-shaping filter was redesigned to be readily adjustable over the range from 10 rad/sec to 300 rad/sec on the time scale of the problem. The next step is to consider how the noise signal might be generated.

### 3.42. Possible Methods of Generating the Desired Noise Spectrum.

There are two basically different ways in which a noise spectrum, such as discussed in the preceding section, can be generated. One method is to generate a spectrum of the desired shape directly, while the other method is to generate essentially white noise and then pass this through suitable filters to produce a spectrum of the desired shape.

One method of generating the spectrum directly would be to cut a random curve on a wheel that is rotated at a constant speed. A random signal could be picked off this wheel by using either a photocell, or a cam follower driving a potentiometer, as the pickoff element. A suitable curve to be cut on the wheel could be synthesized

[REDACTED]

[REDACTED]

by selecting a series of sinusoidal components with frequencies which are not quite even multiples, and with amplitudes which correspond to the power densities at the respective frequencies in the desired power spectrum. The initial phases of sine waves should be chosen at random. The voltage obtained by adding these components point by point would approach a portion of a random curve but would be periodic in the diameter of the wheel. By a proper choice of the diameter of the wheel and its speed of rotation relative to the length of the problem being studied, this periodicity could be made unimportant. Since the speed of the wheel appears as a multiplier on the frequency scale, the bandwidth of the noise signal could be changed merely by changing the speed of rotation of the wheel. As an alternative to cutting the random-signal curve on a wheel, the data could be punched on teletype tape. The speed of reading the tape could be changed to scale the power spectrum as desired.

Instead of putting the sum of various sinusoidal components on a wheel or a tape, a group of generators could be driven from a common motor by a system of gears selected to produce frequencies which were not exact multiples. The outputs of these various generators could then be summed to approximate the desired spectrum.

In the alternate approach to producing a specified spectrum, the first problem is to generate a random signal which is sufficiently broadband to be considered white. Two readily available sources of white noise are the Johnson noise in resistors and the shot-effect noise in vacuum tubes. The noise level developed in each of these

[REDACTED]

cases is usually very small, with the result that a large amount of amplification is required after the noise source. Photomultiplier tubes, because of their very high internal gain, can, however, be made to produce relatively high shot-effect noise outputs. Gas diodes produce an even higher output, particularly when the gas discharge is made to take place in a magnetic field.

Another way to produce a white-noise spectrum is to record a table of random numbers either on teletype tape or as voltages on a magnetic tape. When this recording is read at a suitable speed, a broadband output voltage is produced.

Other means could be devised for generating random signals, the methods given here being merely representative of what could be done, rather than constituting an exhaustive list of possible noise-generating schemes.

### 3.43. Method Adopted for Generating Noise Signals.

After a consideration of the various ways in which noise could be generated and introduced into the computer, the decision was made to use a gas tube as a white-noise source and to follow this by filters designed to shape the noise to the desired power spectrum.

In the circuit of Fig. 3.43-1, noise is developed across a resistor in the plate circuit of a type-884 inert-gas-filled thyatron which is operated as a diode. The amplitude of the noise generated is increased by placing the tube in a magnetic field. An increase of approximately 40 db in the noise amplitude over the output produced without the magnetic field is readily achieved in this way. This

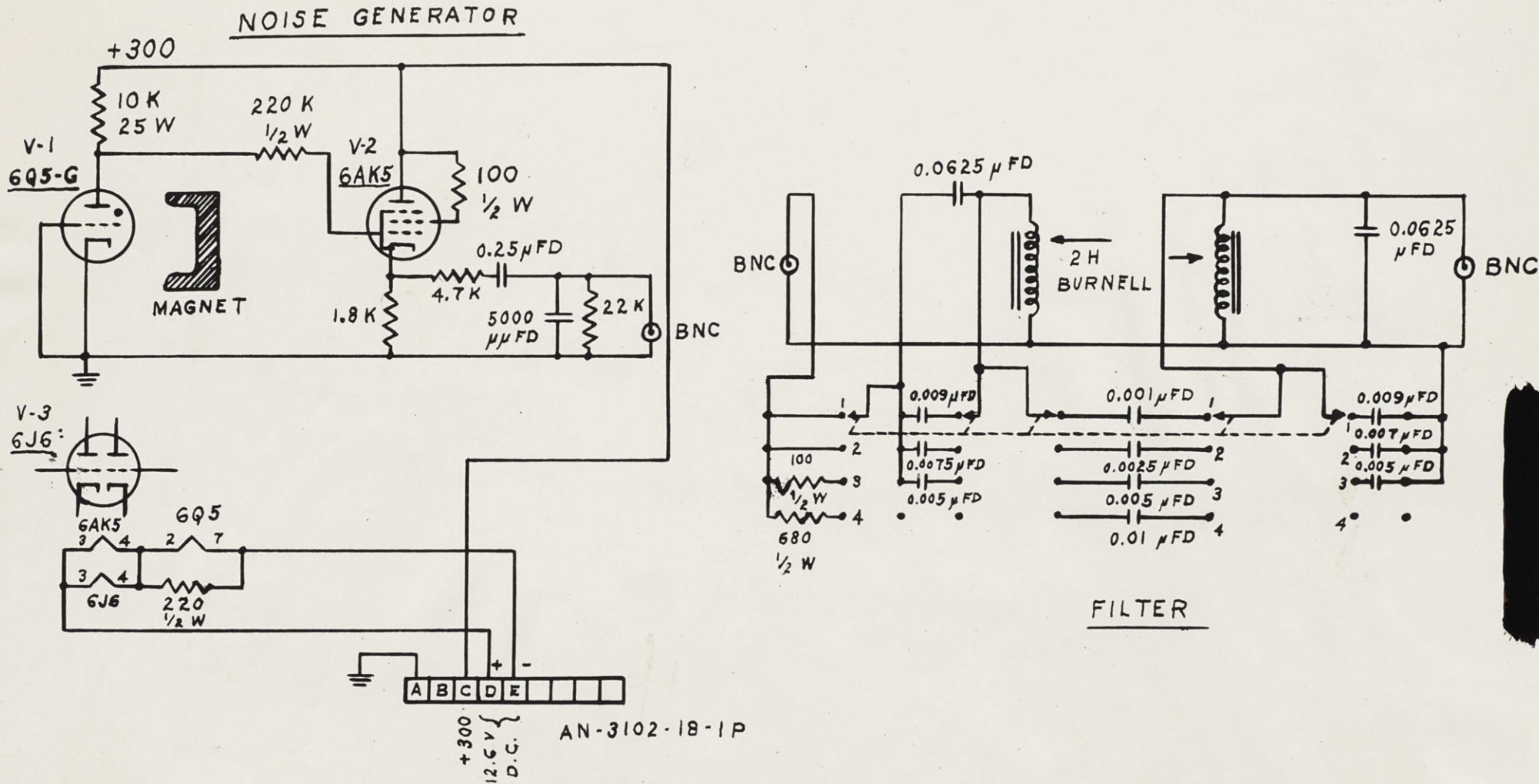


FIG. 3.43-1. SCHEMATIC OF NOISE GENERATOR,  
TYPE N-1.

██████████

increase raises the noise out of the gas tube to a level where only a moderate amount of amplification (the order of 200 times) is required in order to develop the desired spectral power density.

The power spectrum of the noise voltage from the gas tube extends over a band of frequencies from essentially zero to an upper cutoff frequency determined by the resistance and capacitance in the plate circuit of the tube. There are several possible schemes for shaping this power spectrum and introducing the noise into the computer as a 400-cps suppressed-carrier signal. The noise voltage could be passed through a low-pass filter, then through suitable d-c amplifiers, and finally through a modulator giving a suppressed-carrier signal. Because this scheme is subject to zero-drift difficulties common to all high-gain d-c amplifiers, it was not used. An alternative approach is to pass the essentially white noise from the gas tube through a bandpass filter centered at the 400-cps carrier used in the computer. The output of such a filter is similar to a suppressed-carrier noise signal but is random both in phase and in amplitude. Since the computing elements of the system respond only to the inphase components of a signal, care must be taken to interpret the noise correctly. The signal from the bandpass filter may be used directly or it may be demodulated with a phase-sensitive demodulator, and then remodulated, thereby giving a 400-cps noise signal which has random amplitude but is all inphase. The envelope of this signal is random, as it should be to simulate a radar noise signal.

██████████

If the output of the bandpass filter is used directly, several precautions must be observed. In using an ordinary rms-reading voltmeter to set the noise voltage, in order to obtain the desired noise power density, a point to be noted is that the meter reads the quadrature as well as the inphase components of the signal, whereas the computer responds only to the inphase component. A signal with an rms value of  $E$  but made up of components of random phase has an inphase component of  $0.707E$  with a quadrature component of  $0.707E$ . With the assumption of an equivalent square bandpass  $\omega_{ss}$ , the noise power density is given by Eq. (3.3-1) as

$$\Phi_N = \frac{(0.707E)^2}{2\omega_{ss}} \quad (3.43-1)$$

where  $E$  is the reading of an rms-type meter.

Although the servos are built to respond only to inphase 400-cps signals, they are subject to overload by quadrature signals, since the electronic amplifiers provide a very high gain after the error point and the feedback voltage is purely an inphase signal. If the output of the bandpass filter is used directly, the signal is made up of equal parts of inphase and quadrature signals. Therefore, overload by the quadrature component is bound to occur.

In determining the bandwidth of the noise to be injected into the computer, the time-scale-extension factor being used must be considered. Ideally, the integrators can be set to simulate operation over a fairly wide range of time scales. As the extension factor is reduced, however, the possibility that either velocity or acceleration

overloading will occur in the servos is increased. On the other hand, as the factor is extended, the time required for the machine to turn out a solution becomes longer and the integrator drift occurring during a solution increases. A long solution time definitely limits the amount of data which can be obtained, particularly in a statistical study. Eight to one, as used here, was found to be the most satisfactory compromise for this particular class of problems. Although the integrators can be set up for any time scale, a physical filter, such as the bandpass filter used to shape the noise, must necessarily operate in real time. This means that the operation of such a piece of equipment must be reinterpreted when it is used in conjunction with the computer.

A narrow bandpass filter is difficult to build with only passive elements and furthermore, an extremely narrow filter would be undesirable because the carrier frequency employed in the computer is not stabilized. The filter shown in Fig. 3.43-1 proved simple and effective, giving, on the narrowest setting, an over-all bandpass of 16 cps. With an 8-to-1 time-scale extension this is equivalent to an over-all bandpass of 128 cps. The power spectrum introduced into the computer must be considered on a low-pass rather than a bandpass basis in relation to the noise being simulated. If the preceding filter were perfectly symmetrical and perfectly centered about the carrier frequency, the equivalent power spectrum would, therefore, cut off at 64 cps. With this filter, as the amplitude of the noise is raised to give the desired noise power density in the vicinity of zero frequency, the

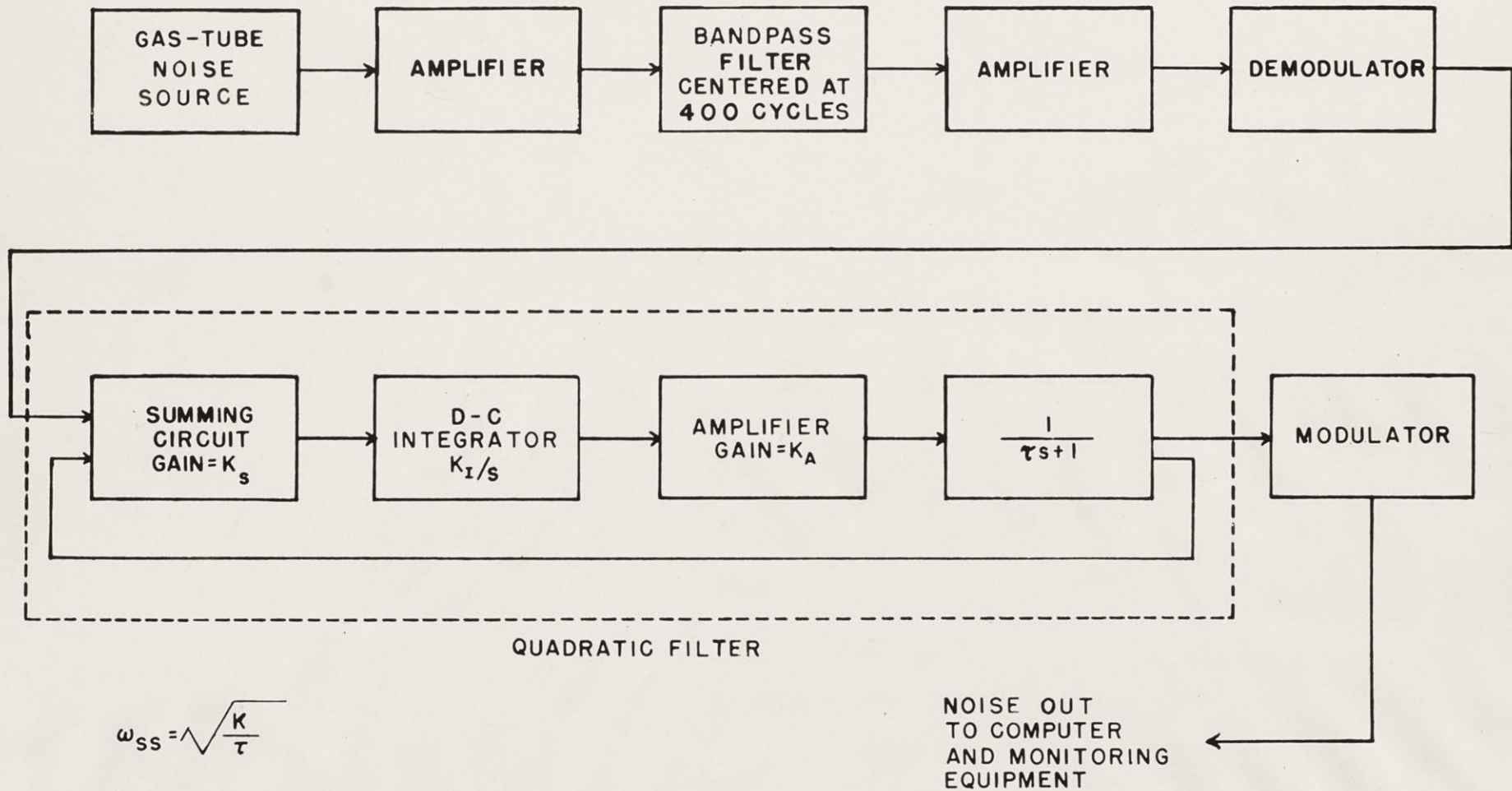
[REDACTED]

electromechanical servos are overloaded by the high-frequency components of noise impressed upon them. The arc-tangent solver (Fig. 2.2-2) gives particular trouble in this respect, and finally the study discussed in Chap. 4 was undertaken to evaluate the behavior of this unit.

The specification of the type of noise power spectrum required for injection into the computer became possible only after some preliminary simulator studies were made. The final requirements were that its bandwidth be readily adjustable over a range from 2 rad/sec to 200 rad/sec without changing the shape of the spectrum. This specification is difficult to meet with a conventional passive bandpass filter. The foregoing considerations led to adopting the approach to the noise-filtering problem which is given in Fig. 3.43-2. The noise generated by the gas tube is amplified and passed through a bandpass filter as before. The filter is operated with a large bandwidth (approximately 75 cps real time) and is used merely to hold the rms value of the noise voltage delivered by this section of the noise-generating equipment at a level well below that causing overloading in subsequent amplifiers. This noise, which has roughly the character of a 400-cps suppressed-carrier signal, is fed into a phase-sensitive demodulator. The output of the demodulator is passed through a semiactive low-pass filter and finally through a modulator to give a true 400-cps suppressed-carrier signal.

The low-pass filter selected for most of the experimental work was a quadratic formed by cascading a passive simple-lag circuit with one of the d-c integrators and closing a feedback loop around the pair as

[REDACTED]



$$\omega_{ss} = \sqrt{\frac{K}{\tau}}$$

$$\zeta_{ss} = \frac{1}{2\sqrt{K\tau}}$$

$$K = K_s K_I K_A$$

FIG. 3.43-2. BLOCK DIAGRAM OF NOISE-GENERATING AND FILTERING EQUIPMENT.

shown in Fig. 3.43-2. The natural frequency and the damping ratio of this filter can be adjusted by selecting a suitable time constant in the simple-lag circuit and providing a suitable gain, as indicated in the figure. Before injection into the computer the output of this filter must be passed through a modulator to form a 400-cps signal.

A simple-lag filter system was also used to some extent, but an analysis of the operation of the electromechanical servos, as given in Chap. 4, showed that the computing errors involved with simple-lag noise were considerably higher than with quadratic noise. This effect occurs because of the relatively large amount of power above the 3-db frequency point in a simple-lag system compared with that in a quadratic system.

The noise filter was set up with d-c computing equipment rather than with a-c because the d-c integrators are not so subject to overload troubles as the electromechanical a-c integrators. Furthermore, the fact that the d-c equipment has a lower static accuracy than the a-c was of little importance in this particular application because the noise was continuously monitored on the output of the filter system, with the result that small changes in gain were unimportant.

The power spectra at the input and output of a linear system are related by the expression

$$\Phi_{\text{out}}(\omega) = |H(i\omega)|^2 \Phi_{\text{in}}(\omega) \quad (3.43-2)^*$$

where  $H(i\omega)$  is the transfer function of the system.

\* This equation, identical with Eq. (4.21-1), is discussed more fully in Chap. 4.

If the assumption is made that the input power spectrum is a constant over a range which is very much broader than the filter system used to shape it, then  $\Phi_{in}(\omega)$  may be assumed constant.

$$\Phi_{in}(\omega) = \Phi_N. \quad (3.43-3)$$

For the simple-lag case

$$H(i\omega) = \frac{1}{\tau(i\omega) + 1}. \quad (3.43-4)$$

Substitution of Eqs. (3.43-3) and (3.43-4) into Eq. (3.43-2) then yields

$$\Phi_{out}(\omega) = \frac{\Phi_N}{\tau^2 \omega^2 + 1}. \quad (3.43-5)$$

For the quadratic case,

$$H(i\omega) = \frac{1}{\frac{(i\omega)^2}{\omega_{ss}^2} + \frac{2\zeta_{ss}(i\omega)}{\omega_{ss}} + 1}, \quad (3.43-6)$$

$$\Phi_{out}(\omega) = \frac{\Phi_N}{\left(1 - \frac{\omega^2}{\omega_{ss}^2}\right)^2 + \left(\frac{2\zeta_{ss}\omega}{\omega_{ss}}\right)^2}. \quad (3.43-7)$$

#### 3.44. Random-square-wave Generator.

The output of the noise generator previously described has an amplitude probability distribution which is very nearly Gaussian. For studying linear problems the specification of the rms-noise voltage and its power spectrum would be sufficient. As was noted in Sec. 3.1, these two quantities do not, however, define a unique noise signal.

Accordingly, in the study of nonlinear problems the amplitude probability distribution of the noise also must be considered. In order to study the effect of a different amplitude probability distribution, a noise generator was constructed which produced square waves of constant amplitude but with random times for crossing from one polarity to the other. This type of signal was selected because the equipment for producing it could be constructed quite readily and because its amplitude probability distribution consisted merely of two impulses. This distribution is about as different as possible from Gaussian distribution produced by the other noise source.

The random square wave is produced by demodulating the output of the noise generator already described, slicing the signal from the demodulator at a convenient level, and then using this portion of the signal, after suitable amplification, to drive a flip-flop which triggers only on positive-going steps. The output of the flip-flop is then used to drive a high-speed, single-pole, double-throw relay through a cathode follower. With a 400-cps signal applied to the contacts of this relay the output becomes a 400-cps, suppressed-carrier, random square wave. The complete circuit, which includes a crossing-rate meter for monitoring purposes, is shown in Fig. 3.44-1.

The power spectrum of this random square wave is

$$\Phi(\omega) = \frac{kx_N^2}{\pi(\omega^2 + k^2)} = \frac{1}{\pi} \frac{\frac{x_N^2}{k}}{\frac{\omega^2}{k^2} + 1} \quad (3.44-1)$$



where  $k$  equals twice the average zero-crossing rate of the square wave and  $\frac{1}{2}x_N$  equals the amplitude of the square wave. A comparison of Eq. (3.44-1) with Eq. (3.43-5) shows that this power spectrum has the same form as that produced by passing white noise through a simple-lag filter.

### 3.45. Method of Injecting Glint Noise into the Computer.

Glint noise represents an uncertainty in the radar center of gravity of a target and appears as a constant distance at the target, irrespective of the range from which the target is being viewed. Therefore, this type of noise could be added to the computer setup of Fig. 2.2-2 by summing a constant noise signal,  $x_N$ , with the output of the  $x$  integrator just before the  $x$  signal is fed into the  $\alpha$  servo. The  $x$  distance measured to the true center of gravity of the target is still given by the output of the  $x$  integrator, while computations involving  $x$  are carried on using a perturbed value of  $x$ . The method is a direct way of inserting the noise and involves no linearizing assumptions, but requires that the  $\alpha$  servo pass the noise faithfully without limiting. The  $\alpha$ -servo operation actually presented a considerable problem that is discussed at length in Chap. 4.

A second means of inserting noise is to compute  $\alpha$  from the true center-of-gravity information and then add a noise perturbation to the value of  $\alpha$  thus obtained. Since the noise is constant in distance at the target, as an angle it varies as the arc tangent of  $x_N/y$  or approximately inversely with the range. Noise can, therefore, be inserted as an angle by passing a constant noise signal through a divider servo and

summing the output with the unperturbed value of  $\alpha$ . This method of inserting noise is equivalent to making a linearizing assumption on the portion of  $\alpha$  due to noise and not on that portion due to target maneuver. Since the variation in  $\alpha$  due to noise is as important as the other part, little justification exists for linearizing one portion of the computation and not the other.

A third means of inserting the noise employs the same linearizing technique as used in the analytic treatment of Chap. 1. Rather than computing the angle  $\alpha$  as the arc tangent of  $(x+x_N)/y$ ,  $\alpha$  is taken merely as  $(x+x_N)/y$ . This setup requires an accurate divider servo, which operates on a smooth and known signal  $y$  but does not have to transmit the noise  $x_N$ . One of the standard integrator-servo units was setup as a divider for this operation with an additional potentiometer arranged to keep the loop gain of the servo constant. Operating on an 8-to-1 time-scale extension the maximum acceleration required for this divider does not exceed the acceleration capabilities of the servo until the last 100 feet of the trajectory. This method of computation has two distinct advantages over using a servo to calculate the arc tangent of  $(x+x_N)/y$ . First, since only potentiometers are required in the computation, there is no restriction that a radian of shaft motion be a simulated radian. Therefore, a potentiometer output may be used without incurring resolution difficulties. Second, the acceleration demanded of the servo which computes  $(x+x_N)/y$  is much less than that required of a servo computing the arc tan of  $(x+x_N)/y$  because the acceleration needed to follow  $1/y$  is much less than that required

to follow  $(x+x_N)/y$  when the range is relatively small.

The divider servo provided the most accurate means available for injecting the noise signal into the computer. Certain limitations, however, result from the linearization associated with this scheme. For example, this arrangement should not be used in computations involving both long ranges and maneuvering targets since, under these conditions, the change in  $\alpha$  during a run may be large enough to invalidate the approximation that the arc tangent of  $x/y$  equals  $x/y$ . Furthermore, even a good divider servo does not operate satisfactorily over a range greater than approximately 400 to 1. This substitution should be regarded as a temporary measure and not a panacea.

#### 3.46. Method of Monitoring the Noise.

Another problem which arises in studies involving noise is that of monitoring the noise injected into the computer. If an ordinary a-c voltmeter is used for this purpose, several difficulties arise. Since the noise is continuously varying in amplitude, the meter reading fluctuates and, even when using a thermal meter with its inherently slow response, an accurate reading of the rms value of the noise is difficult to obtain. Furthermore, the computer operates with a nominal 50 volts as a reference, but since the accuracy of most of the operations involved in the computer does not depend on this reference being an absolute 50 volts or even bearing a constant ratio to true 50 volts, no attempt has thus far been made to regulate it. Therefore, if an ordinary voltmeter is used to monitor the noise, its reading must be modified by the ratio of 50 volts to the reading obtained on the meter

when it is connected to one of the 50-volt reference points in the computer.

Another possible way to check the rms value of the noise is to record a section of noise and then read a number of values of the noise amplitude taken at equal intervals of time along this record. When these readings are squared, summed, and averaged, the mean-square value of the noise is obtained. The precautions noted in Sec. 4.3 must be observed to insure that the values read from the record are sufficiently uncorrelated and a sufficient number of points must be read to insure reasonable accuracy, as described in Sec. 5.1. Although this method provides a relatively accurate method for obtaining the rms value of the noise, it is time consuming and, hence, not practical as a monitoring procedure.

The method shown in block diagram form in Fig. 3.46-1 was finally developed as an accurate and convenient method of obtaining the rms value of the noise as actually seen by the computer. The noise signal to be monitored is passed through an amplifier and a coefficient potentiometer. It is then fed to two of the inputs of one of the high-speed, high-accuracy electromechanical multipliers,<sup>18</sup> which have recently become standard elements of the D.A.C.L. Computer. In this way the square of the noise signal is obtained at the output of the multiplier. The amplifier and potentiometer are used to adjust the level of the signal so that the multiplier is operated over the middle portion of its useful range. The signal from the multiplier is then passed through a low-pass filter. This operation is equivalent to

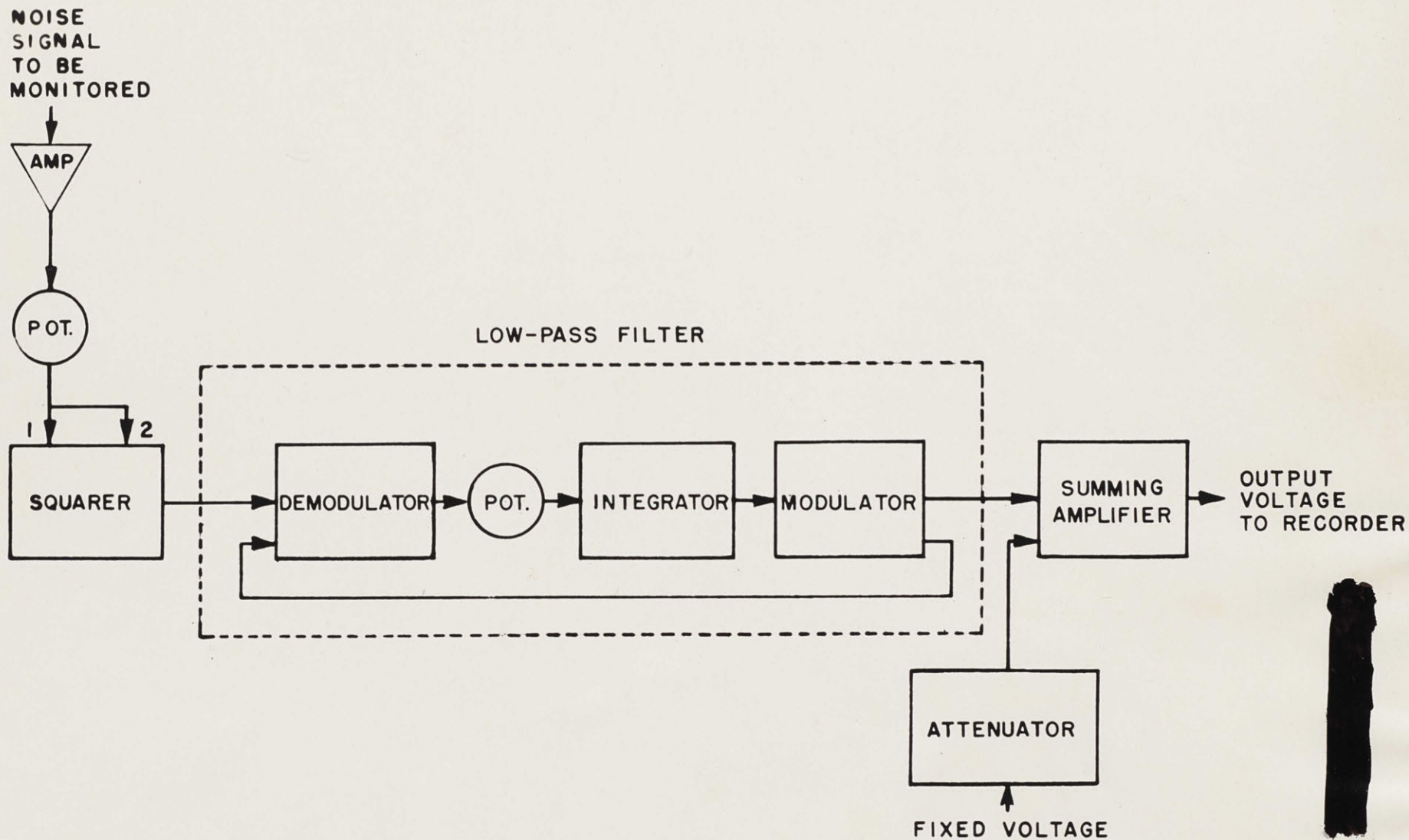


FIG. 3.46-1. NOISE-MONITORING EQUIPMENT.

taking its mean value. Since d-c equipment is used to set up the filter, the signal is first demodulated. It is then passed through a coefficient potentiometer, an integrator, and finally a modulator. An a-c feedback loop is closed around the whole group in such a way that the transfer function from the input to the demodulator to the output of the modulator is

$$F(s) = \frac{1}{\tau s + 1} \quad (3.46-1)$$

where  $\tau$  is the reciprocal of the loop gain of the system. A time constant of the order of 40 to 50 seconds is used. The discrepancy between a computer volt and a standard volt is taken care of automatically by reading the output of the filter on one of the Brush recorders. Improved recording accuracy is achieved by subtracting from the noise-monitor output the desired value of the output and recording merely the difference on a sensitive scale. An over-all calibration constant is obtained by inserting a fixed voltage into the squarer and observing the corresponding output of the filter. The accuracy of the system was checked by determining the rms value of the noise by reading points from a noise record and comparing this result with the average value read from the monitor. The error observed on several trials was less than 3 per cent, a value well within the magnitude of error involved in reading from the recorder the three quantities required to make this check and from calculating the rms value of the noise from a limited number of points (100).

### 3.5. Effect of Using Nonwhite Noise in the Computer.

As this study progressed and the importance of the noise bandwidth employed became more evident, the desirability of investigating the effect of the noise bandwidth on the miss for the case of unlimited missile acceleration became apparent. In order to examine this phenomenon an analytic study was made of the problem of passing white noise, shaped by various filters, through a linear, proportional-navigation system employing in its control equation a filter characterized by a simple time lag, A.

As pointed out in Eq. (1.4-24), the transfer characteristic of such a system, on a distance-to-distance basis, is given by

$$F(s) = 1 - \frac{s^N}{\left(s + \frac{1}{A}\right)^N} \quad (1.4-24)$$

where

$$N = \frac{(b + 1) V_M \cos \beta_0}{V_R} \quad (1.4-18)$$

If white noise with a spectral power density  $\Phi_N$  is passed through a filter with a transfer function  $G(s)$  and the resulting signal is used as the input to the system of Eq. (1.4-24), the rms value of the miss distance can be calculated with the methods outlined in Sec. 4.21. Here, the integral involved assumes the form

$$\overline{x_M^2} = \frac{1}{i} \int_{-i\infty}^{+i\infty} |F(s)|^2 |G(s)|^2 \Phi_N ds. \quad (3.5-1)$$

For the head-on approach with  $(b + 1) = 6$ ,  $V_M = 2000$  ft/sec,  $V_R = 3000$  ft/sec and  $\cos \beta_0 = 1$ , Eq. (1.4-18) gives  $N = 4$ . For the case of a simple-lag filter with a time constant  $\tau$

$$G(s) = \frac{1}{\tau s + 1}$$

and the expression for the mean-square distance becomes

$$\overline{x_M^2} = \frac{\Phi_N}{i} \int_{-i\infty}^{+i\infty} \left| 1 - \frac{s^4}{(s + \frac{1}{A})^4} \right|^2 \left| \frac{1}{\tau s + 1} \right|^2 ds. \quad (3.5-2)$$

When  $u = As$ , Eq. (3.5-2) becomes

$$\overline{x_M^2} = \frac{2\pi\Phi_N}{A} \left( \frac{1}{2\pi i} \int_{-i\infty}^{+i\infty} \left| 1 - \frac{u^4}{(u + 1)^4} \right|^2 \left| \frac{1}{\frac{\tau}{A} + 1} \right|^2 du \right). \quad (3.5-3)$$

The integral of Eq. (3.5-3) may be evaluated with use of the tables given in Appendix C. The details are somewhat lengthy but the final result is

$$\overline{x_M^2} = \frac{\pi\Phi_N}{16A} \left[ \frac{16\left(\frac{\tau}{A}\right)^3 + 69\left(\frac{\tau}{A}\right)^2 + 116\left(\frac{\tau}{A}\right) + 93}{\left(\frac{\tau}{A}\right)^4 + 4\left(\frac{\tau}{A}\right)^3 + 6\left(\frac{\tau}{A}\right)^2 + 4\left(\frac{\tau}{A}\right) + 1} \right]. \quad (3.5-4)$$

Equation (3.5-4) may be nondimensionalized by computing  $A \overline{x_M^2} / \Phi_N$  rather than merely  $\overline{x_M^2}$ . The factor,  $\eta$ , may then be added to normalize the resulting expression in such a way as to make  $A \eta \overline{x_M^2} / \Phi_N$  equal 1, in the case where the noise is passed through a filter of infinite bandwidth, i.e.,  $\tau = 0$ . For this case, the noise at the input to the  $F(s)$  system is white. Thus for  $\tau = 0$

$$\frac{A \overline{\eta x_M^2}}{\Phi_N} = \frac{93\pi\eta}{16} = 1,$$

from which

$$\eta = 0.054763 \quad \text{or} \quad \pi\eta = 0.172043.$$

The final expression then becomes

$$\frac{\eta A \overline{x_M^2}}{\Phi_N} = 0.172043 \left[ \frac{\left(\frac{\gamma}{A}\right)^3 + 4.3125 \left(\frac{\gamma}{A}\right)^2 + 7.25 \left(\frac{\gamma}{A}\right) + 5.8125}{\left(\frac{\gamma}{A}\right)^4 + 4 \left(\frac{\gamma}{A}\right)^3 + 6 \left(\frac{\gamma}{A}\right)^2 + 4 \left(\frac{\gamma}{A}\right) + 1} \right]. \quad (3.5-5)$$

The results of Eq. (3.5-5) are plotted in Fig. 3.5-1. Values of miss can be determined from this curve as

$$\overline{x_M^2} = \frac{\Phi_N}{(0.172043 A)} \left( \frac{\eta A \overline{x_M^2}}{\Phi_N} \right) \quad (3.5-6)$$

where  $\Phi_N$  is given in  $\text{ft}^2/\text{rad}/\text{sec}$  and  $A$  is the time constant in seconds of the missile control system.

These same calculations were made for the case where white noise is passed through a quadratic filter characterized by the constants  $\omega_{ss}$  and  $\zeta_{ss}$ . In this case

$$\overline{x_M^2} = \frac{\Phi_N}{i} \int_{-i\infty}^{+i\infty} \left| 1 - \frac{s^4}{\left(s + \frac{1}{A}\right)^4} \right|^2 \left| \frac{1}{\frac{s^2}{\omega_{ss}^2} + \frac{2\zeta_{ss}s}{\omega_{ss}} + 1} \right|^2 ds. \quad (3.5-7)$$

With

$$u = As \quad \text{and} \quad v = \frac{1}{A\omega_{ss}}$$

$\eta A x_M^2 / \Phi_N$

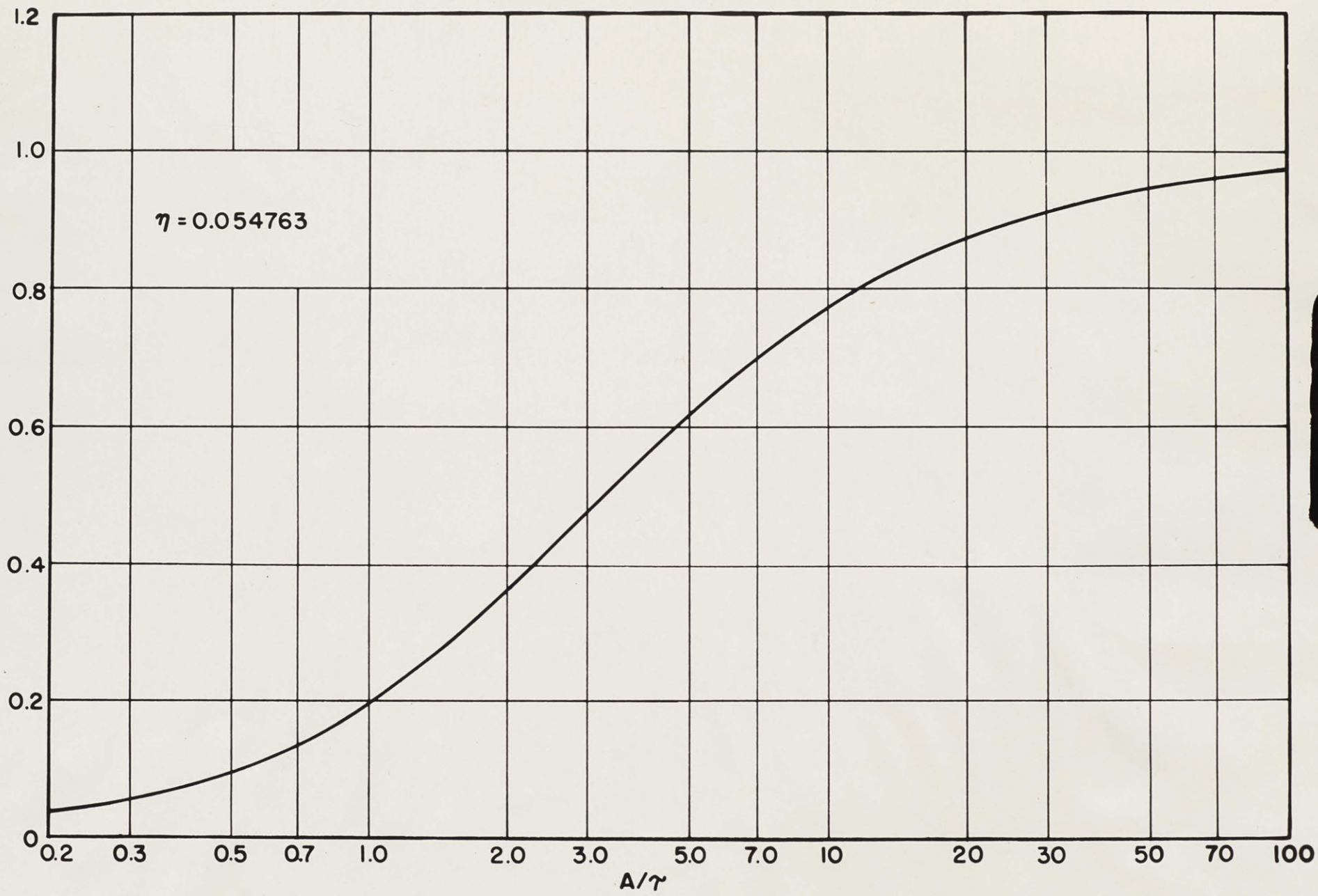


FIG. 3.5-1. SIMPLE-LAG-NOISE - BANDWIDTH EFFECT ON MISS FOR A MISSILE WITH A SIMPLE-LAG CONTROL SYSTEM.

this becomes

$$\overline{x_M^2} = \frac{2\pi\Phi_N}{A} \frac{1}{2\pi i} \int_{-i\infty}^{+i\infty} \left| 1 - \frac{u^4}{(u+1)^4} \right|^2 \left| \frac{1}{v^2 u^2 + 2\zeta_{ss} v u + 1} \right|^2 du. \quad (3.5-8)$$

The result obtained when this equation is evaluated, nondimensionalized, and normalized, as for the simple-lag case, is

$$\frac{\eta A x_M^2}{\Phi_N} = \frac{0.172043}{16\zeta_{ss}} \frac{\left[ \begin{aligned} &8v^7 + 64\zeta_{ss} v^6 + (192\zeta_{ss}^2 + 32)v^5 + (256\zeta_{ss}^3 + 193\zeta_{ss})v^4 \\ &+ (128\zeta_{ss}^4 + 456\zeta_{ss}^2 + 32)v^3 + (276\zeta_{ss}^3 + 326\zeta_{ss})v^2 \\ &+ (232\zeta_{ss}^2 + 128)v + 93\zeta_{ss} \end{aligned} \right]}{\left[ \begin{aligned} &v^8 + 8\zeta_{ss} v^7 + (24\zeta_{ss}^2 + 4)v^6 + (32\zeta_{ss}^3 + 24\zeta_{ss})v^5 \\ &+ (16\zeta_{ss}^4 + 48\zeta_{ss}^2 + 6)v^4 + (32\zeta_{ss}^3 + 24\zeta_{ss})v^3 \\ &+ (24\zeta_{ss}^2 + 4)v^2 + 8\zeta_{ss} v + 1 \end{aligned} \right]} \quad (3.5-9)$$

which is plotted in Fig. 3.5-2.

A discrepancy of a few per cent may be observed, if the miss computed from Eq. (3.5-5) or (3.5-9) for the case of white noise ( $v = 0$ ) is compared with the value computed from Eq. (1.4-27). This difference results from the approximation involved in the evaluation of the integral in Eq. (1.4-26).

$\eta \overline{A^2}_M / \Phi_N$

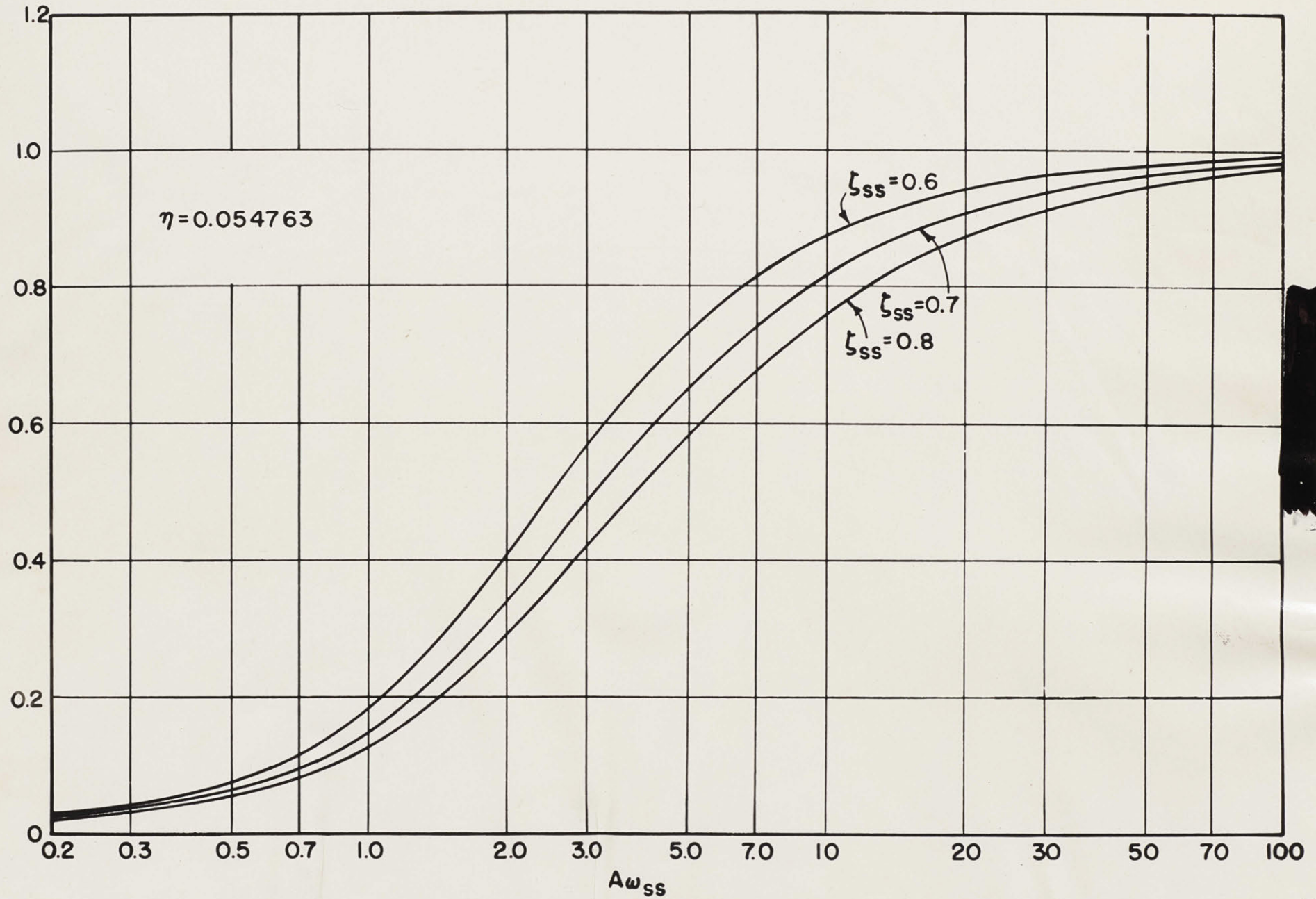


FIG. 3.5-2. QUADRATIC-NOISE-BANDWIDTH EFFECT ON MISS FOR A MISSILE WITH A SIMPLE-LAG CONTROL SYSTEM.

[REDACTED]

## CHAPTER 4

### ANALYSIS OF COMPUTER OPERATION FOR PROPORTIONAL-NAVIGATION

#### PROBLEMS INVOLVING NOISE

##### 4.1. Introduction.

Even after the computer has been set up to solve with a reasonably high degree of accuracy the noise-free, simple-lag, proportional-navigation problem, the addition of noise to the problem imposes numerous further demands that may completely invalidate the solutions.

A brief examination of the ability of the various computer components to handle random noise signals may determine whether the presence of these noise signals introduces additional sources of computing error. Consideration of the number of solutions required to achieve a prescribed accuracy in the rms miss, because of the statistical nature of the noise problem, will be delayed until Chap. 5.

For the purely electronic components in the computer the presence of the relatively broadband signals representing the noise should cause no trouble. The bandwidths of these components, such as repeater amplifiers, resolvers, coefficient potentiometers, modulators, and limiter amplifiers, are in all cases broad enough to pass the noise signals. Furthermore, as the frequency of the signal fed into these units is increased, the amplitude may be held constant without fear of overloading.

For the electromechanical units broadband signals do present a problem because the finite velocity and acceleration capabilities of the electromechanical transducers employed cause the units to become

[REDACTED]

nonlinear for high-amplitude, high-frequency signals. The two types of units falling into this class are the high-speed multipliers and the electromechanical servos. Since the multipliers have very high acceleration capabilities, they are able to handle full-scale signals up to frequencies considerably above those of interest in the noise employed in this study. Furthermore, the only multiplier used appears in the noise-monitoring channel where a favorable signal level can easily be selected. Experimental checks have indicated no serious troubles with the unit.

For the integrator servos the situation differs substantially because of the limited acceleration capabilities of the motors employed. Although these units are used both as integrators and as position servos, the presence of noise places the most severe requirements on the particular unit designated in Chap. 2 as the  $\alpha$  servo. Attention will therefore be directed toward an analysis of this particular unit when handling noise signals.

#### 4.2. Analysis of $\alpha$ -servo Operation.

##### 4.21. Basis of Analysis.

The function of the  $\alpha$  servo is to convert range information, given as  $x$  and  $y$  in rectangular coordinates, to polar coordinates involving the angle  $\alpha$  and the range. For the calculations involved in the present problem, since the angle is actually the only component of interest, the  $\alpha$  servo could be any device capable of computing the arc tangent

of  $x/y$ . This computation involves determining the components of the vectors  $x$  and  $y$  in a system of coordinates which has been rotated through an angle  $\alpha$  from the reference system as shown in Fig. 4.21-1. The difference between the projections of the  $x$  and  $y$  vectors on the

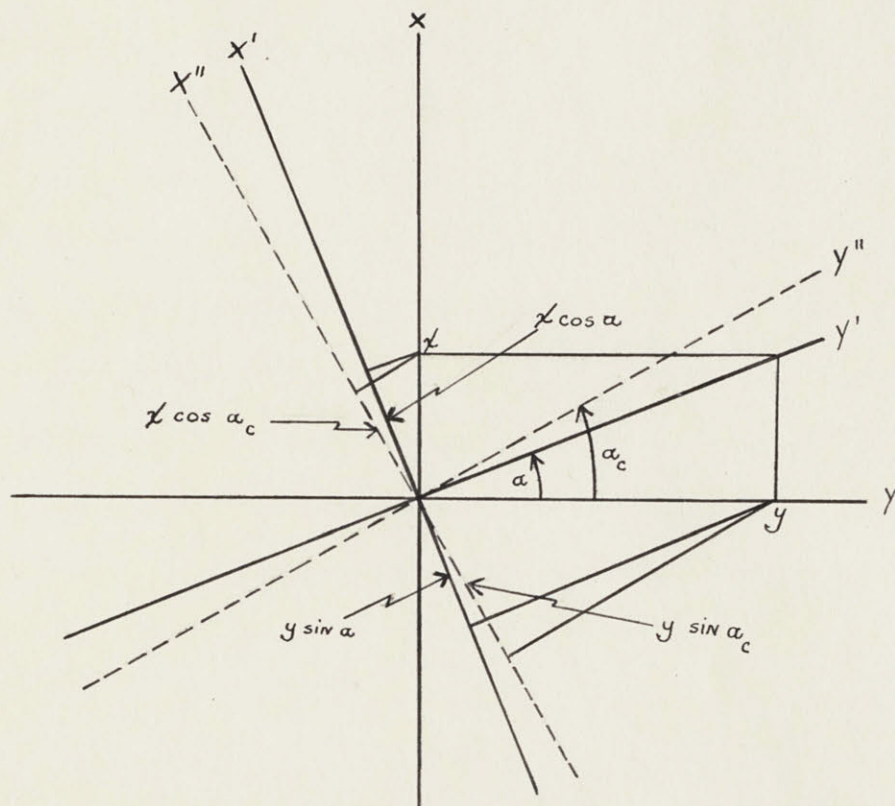


Fig. 4.21-1. Coordinate system of the  $\alpha$  servo.

$x'$  axis may then be used as the error signal to drive a position servo. This error signal may be obtained by mounting a resolver on the output shaft of a position servo and using the quantities  $x$  and  $y$  as inputs to the resolver. One output of this resolver is then  $(-x \cos \alpha_c + y \sin \alpha_c)$ , where  $\alpha_c$  is the angle through which the output shaft has actually been

turned. As shown in Fig. 4.21-1, if  $\alpha_c$  is larger than  $\alpha$ , the component  $x \cos \alpha_c$  becomes smaller than  $y \sin \alpha_c$  so that a positive error signal is developed. This signal then drives the servo in such a direction as to reduce the angle  $\alpha_c$ . On the other hand, if  $\alpha_c$  is smaller than  $\alpha$ , a negative error is developed and  $\alpha_c$  is increased. In this way, ideally at least, the error signal is reduced to zero and the output shaft assumes the correct angle  $\alpha$ . A voltage proportional to  $\alpha$  may be obtained from a potentiometer or, if the angle is always small, from a resolver mounted on the shaft which carries the first resolver. The second output from the first resolver is  $(x \sin \alpha + y \cos \alpha)$ , the magnitude of the range vector. One of the standard D.A.C.L. integrator units<sup>7</sup> was used for this arc-tangent computation by using the error signal  $(-x \cos \alpha_c + y \sin \alpha_c)$  to close a position loop around it. A greatly simplified diagram of this arc-tangent solver is given in Fig. 4.21-2.

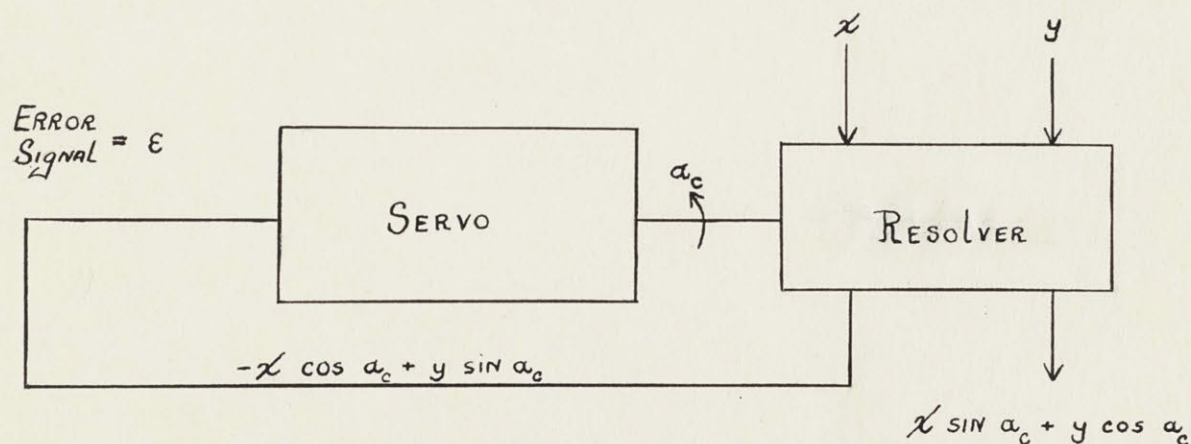


Fig. 4.21-2. Simplified diagram of arc-tangent solver.

To obtain correct results from the computer it is essential that the servo provide an accurate solution for  $\alpha$ . The methods employed in

the analysis of the operation of the  $\alpha$  servo must therefore indicate the magnitude of the errors involved for the class of signals handled as well as indicate the limits of linear servo operation.

The analysis of the system of Fig. 4.21-2 can be greatly simplified in the case where the angle  $\alpha_c$  is always very small. Here the expression for the error signal,  $\epsilon$ , can be reduced to the form

$$\epsilon = x - y\alpha_c.$$

If, in addition,  $y$  is then held constant, the quantity  $x$  may be considered as the input to a servo in which  $-K_1\alpha_c$  is the feedback signal. This servo then assumes the more usual form shown in Fig. 4.21-3.

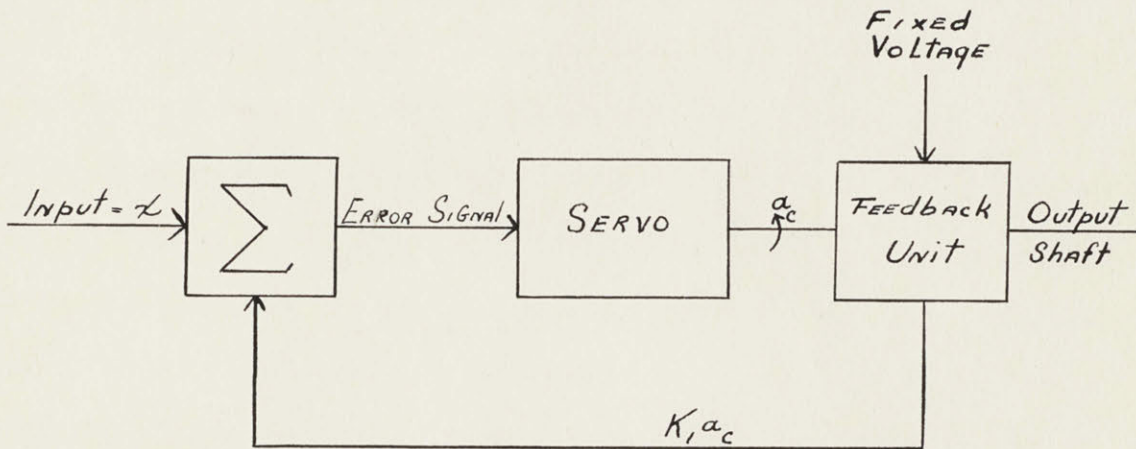


Fig. 4.21-3. Representation of Fig. 4.21-2, valid when  $\alpha_c$  is small and  $y$  is constant.

By the usual methods of servo analysis the output angle  $\alpha_c$  could be computed for a step-function input signal and for sinusoidal inputs of various frequencies. For the step input the rise time and overshoot characteristics of the output are examined, while for the sinusoidal

input the amplitude and phase characteristics of the output are studied for various input-signal frequencies. Although much valuable data can be obtained from such analyses they are subject to several serious deficiencies. First, the input signals which the servo must handle in actual operation are neither widely separated steps nor sinusoids. Second, the effects of limiting in the system are not considered. The usual analytic treatments describe a servo as a linear, constant-coefficient transfer function. Since actual systems, on the other hand, are linear over only a very limited range of operation, the results obtained from a purely linear analysis may be considerably in error. In experimentally checking the step response and even the sinusoidal response of a servo, great care must be taken to confine the operation to the linear region if the results obtained are to agree with the calculations. This means that, in practice, the step-input signals employed must be only a small fraction of full scale. In testing the D.A.C.L. integrator servos it has been virtually impossible to find a step-input amplitude which gives meaningful results. Since these units employ a d-c compensation section, output drift must also be considered. The output resulting from a small input signal is overshadowed by drift, whereas a signal large enough to override the effects of drift causes saturation. In testing with sinusoidal signals the amplitude of the input must be decreased as its frequency is increased. Frequencies are soon reached where the allowable shaft motion of the servo is so small that poor resolution in the transducer used to convert shaft motion to electrical signal sets a new limit on the accuracy

obtained.

Even after the response characteristics have been obtained (either analytically or experimentally), a problem remains in deciding on the response which gives the best possible servo. A. C. Hall<sup>19</sup> introduced the idea of using and minimizing the integral-squared error resulting from a step input as a criterion of goodness to obtain the best servo. A deficiency still exists, however, since even after the step or sinusoidal response of the servo is obtained, this information does not permit prediction of the operation of the servo when more complicated input signals are introduced.

The study of other systems, such as filters and amplifiers, had also been restricted principally to analyses employing sinusoids and step functions. In order to extend system analyses to more general input functions Wiener<sup>10, 20</sup> introduced the idea of describing a random signal by a power spectrum. He further showed that the power spectrum used in communication engineering and autocorrelation function used in statistics are Fourier transforms of each other. Wiener,<sup>21</sup> Y. W. Lee<sup>22</sup> and others applied these ideas to the design of optimum (on an rms basis) linear filters and predictors. These ideas have also been employed to a limited extent in the study of more general linear problems in the field of fire-control systems<sup>23</sup> and guided-missile control systems.<sup>5</sup> The applications of such analyses are, however, severely restricted by the nonlinearities which are unavoidably present in all physical systems. In practical servos, limits on the position, velocity, or acceleration of the output may become very important and lead

██████████

to results that are considerably different from those predicted by the linear theory. G. C. Newton,<sup>24</sup> in his doctoral thesis, extended the linear analysis still further by considering the problem of optimizing a linear system which has constraints imposed on the rms output or the rms derivatives of the output. His analysis provides a basis on which to handle nonlinearities but makes no attempt to correlate the mathematical value of the constraint imposed and the maximum value of the quantity actually available. In the absence of any purely mathematical approach to the nonlinear problem the determination of the correlation between the value of the constraint to be used in an analysis such as Newton proposed and the maximum value actually available must be experimental. The remainder of this chapter is concerned with an evaluation of this correlation for a particular servo system (the  $\alpha$  servo) in which the output-shaft acceleration is limited. Once the correlation factors have been evaluated for the cases of practical interest, a complete method of analysis will be available which overcomes to a large degree the deficiencies of the usual approaches to the problem of servo design and analysis.

For this extended analysis the input signal is defined only statistically and its power spectrum rather than its amplitude-versus-time relation is specified. The limitation is not serious because ordinarily the input signals met in practice can be defined only in such statistical terms as their power spectra, rms amplitude, and amplitude probability distributions. As in the usual analyses, considerable insight into the operation of a servo can be obtained by calculating such

██████████

quantities as the error signal, the output, and derivatives of the output. Here, because of the generality of the input signal employed, it is not possible to calculate the error or the output as a function of time but it is possible to obtain the rms values of these quantities and from these to obtain some very definite measures of the performance of the servo for the class of signals being considered.

The basic expression to be used relates the power spectra appearing at the input and at the output of a linear system. If the system function is specified as  $H(i\omega)$ , the power spectra of the input  $\Phi_{in}(\omega)$  and of the output  $\Phi_{out}(\omega)$  are related by the expression\*

$$\Phi_{out}(\omega) = |H(i\omega)|^2 \Phi_{in}(\omega). \quad (4.21-1)$$

However,\*\*

$$\overline{E_{out}^2} = \int_{-\infty}^{+\infty} \Phi_{out}(\omega) d\omega, \quad (4.21-2)$$

so

$$\overline{E_{out}^2} = \int_{-\infty}^{+\infty} |H(i\omega)|^2 \Phi_{in}(\omega) d\omega. \quad (4.21-3)$$

Substitution of  $s$  for  $i\omega$  and extraction of the square root of the resulting expression, give the rms output voltage as

\* Expression 4.21-1 can be developed either by using the autocorrelation functions of the input and output signals or by considering a Fourier series representation of the input and output signals.

\*\* The bar over  $E_{out}^2$  denotes that the mean value of  $E_{out}^2$  is to be considered.

$$E_{\text{out}} = \left[ \frac{1}{i} \int_{-i\infty}^{+i\infty} |H(s)|^2 \Phi_{\text{in}}\left(\frac{s}{i}\right) ds \right]^{1/2}. \quad (4.21-4)$$

A proper choice of the function  $H(s)$  allows assignment of various meanings to the quantity  $E_{\text{out}}$ . For example,  $E_{\text{out}}$  may be the error signal, the output voltage or shaft motion or the velocity or acceleration of the output shaft motion.

#### 4.22. Rms Error and Acceleration Calculations for the $\alpha$ Servo.

In the class of problems for which the  $\alpha$  servo is here being used, the input signal  $x$  of Fig. 4.21-3 consists of two parts. The first is a slowly varying signal which remains small until the very end of the problem if the missile accurately follows the target. The second portion of the input signal is the noise which, as was pointed out in Chap. 3, appears to have a constant value,  $x_N$ , in distance and may extend over a frequency range of 100 rad/sec or more. During the terminal portion of the flight the variations in the angle  $\alpha$  caused by the constant,  $x_N$ , may reach considerable amplitudes. The  $\alpha$  servo is able to follow adequately the first type of input signal, if it occurs alone, but has considerably more difficulty with signals of the second class. A simple example of the kind of difficulty encountered arises in the following situation. An input consisting of a single low-frequency sinusoid, which the servo is capable of following faithfully, is first applied. Next the input is made a high-frequency sinusoid. The second signal causes limiting within the servo but produces negligible output.

If the two signals are next applied simultaneously, it should not be assumed that the low-frequency signal will be transmitted with exactitude. The system is now being driven beyond the limits of linearity and the principle of superposition no longer applies. This illustration points out a serious deficiency of servo analyses using single sinusoidal input signals.

Since the difficult portion of the  $\alpha$ -servo input signal is the noise component, the servo should be analyzed on the basis of such an input. As stated in Chap. 3, the noise signal most generally employed in this study is obtained by passing white noise through a quadratic filter characterized by a natural frequency  $\omega_{ss}$  and a damping  $\zeta_{ss}$ . When Eq. (4.21-1) is applied the power spectrum of the filtered noise becomes

$$\Phi_{\text{out}}(\omega) = \left| \frac{1}{s^2 + \frac{2\zeta_{ss}s}{\omega_{ss}} + 1} \right|^2 \Phi_N(\omega) \quad (4.22-1)$$

where  $\Phi_N(\omega)$  is a constant.

Fuchs<sup>7,\*</sup> found that over the range of linear operation the transfer function of the integrator servo could be described fairly accurately as

$$H(s) = \frac{K}{s(\tau_1 s + 1)} \quad (4.22-2)$$

where the factor  $K$  can be selected so that the output is given in terms of either the output-shaft position or a voltage proportional to the output-shaft position.

\* Fuchs, op. cit., p. 90

Figure 4.22-1 shows the over-all system with a position loop closed around the integrator servo.

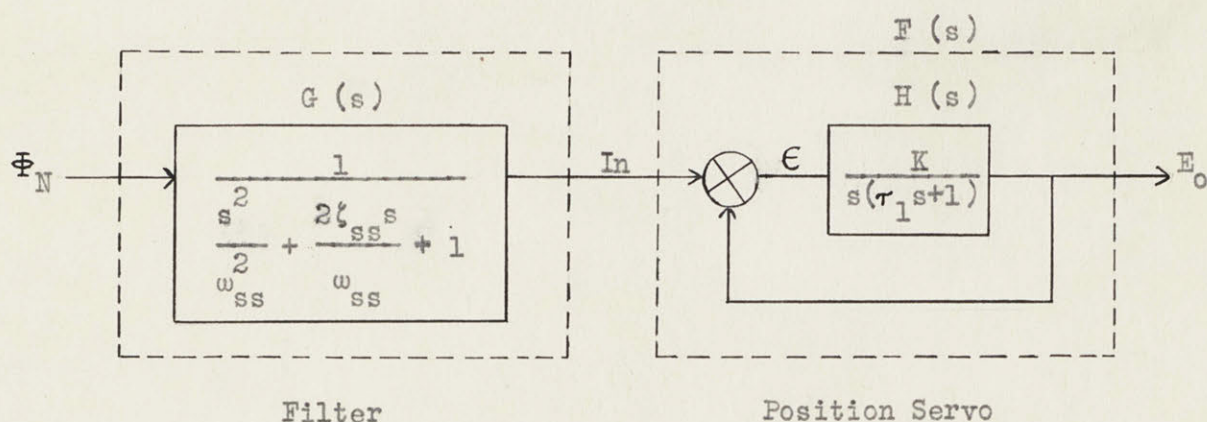


Fig. 4.22-1. Representation of input signal and servo system studied analytically.

The transfer characteristic of the resulting position servo, from its input to its output, then becomes

$$F(s) = \frac{1}{\frac{\tau_1 s^2}{K} + \frac{s}{K} + 1} \quad (4.22-3)$$

where  $K$  must now have dimensions which give the output as a voltage measured on the same level as the input signal.

For the system of Fig. 4.22-1 there are two transfer functions in cascade between the white-noise input, characterized by the constant  $\Phi_N$  and the output. The mean-square output is then given as

$$\overline{E_o^2} = \frac{1}{i} \int_{-i\infty}^{+i\infty} |G(s)|^2 |F(s)|^2 \Phi_N ds. \quad (4.22-4)$$

The corresponding expression for the error voltage developed at the

input to the forward gain section,  $H(s)$ , of the servo is then

$$\overline{\epsilon^2} = \frac{1}{i} \int_{-i\infty}^{+i\infty} \left| G(s) \right|^2 \left| F(s) \right|^2 \left| \frac{1}{H(s)} \right|^2 \Phi_N ds. \quad (4.22-5)$$

When the expressions for  $G(s)$ ,  $F(s)$ , and  $\frac{1}{H(s)}$  are inserted in Eq. (4.22-5) the expression for the error becomes:

$$\overline{\epsilon^2} = (2\pi\Phi_N) \frac{1}{2\pi i} \int_{-i\infty}^{+i\infty} \left| \frac{1}{s^2 + \frac{2\zeta_{ss}s}{\omega_{ss}} + 1} \right|^2 \left| \frac{s(\tau_1 s + 1)}{K \left( \frac{\tau_1 s^2}{K} + \frac{s}{K} + 1 \right)} \right|^2 ds. \quad (4.22-6)$$

Integrals of the type appearing in Eq. (4.22-6) may be evaluated using the tables given by James, Nichols, and Phillips.<sup>23\*</sup> Under the direction of R. C. Booton of the D.A.C.L., the work of Phillips has been extended and the notation somewhat changed. The resulting set of tables is presented here as Appendix C.

With  $\epsilon_1 = 2\zeta_{ss}/\omega_{ss}$  and  $\epsilon_2 = 1/\omega_{ss}^2$  and the use of the expression for  $I_4$  given in Appendix C, the mean-square error, after some simplification, becomes

$$\overline{\epsilon^2} = \frac{\pi\Phi_N}{K^2} \left\{ \frac{K\epsilon_1\tau_1^2 + \tau_1^2 + \epsilon_2 + \epsilon_1\tau_1}{\frac{1}{K^2} (\epsilon_1^2\tau_1 + \epsilon_1\tau_1^2 + \epsilon_1\epsilon_2) + \frac{1}{K} (\epsilon_1^3\tau_1 + \epsilon_1^2\epsilon_2 - 2\epsilon_1\epsilon_2\tau_1) + \epsilon_1\epsilon_2^2} \right\} \quad (4.22-7)$$

The effect of the gain of the system on the error may be conveniently expressed by normalizing the preceding expression in terms of the

\* James, Nichols, and Phillips, op. cit., pp. 369-370.

signal appearing at the input to the servo. This will be denoted as  $\epsilon_0$  since it is the same as the error signal obtained if  $K$  is made zero. From Eq. (4.22-7)  $\epsilon_0$  is obtained as

$$\epsilon_0 = \frac{\pi \Phi_N}{\xi_1} \quad (4.22-8)$$

A normalized expression for error is then given by

$$\frac{\epsilon}{\epsilon_0} = \frac{1}{K} \left[ \frac{K \xi_1 \tau_1^2 + \tau_1^2 + \xi_2 + \xi_1 \tau_1}{\frac{1}{K^2} (\tau_1^2 + \xi_2 + \xi_1 \tau_1) + \frac{1}{K} (\xi_1^2 \tau_1 + \xi_1 \xi_2 - 2 \xi_2 \tau_1) + \xi_2^2} \right]^{1/2} \quad (4.22-9)$$

Figure 4.22-2 shows the normalized error plotted as a function of the gain  $K$  for noise-filter bandwidths of 1, 2.5, 5, 10, 20, and 40 rad/sec. The delay  $\tau_1$  associated with the integrator servo was taken as 0.0016 sec. This value is slightly larger than that found by Fuchs<sup>7,\*</sup> but was obtained for a servo with somewhat different compensation than he used.

Equation (4.22-9) was derived purely on the basis of linear theory, whereas signals of the class now being considered are very apt to drive the servomotor into the region of acceleration limiting. Therefore, as a next step in the analysis, the acceleration required at the output of the  $\alpha$  servo was calculated. Since the acceleration is the second derivative of the output-shaft position, the expression for the mean-square acceleration is given as

$$\overline{a^2} = \frac{1}{i} \int_{-i\infty}^{+i\infty} |s^2 F(s)|^2 |G(s)|^2 \Phi_N ds. \quad (4.22-10)$$

\* Fuchs, op. cit., pp. 125, 126.

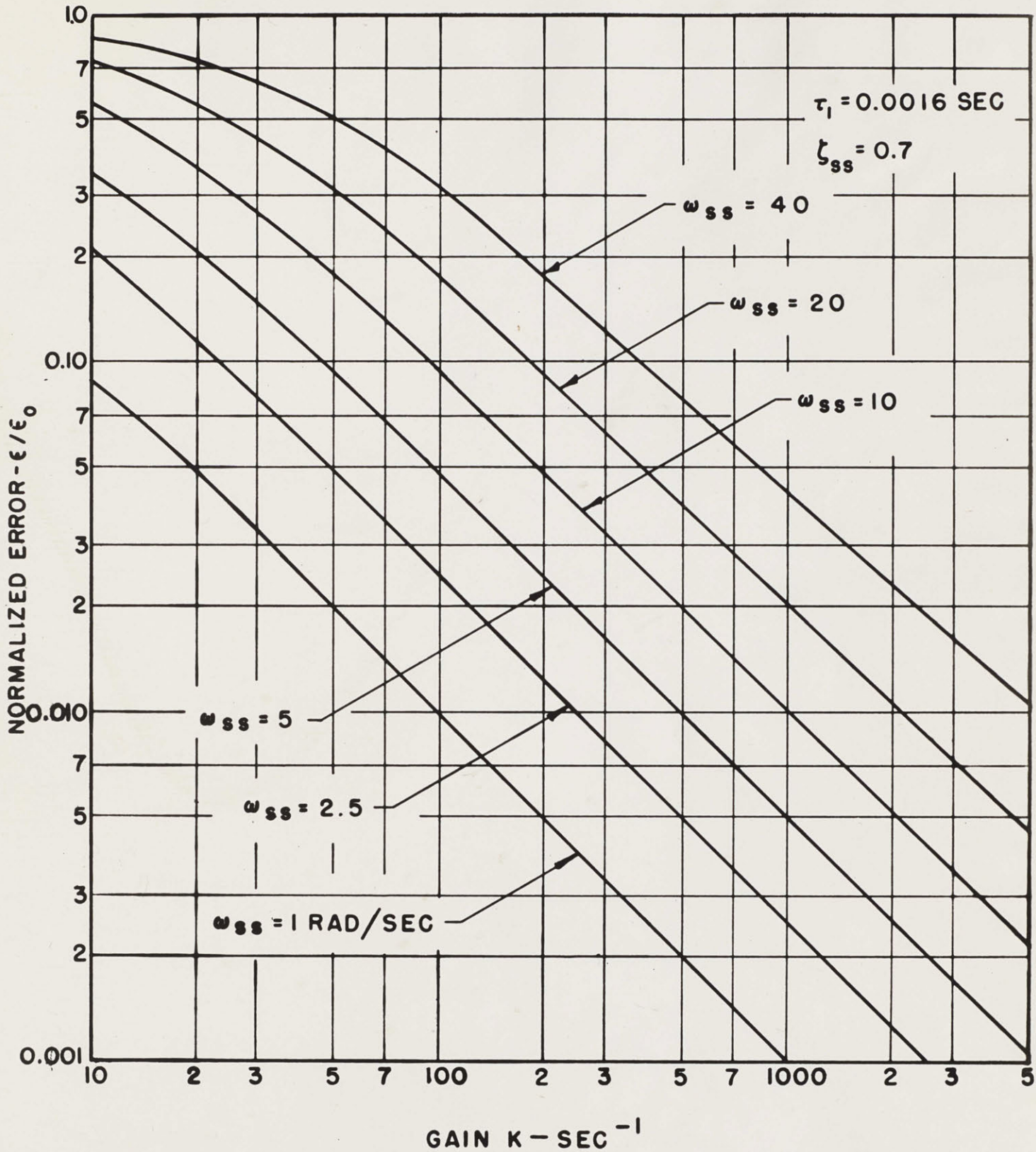


FIG. 4.22-2. NORMALIZED ERROR FOR POSITION SERVO FOLLOWING QUADRATIC NOISE.

With substitution of the foregoing expressions for  $F(s)$  and  $G(s)$  Eq. (4.22-10) becomes

$$\overline{a^2} = 2\pi\Phi_N \frac{1}{2\pi i} \int_{-i\infty}^{+i\infty} \left| \frac{s^2}{\frac{\tau_1 s^2}{K} + \frac{s}{K} + 1} \right|^2 \left| \frac{1}{\frac{s^2}{\omega_{ss}^2} + \frac{2\zeta_{ss}s}{\omega_{ss}} + 1} \right|^2 ds. \quad (4.22-11)$$

After evaluation of this integral the expression for the mean-square acceleration divided by the noise power density  $\Phi_N$  becomes

$$\frac{\overline{a^2}}{\Phi_N} = \frac{\pi \left[ \omega_{ss}^5 K^2 + 2\zeta_{ss} \omega_{ss}^4 K^3 \right]}{2\zeta_{ss} \left[ \tau_1^2 \omega_{ss}^4 + 2\zeta_{ss} \tau_1 \omega_{ss}^3 + (4\zeta_{ss}^2 \tau_1 K - 2\tau_1 K + 1) \omega_{ss}^2 + 2\zeta_{ss} K \omega_{ss} + K^2 \right]}. \quad (4.22-12)$$

The square root of Eq. (4.22-12) is plotted as a function of the gain  $K$  in Fig. 4.22-3.

An inspection of Figs. 4.22-2 and 4.22-3 shows that the gain of the servo should be made large if the error is to be kept small but that as the gain is increased the rms acceleration required at the output shaft of the servo increases rapidly, with the result that the operation soon becomes nonlinear. To determine what gain gives the minimum error for such a system, a servo was set up and investigated experimentally under the conditions which would occur in problem operation if the  $y$  input were fixed.

As noted in Appendix B, a range of plug-in gearboxes is available for use with the standard D.A.C.L. integrator units. These boxes provide speed reductions from the motor-tachometer shaft to the output units with a range from a minimum of 15 to 1 to a maximum of 3840 to 1.

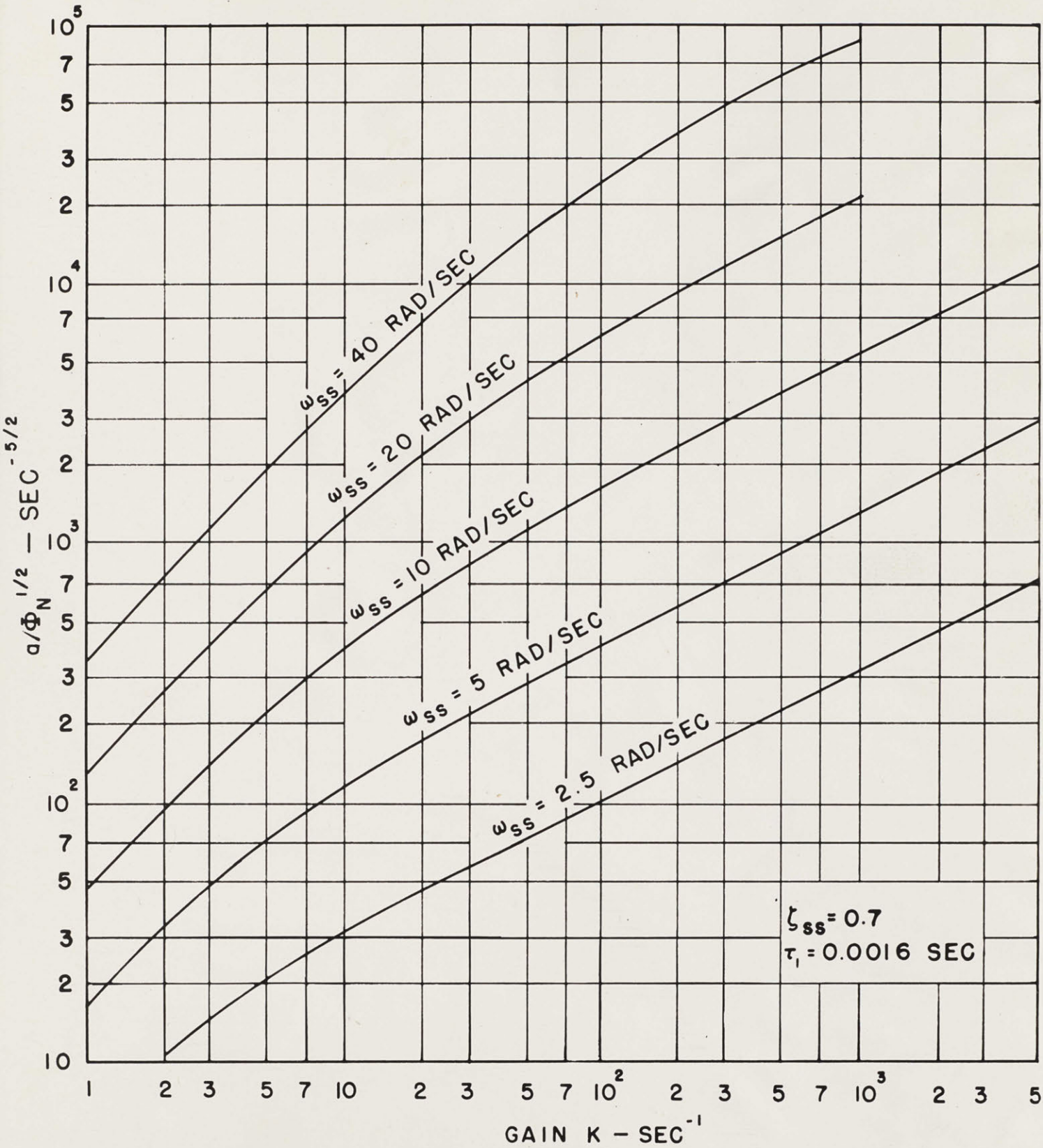


FIG. 4.22-3.  $a/\Phi_N^{1/2}$  VERSUS  $K$ , FOR SERVO FOLLOWING QUADRATIC NOISE.

Since one of the primary interests in this application is to obtain the maximum available acceleration at the output shaft, the 15-to-1 gearing was selected.

The servomotors provide a maximum acceleration of  $4000 \text{ rad/sec}^2$  at their shaft. Nevertheless, measurements indicated that for the smaller gear ratios this acceleration is significantly reduced. With the 15-to-1 gearing, limiting began at  $2000 \text{ rad/sec}^2$  at the motor shaft or  $2000/15 \text{ rad/sec}^2$  at the output shaft, and the maximum available acceleration was approximately 30 per cent above this value. A smaller gear ratio, even if available, would not increase the available acceleration since the loading reflected to the motor shaft then reduces the acceleration faster than it is increased by the gear reduction.

Figure 4.22-4 shows the particular arrangement of the servo which was studied. Mention should be made that  $x$  and  $y$  in both Fig. 4.22-4

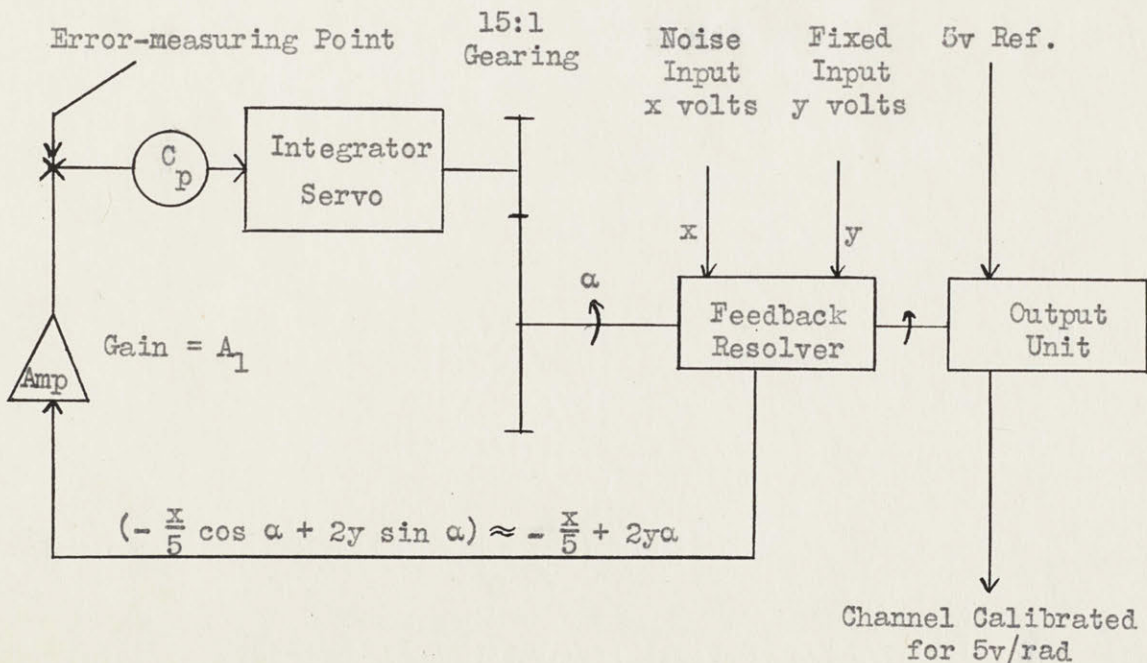


Fig. 4.22-4. Arrangement of  $\alpha$  servo studied experimentally.

and Eq. (4.22-13) through (4.22-16) are in volts. The detail is important because the scale factors (conversion factor from feet to volts) used for  $x$  and  $y$  are different.

In the circuit, the resolver used on the output shaft replaces the summing circuit appearing at the input to a conventional position servo employing a potentiometer feedback element. With the particular gains employed in the input and output channels of the resolver the error signal used to drive the servo becomes

$$\epsilon = -\frac{x}{5} \cos \alpha + 2y \sin \alpha \text{ volts} \quad (4.22-13)$$

where  $x$  and  $y$  are the signals fed into the two resolver input channels, expressed in volts and  $\alpha$  is the angle through which the output shaft is turned. Since the operation is to be restricted to only a few degrees, the usual small-angle approximation may be made and gives

$$\epsilon = -\frac{x}{5} + 2y \alpha. \quad (4.22-14)$$

Use of Eq. (4.22-14) reveals that the system of Fig. 4.22-4 may be reduced to the more familiar form of Fig. 4.22-5.

For convenience of calculation all input quantities will be referred to the input of the summing circuit.

The loop gain of this servo is

$$\begin{aligned} K &= C_p \left( \frac{300 \text{ rad/sec}}{5 \text{ v}} \right) \left( \frac{1}{15} \right) (2y \text{ v/rad}) A_1 \\ &= 8y A_1 C_p \text{ sec}^{-1}, \end{aligned} \quad (4.22-15)$$

where the tachometer feedback constant of the integrator is adjusted to produce a velocity at the servomotor shaft of 300 rad/sec for an input

signal of 5 volts.

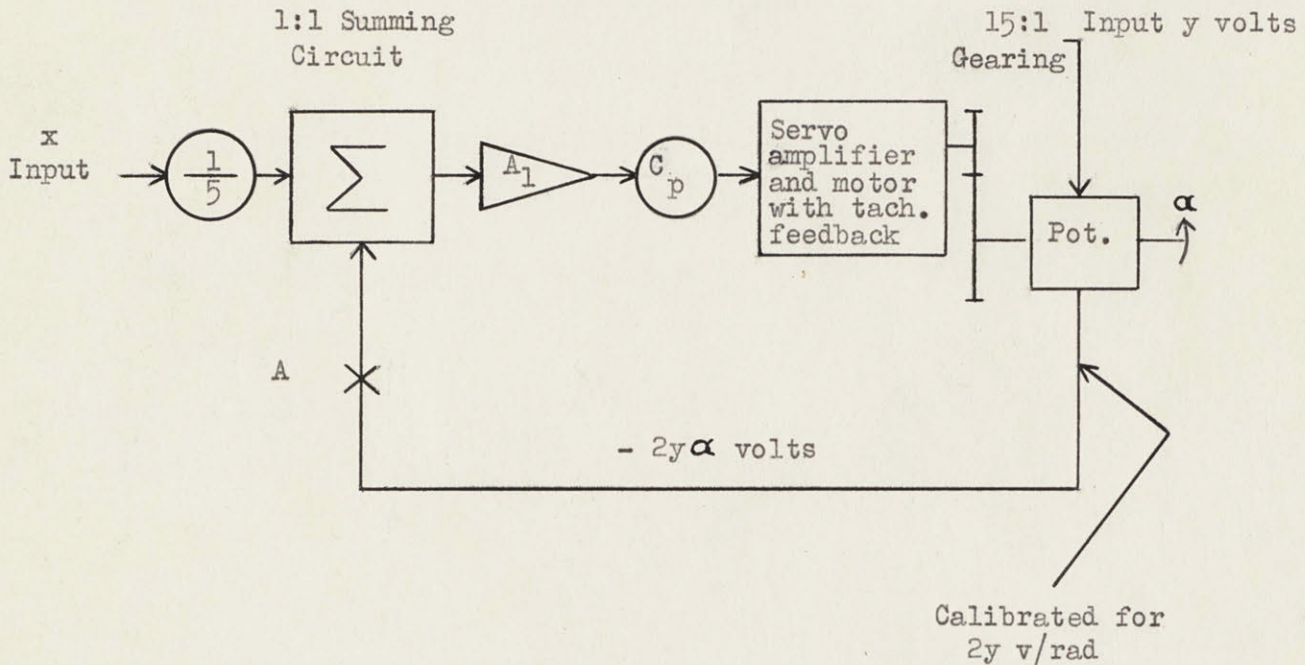


Fig. 4.22-5. Equivalent form of Fig. 4.22-4 for small-angle operation.

The maximum available acceleration of the servo referred to point A is

$$\begin{aligned}
 a_{\max} &= \left( \frac{2000}{15} \text{ rad/sec}^2 \right) (2y \text{ v/rad}) \\
 &= 267y \text{ v/sec}^2. \qquad (4.22-16)
 \end{aligned}$$

Since the effective amplitude of the signal referred to the input of the summing circuit is  $x/5$ , the equivalent power density  $\Phi'_N$  to be used in Eq. (4.22-12) is  $\Phi_N/25$ .

Experience with solving the proportional-navigation problem shows that for accurate solutions the  $\alpha$  servo must operate with a small error to a range of approximately 200 feet but that appreciable errors may occur at smaller ranges without markedly affecting the miss distance

obtained. The problem requires a consideration of noise bandwidths up to 200 rad/sec with power densities up to 50 ft<sup>2</sup>/rad/sec. In the preceding sentence time is measured in problem seconds. In the remainder of this section, however, time will be measured in computer seconds because an 8-to-1 time-scale-extension factor was used during this study, as pointed out in Chap. 2. Measured in computer seconds the noise bandwidth then becomes 25 rad/sec and the spectral density, 400 ft<sup>2</sup>/rad/sec.

The following conditions could then be assumed as the most severe requirements imposed on the system of Fig. 4.22-5:

$$y = 0.2 v,$$

$$\omega_{ss} = 25 \text{ rad/sec, with } \zeta_{ss} = 0.7$$

$$\Phi_N' = 0.0016 v^2/\text{rad/sec},$$

measured at the input to the summing circuit on the basis that one volt at x (ahead of the 1/5 factor in Fig. 4.22-5) represents 100 feet.

Under these conditions the maximum acceleration available at point A of Fig. 4.22-5 is

$$a_{\max} = (267) (0.2) = 53.4 v/\text{sec}^2$$

which gives

$$\frac{a_{\max}}{(\Phi_N')^{1/2}} = \frac{53.4 v/\text{sec}^2}{(0.0016 v^2/\text{sec})^{1/2}} = 1333 \text{ sec}^{-5/2}.$$

The rms input to the summing circuit, under these conditions, is

$$E = \left( 2\omega_{ss} \Phi_N' \right)^{1/2} = \left[ (2) (25) (0.0016) \right]^{1/2}$$

$$= 0.282 \text{ v.}$$

The rms output-shaft movement is therefore approximately

$$\alpha = \frac{0.282}{2y} = \frac{0.282}{(2) (0.2)} = 0.705 \text{ rad}$$

$$= 40.4 \text{ deg.}$$

The movement actually required will not be as great as this because there is considerable difference between an angle and its tangent for large angles.

Several experimental curves of the error of this servo as a function of the gain are shown in Fig. 4.22-6. The results were obtained by feeding quadratic noise of various bandwidths into the servo and measuring the error signal, with the noise-monitoring equipment discussed in Chap. 3 to obtain the rms value.

The theoretical curves of Fig. 4.22-6 are drawn for a  $\tau_1$  of 0.003 second since this was the value which best characterized the servo on which these tests were made. This small change in the value of  $\tau_1$  makes a scarcely noticeable difference between the curves of Fig. 4.22-2 and 4.22-6. For example, with  $K = 100 \text{ sec}^{-1}$ ,  $\omega_{ss} = 6.9 \text{ rad/sec}$ , and  $\zeta_{ss} = 0.78$ , the value of  $\epsilon/\epsilon_0$  obtained for  $\tau_1 = 0.0016$  second is 0.06605, whereas with  $\tau_1 = 0.003$  second the value obtained is 0.0675. Changes in  $\zeta_{ss}$  over the range from 0.5 to 1.0 can also be tolerated without making appreciable changes in the results.

In each case the results presented in Fig. 4.22-6 show good agreement between the error predicted by the linear theory and the experimental

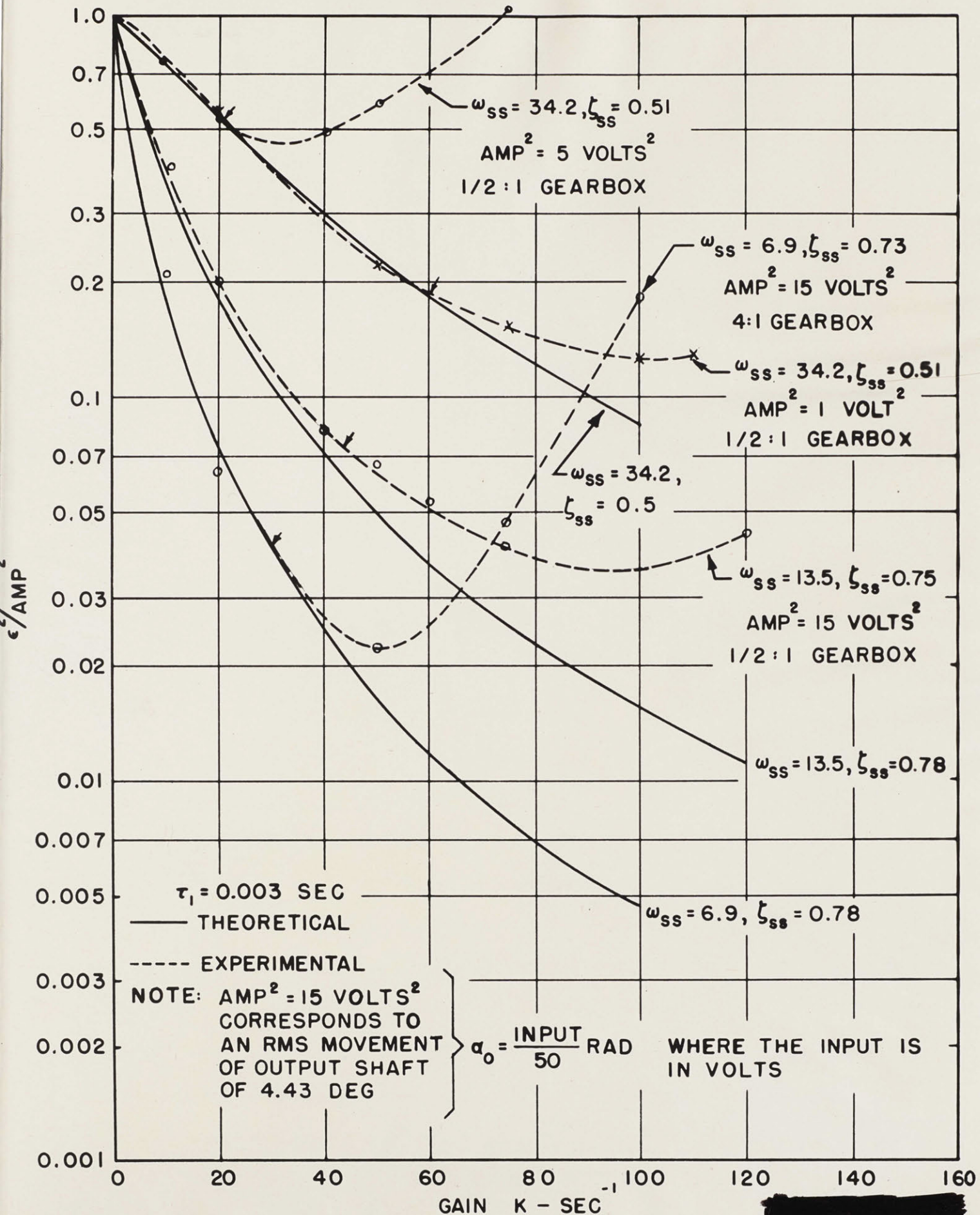


FIG. 4.22 - 6. CURVES OF ERROR VERSUS GAIN.

error, for gains below that at which the rms called-for acceleration equals approximately the maximum available acceleration. As this value is exceeded slightly the error continues to decrease somewhat but as the gain is increased still more the error increases again. These results show that the best operation of the servo is obtained when the gain is so adjusted that the rms called-for acceleration is approximately equal to the maximum available acceleration. Although only a few situations have been studied experimentally this appears to be a general criterion by which to calculate the optimum gain of servos which must be operated close to the limits of acceleration limiting, at least when the input signal has a Gaussian amplitude distribution. Actually, in the servo studied, the torque rather than the acceleration is limited. Nevertheless, if a purely inertial load is assumed, limiting the torque and limiting the acceleration are equivalent. With this criterion, Figs. 4.22-7 and 4.22-8 were plotted to show the minimum error and the corresponding gain setting required for various bandwidths of the input signal with the quantity  $a_{\max}/(\Phi_N^1)^{1/2}$  as a parameter.

Even if no acceleration difficulties occur, present equipment cannot be operated with loop gains much in excess of 400, because noise and phase shift then cause poor servo operation.

The results in Figs. 4.22-7 and 4.22-8, together with gain restrictions, show that, unless the bandwidth of the input signal and the rms shaft output are severely limited, large errors are introduced by this servo. In actual problem operation the  $\alpha$  servo is called upon to transmit a slowly varying signal as well as the noise signal, whereupon, as

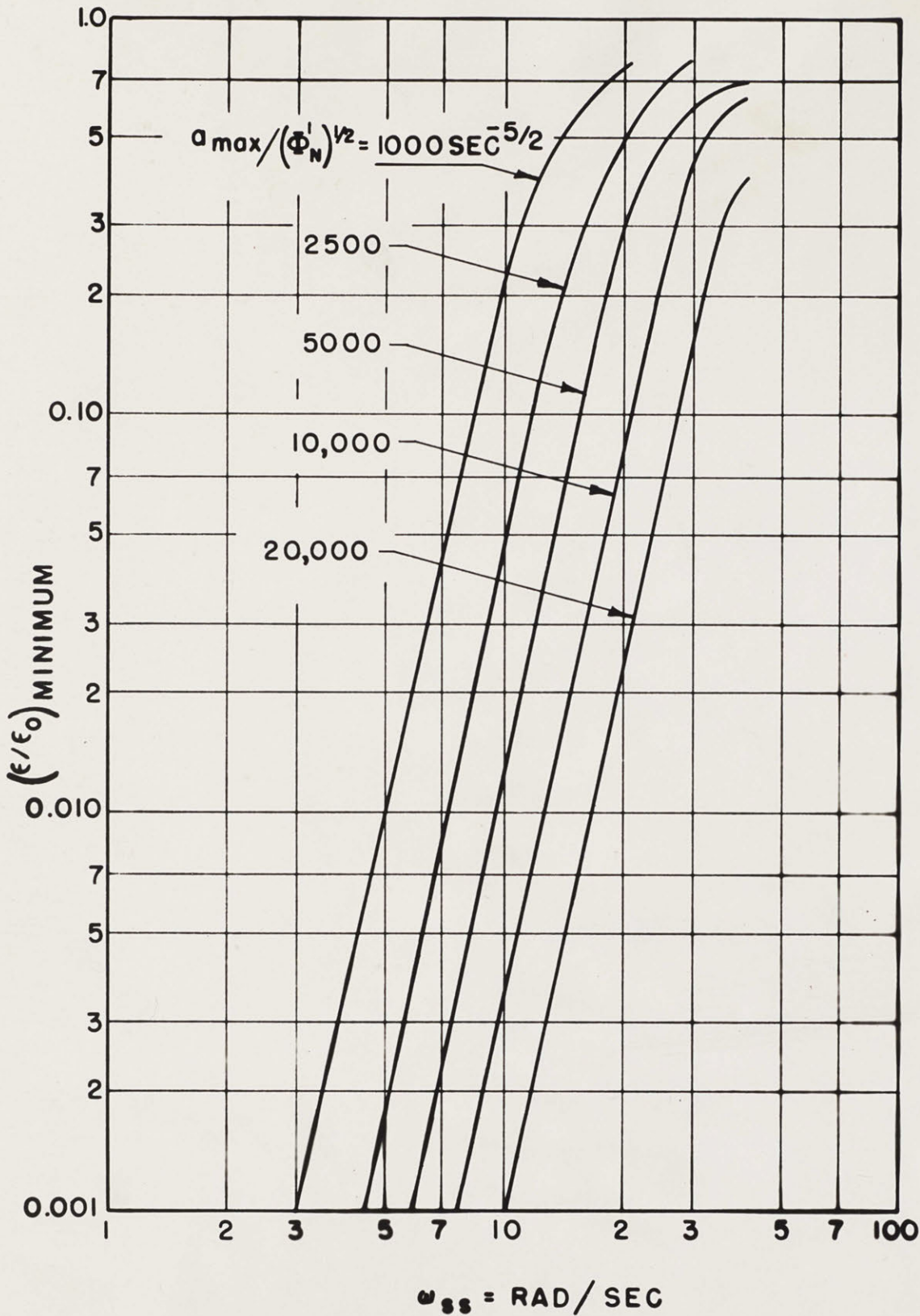


FIG. 4.22 - 7. MINIMUM ERROR AS A FUNCTION OF THE FREQUENCY OF THE INPUT SIGNAL AND THE FACTOR  $a_{\max}/(\Phi'_N)^{1/2}$

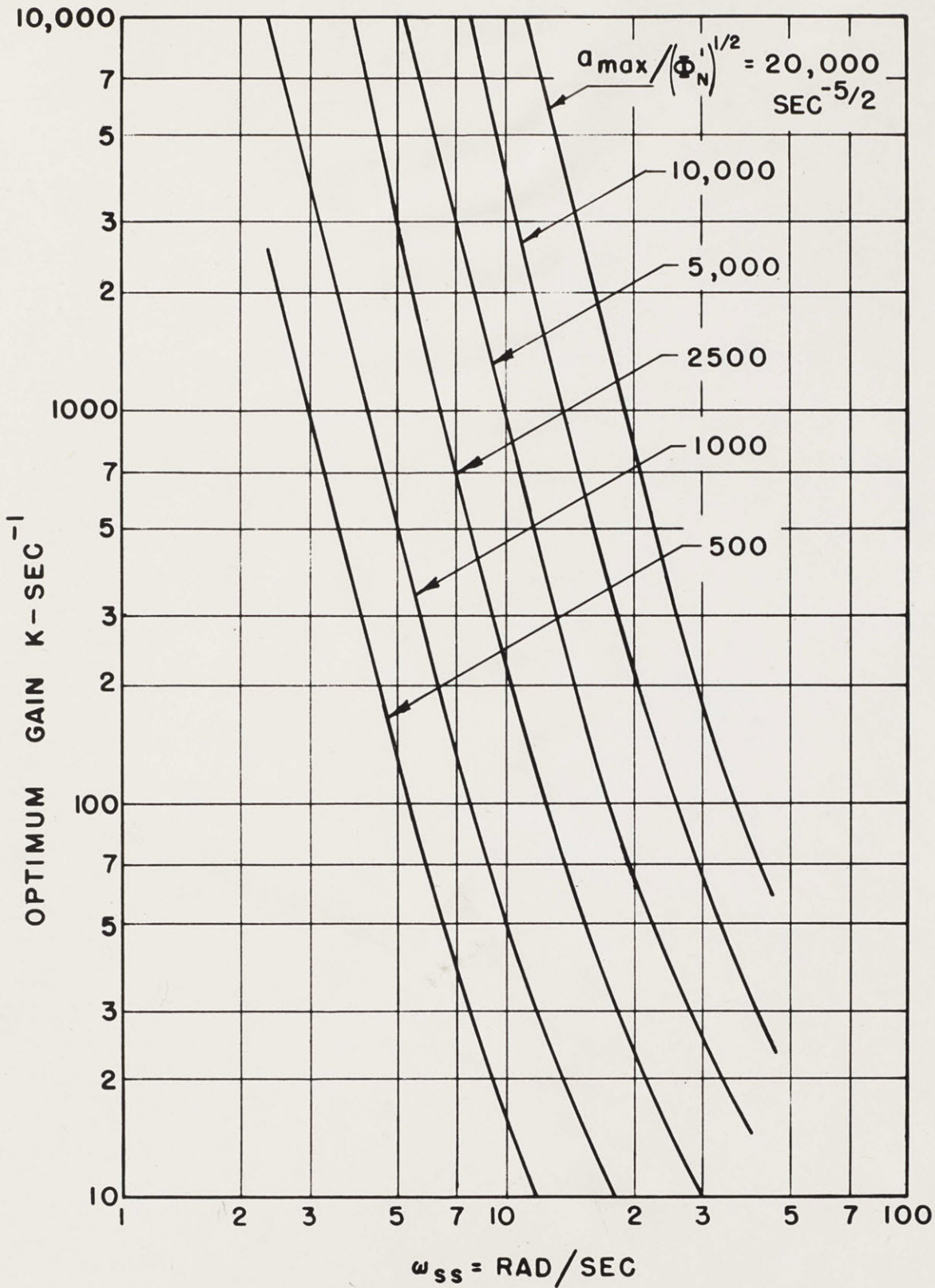


FIG. 4.22-8. OPTIMUM GAIN AS A FUNCTION OF THE FREQUENCY OF THE INPUT SIGNAL AND THE FACTOR  $a_{\max} / (\Phi_N')^{1/2}$

soon as the noise calls for the maximum available acceleration, the low-frequency component may cease to be transmitted faithfully.

If the calculations and experiments are repeated for the case where white noise is shaped by a simple-lag filter, the results obtained show considerably poorer servo operation because at high frequencies the simple-lag power density spectrum falls off only as  $\omega^2$ , whereas in the quadratic case it falls off as  $\omega^4$ . Analysis reveals that there is an optimum nonzero time constant which should be built into a servo required to handle simple-lag noise, but the optimum time constant is zero for a servo handling quadratic noise.

These results emphasize the danger of analyzing the performance of a servo, required to handle a random signal, by the usual single-frequency sinusoidal methods which indicate that the servo here considered should be able,<sup>7,\*</sup> to follow faithfully (0.1 per cent error) a 65 rad/sec input signal giving a motion at the output shaft of approximately 4 degrees.

In this section the  $\alpha$  servo has been analyzed as an isolated computing element and has been found to be seriously limited in ability to handle random signals. In this investigation the fact that the  $y$ -input signal varies has not been considered. The effect has been neglected because of lack of means for handling the additional complication. Nonetheless, variations in  $y$  may appreciably increase the acceleration demands made upon the servo near the end of the run, where changes in  $y$  are as significant as changes in  $x$ . Since the  $\alpha$  servo is only one part of the complete proportional-navigation problem setup, its effect should

\* Fuchs, A. M., op. cit., p. 105.

██████████

be considered in relation to the operation of the whole computer system. A complete analysis of this problem is not possible but a partial evaluation is presented in Sec. 4.4, where more evidence is obtained pointing toward the serious deficiencies of the presently available  $\alpha$  servo. Although the difficulties encountered when this servo becomes part of a larger loop result from the basic shortcoming observed when the servo is studied as an independent element, they may assume additional characteristics because of the presence of over-all feedback.

In certain restricted problems approximations such as substituting  $x/y$  for  $\alpha$  may be valid or the time scale may be slowed down so that the present  $\alpha$  servo may be satisfactory. These are temporary measures, however, and the basic demand for a higher gain, higher acceleration position servo will remain so long as problems are to be solved on the computer. A brief consideration of what might be accomplished toward obtaining a more suitable high-speed position servo therefore appears appropriate.

#### 4.23. Procedures for Improving the $\alpha$ Servo.

A redesign of the  $\alpha$  servo should increase the loop gain of the system and the acceleration available at the output shaft. Such a design can be achieved by using the methods discussed in Sec. 4.22. As a first step, the results of the preceding section should be used to determine roughly what gain and acceleration should be sought in an improved servo. To accomplish this, the input signals to be handled, the mechanical output desired, and the limits of acceptable accuracy should be reviewed.

██████████

On a one-to-one time scale the system should be able to handle quadratic noise signals with  $\omega_{ss}$  as great as 200 rad/sec and  $\zeta_{ss} = 0.7$ . A more realistic approach, however, from the point of view of what might be achieved in the servo, would be either to restrict the noise bandwidth or to change the time scale so that the servo is called upon to handle a maximum  $\omega_{ss}$  of 20 rad/sec (in computer seconds). If an rms error of two per cent is to be allowed, the loop gain must then be increased to approximately  $1000 \text{ sec}^{-1}$ , as shown by Fig. 4.22-2. With this gain and  $\omega_{ss} = 20 \text{ rad/sec}$ , the corresponding value of  $a/\Phi_N^{1/2} = 22,000 \text{ sec}^{-5/2}$ . If an input noise power density of  $0.001 \text{ v}^2/\text{rad/sec}$  measured at the summing circuit of Fig. 4.22-5 is to be used with  $y = 1$  volt to give an rms output-shaft movement of 0.1 radian, then the rms acceleration called for is  $a = 22,000 (0.001)^{1/2} = 700 \text{ v/sec}^2$ . The acceleration available with the present units under these operating conditions is given by Eq. (4.22-16) as  $267 \text{ v/sec}^2$ . The preceding conditions therefore require an increase in acceleration capabilities of approximately 2.5 times to be able to meet very modest specifications. If a potentiometer is being used, then an rms shaft movement of 0.1 radian is not great enough to permit neglect of the resolution errors caused by a finite number of wires in the potentiometer winding. Furthermore, a two per cent error is large. If the error is to be reduced to 0.5 per cent and the rms shaft movement simultaneously increased to 0.25 radian, then the gain required becomes approximately  $4500 \text{ sec}^{-1}$  for  $\omega_{ss} = 20 \text{ rad/sec}$ . The corresponding value of  $a/\Phi_N^{1/2}$  is then approximately  $50,000 \text{ sec}^{-5/2}$ . If the increased shaft movement is obtained by

reducing  $y$  to 0.4 volt but by keeping  $\Phi_N = 0.001 \text{ v}^2/\text{rad}/\text{sec}$ , then the required value of  $a = 50,000 (0.001)^{1/2} = 1580 \text{ v}/\text{sec}^2$ , compared with an available acceleration of  $(267)(0.4) = 107 \text{ v}/\text{sec}^2$ . Here the available acceleration is down by a factor of 15 times from the required value.

For operation on a one-to-one time scale (this is particularly desirable if the generalized portion of the computer is to be used with the gimbals for testing physical components), the acceleration requirements increase considerably. Although Fig. 4.22-3 does not show  $\omega_{ss}$  equal to 200 rad/sec, the called-for acceleration increases approximately as the square of  $\omega_{ss}$  for a fixed value of  $K$ . Furthermore, in order to maintain a constant error as  $\omega_{ss}$  is increased,  $K$  must be increased approximately in proportion to  $\omega_{ss}$ , except in the region of very large or very small errors. Figure 4.22-2 shows that a gain of 10,000 would, therefore, be required to keep the error to two per cent for an  $\omega_{ss}$  of 200 rad/sec. For this value of  $K$  and  $\omega_{ss} = 200 \text{ rad}/\text{sec}$  Fig. 4.22-3 indicates that the value of  $a/\Phi_N^{1/2}$  required is of the order of  $5 \times 10^7 \text{ sec}^{-5/2}$ . With  $\Phi_N = 0.001 \text{ v}^2/\text{rad}/\text{sec}$  the required value of  $a = 5 \times 10^7 \times (0.001)^{1/2} = 1,580,000 \text{ v}/\text{sec}^2$ , compared with an acceleration of  $107 \text{ v}/\text{sec}^2$  available when  $y$  is 0.4 volt. In this case the available acceleration is down by a factor of 15,000 times from that required! The problem is doubly difficult because the realization of a loop gain of  $10,000 \text{ sec}^{-1}$  will be as difficult as the attainment of the desired acceleration.

██████████

The foregoing calculations demonstrate that if a servo is to be constructed to handle adequately the assumed class of input signals, the design must be a radical departure from that of the standard D.A.C.L. integrator servos.

There are two methods of obtaining a higher output acceleration than is available in the existing servo:

- 1) The acceleration capabilities of the motor may be increased.
- 2) The gearing between the motor and the output units may be eliminated.<sup>25</sup>

Since no commercial electric motor produces sufficient torque in the desired velocity range and still has a torque-to-inertia ratio substantially greater than the Bendix CK-3000-1A 2-phase induction motor in current use, increasing the acceleration capabilities of the motor presents a major problem. Dry disc or fluid magnetic clutches may provide a solution to this problem, but considerable developmental work would be required to make such units operationally practical. Another possible solution lies in using a hydraulic motor, but here again developmental problems arise, particularly in regard to drift and noise considerations.

As a temporary measure an appreciable improvement could be achieved by eliminating the gearing between the motor and the output units by connecting a pair of resolvers directly to the motor shaft and doing away with the tachometer, which is unnecessary in a servo designed specifically as a position device. By eliminating the tachometer

██████████

and the gearing and thus reducing the versatility of the unit, both the inertia and friction loading reflected to the motor could be reduced, thereby increasing the available acceleration. The question then arises as to whether the increased mechanical gain resulting from the elimination of the gearing could be utilized to realize the advantage of the added acceleration capabilities or whether higher order terms in the system would come into play and consequently prevent any appreciable improvement. An analysis was, therefore, made of the effect of a second time lag in the system such that the forward transfer function assumed the form

$$\frac{K}{s(\tau_1 s + 1)(a_1 \tau_1 s + 1)} \quad (4.23-1)$$

The error squared corresponding to Eq. (4.22-6) is then

$$\overline{\epsilon^2} = (2\pi\Phi_N) \frac{1}{2\pi i} \int_{-i\infty}^{+i\infty} \left| \frac{1}{\frac{s^2}{\omega_{ss}^2} + \frac{2\zeta_{ss}s}{\omega_{ss}} + 1} \right|^2 \left| \frac{s(\tau_1 s + 1)(a_1 \tau_1 s + 1)}{K \left( \frac{a_1 \tau_1^2 s^3}{K} + \frac{(1+a_1)\tau_1 s^2}{K} + \frac{s}{K} + 1 \right)} \right|^2 ds. \quad (4.23-2)$$

The expression for  $\overline{\epsilon^2}$  given by Eq. (4.23-2) is meaningful only for a stable system. As the system approaches instability,  $\epsilon$  approaches infinity. The gain at which this occurs may be determined by applying the Hurwitz criterion to the denominator of the system transfer function. From this criterion, which is a relation required among the coefficients of a polynomial for the zeros to be in the left half-plane, the gain at which the system becomes unstable may be calculated. The particular expression involved here is the cubic term in the denominator of

Eq. (4.23-2), namely,

$$\frac{a_1 \tau_1^2 s^3}{K} + \frac{(1+a_1)}{K} \tau_1 s^2 + \frac{s}{K} + 1. \quad (4.23-3)$$

For a cubic the gain which results in instability is determined by equating the products of the inner and outer coefficients

$$\frac{(1+a_1) \tau_1}{K} \frac{1}{K} = \frac{a_1 \tau_1^2}{K} \quad (4.23-4)$$

and yields

$$K = \frac{(1+a_1)}{a_1 \tau_1}. \quad (4.23-5)$$

For

$$a_1 = 0.2 \text{ and } \tau_1 = 0.0016 \text{ sec,}$$

a gain of

$$K = \frac{1.2}{(0.2)(0.0016)} = 3750 \text{ sec}^{-1}$$

results in an unstable system.

The integral in Eq. (4.23-2) was also evaluated to determine the gain required to give the minimum error in such a servo. The expression obtained is quite long and will not be given here, but Fig. 4.23-1 shows a curve of the normalized error obtained for the case when

$$a_1 = 0.2$$

$$\tau_1 = 0.0016 \text{ sec}$$

$$\omega_{ss} = 2.5 \text{ rad/sec}$$

$$\zeta_{ss} = 0.7.$$

The error obtained for  $a_1 = 0.2$  is essentially the same as that obtained for the simpler case where  $a_1 = 0$ , so long as the gain is kept below

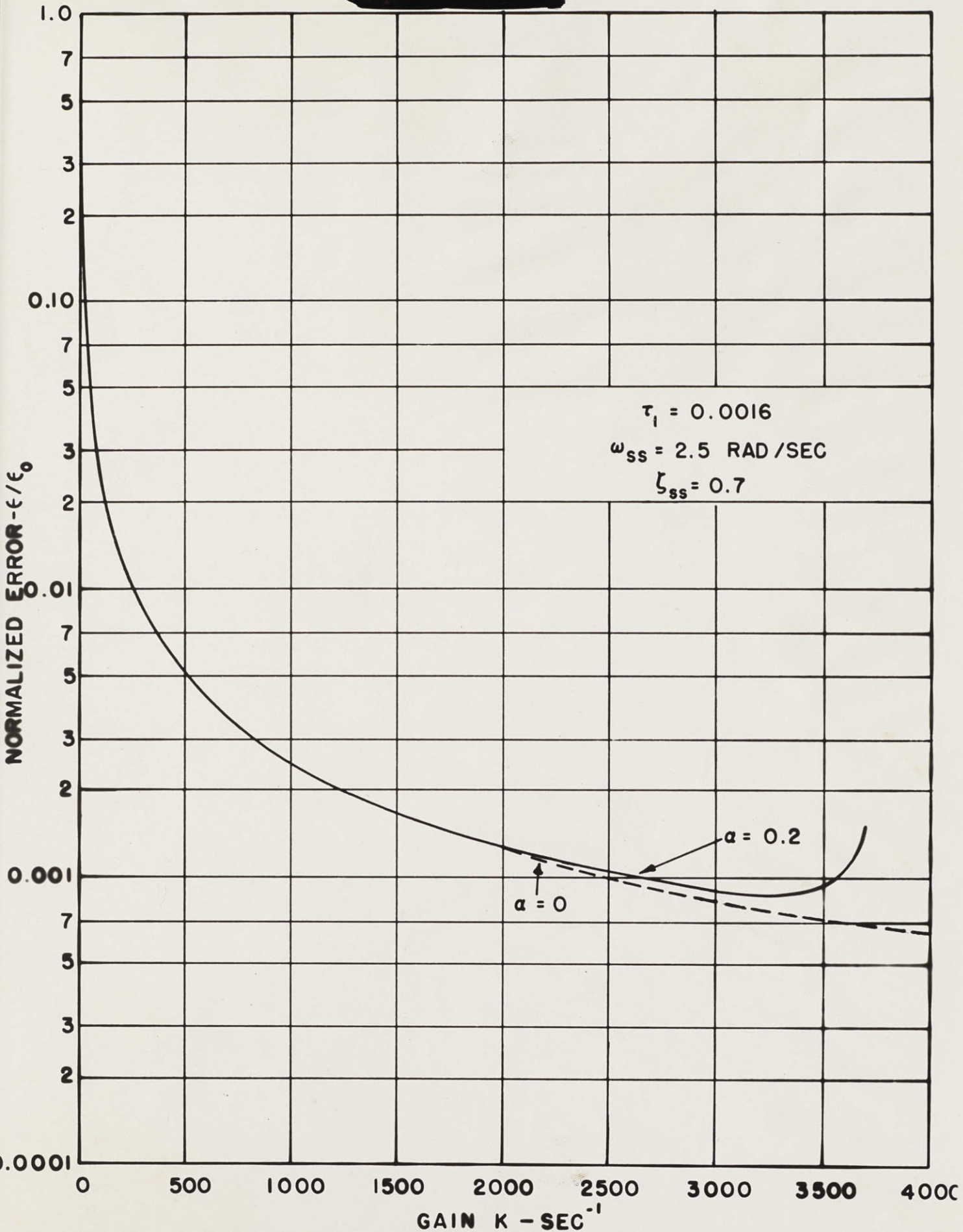


FIG. 4.23-1. NORMALIZED ERROR FOR POSITION SERVO FOLLOWING QUADRATIC NOISE.

about 3000. Previous calculations, however, showed that the use of gains greater than 3000 may be necessary to reduce the error to an acceptable value. To be able to utilize these higher gains,  $\tau_1$  and  $a_1$  of Eq. (4.23-1) must be reduced.

Before much effort is expended toward the design of a servo to meet the acceleration, gain, and time-constant requirements outlined, the noise to be expected in such a high-gain system should be carefully considered since noise will also set a limit to the maximum gain which can be realized.

The servo designer appears to be faced here with a set of requirements which, with present knowledge and equipment, may well be unattainable. For the computer operator, on the other hand, the need for a more suitable servo is very real. The final solution may lie in a combination of appreciably faster servos than those now possible and a modification of computer operating techniques in order to make less severe demands upon the servos.

#### 4.3. Computer Checking When Noise Is Inserted.

After the computer has been adjusted to operate properly in the noise-free unlimited version of the proportional-navigation-with-simple-lag problem, the next step is to check the operation with noise, and the value of noise injected into the computer. A simple and effective test can be obtained by locking the y servo at an appropriate range and observing the rms value of x resulting from the noise from a fixed target. Figure 4.3-1 shows the kinematic arrangement involved.

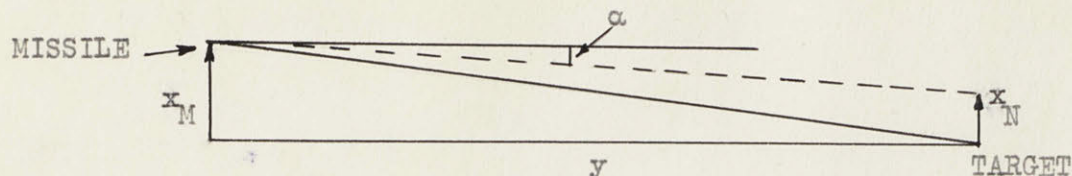


Fig. 4.3-1. Geometry of target and missile.

If  $y$  is so chosen that the angles involved are small, the linearized equations can be used, giving

$$\dot{x}_M = V_M \theta \quad (4.3-1)$$

and

$$\alpha = \frac{x_N - x_M}{y} \quad (4.3-2)$$

where here, and in the remainder of this section,  $x$  and  $y$  are measured in feet. Substituting these values into the control equation,

$$A\dot{\theta} + \theta = (b+1) \alpha \quad (4.3-3)$$

gives

$$\frac{A\ddot{x}_M}{V_M} + \frac{\dot{x}_M}{V_M} = (b+1) \frac{(x_N - x_M)}{y} \quad (4.3-4)$$

Solution of Eq. (4.3-4) for  $x_M$  yields

$$x_M = \frac{x_N}{\left[ \frac{Ays^2}{V_M(b+1)} + \frac{ys}{V_M(b+1)} + 1 \right]} \quad (4.3-5)$$

With  $y$  locked, the system has a quadratic transfer function with a natural frequency given by

$$\omega_o = \sqrt{\frac{V_M(b+1)}{Ay}} \quad (4.3-6)$$

and a damping coefficient

$$\zeta_0 = \frac{1}{2} \sqrt{\frac{y}{AV_M(b+1)}} \quad (4.3-7)$$

Experimentally the mean-square value of  $x_M$  is of interest. This is given for the case of white noise by

$$\overline{x_M^2} = \frac{1}{i} \int_{-i\infty}^{+i\infty} \left| \frac{1}{\frac{Ays^2}{V_M(b+1)} + \frac{ys}{V_M(b+1)} + 1} \right|^2 \Phi_N ds. \quad (4.3-8)$$

For noise characterized by a quadratic with a natural frequency of  $\omega_{ss}$  and a damping coefficient  $\zeta_{ss}$ , the mean-square value of  $x_M$  is given by

$$\overline{x_M^2} = \frac{1}{i} \int_{-i\infty}^{+i\infty} \left| \frac{1}{\frac{Ays^2}{V_M(b+1)} + \frac{ys}{V_M(b+1)} + 1} \right|^2 \left| \frac{1}{\frac{s^2}{\omega_{ss}^2} + \frac{2\zeta_{ss}s}{\omega_{ss}} + 1} \right|^2 \Phi_N ds. \quad (4.3-9)$$

The integral tables in Appendix C yield for white noise

$$I_2 = \frac{V_M(b+1)}{2y} \quad (4.3-10)$$

and

$$\overline{x_M^2} = n\Phi_N \frac{V_M(b+1)}{y}. \quad (4.3-11)$$

With use of the integration tables Eq. (4.3-9) gives for quadratic noise,

$$\overline{x_M^2} = \frac{\pi \Phi_N \left[ \frac{1}{\omega_{ss}^3} + \frac{2\zeta_{ss} y}{V_M(b+1)} \left( \frac{1}{\omega_{ss}^2} + \frac{2\zeta_{ss} A}{\omega_{ss}} + A^2 \right) \right]}{2\zeta_{ss} \left[ \frac{1}{\omega_{ss}^4} + \frac{2\zeta_{ss} y}{V_M(b+1)\omega_{ss}^3} + \frac{y}{V_M(b+1)\omega_{ss}^2} \left( \frac{y}{V_M(b+1)} - 2A + 4\zeta_{ss}^2 A \right) + \frac{2\zeta_{ss} A y^2}{V_M^2(b+1)^2 \omega_{ss}} + \frac{A^2 y^2}{V_M^2(b+1)^2} \right]} \quad (4.3-12)$$

Two typical cases follow:

CASE I

$$V_M = 2000 \text{ ft/sec}$$

$$(b+1) = 6$$

$$y = 1000 \text{ ft}$$

$$\Phi_N = 10 \text{ ft}^2/\text{rad/sec}$$

$$A = 1/2 \text{ sec}$$

For white noise  
Eq. (4.3-11) yields

$$\overline{x_M^2} = 120 \pi \text{ ft}^2$$

or

$$x_{M,rms} = 19.4 \text{ ft}$$

CASE II

$$V_M = 2000 \text{ ft/sec}$$

$$(b+1) = 4$$

$$y = 4000 \text{ ft}$$

$$\Phi_N = 10 \text{ ft}^2/\text{rad/sec}$$

$$A = 1 \text{ sec}$$

For white noise  
Eq. (4.3-11) yields

$$\overline{x_M^2} = 20 \pi \text{ ft}^2$$

or

$$x_{M,rms} = 7.93 \text{ ft}$$

The influence of the  $\omega_{ss}$  and  $\zeta_{ss}$  used in the noise filter can be obtained by considering the ratio  $\overline{x_M^2}/\overline{x_{M,\infty}^2}$  where  $\overline{x_{M,\infty}^2}$  is the mean-square miss caused by white noise and  $\overline{x_M^2}$  is the miss given by Eq. (4.3-12). This ratio is plotted in Fig. 4.3-2 for the parameters of Case I and  $\zeta_{ss}$  of

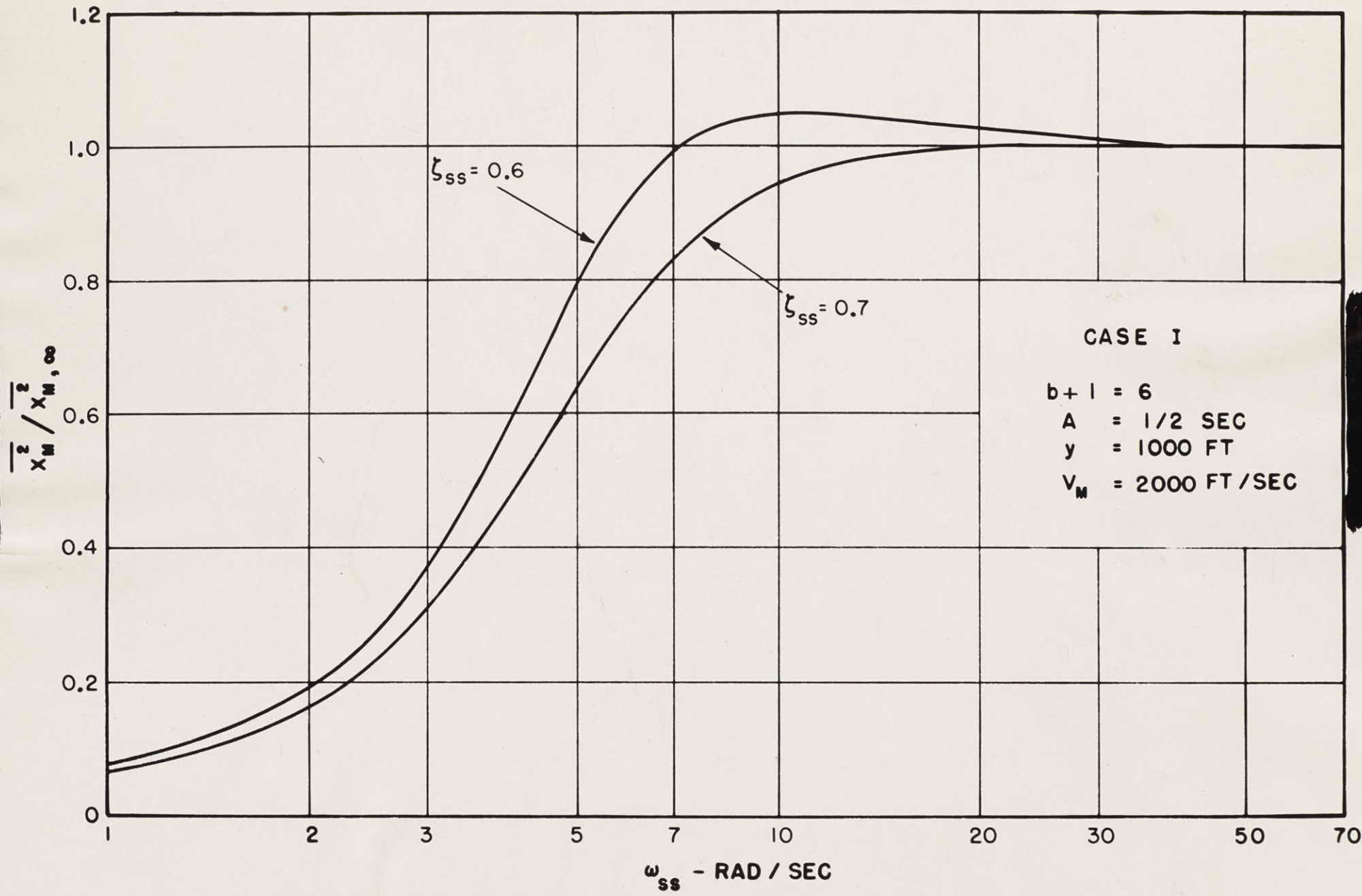


FIG. 4.3-2. QUADRATIC NOISE INTO y-LOCKED SYSTEM.

0.6 and 0.7. This figure shows that noise shaped by a quadratic filter can, for a given  $\Phi_N$ , cause a larger miss than white noise, provided the damping coefficient and natural frequency of the filter bear the proper relation to those of the y-locked system. For this same case Eqs. (4.3-6) and (4.3-7) yield  $\omega_0 = \sqrt{24}$  and  $\zeta_0 = 1/\sqrt{24}$ .

Experimentally, the rms value can readily be obtained by reading a number of x values taken at equal intervals from a recording of x, squaring these, averaging them, and then taking their square root.

Since, in this test,  $x_M$  is obtained as a continuous function of time, both the time between successive points read from the curve and the number of points read must be considered in arriving at the accuracy to be expected. Consideration of the number of uncorrelated readings which must be taken to achieve a specified accuracy will be postponed until Sec. 5.1. At this point merely the problem of obtaining uncorrelated readings will be considered.

If a fixed number n of values is to be read from the x recording, the rms value of x is obtained with much better accuracy if the correlation between successive points is relatively small than if the points are chosen so close together that successive points have a high correlation. An appropriate spacing for successive readings may be obtained by calculating the autocorrelation function of x obtained for the y-locked case. The power spectrum of  $x_M(t)$ ,  $\Phi_{x,M}(\omega)$ , corresponding to Eq. (4.3-5) is in accord with Eq. (4.21-1) given by

$$\Phi_{x,M}(\omega) = \frac{\Phi_N(\omega)}{\left| \frac{Ays^2}{V_M(b+1)} + \frac{ys}{V_M(b+1)} + 1 \right|^2} \quad (4.3-13)$$

The autocorrelation function of  $x_M(t)$ ,  $\phi_{x,M}(\tau)$ , is the inverse Fourier transformation of  $\Phi_{x,M}(\omega)$ . For white noise,  $\Phi_N(\omega)$  is a constant  $\Phi_N$ . With

$$\mu = \frac{Av}{V_M(b+1)}$$

and

$$\nu = \frac{V}{V_M(b+1)},$$

$$\phi_{x,M}(\tau) = \frac{\Phi_N}{\mu^2} \mathcal{L}^{-1} \left| \frac{1}{s^2 + \frac{\nu s}{\mu} + \frac{1}{\mu}} \right|^2. \quad (4.3-14)$$

The autocorrelation function can be evaluated in the following manner.

$$\left| \frac{1}{s^2 + \frac{\nu s}{\mu} + \frac{1}{\mu}} \right|^2 = \frac{1}{s^2 + \frac{\nu s}{\mu} + \frac{1}{\mu}} \frac{1}{s^2 - \frac{\nu s}{\mu} + \frac{1}{\mu}}. \quad (4.3-15)$$

Breaking this into two parts, one of which has poles only in the right half-plane and the other, poles only in the left half-plane, yields

$$\frac{1}{s^2 + \frac{\nu s}{\mu} + \frac{1}{\mu}} \frac{1}{s^2 - \frac{\nu s}{\mu} + \frac{1}{\mu}} = \frac{Ms + N}{s^2 + \frac{\nu s}{\mu} + \frac{1}{\mu}} \frac{-Ms + N}{s^2 - \frac{\nu s}{\mu} + \frac{1}{\mu}}. \quad (4.3-16)$$

Therefore,

$$M = \frac{\mu^2}{2\nu} \text{ and } N = \frac{\mu}{2}.$$

Writing the transform in Eq. (4.3-14) in integral form gives:

$$\phi_{x,M}(\tau) = \frac{\Phi_N}{\mu^2} \frac{1}{2\pi i} \int_{-i\infty}^{+i\infty} \left| \frac{1}{s^2 + \frac{\nu s}{\mu} + \frac{1}{\mu}} \right|^2 e^{\tau s} ds. \quad (4.3-17)$$

Equation (4.3-17) can then be written:

$$\phi_{x,M}(\gamma) = \frac{\Phi N}{\mu^2} \frac{1}{2\pi i} \left[ \int_{-i\infty}^{+i\infty} \frac{Ms + N}{s^2 + \frac{\nu s}{\mu} + \frac{1}{\mu}} e^{\gamma s} ds + \int_{-i\infty}^{+i\infty} \frac{-Ms + N}{s^2 - \frac{\nu s}{\mu} + \frac{1}{\mu}} e^{\gamma s} ds \right]. \quad (4.3-18)$$

The first integrand has poles only in the left half-plane and can be evaluated for  $\gamma > 0$  by closing a large arc around the left half-plane since the integral along this path and the  $i$  axis is equal to the residues at the enclosed poles. The integral along the large arc approaches zero for this term, therefore the integral along the imaginary axis is equal to the sum of the residues at the poles in the left half-plane. The second integral is zero around this same complete path because the integrand has no poles in the left half-plane. Since the exponential is bounded for positive values of  $\gamma$  and negative real values of  $s$ , the integral along the arc approaches zero. Consequently, the integral along the imaginary axis is zero. Thus, for  $\gamma > 0$  the value of  $\phi(\gamma)$  is given by the first integral alone. A similar line of reasoning shows that for  $\gamma < 0$  the value of  $\phi(\gamma)$  is given by the second integral. Therefore, for  $\gamma > 0$

$$\phi_{x,M}(\gamma) = \frac{\Phi N}{\mu^2} \mathcal{L}^{-1} \left[ \frac{Ms + N}{s^2 + \frac{\nu s}{\mu} + \frac{1}{\mu}} \right] \quad (4.3-19)$$

$$= \frac{\Phi N}{2\nu} \mathcal{L}^{-1} \left[ \frac{s + \frac{\nu}{\mu}}{\left(s + \frac{\nu}{2\mu}\right)^2 + \left(\frac{1}{\mu} - \frac{\nu^2}{4\mu^2}\right)} \right]. \quad (4.3-20)$$

When the inverse transform of Eq. (4.3-20) is taken

$$\phi_{x,M}(\gamma) = \frac{2\pi\Phi_N}{2\nu} \left\{ \frac{1}{\left(\frac{1}{\mu} - \frac{\nu^2}{4\mu^2}\right)^{1/2}} \frac{e^{-\frac{\nu}{2a}}}{\mu^{1/2}} \sin \left[ \left(\frac{1}{\mu} - \frac{\nu^2}{4\mu^2}\right)^{1/2} \gamma + \psi \right] \right\} \quad (4.3-21)$$

where

$$\psi \triangleq \tan^{-1} \left[ \frac{2\mu}{\nu} \left(\frac{1}{\mu} - \frac{\nu^2}{4\mu^2}\right)^{1/2} \right].$$

Substitution of the values of  $\mu$  and  $\nu$  gives for  $\gamma > 0$

$$\phi(\gamma) = \frac{\pi\Phi_N V_M(b+1)}{y} \left\{ \left[ \frac{\frac{V_M(b+1)}{Ay}}{\frac{V_M(b+1)}{Ay} - \frac{1}{4a^2}} \right]^{1/2} e^{-\frac{\gamma}{2A}} \sin \left[ \left( \frac{V_M(b+1)}{Ay} - \frac{1}{4a^2} \right)^{1/2} \gamma + \psi \right] \right\} \quad (4.3-22)$$

where

$$\psi \triangleq \tan^{-1} 2 \left( \frac{AV_M(b+1)}{y} - \frac{1}{4} \right)^{1/2}.$$

Evaluation of  $\phi(\gamma)$  for  $\gamma = 0$  yields

$$\phi(0) = \frac{\pi\Phi_N V_M(b+1)}{y}$$

which checks Eq. (4.3-11) for the value of  $x_{M,rms}$ , as it should.

Successive points on the x plot can be considered sufficiently uncorrelated if  $\phi(\gamma)$  is only 10 per cent of the  $\phi(0)$  value. This requires the  $e^{-\gamma/2A}$  factor to be approximately  $e^{-2}$  or  $\gamma = 1$  second for  $A = 1/2$  second. Since the computer was run with an 8-to-1 time-scale extension, 8 seconds of running time are required to simulate one second between adjacent points.

Tests with  $y$  locked proved a very valuable means of checking the accuracy of the computer when operating with noise signals because 100 samples for a  $y$ -locked check can be obtained in roughly one seventh the time required to make 100 complete runs with noise. After the final noise-generating and-monitoring schemes discussed in Chap. 3 were adopted and the  $\alpha$  servo was replaced by the divider servo, the computer gave experimental points which matched the curve of Fig. 4.3-2 to within approximately 5 per cent for 100 points. This accuracy is essentially that expected because of the statistical nature of the problem as discussed in Sec. 5.1.

#### 4.4. Effect of Time Lag in the $\alpha$ Servo.

The maximum gain which can be utilized in the  $\alpha$  servo can be determined according to the methods of Sec. 4.2. When this servo is used as part of a complete problem, the effect of the time constant  $\tau_1$  on the over-all accuracy should be determined. Unfortunately, such an analysis cannot be made for the general problem but the special  $y$ -locked problem discussed in Sec. 4.3 has been studied. In this case the actual  $\alpha$  obtained is found by multiplying the expression for  $\alpha$ , Eq. (4.3-2), by the transfer function of the  $\alpha$  servo given in Eq. (4.22-3). Then

$$\alpha = \left( \frac{x_N - x_M}{y} \right) \left( \frac{1}{\gamma_1 s^2 + \frac{s}{K} + 1} \right). \quad (4.4-1)$$

Substituting the value for  $\alpha$  from Eq. (4.4-1) into Eq. (4.3-3) gives

$$x_M \left( \frac{As^2}{V_M} + \frac{s}{V_M} \right) = (b+1) \left( \frac{x_N - x_M}{y} \right) \left( \frac{1}{\frac{\gamma_1 s^2}{K} + \frac{s}{K} + 1} \right). \quad (4.4-2)$$

The solution of Eq. (4.4-3) for  $x_M$  then yields

$$x_M = \frac{\left( \frac{b+1}{y} \right) x_N}{\left[ \frac{A\gamma_1 s^4}{V_M K} + \left( \frac{A}{V_M K} + \frac{\gamma_1}{V_M K} \right) s^3 + \left( \frac{A}{V_M} + \frac{1}{V_M K} \right) s^2 + \frac{s}{V_M} + \frac{b+1}{y} \right]}. \quad (4.4-3)$$

The mean-square value of  $x$  is then written as

$$\overline{x^2} = \frac{1}{i} \int_{-i\infty}^{+i\infty} \frac{\left( \frac{b+1}{y} \right)^2 \Phi_N(\omega)}{\left| \frac{A\gamma_1 s^4}{V_M K} + \left( \frac{A}{V_M K} + \frac{\gamma_1}{V_M K} \right) s^3 + \left( \frac{A}{V_M} + \frac{1}{V_M K} \right) s^2 + \frac{s}{V_M} + \frac{b+1}{y} \right|^2} ds \quad (4.4-4)$$

where  $\Phi_N(\omega)$  is the power spectrum of  $x_N(t)$ . For the case of white noise  $\Phi_N(\omega)$  is constant.

$$\Phi_N(\omega) = \Phi_N. \quad (4.4-5)$$

When  $\Phi_N$  is substituted and the integral evaluated, the expression for  $\overline{x_M^2}$  becomes

$$\overline{x_M^2} = \pi \Phi_N \left\{ \frac{A^2 + \frac{A}{K} + \frac{\gamma_1}{K}}{\left[ -\frac{1}{K} (A + \gamma_1)^2 + \left( \frac{y}{b+1} \right) \left( \frac{1}{V_M} \right) \left( A^2 + \frac{A}{K} + \frac{\gamma_1}{K} \right) \right]} \right\} ft^2. \quad (4.4-6)$$

When  $K \rightarrow \infty$  Eq. (4.4-6) yields the result of Eq. (4.3-11),

$$\overline{x_{M,K \rightarrow \infty}^2} = \pi \Phi_N \frac{V_M (b+1)}{y}. \quad (4.4-7)$$

Use of this value as a normalizing factor gives

$$\frac{\overline{x_M^2}}{\overline{x_{M,K \rightarrow \infty}^2}} = \left[ \frac{(A^2 K + A + \gamma_1)}{A^2 K + A + \gamma_1 - \frac{V_M(b+1)}{y} (A + \gamma_1)^2} \right]. \quad (4.4-8)$$

In Fig. 4.4-1  $\overline{x_M^2}/\overline{x_{M,K \rightarrow \infty}^2}$  is plotted as a function of the servo gain  $K$ . This figure shows that if  $K$  is reduced to 14.1 an oscillation of the over-all loop takes place as a result of the time lag in the  $\alpha$  servo. Even if the gain is increased to  $K = 60$  (approximately the maximum allowed by the acceleration limitations of the servo, as discussed in Sec. 4.22), the error introduced by this servo in solving the  $y$ -locked problem at 1000 feet is still approximately 3.5 per cent of the simple-lag case with  $A = 1/2$  sec and  $(b+1) = 6$ .

Unfortunately, this same type of error analysis cannot, at present, be extended to the proportional-navigation problem with time-varying parameters, but the preceding analysis indicates that the combination of the inherent time lag and the limited gain which can be utilized in the  $\alpha$  servo introduces appreciable computing errors, particularly toward the end of the problem.

The discussions in this chapter show that until a servo is available which possesses greater acceleration capabilities and a smaller time constant than the present D.A.C.L. electromechanical servos, considerable error will be introduced whenever the computation of an arc tangent is required. Fortunately, for the type of problem being studied here,  $x/y$  may be substituted for  $\alpha$  with negligible error, since  $\alpha$  never exceeds approximately 10 degrees until the last 200 feet or

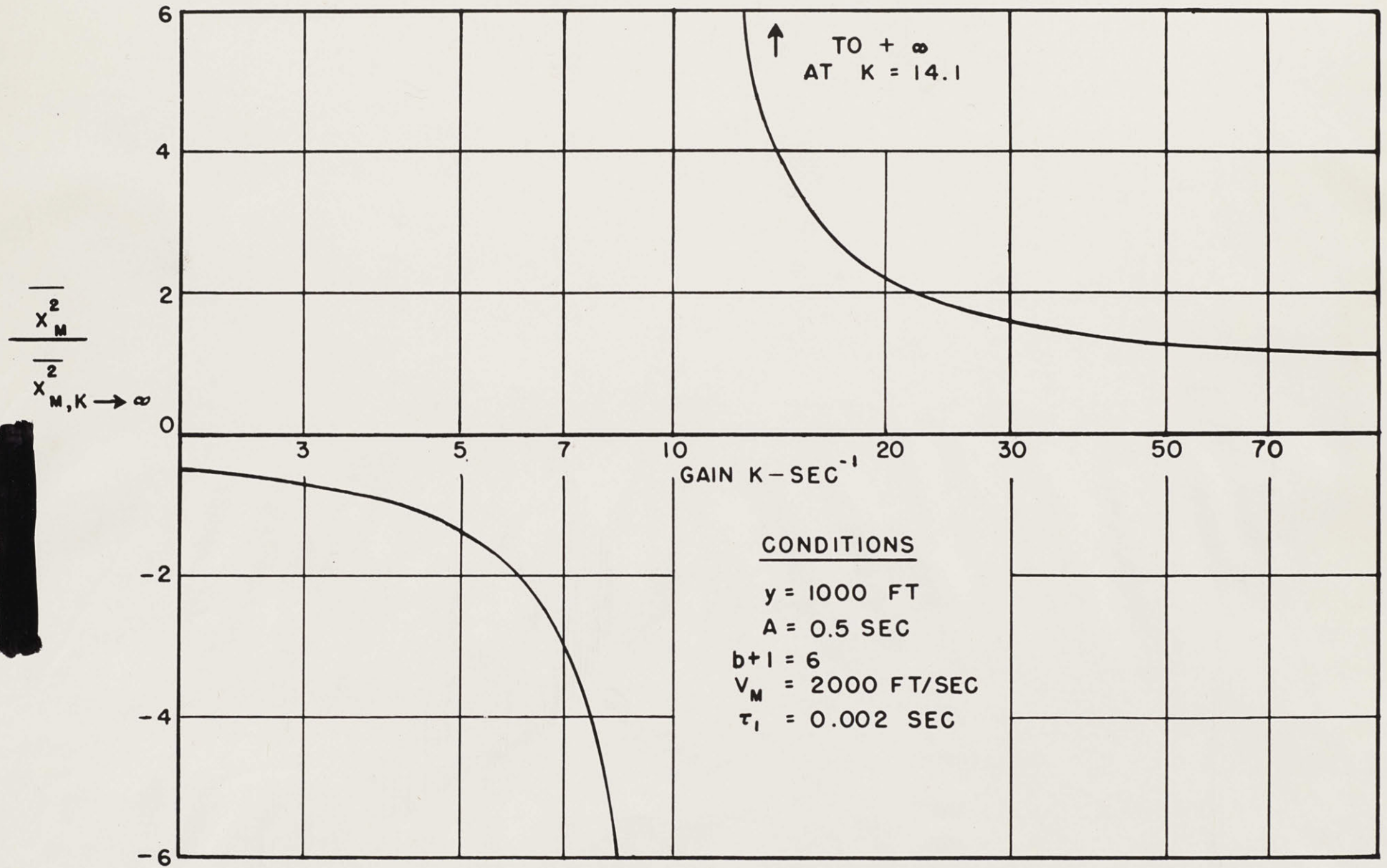


FIG. 4.4 - I. EFFECT OF LIMITED  $\alpha$ -SERVO GAIN IN A STUDY OF THE  $y$ -LOCKED PROBLEM.

less of the problem. For these close ranges the difference between  $x/y$  and  $\alpha$  causes negligible error. This substitution should not, however, be relied upon to give accurate answers to problems involving initial ranges greater than 5000 to 10,000 feet.

[REDACTED]

## CHAPTER 5

### PRESENTATION AND INTERPRETATION OF EXPERIMENTAL RESULTS

Operating experience with the M.I.T. Flight Simulator indicates that extreme care must be exercised if meaningful results are to be obtained from any large-scale computer. Use must be made of every available procedure whereby portions of the computer setup can be analyzed separately to check analytic solutions against simplified cases of the general problems being studied. Furthermore, it is important to distinguish between the accuracy limitations imposed by the equipment involved and by the nature of the problem itself. In this way machine errors can be identified and corrected but time will not be wasted trying to achieve higher accuracy than the nature of the problem allows.

The probable error imposed by the statistical nature of the noise problem and the results obtained in checking computer solutions against analytic results for the linear case are accordingly discussed before treating the general problem involving limiting.

#### 5.1. Probable Error Imposed by the Statistical Nature of the Problem.

Since a statistical distribution of miss distances is expected in any problem involving noise, the probable error expected from taking only a limited number of runs should be considered. It is desired to determine the probable error expected in checking the rms value of the misses obtained experimentally with the standard deviation of the miss obtained analytically. The simplest case occurs when the missile is

[REDACTED]

attacking a target flying a straight-line course. For a missile initially on a collision course, noise alone causes the miss. If the noise is normally distributed about zero and, if no limiting occurs, the miss distances will be distributed normally about zero.

Some of the accuracy considerations involved in making statistical studies have been investigated by R. C. Booton. A heretofore unpublished note by him is included as Appendix D. There he points out, for the case where the variable (miss distance) is normally distributed about zero, that approximately 800 solutions are required to insure a 95 per cent probability that the standard deviation calculated from the finite number of samples be within 5 per cent of the true standard deviation. On the other hand, if a 50 per cent probability of being within 5 per cent can be tolerated, only 90 samples are required. Since the collection and processing of data are very time-consuming operations, a balance must be struck between the accuracy to be expected in an answer and the time required to obtain the answer. For most of the results reported, approximately 100 samples were collected in each instance. There is, therefore, a 50 per cent probability that the results are within 5 per cent, or a 95 per cent probability that they are within 14 per cent of the true results, on the basis of statistics alone. The accuracy figures may be somewhat in error because the samples are not in all cases normally distributed about zero. However, on the basis of experimental observations there appears to be little reason to suspect any large discrepancies.

5.2. Comparison between Experimental and Analytic Results for the Case of Linear Operation.

The first situation investigated in this computer study applied to a missile having a proportional-navigation-with-simple-time-lag control system and unlimited available acceleration. The control equation for this case is

$$A\ddot{\theta} + \dot{\theta} = (b+1)\dot{\alpha} \quad (5.2-1)$$

and the corresponding basic computer setup diagram is given in Fig. 5.2-1, which is essentially a more detailed version of Fig. 2.2-2.

In order to set up the computer a detailed setup sheet is required for each integrator as well as for special equipment such as the limiter, noise generator, and noise monitor. For this case, the limiter of Fig. 5.2-1 is set on "no limits" and the filter  $sF(s)$  between  $(b+1)\dot{\alpha}$  and  $\dot{\theta}$  becomes  $s/(As+1)$ , which is equivalent to  $1/(As+1)$  between  $(b+1)\dot{\alpha}$  and  $\dot{\theta}$ .

A computer study of the situation where the missile is capable of unlimited acceleration is of considerable importance because analytic miss-distance data are available as checks. A typical solution obtained with the preceding setup is illustrated in Fig. 5.2-2. Since solution coding and data recording play an important role in a study of this type, some of the techniques developed during this study are considered in Appendix E.

Other studies<sup>4</sup> had established the fact that the target maneuver producing the greatest miss involves a head-on approach, with the target making a single circular turn at a critical range which occurs between 3000 and 8000 feet for the usual missile-control-system parameters.

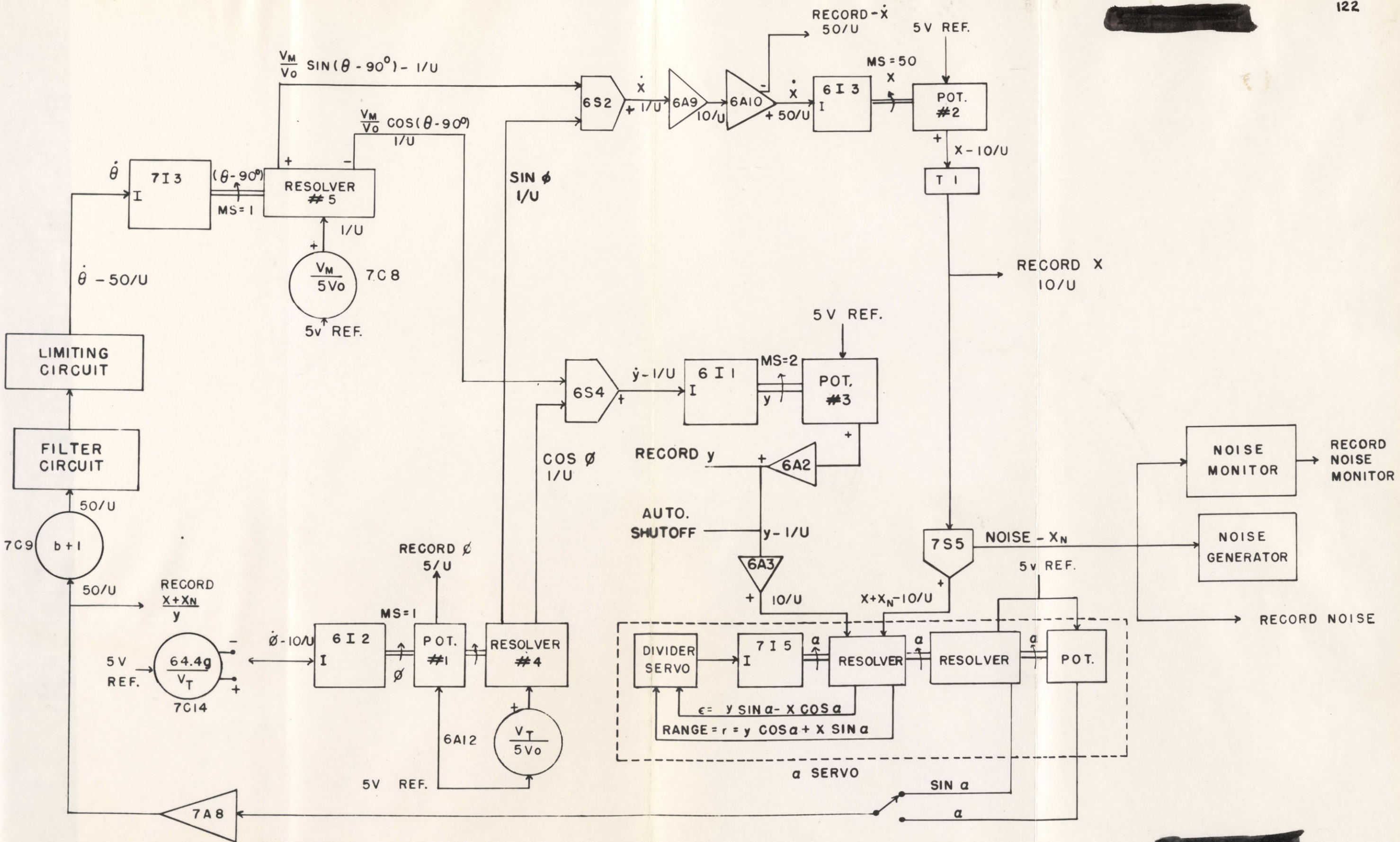
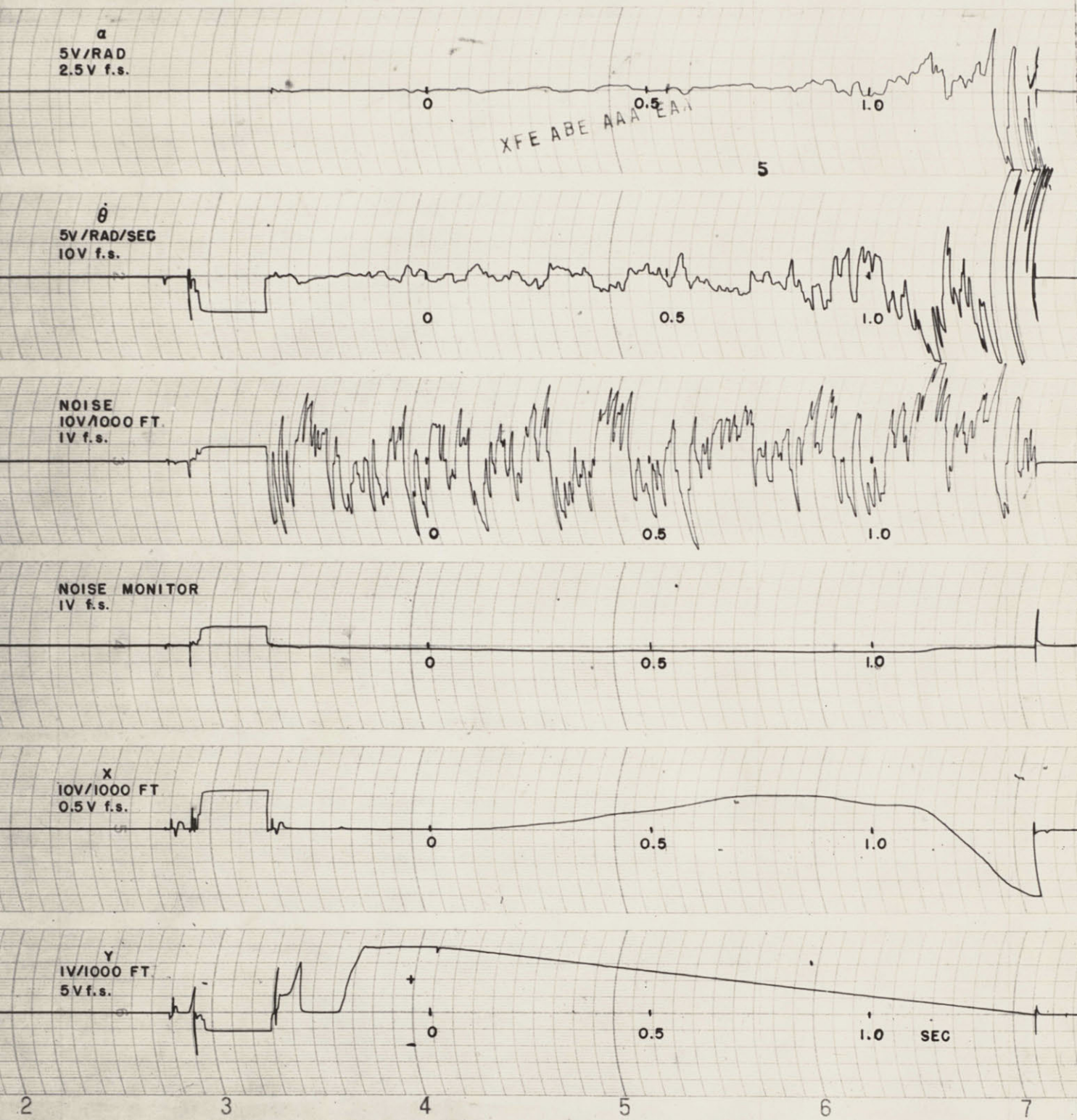


FIG. 5.2-1. BASIC COMPUTER SETUP DIAGRAM FOR CODES AA, AB, AC, AND AD.

FIG. 5.2-1.



FLIGHT SIMULATOR CHART NO. GC-265

FLIGHT SIMUL

$b=1.6$

$\Phi_N = 10 \text{ FT}^2/\text{RAD/SEC}$

$a_T = 4g$

$r_1 = 4000 \text{ FT}$

$\omega_{SS} = 108 \text{ RAD/SEC}$

$A = 0.5 \text{ SEC}$

FIG. 5.2-2. TYPICAL SOLUTIONS WITH SIMPLE-LAG FILTER, NOISE, AND NO LIMITING.

██████████

This work, in addition to the analysis discussed in Chap. 1, had indicated that for the unlimited case, at least, values of  $A = 0.5$  sec and  $(b+1) = 6$  are nearly optimum.

Furthermore, with these values and a maximum available lateral acceleration of  $10g$ , which corresponds to what the best missiles now under development can achieve at altitudes up to approximately 25,000 feet, and a target turn of  $4g$ , which is also reasonable at low altitudes, the maximum miss in the head-on noise-free case occurs if the target begins to turn at a range of approximately 4000 feet. This tactical situation was, therefore, used as a standard for the greatest portion of this investigation, since it was felt that a control system which gave acceptable results in this case would also be acceptable in the majority of situations. To obtain a complete evaluation, the final system should, of course, be studied under other situations and should also be evaluated in relation to its ability to remove initial launching errors.

In this study, the rms value of the miss was generally used as a criterion of the worth of a particular system, although the probability of a miss less than 50 feet was also calculated for some cases as a figure of merit. In a final analysis, it can be argued that the "probability of kill" is a better criterion. The calculation of this probability depends basically on the rms value of the miss distance but, in addition, depends upon the exposed area and vulnerability of the target, as well as the nature of the warhead used in the missile. It is

██████████

felt that such factors unnecessarily complicate a basic investigation without aiding much in evaluating the relative worth of various control systems.

In the first studies involving noise, the noise was injected ahead of the  $\alpha$  servo as a distance  $x_N$  and a perturbed angle  $\alpha$  was calculated (Sec. 3.45), as shown in the setup diagram of Fig. 5.2-1. In spite of the fact that the  $\alpha$  servo was being overloaded by the noise toward the end of each run, this setup gave reasonably good results in the unlimited case, since for this case the miss was essentially independent of the bandwidth of the noise. Later work on the limited-acceleration case showed the necessity of avoiding unintentional limiting of any type. In an effort to avoid limiting difficulties, the second scheme discussed in Sec. 3.45 for inserting noise was tried. The setup diagram of Fig. 5.2-3 shows the arrangement used in this method of calculation. A few runs were made with this scheme but, since the divider servo employed was not sufficiently accurate to be considered a true computing element, very little was learned from these tests.

The third method discussed in Sec. 3.45 was finally adopted as being the best available computing arrangement. This setup, shown in Fig. 5.2-4, employs the same linearization in the computation of  $\alpha$  as was used in the analytic work. The angle  $\alpha$  is taken merely as  $(x + x_N)/y$ , rather than as the arc tangent of  $(x + x_N)/y$ .

For maneuvering targets and no noise, a comparison of the results derived from the analytic study with those obtained using point-by-point



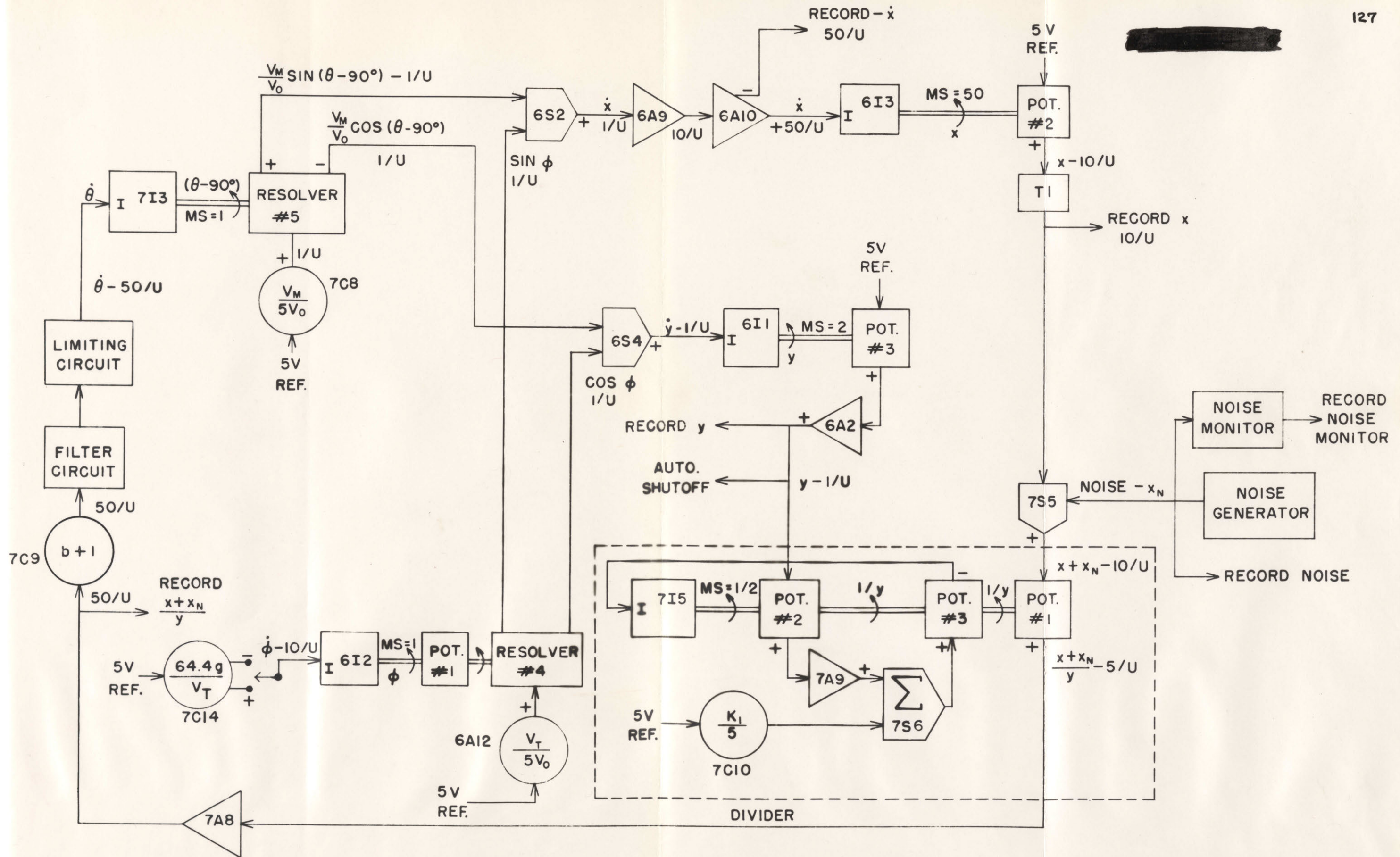


FIG. 5.2-4. COMPUTER SETUP WITH DIVIDER SERVO REPLACING  $\alpha$  SERVO.

integration with desk calculators verified that this approximation yielded a very high degree of accuracy. In the noise studies without limiting the close agreement finally obtained between experimental and analytical results is demonstrated in Fig. 5.2-5 for a particular set of parameters. Each point on this curve corresponds with the analytic value to within the error to be expected from the statistical nature of the problem, plus the expected machine errors.

The histogram obtained from a typical set of runs with unlimited available acceleration is shown in Fig. 5.2-6. The dotted curve in this figure is an approximation to the experimental data while the solid line is a normal distribution curve drawn with the standard duration obtained using Eq. (1.4-7).

### 5.3. Methods of Introducing Limiting.

Two different ways of instrumenting the equation

$$A\ddot{\theta} + \dot{\theta} = (b+1)\dot{\alpha}, \quad \text{for } \dot{\theta}_c < \dot{\theta}_{lim} \quad (5.3-1)$$

are shown in Fig. 5.3-1. For convenience in machine setup, the input to this portion of the computer is taken as  $(b+1)\dot{\alpha}$  rather than  $(b+1)\ddot{\alpha}$ . In method "a" the quantity  $(b+1)\dot{\alpha}$  is filtered to give  $\dot{\theta}_c$ , which might be termed the called-for acceleration. Replacing the filter  $1/(As+1)$  operating on an input signal  $(b+1)\dot{\alpha}$  by a filter  $s/(As+1)$  with an input  $(b+1)\ddot{\alpha}$  gives the same output. The resulting  $\dot{\theta}_c$  signal is then limited and passed through an integrator to give  $\theta$ . For case "a",

$$A\ddot{\theta}_c + \dot{\theta}_c = (b+1)\ddot{\alpha}$$

This case might therefore represent the situation where an electronic filter, with a transfer function of  $(b+1)/(As+1)$ , occurs in the missile

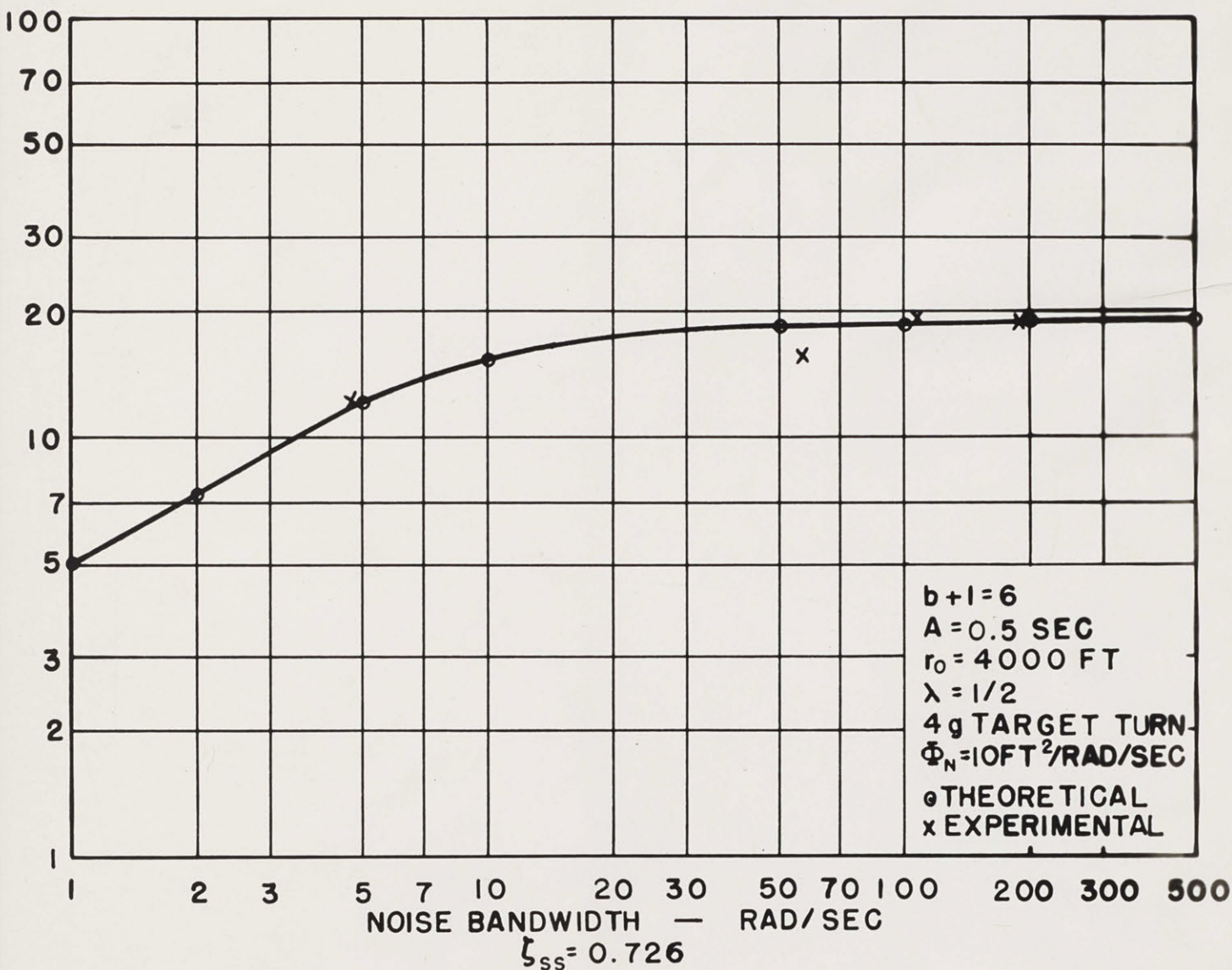


**FIG. 5.2-5. COMPARISON BETWEEN ANALYTIC AND MACHINE RESULTS OF MISS vs. NOISE BANDWIDTH IN UNLIMITED ACCELERATION CASE.**

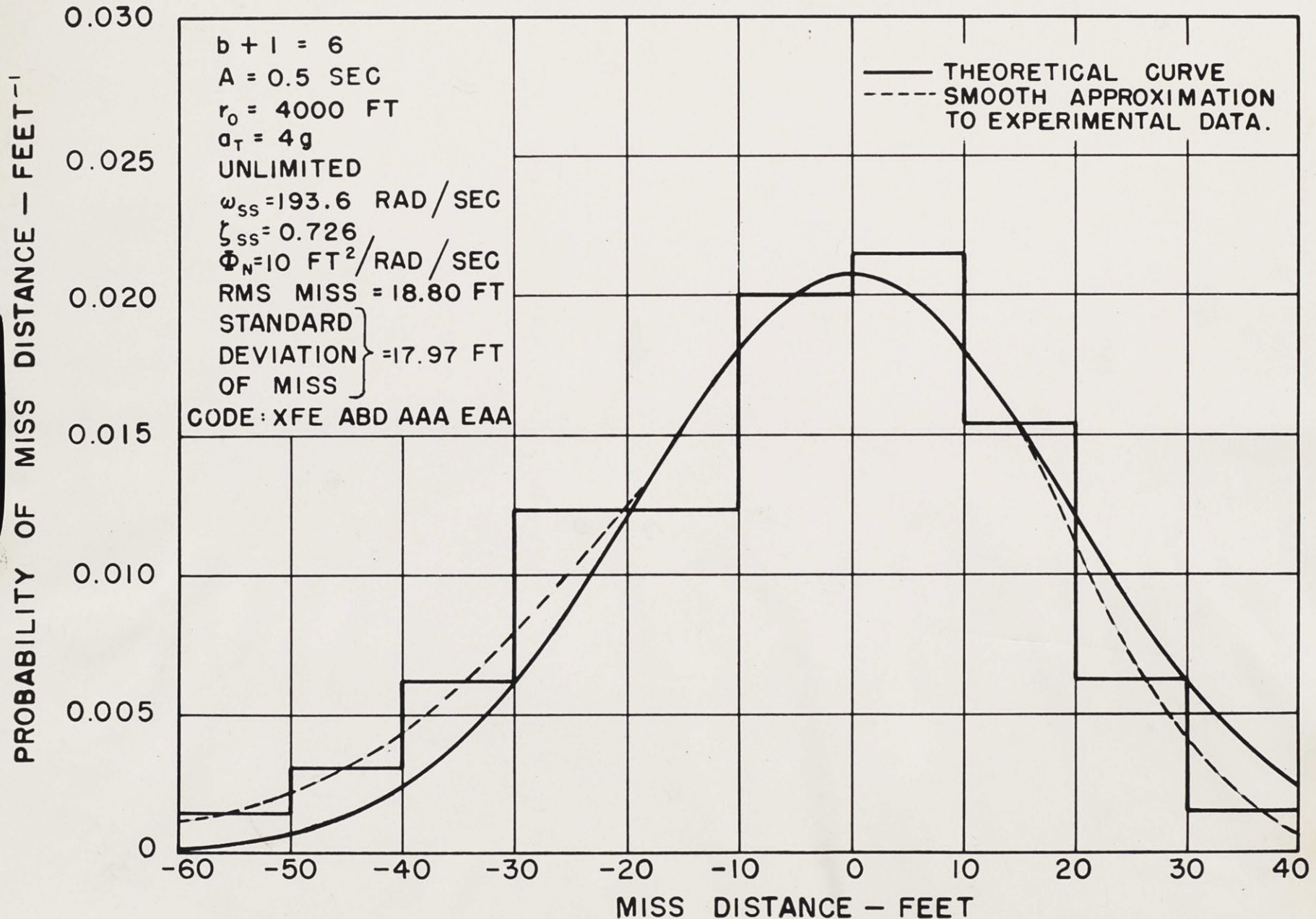
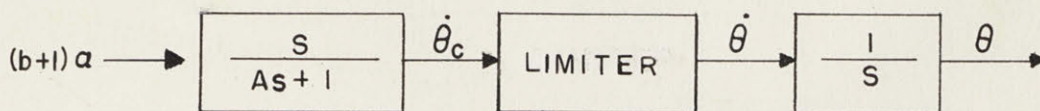
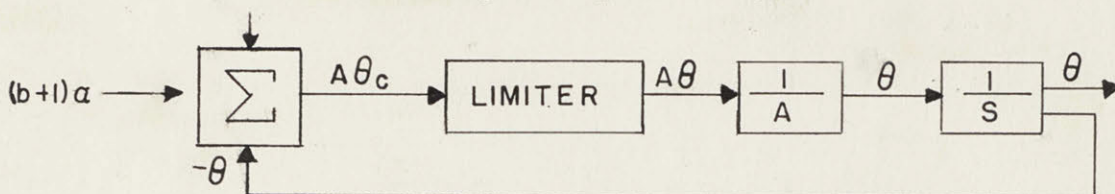


FIG. 5.2-6. HISTOGRAM OF MISS DISTANCES IN UNLIMITED ACCELERATION CASE.

between the  $\dot{\alpha}$  signal and the  $\dot{\theta}_c$  signal. Limiting takes place on the  $\dot{\theta}_c$  signal with no local feedback from the actual missile  $\dot{\theta}$  or  $\theta$ .



a. Open-loop limiting.



b. Closed-loop limiting.

Fig. 5.3-1. Two means of introducing limiting.

In method "b" limiting occurs within a feedback loop and the control equation assumes the form

$$A\ddot{\theta}_c + \dot{\theta} = (b+1)\dot{\alpha}.$$

This represents the situation where a feedback signal corresponding to  $\dot{\theta}$  is obtained locally either from an angular accelerometer or a gyro mounted on the missile. This second setup requires that a constant of integration,  $-\gamma$ , be added to account for the fact that one integration of Eq. (5.3-1) has already been performed.

If the limits are not exceeded, both of these arrangements give exactly the same output, but when limiting occurs the results may differ. Furthermore, so long as the called-for acceleration always

remains above the limiting value, once this value is attained, the two schemes give the same results. Different acceleration programs would be expected, however, in cases where  $\dot{\theta}_c$  is going into and out of the limits.

A general study might well concern itself with either one or both of these arrangements or possibly additional arrangements. In the study of a particular missile a careful analysis should be made to insure that the filtering and limiting be simulated in the manner in which they actually occur.

Some of the earliest simulator work done for this study employed closed-loop limiting, as shown in Fig. 5.3-1b. This setup was used principally to save an integrator, but might well have represented a practical missile system. Later studies employed the open-loop limiting represented in Fig. 5.3-1a because it was felt that this more nearly approximates the type of limiting occurring in the Meteor missile.

Another condition to be considered concerns limiting and energy storage. A simple example of this situation is shown in Fig. 5.3-2.

In Fig. 5.3-2a the output voltage is limited when the voltage across the condenser C exceeds the limiting level, but the voltage across C continues to rise as the input is further increased. In Fig. 5.3-2b, the voltage across C is fixed at the limiting level, once this level is reached, regardless of how high the input signal may rise subsequently. It makes no difference in the output signal which method is used, so long as there is no question of the output signal dropping

below the limiting level, once this level is attained. It is readily seen, however, that for certain types of decreasing input signals the output could come out of the limits much earlier in the setup of Fig. 5.3-2b than in Fig. 5.3-2a.

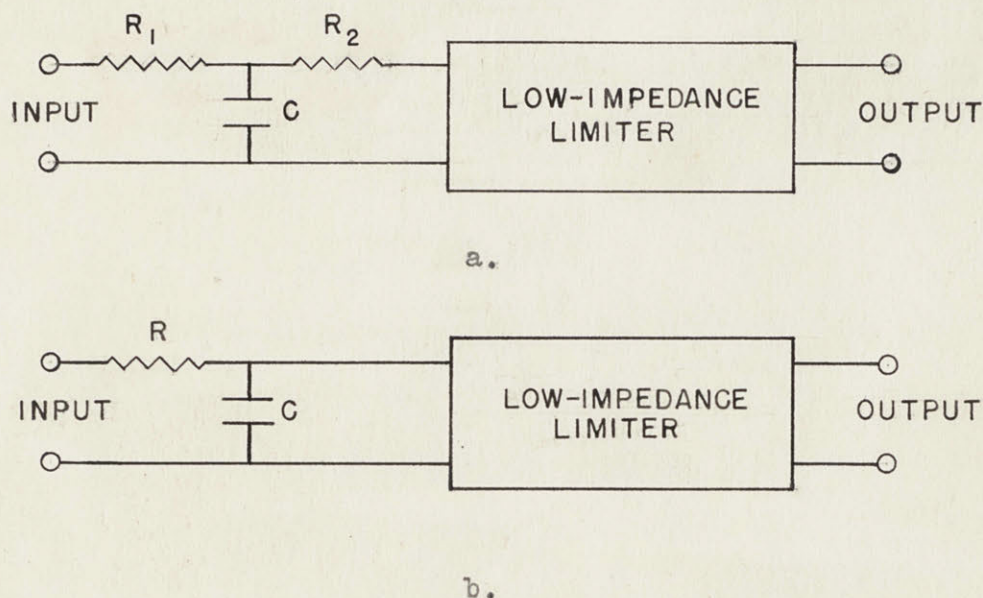


Fig. 5.3-2. Energy storage possibilities in a system with limiting.

In the case of higher order filters, such as quadratic and cubic systems, the number of energy-storage situations to be considered rises to two and three respectively.

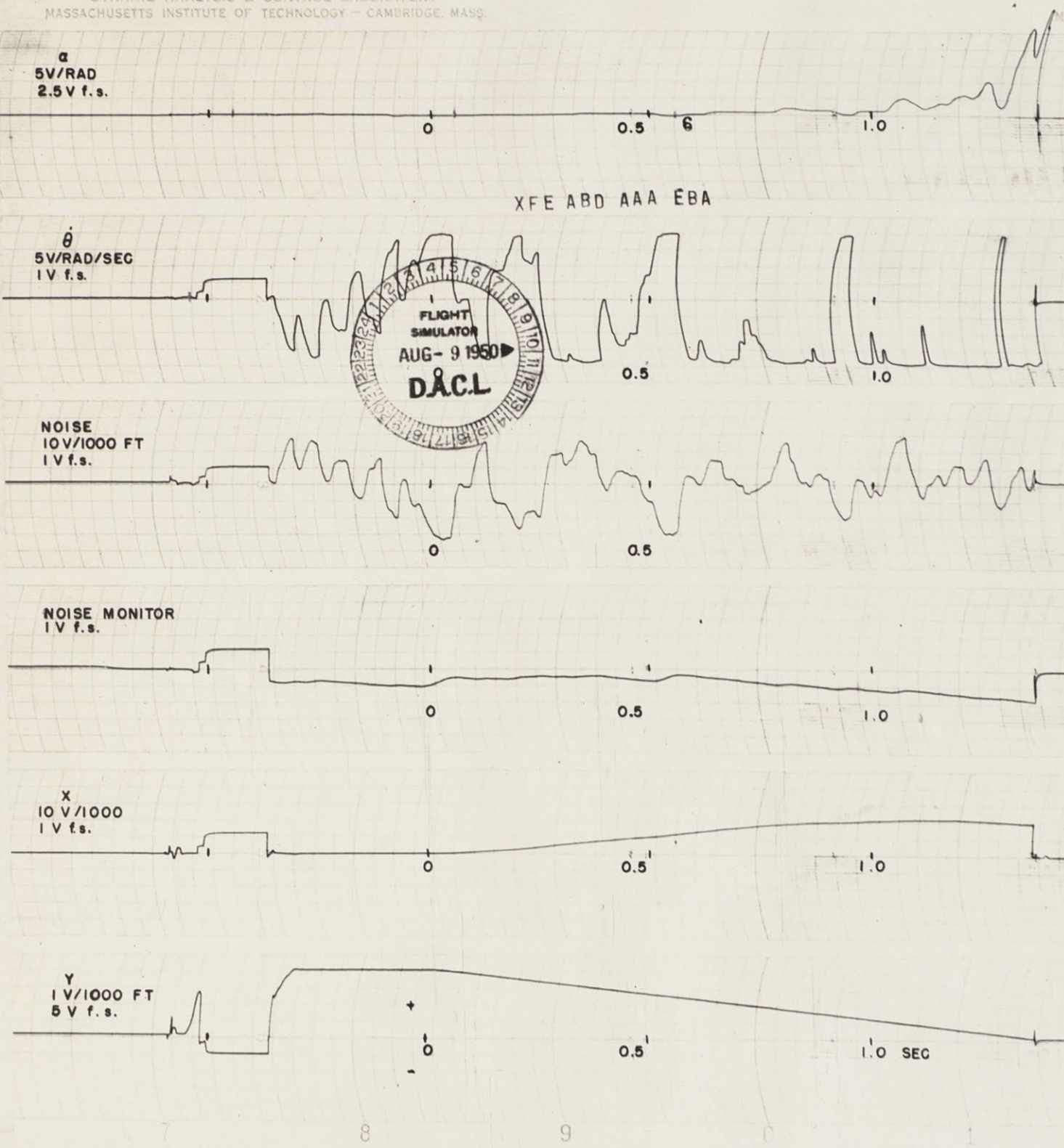
In this computer study the filters were simulated using electro-mechanical servo integrators and the limiters were of a completely nonreacting type. The limiter had no effect on the filter and the shafts of the integrators were free to continue to turn after the output signal reached the limits.

5.4. Results Obtained with Noise, Target Maneuver, and Limiting for the Proportional-navigation Problem Involving a Simple-lag Filter.

Figure 5.4-1 shows a typical simulator solution for a homing-missile trajectory problem involving a proportional-navigation-with-simple-lag control system, target maneuver, radar noise and acceleration limiting. When all cases of unintentional limiting in the simulator were eliminated, so that the broadband noise could be used, it was found that there is a marked dependence of miss on noise bandwidth for the problem involving noise, target maneuver, and limiting. It therefore becomes impossible to specify miss distances without also giving a complete description of the noise power spectrum.

Figure 5.4-2 shows as a function of the bandwidth of the noise the rms misses obtained in the standard tactical situation described in Sec. 5.2 for the cases of no limiting, a 10g limit, and a 5g limit. In these cases, the zero-frequency noise power density  $\Phi_N$  was held at  $10 \text{ ft}^2/\text{rad}/\text{sec}$ , with the consequence that the rms value of the glint noise increases along with its bandwidth. With the preceding power density, a bandwidth of 200 rad/sec represents an rms noise of 65 feet. This figure may be high by a factor of two but is still only approximately 90 per cent of the half-wing span of a B-29 and is therefore possible. Figure 5.4-3 shows a histogram of the miss distances obtained for a typical simple-lag control system.

DYNAMIC ANALYSIS & CONTROL LABORATORY  
 MASSACHUSETTS INSTITUTE OF TECHNOLOGY - CAMBRIDGE, MASS.



FLIGHT SIMULATOR CHART NO. GC 265

$b+1=6$   
 $r_1=4000$  FT

$\Phi_N = 10$  FT<sup>2</sup>/RAD/SEC  
 $\omega_{ss} = 55.2$  RAD/SEC

$a_T = 4g$   
 $A=0.5$  SEC

$a_{M,MAX} = 10g$

FIG. 5.4-1. TYPICAL SOLUTIONS WITH SIMPLE-LAG FILTER, NOISE, AND LIMITING.

$$A\ddot{\theta} + \dot{\theta} = (b+1)\dot{a}$$

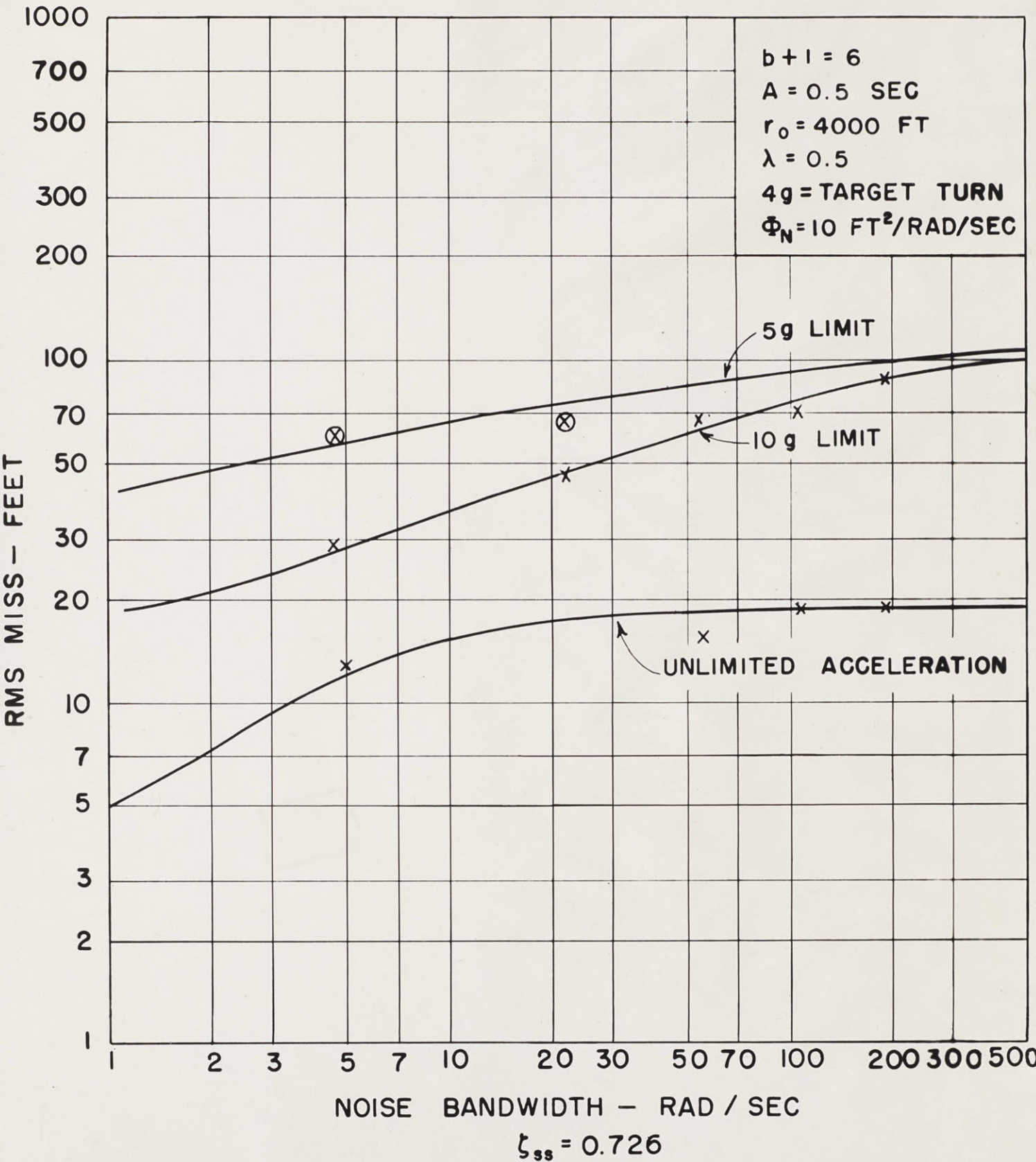


FIG. 5.4-2. RMS MISS DISTANCE VS. NOISE BANDWIDTH FOR SIMPLE-LAG CONTROL SYSTEMS.

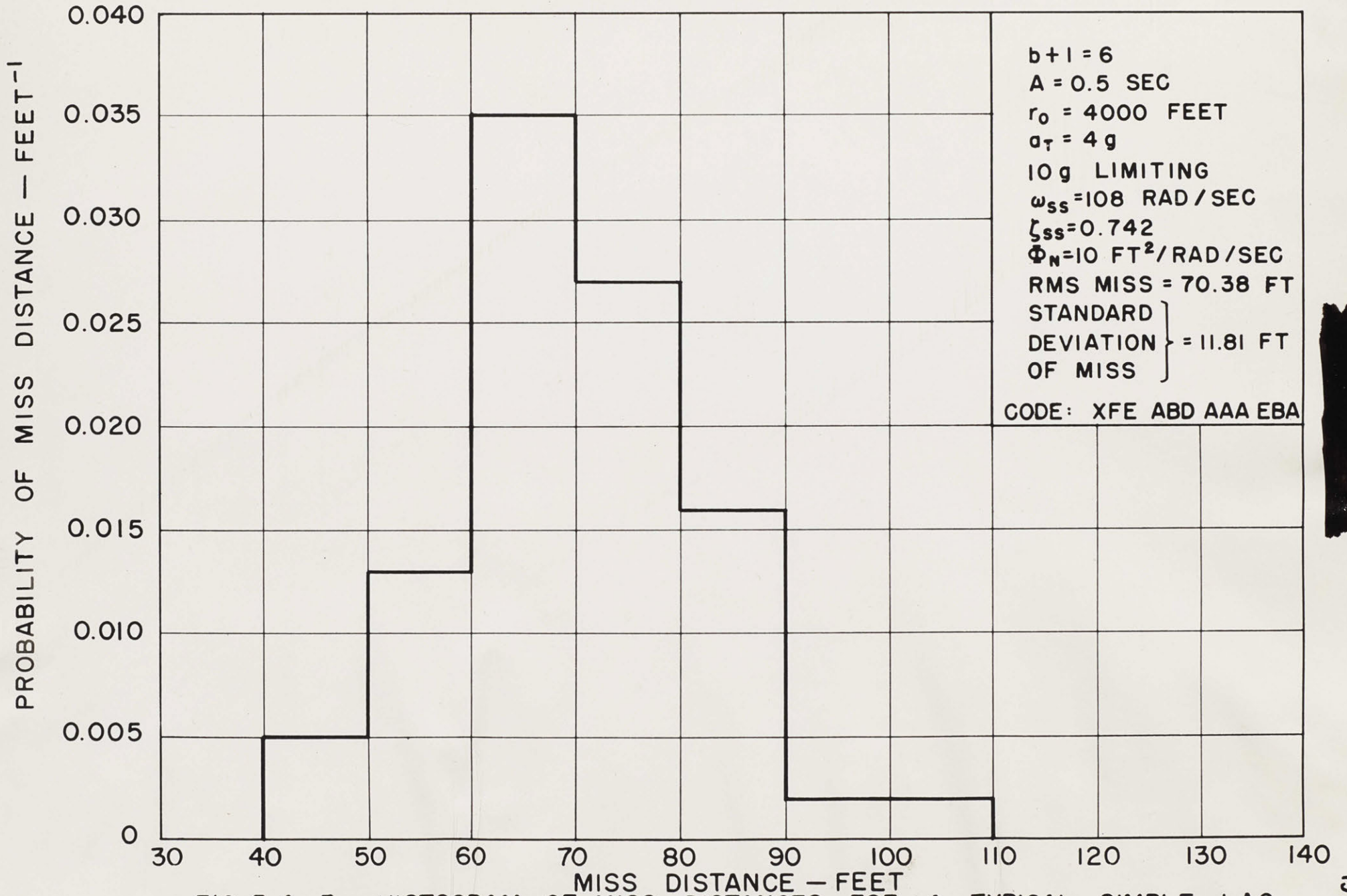


FIG. 5.4-3. HISTOGRAM OF MISS DISTANCES FOR A TYPICAL SIMPLE-LAG CONTROL SYSTEM.

The analysis of Figs. 5.4-2 and 5.4-3 is facilitated by calculating the distance the target moves normal to the line of sight from the beginning of its maneuver until collision. This distance is given by

$$x_T = (0.5)a_T t_f^2 \quad \text{ft} \quad (5.4-1)$$

where  $a_T$  is the lateral acceleration of the target in  $\text{ft}/\text{sec}^2$  and  $t_f$  is the time of flight in seconds.

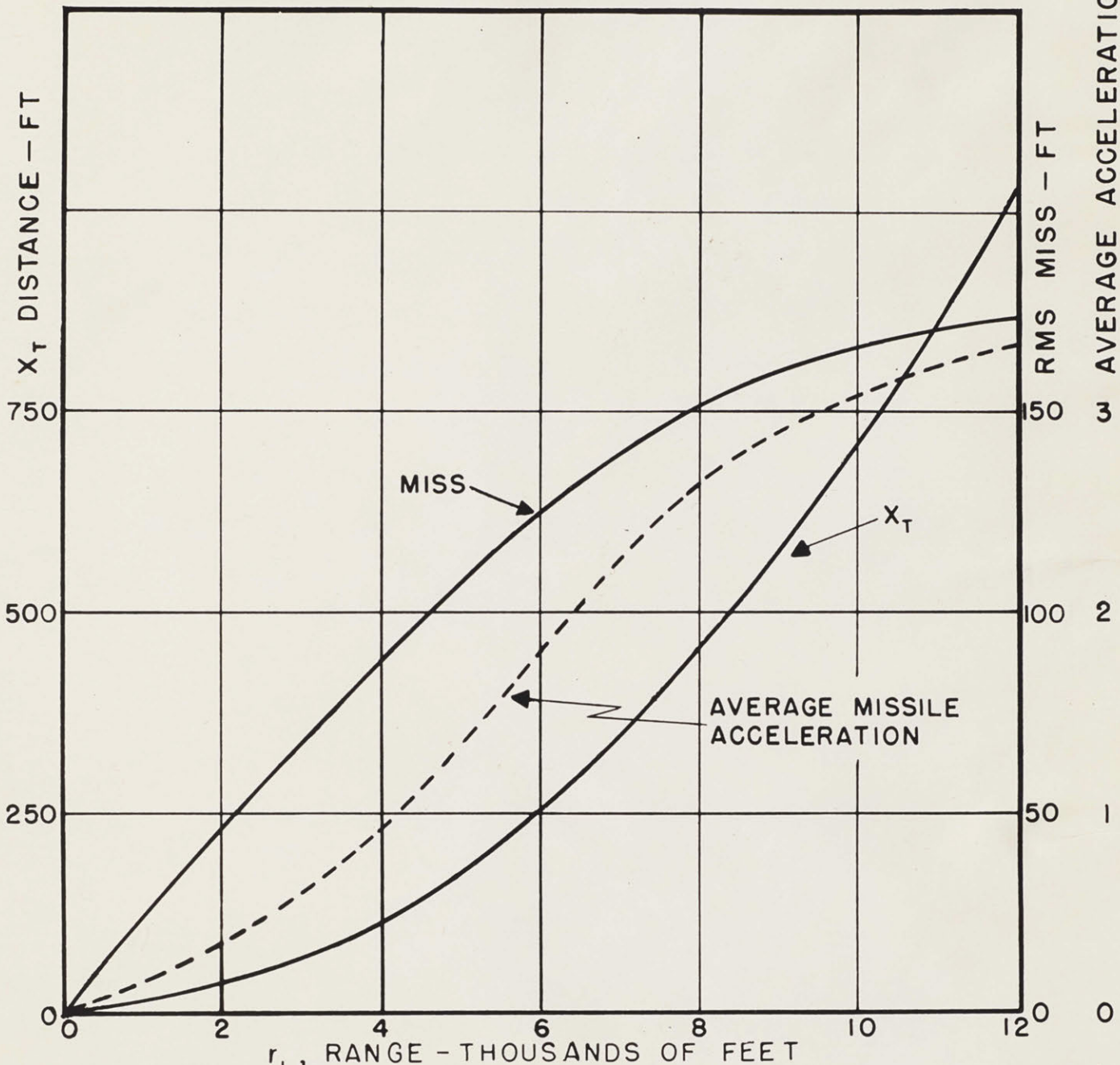
For the head-on case with a 4g turn beginning at 4000 feet

$$\begin{aligned} x_T &= (0.5)(32.2)(4)\left(\frac{4000}{2000 + 1000}\right)^2 \\ &= 114.5 \text{ ft.} \end{aligned}$$

For the preceding case the simulator gave an rms miss of 88 feet for a noise bandwidth of 193.6 rad/sec. This result shows that the missile has moved laterally only 26.5 feet during the time of flight. Therefore, the missile has developed an average acceleration of only 0.93g, whereas it is capable of 10g.

Figure 5.4-4 shows the results of similar calculations made for ranges up to 12,000 feet. The calculations show that, although the missile misses its target by a large amount, it is, on the average, developing only a fraction of its full acceleration. A more complete picture of what is taking place can be gained by comparing the  $\dot{\theta}$  programs obtained in typical solutions to the foregoing problems with the corresponding  $\dot{\theta}$  programs obtained for noise-free cases (Fig. 2.3-1 vs. Fig. 5.4-1).

For the 4000-foot case with broadband noise ( $\omega_{ss} = 193.6 \text{ rad/sec}$ ), the noise causes nearly the limiting value of  $\dot{\theta}$  to be developed, first



CONDITIONS:

1. INITIAL-COLLISION COURSE WITH A 4g TARGET TARGET TURN BEGINNING AT  $r_1$ .
2. MAXIMUM LATERAL ACCELERATION OF THE MISSILE EQUAL TO 10g.
3.  $\Phi_N = 10 \text{ FT}^2/\text{RAD}/\text{SEC}$ ,  $\omega_{SS} = 193.6 \text{ RAD}/\text{SEC}$ .

FIG. 5.4-4. TARGET MOVEMENT, MISS DISTANCE, AND AVERAGE MISSILE ACCELERATION VS. RANGE.

in one direction and then in the other, during the full length of the trajectory. The constant-turn target maneuver superimposes a bias, which increases steadily in one direction during the course of the flight, on the  $\dot{\theta}$  called for by the noise. If the noise were large enough to override completely the biasing term, the resulting acceleration would jump back and forth between the limiting values, following only the noise. Since the noise is distributed about zero with an average value of zero, the average acceleration developed by the missile in this case would, therefore, be zero with the result that the missile would develop no average lateral displacement during the flight (see Sec. 5.7). In the meantime, the target moves over by the amount

$$x_T = (0.5)a_T t_f^2 \text{ ft,} \quad (5.4-1)$$

which then becomes the value of the miss.

The effect of changes in the various parameters of the system may now be discussed in a qualitative way. Both the bandwidth and the zero-frequency power density of the noise become important in this situation. If these quantities are sufficiently large, the missile will develop no average acceleration during the course of the flight. The value of the noise required to produce this situation, however, depends on the range and the maximum acceleration the missile is able to develop.

If the noise were extremely large, the miss would increase with the square of the range. At an acceleration of 4g and a velocity of 1000 ft/sec the target flies in a circle with a radius of 7800 feet

and a period of 49 seconds. Accordingly, the  $(0.5)a_T t_f^2$  approximation to the lateral movement of the target is within approximately 3.5 per cent for values of  $t_f$  as large as 5 seconds. This means that, for head-on attack with ranges up to 15,000 feet or for tail attack with ranges up to 5000 feet, the  $(0.5)a_T t_f^2$  approximation is valid. With a power spectral density of  $\Phi_N = 10 \text{ ft}^2/\text{rad}/\text{sec}$  and a bandwidth of 193.6 rad/sec, the noise does not call for the full 10g acceleration from one side to the other until the range becomes approximately 4000 feet, or less. This figure can be obtained by inspection of the test solutions or can be calculated approximately with the assumption that  $\alpha$  and  $\dot{\theta}$  are related by a pure integration; that is,

$$\dot{\theta} = \left(\frac{b+1}{A}\right)\alpha.$$

With

$$V_M \dot{\theta}_{\max} = 10g = 322 \text{ ft}/\text{sec}^2,$$

$$\frac{b+1}{A} = 12,$$

and

$$\alpha = \frac{x_N}{r} = \frac{63}{r},$$

the range at which the rms called-for acceleration exactly equals the limiting value is determined as

$$r = \left(\frac{b+1}{A}\right) x_N \frac{V_M}{322} = \frac{(12)(63)(2000)}{322} = 4700 \text{ ft.}$$

For turns beginning at shorter ranges the miss would increase approximately as the square of the range. At the beginning of longer

range trajectories, however, since the noise does not require the full available acceleration, some is available for following the target maneuver, and the miss no longer increases appreciably with the range at which the maneuver is begun.

As the rms noise is increased by increasing the spectral density or the bandwidth, the range at which the noise requires the maximum available acceleration increases. For these longer ranges the miss is, therefore, larger with greater noise, whereas for the shorter ranges it is affected very little.

Analogous reasoning indicates that, as the maximum lateral acceleration which the missile is able to develop is reduced, the range at which noise alone drives  $\dot{\theta}$  from one limit to the other is also reduced or, for a given range, the spectral power density or the bandwidth of noise which calls for the full acceleration capabilities of the missile is reduced. Each of these effects tends to increase the miss with a decrease in the acceleration capability of the missile. The effect of a decrease in  $V_{M \max} \dot{\theta}$  from 10g to 5g, for example, is pronounced in those regions of operation where the 10g missile gives fair results in reducing the miss but is hardly recognizable where the missile already operates poorly.

So far, no mention has been made of the effect on the miss of the control-system parameters  $A$  and  $(b+1)$ . In the case of unlimited missile-acceleration capabilities a fairly sharp minimum in the miss distance is observed as either  $A$  or  $(b+1)$  is varied while the other is held constant (Fig. 5.4-5). In this case, an optimum ratio of  $A$  to  $(b+1)^{1.25}$  can be calculated for specific values of noise and target

A = 0.5 SEC  
 $r_0 = 4000$  FT  
 $\lambda = 1/2$   
 4g TARGET TURN

$\Phi_N = 10$  FT<sup>2</sup>/RAD/SEC  
 $\omega_{SS} = 100$  RAD/SEC  
 $\zeta_{SS} = 0.7$   
 INITIAL HEAD-ON COLLISION COURSE

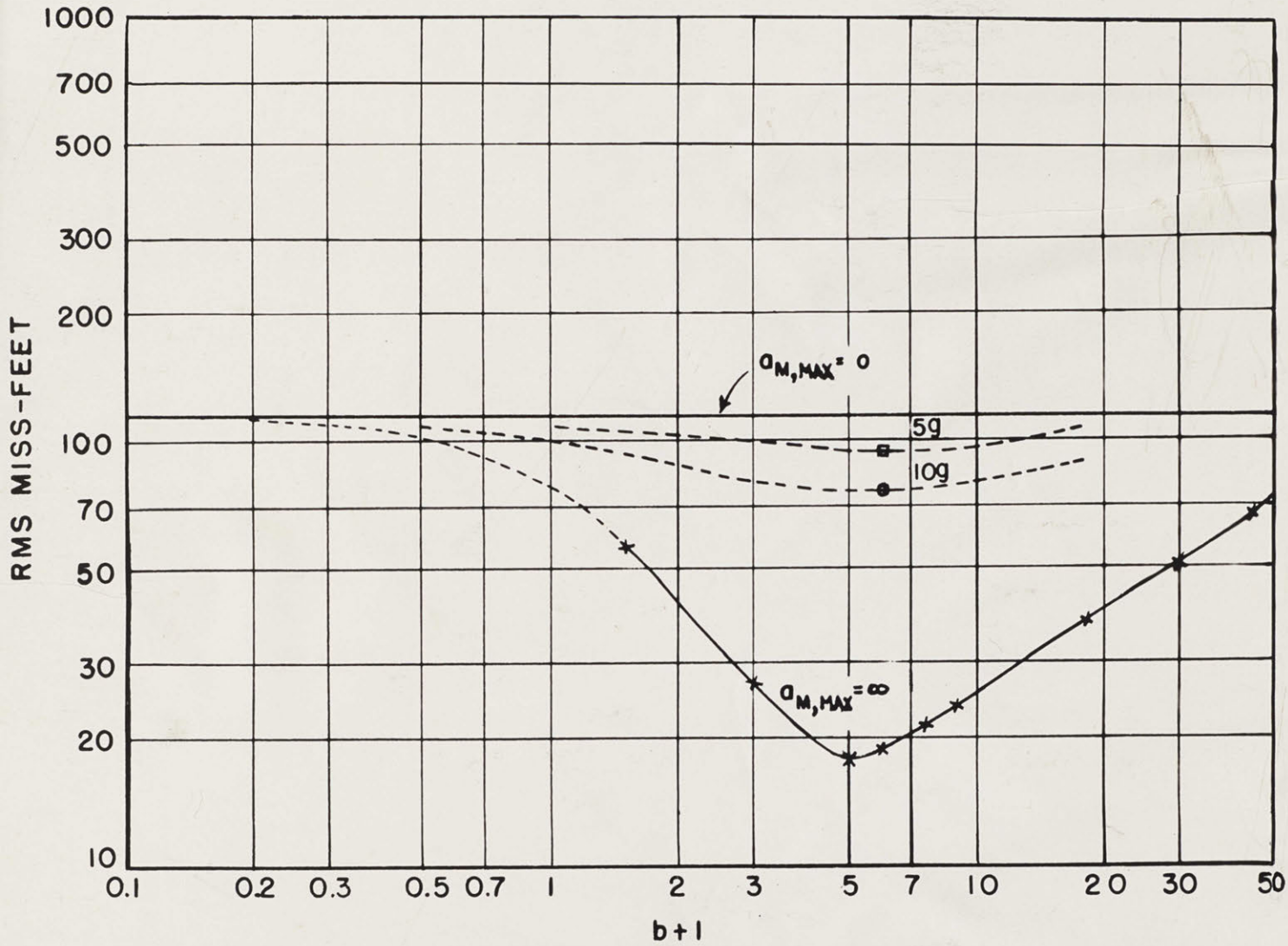


FIG. 5.4-5. RMS MISS vs. NAVIGATION CONSTANT.

maneuver by using Eq. (1.4-28). When  $A$  is independently made very large or  $(b+1)$  approaches zero, the miss approaches the  $(0.5)a_T t_f^2$  value.

As the acceleration capabilities of the missile are reduced, the minimum in the miss distance increases and becomes very broad, finally becoming merely the value  $(0.5)a_T t_f^2$  for all values of  $A$  and  $(b+1)$ , when the lateral acceleration is limited to zero. In cases where the missile acceleration is limited to the order of  $10g$ , the choices of  $A$  and  $(b+1)$  become very noncritical on the basis of miss alone. Nevertheless, lower values of  $A$  and higher values of  $(b+1)$  tend to make the control surfaces of the missile follow the noise to a larger degree. As a result, increased power is required to move the flaps and the drag is increased, thereby decreasing the velocity or requiring additional propulsive power if a constant velocity is to be maintained. Values of  $A$  from 0.5 to 1 second and values of  $(b+1)$  of 5 to 6 appear to be most suitable. The results given here show that the simple-lag system would perform poorly in the face of broadband noise, both as regards excessive miss distance (greater than 50 feet) and excessive power requirements. Since no information is available at this time to show that the noise does not spread over a band of 100 or more rad/sec, the only safe approach appears to be to attempt to design a control system which operates satisfactorily in the face of broadband noise. Consequently, control systems employing quadratic and cubic filters are examined.

### 5.5. Proportional-navigation System with Quadratic Filter.

The simple-lag system is represented as

$$\left[ \frac{(b+1)}{As+1} \right] \dot{a} = \dot{\theta} . \quad (5.5-1)$$

The corresponding quadratic system is

$$\left[ \frac{(b+1)}{\frac{s^2}{\omega_F^2} + \frac{2\zeta_F s}{\omega_F} + 1} \right] \dot{a} = \left[ \frac{(b+1)}{d_2 s^2 + d_1 s + 1} \right] \dot{a} = \dot{\theta} . \quad (5.5-2)$$

A starting point for investigating this system can be obtained by equating the effective bandwidths of the simple-lag and quadratic systems.

$$\frac{\pi}{2} \frac{1}{A} = \frac{\pi}{4\zeta_F} \omega_F$$

or

$$\frac{\omega_F}{\zeta_F} = \frac{2}{A} . \quad (5.5-3)$$

With  $A = 0.5$  second and  $\zeta_F = 0.707$ , Eq. (5.5-3) yields  $\omega_F = 2.8$  rad/sec.

The simulator setup used in the study of the quadratic system is the same as shown in Fig. 5.2-4, but with the quadratic-filter arrangement shown in Fig. 5.5-1.

The first tests made during the study of the quadratic system were for the purpose of evaluating the ability of the system to follow target maneuvers in the absence of noise. All systems which, in this test, gave a miss distance greater than 50 feet could be eliminated immediately on the grounds of being too slow. The results of these tests in the standard tactical situation discussed in Sec. 5.2

$$\frac{\dot{\theta}}{(b+1)\alpha} = sF(s) = s \left[ \frac{c_1 s + 1}{d_2 s^2 + d_1 s + 1} \right]$$

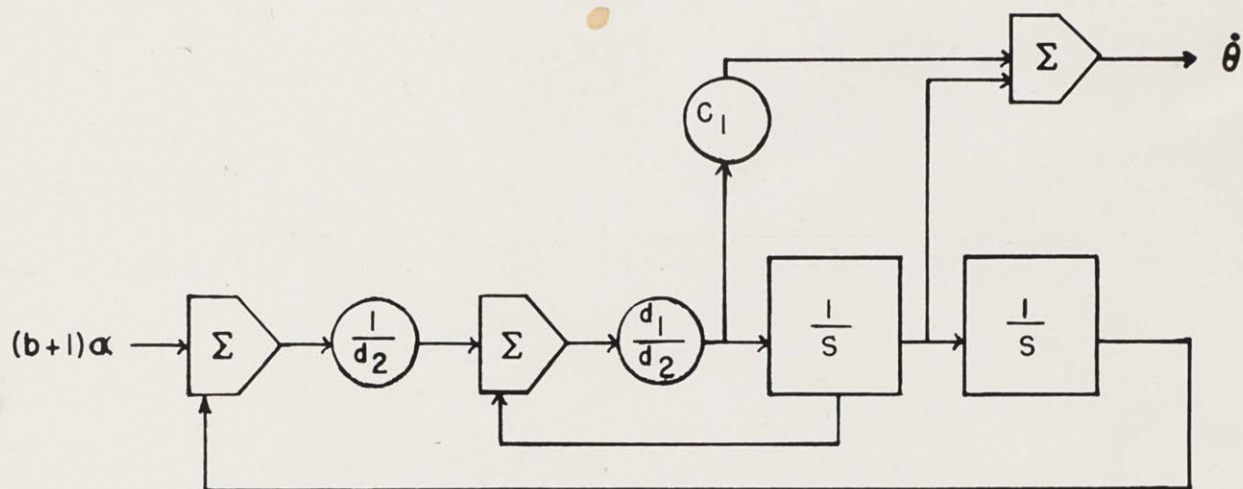


FIG. 5.5-1. BLOCK DIAGRAM OF QUADRATIC FILTER.

(maximum missile acceleration of 10g, head-on approach with 4g target turn beginning at 4000 feet) are shown in Fig. 5.5-2 for several combinations of  $(b+1)$ ,  $\omega_F$ , and  $\zeta_F$ . These tests indicate that systems with  $\omega_F$  greater than approximately 2 rad/sec and  $(b+1)$  larger than 4 are fast enough to keep the miss distance below 50 feet from this type of target maneuver.

Acceptable miss distances (less than 50 feet) can be achieved with filter bandwidths as low as 1.0 rad/sec if very large values of  $(b+1)$  are employed. A strong possibility exists, however, that systems with such high values of  $(b+1)$  will lead to instability problems in actual missile systems.

Figure 5.5-3 shows the effect on the miss distance of the range at which the target begins its turn for the case of a quadratic-filter system with  $\omega_F = 3.33$  rad/sec and  $\zeta_F = 1.0$ . These results indicate that in order to keep the no-noise miss below 50 feet for all ranges the value of  $(b+1)$  must be at least 6.

Noise was next added to the system and further tests were made. The increased number of parameters in the quadratic system and the statistical nature of the general problem, made impossible the collection of sufficient data to allow the formulation of definite conclusions. The principle results obtained are shown in Fig. 5.5-4; a typical solution involving noise, limiting, and a quadratic control system is shown in Fig. 5.5-5; a histogram of miss distances for this same system is shown in Fig. 5.5-6. It appears from the limited data that the optimum is rather broad and occurs for a system with an  $\omega_F$

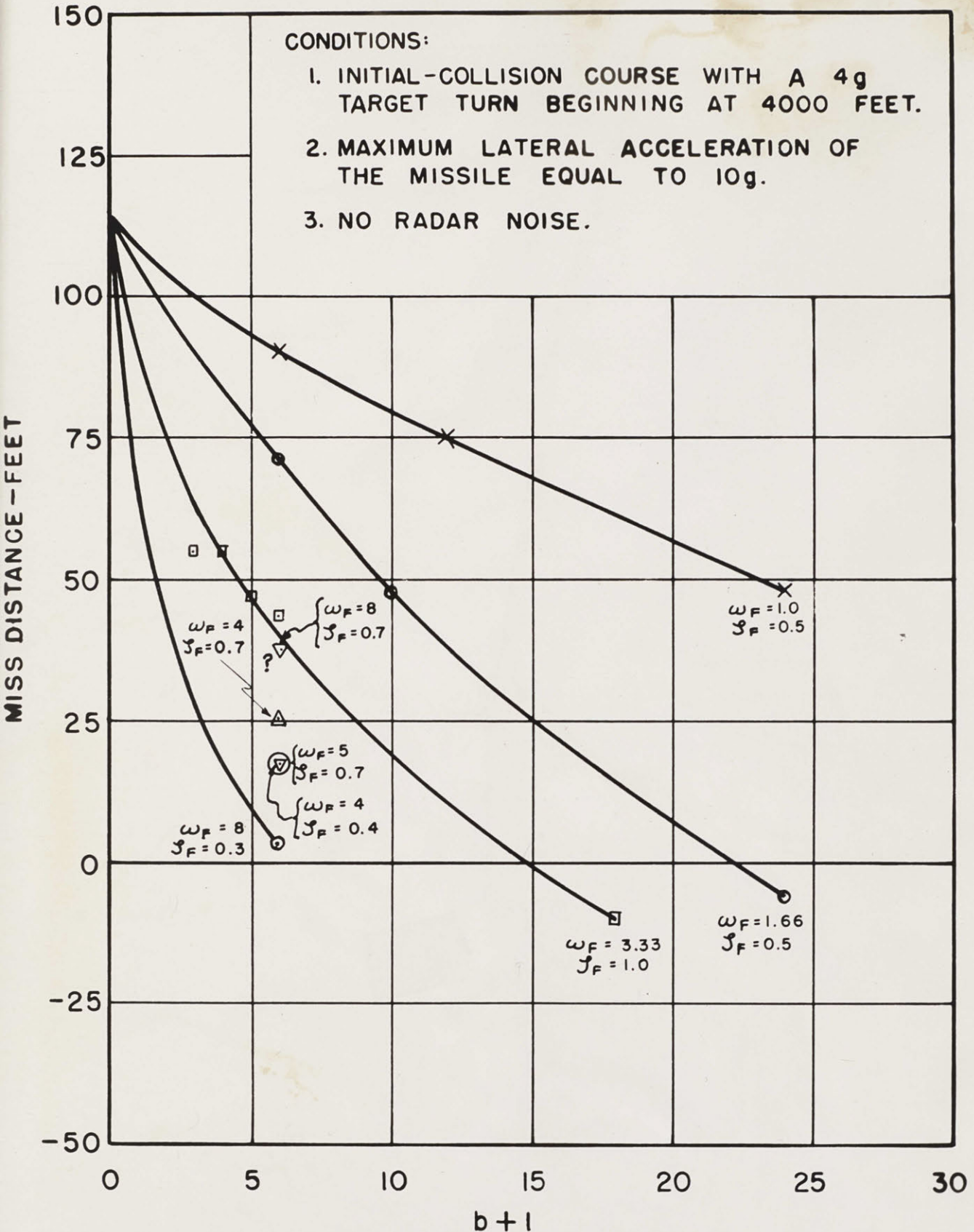


FIG. 5.5-2. MISS DISTANCES OBTAINED WITH MISSILES USING QUADRATIC CONTROL SYSTEMS AND OPERATING IN THE ABSENCE OF RADAR NOISE.

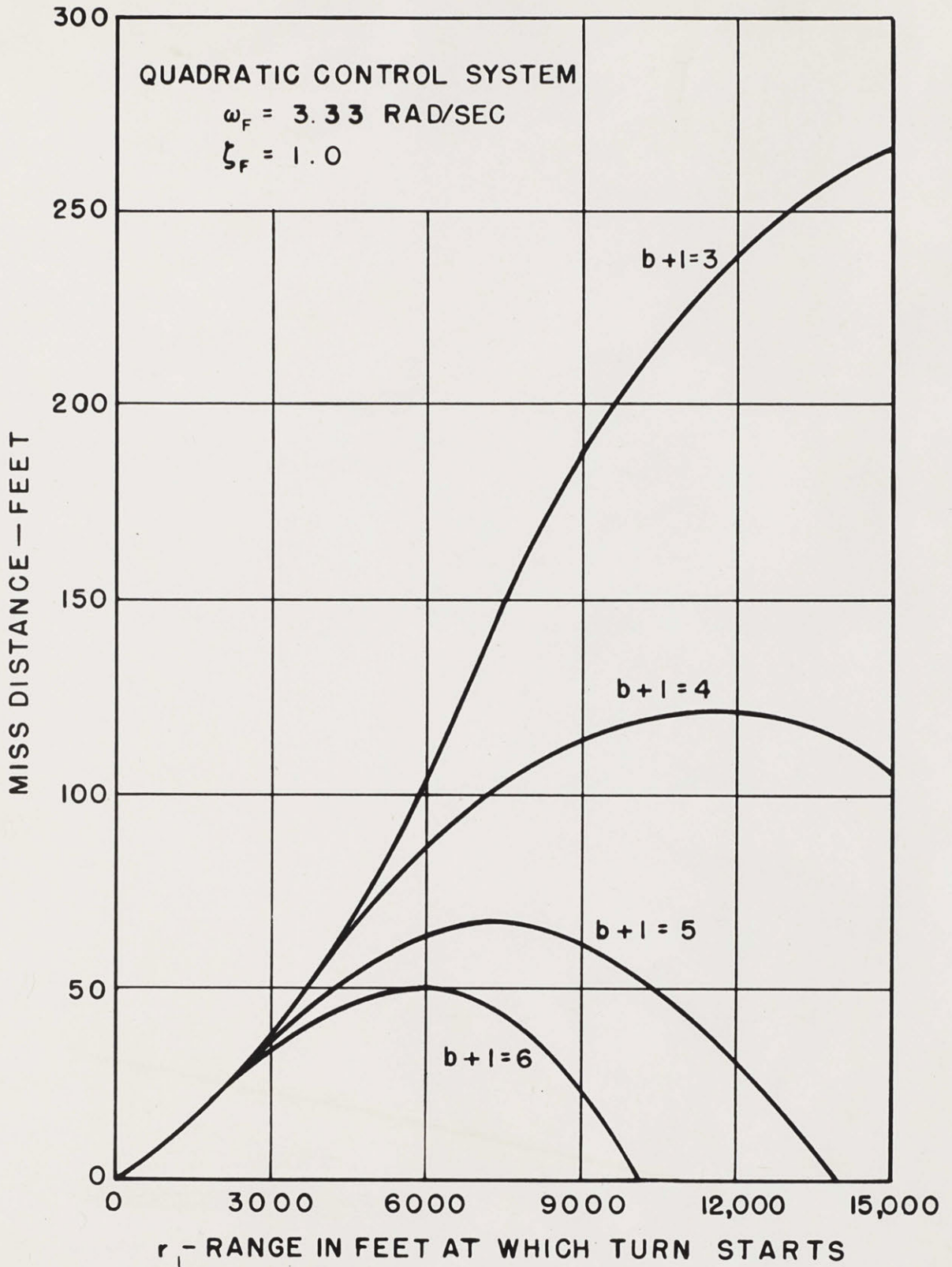


FIG. 5.5-3. MISS DISTANCE CAUSED BY TARGET MANEUVER. NO LAUNCHING ERROR. NO NOISE.

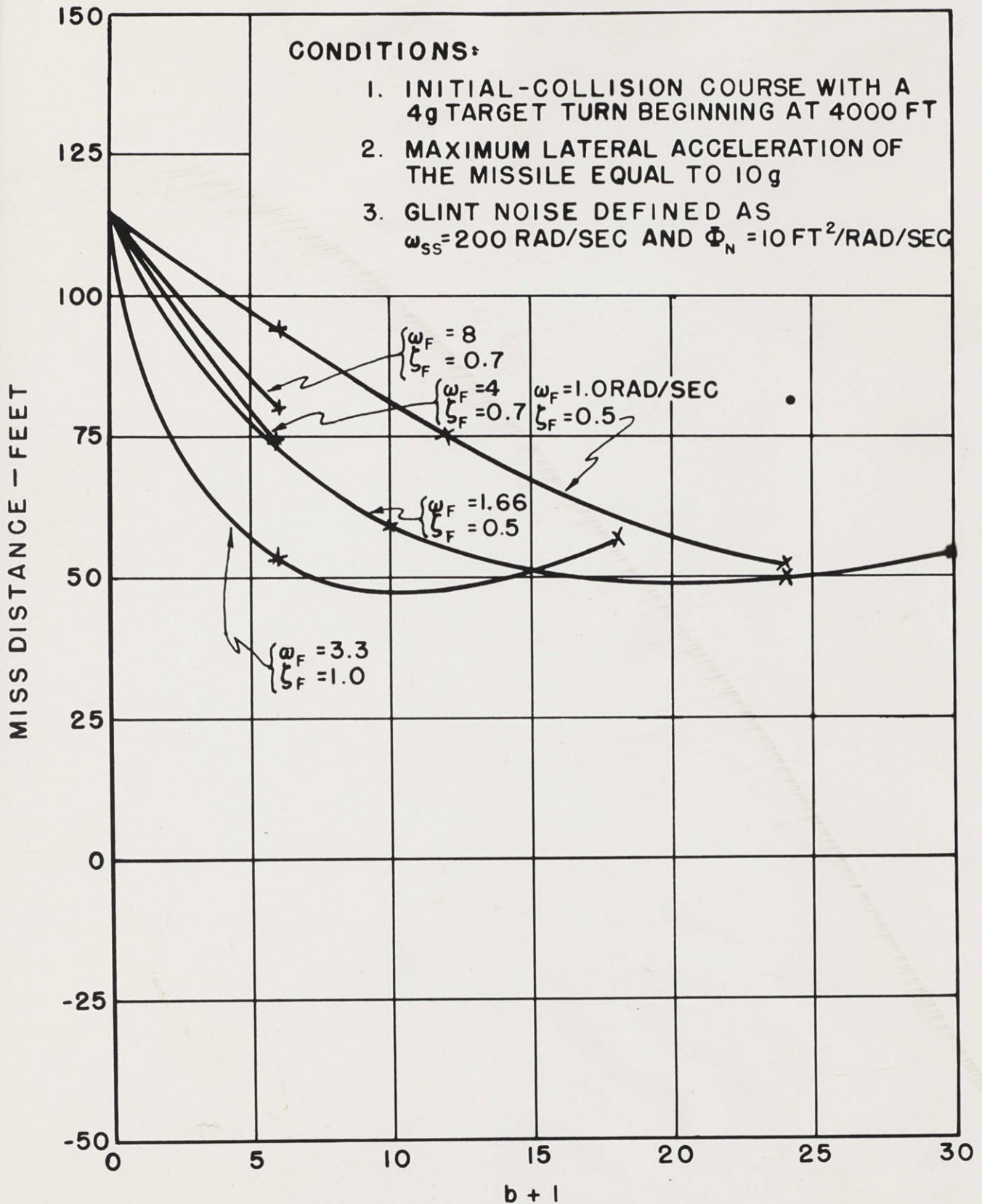


FIG. 5.5-4. MISS DISTANCES OBTAINED WITH MISSILES USING QUADRATIC CONTROL SYSTEMS AND OPERATING IN THE PRESENCE OF RADAR NOISE.



$a = \frac{1}{4}$   
 5v/RAD/SEC  
 2.5v f.s.

ACA BBH BAA ABB

19

$\theta$   
 5v/RAD/SEC  
 1v f.s.

NOISE  
 10v/1000FT  
 2.5v f.s.

NOISE MONITOR  
 1v f.s.

X  
 10v/1000 FT  
 1v f.s.

Y  
 1v/1000 FT  
 5v f.s.

+

0

-

→ SEC

FLIGHT SIMULATOR CHART NO. GC-265

$b + 1 = 6$   
 $r_1 = 4000 \text{ FT}$

$\Phi_N = 10 \text{ FT}^2 / \text{RAD/SEC}$   
 $\omega_{SS} = 194. \text{ RAD/SEC}$

$\omega_F = 4 \text{ RAD/SEC}$   
 $\zeta_F = 0.7$

$a_T = 4g$   
 $a_{M \text{ MAX}} = 10g$

FIG. 5.5-5. TYPICAL SOLUTION INVOLVING NOISE, TARGET MANEUVER, LIMITING, AND A QUADRATIC CONTROL SYSTEM.

PROBABILITY DENSITY OF MISS DISTANCE - FEET<sup>-1</sup>

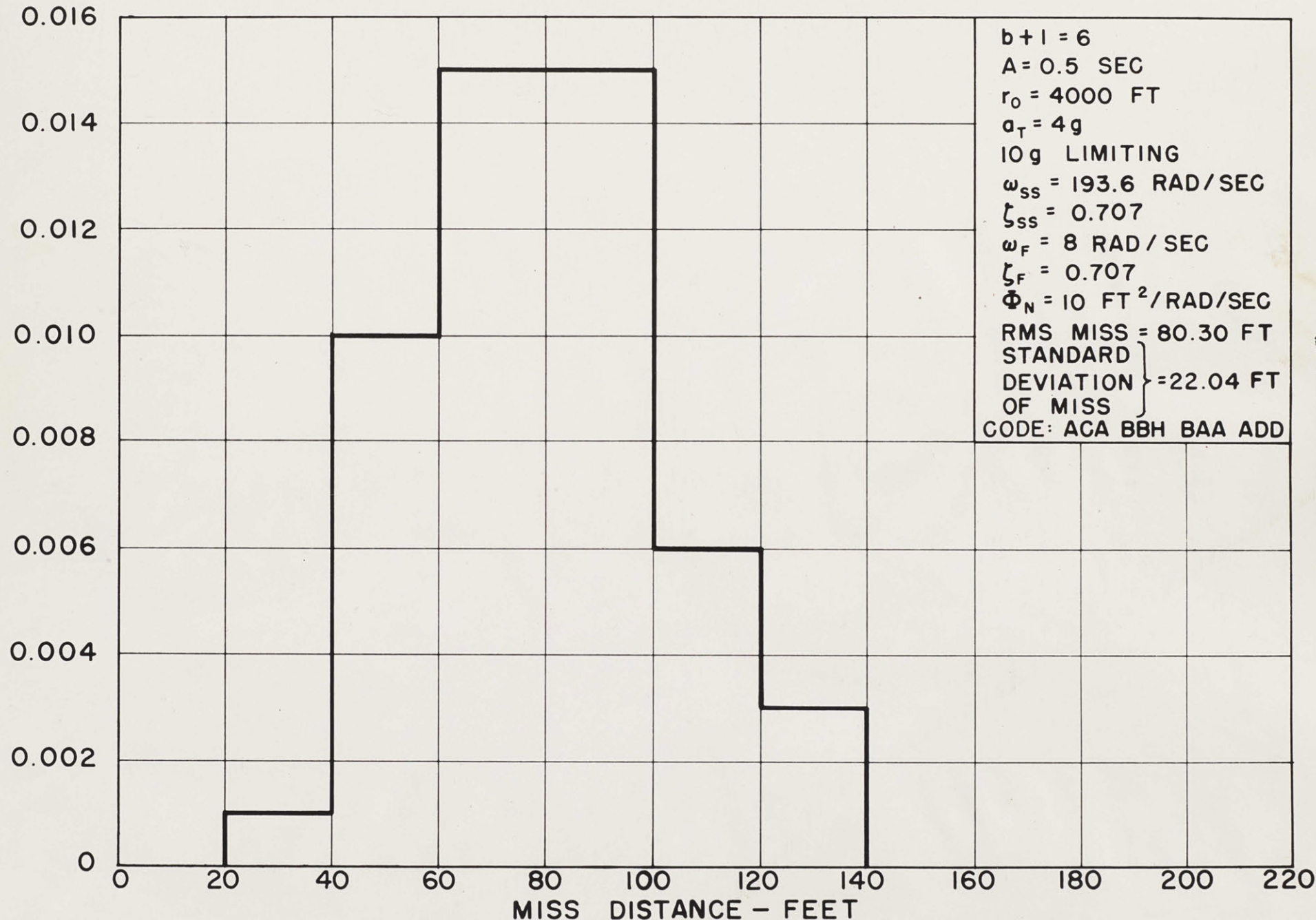


FIG. 5.5-6. HISTOGRAM OF MISS DISTANCES FOR MISSILE WITH A QUADRATIC CONTROL SYSTEM.

of approximately 3.3 rad/sec, a  $\zeta_F$  of 1.0 and a  $(b+1)$  of 5 or 6. A partial rerun of these data was made several months after these values were selected and it was found that somewhat better results were obtained with higher values of  $\omega_F$  (of the order of 8 rad/sec). The large value of miss obtained with no noise for the system with  $\omega_F = 8$  rad/sec and  $\zeta_F = 0.707$  (see Fig. 5.5-2) leads to the conclusion that some parameter in the computer was probably incorrectly set during this part of the study. Further studies should be made to clear up this ambiguity.

For the value of the spectral density of the noise which was used in collecting the data of Fig. 5.5-4 a comparison of the results presented in Figs. 5.5-2 and 5.5-4 indicates that the quadratic system with  $\omega_F$  equal to one radian per second behaves the same, whether or not noise is present in the system. Even for an  $\omega_F$  equal to 3.3 radians per second, the miss is essentially independent of the noise bandwidth so long as  $(b+1)$  is less than 6. One general conclusion may be drawn from a comparison of the results obtained for simple-lag systems (see Fig. 5.4-2 and Ref. 4) with those for systems employing quadratic filters of comparable bandwidths and using comparable values of  $(b+1)$ . With no noise the simple-lag systems yield smaller miss distances than the quadratic systems of equivalent bandwidths. Simple-lag systems, on the other hand, produce larger misses than quadratic systems if, when the simple-lag system is used, the noise bandwidth is large enough to drive the called-for acceleration from one limit to the other during an appreciable portion of the trajectory. Some further

consideration of these effects is given in Sec. 5.8.

### 5.6. Proportional-navigation System with Cubic Filter.

The most general cubic system is represented as

$$\frac{(b+1)(c_2s^2 + c_1s + 1)}{d_3s^3 + d_2s^2 + d_1s + 1} \ddot{a} = \dot{\theta}. \quad (5.6-1)$$

By making  $c_1$  and  $c_2$  equal to zero, a pure cubic system, which attenuates the high-frequency noise at 18 db per octave, is obtained.

Lead terms are inserted by assigning appropriate values to  $c_1$  and  $c_2$ .

The results of a number of tests of noise-free trajectories are given in Table 5.6-1 and Fig. 5.6-1. Table 5.6-1 shows that a denominator of  $(0.072s^3 + 0.48s^2 + 0.8s + 1)$  gives satisfactory operation when used with a  $(b+1)$  of 6 and a lead term of  $(0.8s + 1)$ . The effect of the lead term was investigated for cubics with the preceding denominator. This investigation showed that a pure cubic system ( $c_1 = c_2 = 0$ ) is too slow to follow a target maneuver. If  $c_2$  is made equal to zero and  $c_1$  equal to 0.2, the numerator becomes a factor of the denominator and the system degenerates to a quadratic with  $\omega_F = 1.66$  rad/sec and  $\zeta_F = 0.5$  (see Fig. 5.5-2). The study of quadratic systems indicated that this system was also too slow to follow a maneuvering target. Therefore, a lead term larger than 0.2s is required if an acceptable cubic system is to be achieved. Tests showed that a lead term of at least 0.8s was necessary to give satisfactory no-noise operation and that a system with this amount of lead also performed reasonably well in the face of noise. The transfer function finally selected as being

## CONDITIONS:

1. CUBIC CONTROL SYSTEM DEFINED BY  $\left[ \frac{(6)(C_1 s + 1)}{0.072 s^3 + 0.48 s^2 + 0.8 s + 1} \right] \dot{\alpha} = \dot{\theta}$
2. INITIAL-COLLISION COURSE WITH A 4G TARGET TURN BEGINNING AT  $r_0$
3. MAXIMUM LATERAL ACCELERATION OF MISSILE EQUAL TO 10g
4. NO NOISE

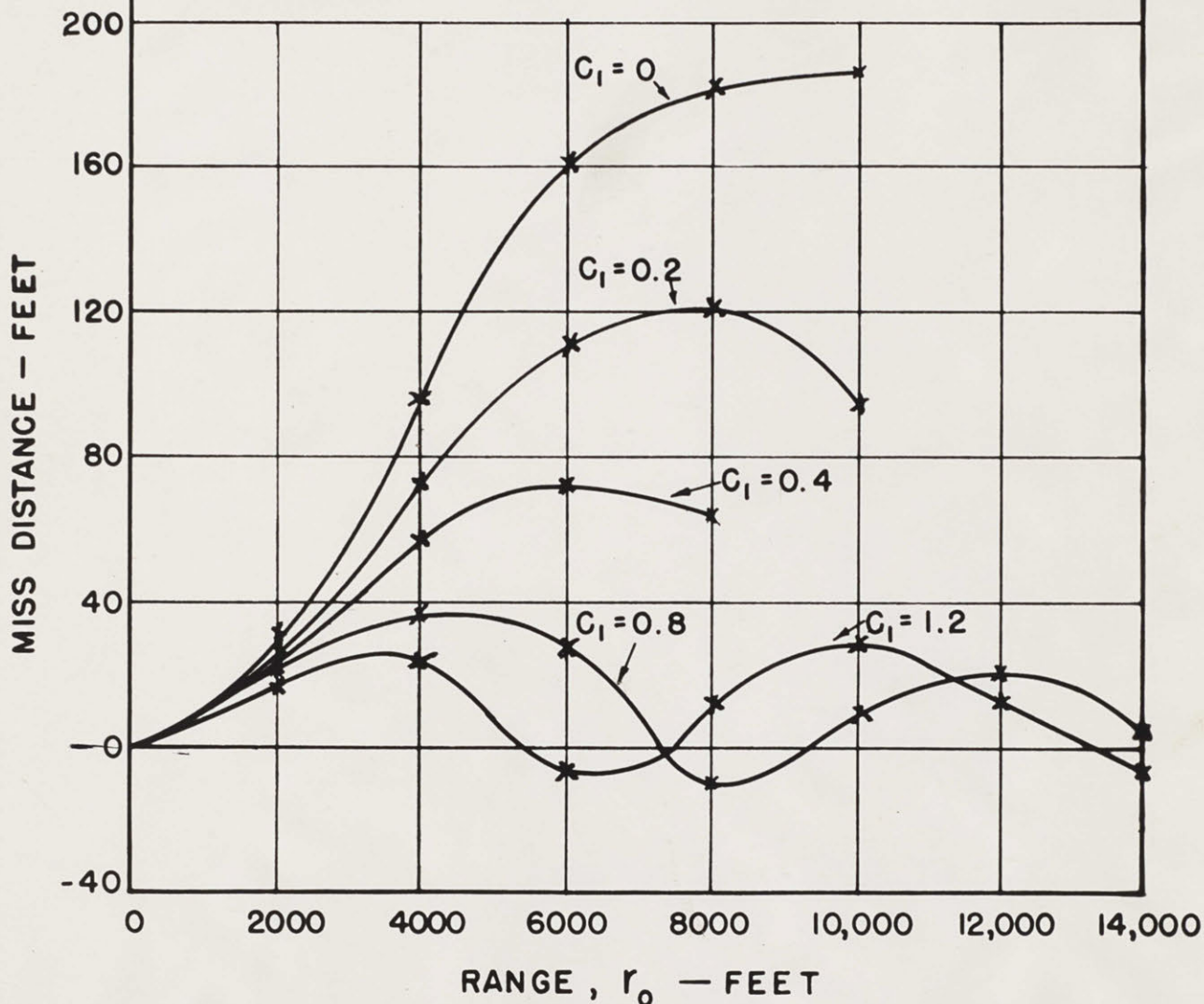


FIG. 5.6-1. MISS DISTANCES OBTAINED WITH CUBIC CONTROL SYSTEMS.

Table 5.6-1

Miss Distances Obtained with Cubic Control Systems

Conditions:

1. Cubic control system defined by

$$\left[ \frac{6(0.8s + 1)}{d_3s^3 + d_2s^2 + d_1s + 1} \right] \dot{\alpha} = \dot{\theta}.$$

2. Initial collision course with a 4g target turn beginning at  $r_0$ .
3. Maximum lateral acceleration of missile equal to 10g.
4. No radar noise.

		Range, $r_0 = 4000$ ft			Range, $r_0 = 8000$ ft		
$d_3$	$d_2$	0.24	0.48	0.72	0.24	0.48	0.72
	$d_1$	(ft)	(ft)	(ft)	(ft)	(ft)	(ft)
0.036	0.4	6	24	35	45	-6	-11
	0.8	12	27	38	7	-7	18
	1.2	17	32	40	1	12	48
0.072	0.4	22	35	42	32	-20	10
	0.8	24	36	45	19	-7	30
	1.2	28	38	46	2	18	52
0.108	0.4	35	42	48	-18	-17	21
	0.8	38	44	54	0	2	42
	1.2	38	44	54	2	25	60

acceptable is

$$\left[ \frac{6(0.8s + 1)}{0.072s^3 + 0.48s^2 + 0.8s + 1} \right] \dot{\alpha} = \dot{\theta}. \quad (5.6-2)$$

The lead term in this function is so important that the resulting medium frequency response differs very little from that given by the quadratic approximation obtained by dividing out the lead term. The natural frequency of the resulting quadratic is 3.33 rad/sec and the damping 1.0.

For the standard tactical situation which has been employed, and an  $r_0$  of 4000 feet, the system defined by Eq. (5.6-2) yields a miss of 36 feet for the noise-free case. Figure 5.5-2 shows that when  $(b+1)$  is 6 the corresponding quadratic system ( $\omega_F = 3.33$  rad/sec,  $\zeta_F = 1.0$ ) gives a miss of 40 feet. With noise ( $\omega_{SS} = 200$  rad/sec,  $\Phi_N = 10$  ft<sup>2</sup>/rad/sec), the cubic system yields an rms miss of 56 feet for an  $r_0$  of 4000 feet, whereas the quadratic system yields a miss of 53 feet for the same situation. The small disparity noted between the two cases may result as much from the differences in machine operation as from inherent dissimilarities in the two systems.

Patterson and Graham<sup>26</sup> attached considerable importance to the zero-frequency phase-slope of the control-system transfer function. This dependence is not borne out by the preceding tests. The system of Eq. (5.6-2) has zero phase-slope at the origin. The operation of this system was compared with that of a system having a control equation

$$\left[ \frac{24(0.2s + 1)}{0.072s^3 + 0.48s^2 + 0.8s + 1} \right] \dot{\alpha} = \dot{\theta}. \quad (5.6-3)$$

Since the numerator of Eq. (5.6-3) is a factor of the denominator, the system is actually a quadratic with  $\omega_F = 1.66$  rad/sec and  $\zeta_F = 0.5$ . Substitution of  $(b+1)$  of 24 in Eq. (5.6-3) gives this system the same high-frequency characteristics as the cubic of Eq. (5.6-2). The low-frequency characteristics of the two systems are quite different, as the quadratic system shows a zero-frequency phase-slope of minus 32 deg/rad/sec. For an initial range of 6000 feet and a noise defined by  $\omega_{ss} = 200$  rad/sec and  $\Phi_N = 10$  ft<sup>2</sup>/rad/sec, the rms miss obtained with the cubic system was 58 feet, whereas with the quadratic system it was only 40 feet.

These tests indicate that a consideration of only the steady-state sinusoidal response of the transfer function of the control system does not suffice. In fact, the problem of a missile following such a target maneuver is essentially a transient problem, with a signal  $(0.5)a_T t^2$  as the forcing function. A better indication of the action of a system probably can be obtained from the initial portion of the step response than from the low-frequency steady-state characteristics. Step responses for the cubic of Eq. (5.6-2) and the quadratic corresponding to Eq. (5.6-3) are given in Fig. 5.6-2. Actual rather than normalized gains are used in these plots. Since the systems should be compared on a high-frequency rather than on a low-frequency basis (because the times of flight are of the order of 1 to 3 seconds), attention should be focused on the initial portion of these transients. When compared on this basis, the average rate of rise of the response of the quadratic system for the first second is approximately twice that of the

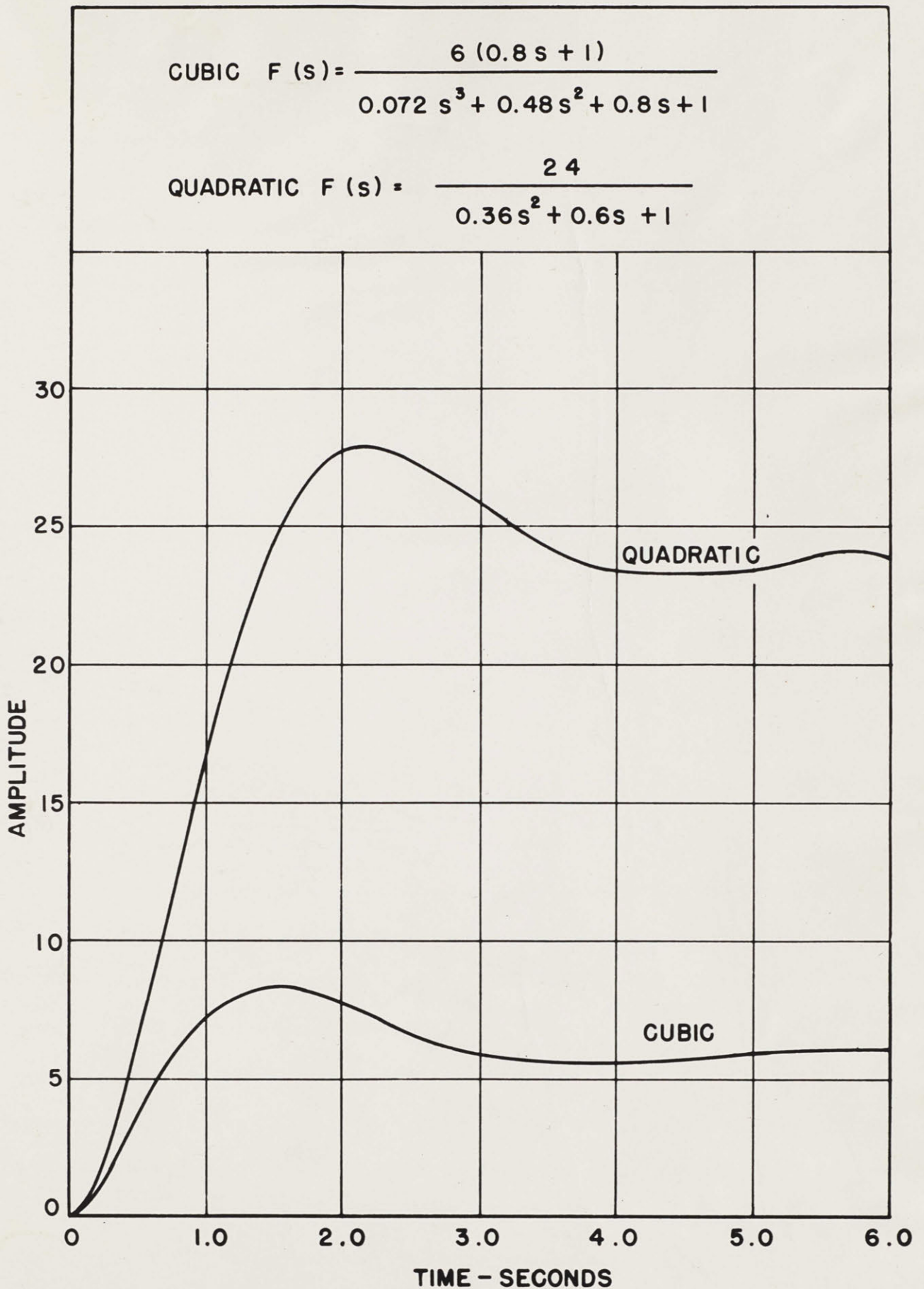


FIG. 5.6-2. STEP RESPONSES OF CUBIC AND QUADRATIC SYSTEMS.

cubic system. The overshoot of the quadratic response is 15 per cent, compared with an overshoot of 36 per cent for the cubic. Furthermore, the steady-state gain of the quadratic system is 4 times that of the cubic system. The zero-frequency phase-slope appears, in fact, to have little significance.

#### 5.7. Calculation of Mean-square Miss Distance for a Missile Subject to Random-square-wave Acceleration.

As was shown in Chap. 1, the unlimited missile problem involving noise can be handled analytically. At the other extreme, the rms miss can also be calculated analytically for the following special case.

At high frequencies a simple-lag system, which is characterized by the relation

$$\frac{(b + 1)}{(As + 1)} \dot{a} = \dot{\theta}, \quad (5.5-1)$$

acts like a pure integrator. If the radar glint noise received by such a system is defined by a random square wave, measured in position at the target, then  $\dot{a}$  consists of a train of randomly spaced impulses (positive and negative). Therefore, if only the high-frequency operation of the system is taken into account, the missile acceleration  $\dot{\theta}$  follows a random-square-wave program. The preceding situation will be studied for the particular case where the called-for acceleration is large enough to drive the missile from one acceleration limit to the other, in the manner of a random square wave. The radar noise need not actually have the form of a random square wave for this analysis to be applicable, because essentially a random-square-wave acceleration

will be produced, even by Gaussian noise, if its amplitude is so great that the resulting called-for acceleration is much higher than the limiting level.

If consideration is given to a large number of trajectories, of missiles initially on straight-line collision courses but which, for a time  $t_f$  before the collision point, are subjected to a random-square-wave acceleration program, there will be an increase in the standard deviation from the straight-line course as the time increases from zero to  $t_f$ .

The mean-square divergence of the missiles from a straight-line course can be expressed in accord with Eq. (4.21-3) as

$$\overline{M^2} = \int_{-\infty}^{\infty} |F(i\omega)|^2 \Phi(\omega) d\omega. \quad (5.7-1)$$

Because the system being considered has a finite settling time,  $F(i\omega)$  is not a rational function and Eq. (5.7-1) cannot be evaluated from the integral tables of Appendix C.

Since position is obtained by twice integrating acceleration, twice integrating the random square wave of missile acceleration gives the random position of the missile which, in turn, is a function of the time of flight. The impulse response of the system with respect to the final time  $t_f$ ,\* from acceleration to position, is therefore a ramp and may be defined as

$$\begin{aligned} f(\tau) &= \tau & \text{for } \tau < t_f \\ f(\tau) &= 0 & \text{for } \tau > t_f \end{aligned}$$

\* Because this is a time-varying system, the impulse response must be taken with respect to a definite time.

where

$t_f$  = the time of flight.

The power spectrum from the random square wave of missile acceleration is

$$\Phi(\omega) = \frac{k a_M^2}{\pi(\omega^2 + k^2)} \quad (5.7-2)$$

where

$a_M$  = the peak value of missile acceleration,

and

$k$  = twice the average crossing rate of the random square wave of acceleration.

When  $\Phi(\omega)$  from Eq. (5.7-2) is substituted in Eq. (5.7-1) and the variable is changed from  $\omega$  to  $s/i$ , the expression for the miss becomes

$$\overline{M^2} = \frac{k a_M^2}{\pi i} \int_{-i\infty}^{+i\infty} |F(s)|^2 \left| \frac{1}{s+k} \right|^2 ds. \quad (5.7-3)$$

If  $F(s)$  is the transform of  $f(\tau)$ , then by means of real convolution Eq. (5.7-3) becomes

$$\overline{M^2} = 2k a_M^2 \int_0^{\infty} |b(\tau)|^2 d\tau \quad (5.7-4)$$

where

$$b(\tau) = f(\tau) * e^{-k\tau}.$$

Writing out the convolution gives

$$b(\tau) = \int_0^{\tau} f(\tau_2) e^{-k(\tau-\tau_2)} d\tau_2. \quad (5.7-5)$$

Then

$$\begin{aligned} e^{k\tau} b(\tau) &= \int_0^{\tau} f(\tau_2) e^{k\tau_2} d\tau_2 \\ &= \int_0^{\tau} \tau_2 e^{k\tau_2} d\tau_2 \quad \text{for } \tau < t_f \end{aligned}$$

and

$$= \int_0^{t_f} \tau_2 e^{k\tau_2} d\tau_2 \quad \text{for } \tau > t_f.$$

Another change of variable ( $\tau_2 = \rho/k$  or  $\tau = P/k$ ) yields

$$\overline{M^2} = 2a_M^2 \int_0^{\infty} \left| b\left(\frac{P}{k}\right) \right|^2 dP \quad (5.7-6)$$

and

$$\begin{aligned} e^P b\left(\frac{P}{k}\right) &= \frac{1}{k^2} \int_0^P f(\rho) e^{\rho} d\rho \\ &= \begin{cases} \frac{1}{k^2} \int_0^P \rho e^{\rho} d\rho & \text{for } 0 < P < T \\ \frac{1}{k^2} \int_0^T \rho e^{\rho} d\rho & \text{for } T < P \end{cases} \quad (5.7-7) \end{aligned}$$

where

$$T = kt_f.$$

Integrating Eq. (5.7-7) then gives

$$b \left( \frac{P}{k} \right) = \begin{cases} \frac{1}{k^2} [P - 1 + e^{-P}] & \text{for } 0 < P < T \\ \frac{1}{k^2} [Te^{-(P-T)} - e^{-(P-T)} + e^{-P}] & \text{for } T < P \end{cases} \quad (5.7-8)$$

Squaring Eq. (5.7-8), substituting it into Eq. (5.7-6), and then integrating the first part from zero to  $T$  and the second from  $T$  to infinity yield, after some simplification,

$$\overline{M^2} = \frac{2a_M^2}{k^4} \left[ \frac{T^3}{3} - \frac{T^2}{2} + T + 1 - e^{-T}(1 + 2T) \right]. \quad (5.7-9)$$

For  $T = kt_f \gg 1$ , Eq. (5.7-9) simplifies to

$$\overline{M^2} = \frac{2a_M^2 t_f^3}{3k}. \quad (5.7-10)$$

If the missile and the target are initially on a collision course and the target continues to fly in a straight line, Eq. (5.7-9) or Eq. (5.7-10) gives the mean-square miss distance. In Fig. 5.7-1 the rms miss is plotted as a function of the limiting value of the missile acceleration, with the average crossing rate of the acceleration program as a parameter. The initial range was taken as 4000 feet and the missile and the target were initially on a head-on collision course. Figure 5.7-1 shows that for the particular case of an initial collision course the rms miss is reduced as the maneuverability of the missile is reduced. This result is interesting but hardly affords a practical way

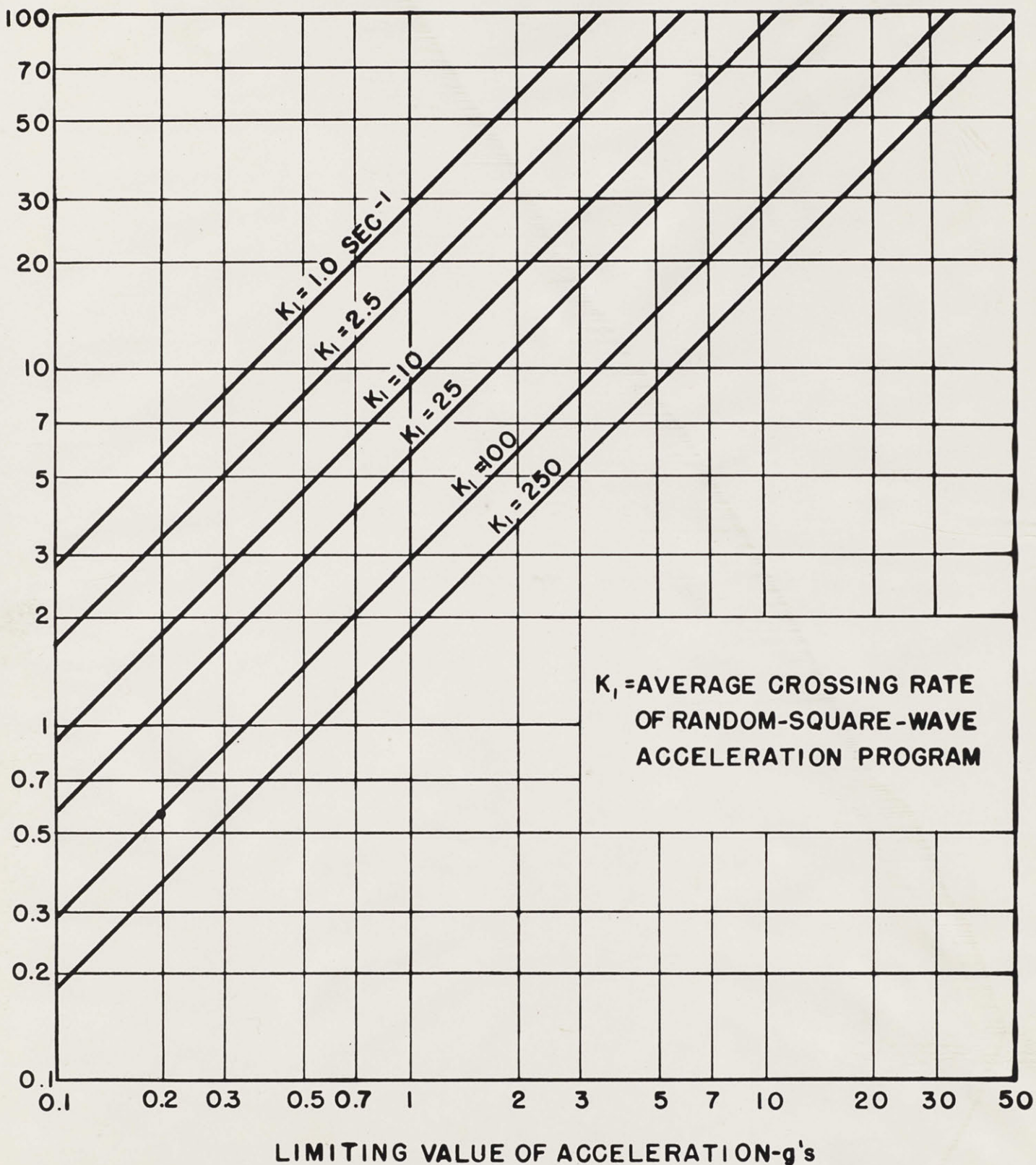


FIG. 5.7-1. RMS MISS DISTANCE AS A FUNCTION OF THE LIMITING VALUE OF THE MISSILE ACCELERATION FOR THE CASE OF A RANDOM-SQUARE-WAVE ACCELERATION PROGRAM.

[REDACTED]

of reducing the miss because neither an initial collision course nor a nonmaneuvering target can be assumed for all trajectories. Even in those cases where small initial errors and nonmaneuvering targets may be assumed probable, this and other work indicate that better operation results from using additional filtering than from reducing the acceleration limits of the missile. If the target maneuvers during the course of the flight, the miss distance can be calculated by applying the principles of Sec. 5.4. In any case where the noise markedly influences the behavior of the missile, this analysis shows that the standard deviation of the miss distance about its mean value would be reduced as the acceleration capabilities of the missile are reduced, or as the bandwidth of the noise is increased.

#### 5.8. Effect of Changes in the Amplitude Probability Distribution of the Noise.

One further characteristic of the noise should be discussed in connection with the limiting problem. As pointed out in Chap. 3, a unique relationship does not exist between the power spectrum of a signal and its amplitude-versus-time function. The consequent ambiguity leads to no difficulty in the unlimited problem, where the noise is sufficiently specified by its power spectrum. In the problem involving limiting, however, the voltage-time relationship of the noise could be important in determining the miss, even for closely matched power spectra.

The noise source employed in obtaining the data of Fig. 5.4-2 produces a signal with an amplitude probability distribution which is

[REDACTED]

approximately Gaussian. Such an amplitude distribution seems reasonable for the noise return from an airplane, but there is also the possibility that, if the radar return were received principally from two well-defined areas on the plane, the noise signal would approximate a constant-amplitude square wave with random times for the zero crossings. The amplitude probability density of such a signal would consist merely of two impulses. Such a signal does not occur in practice, but plans were made for conducting some tests with this type of signal, in order to determine how the miss depends on the amplitude-time function of the noise. The random-square-wave generator discussed in Sec. 3.44 was constructed with the intent of using it as a noise source for some simulator studies in which several significant problems would be studied. The wave form of the noise should have the most influence on the miss under conditions for which the missile is fast enough to respond reasonably to the noise but still not so fast as to lose completely intelligence from noise saturation. Furthermore, examination of the power spectrum,  $\Phi(\omega)$ , of a random-square-wave signal shows it to be identical in form with the spectrum obtained by passing white noise through a simple-lag filter. For the random-square-wave signal

$$\Phi(\omega) = \frac{kx_N^2}{\pi(\omega^2 + k^2)} = \frac{1}{\pi} \frac{\frac{x_N^2}{k}}{\frac{\omega^2}{k^2} + 1} \quad (3.44-1)$$

and for the signal obtained by passing white noise through a simple-lag

filter

$$\Phi(\omega) = \Phi_N \left| \frac{1}{\tau s + 1} \right|^2 = \frac{\Phi_N}{\tau^2 \omega^2 + 1} \quad (5.8-1)$$

where  $\Phi_N$  is the zero-frequency power density of the noise and  $\tau$  is the time constant of the simple-lag filter.

The most significant comparison of results would, therefore, be obtained if the behavior of the system were studied first with random-square-wave noise and then with white noise passed through a simple-lag filter. In order that the results be directly comparable, the following conditions should be met:

$$\left. \begin{aligned} \tau &= \frac{1}{k} \\ \Phi_N &= \frac{x_N^2}{\pi k} \end{aligned} \right\} \quad (5.8-2)$$

Unfortunately, even though the square-wave generator had been built and tested, no time was available to perform this test, hence no conclusions can be drawn on this point.

#### 5.9. Use of Nonlinear Filter Systems in Missiles.

The results given in Secs. 5.4 through 5.6 indicate that with linear filter systems the minimum rms miss obtainable for 200 rad/sec noise and the assumed tactical situation is approximately 55 feet. Since this miss distance is large, a heavy warhead must be carried if the probability of a kill is to approach unity. The question arises as to whether a nonlinear filter system could be devised which would

result in a smaller miss distance. In using such a system there is even greater danger than in the case of a linear system that a small miss may result from a set of circumstances peculiar to a particular tactical situation, whereas the system may show very poor operation under other conditions. The following situation illustrates an exaggerated example of this danger for the case of an initial head-on approach, a single 4g target turn beginning at 4000 feet, broadband noise, and a maximum missile acceleration of 10g. If definite knowledge were available that the target would execute this maneuver, then the missile control system could be arranged to fly the missile in a straight line to a range of 2530 feet and then execute a fixed 10g turn. A hit would inevitably result. The direction in which the target maneuvers can be determined by filtering the  $\dot{\alpha}$  information over the 4000- to 2530-foot interval. Obviously, the construction of such a control system would be asinine, since an intelligent target must be dealt with and a priori knowledge of the future tactical situation is unattainable.

A simplification of the type of signal which typically appears in the control system of a missile is shown in Fig. 5.9-1. This signal, which is composed of a d-c signal with a superimposed random noise having an average value of zero, is used to position the control surfaces of the missile and thus determine its lateral acceleration. If this composite signal is passed through a linear filter system, the average value of the output is the d-c signal. Since acceleration of the missile is in reality limited, the actual system is nonlinear. The

more filtering which can be tolerated ahead of the limits, the smaller fraction of the time the signal will be in the limits. The filtering which can be used, however, is limited if the missile is to follow target maneuvers adequately. With the assumption that the signal of Fig. 5.9-1 is obtained when the maximum allowable filtering is used,

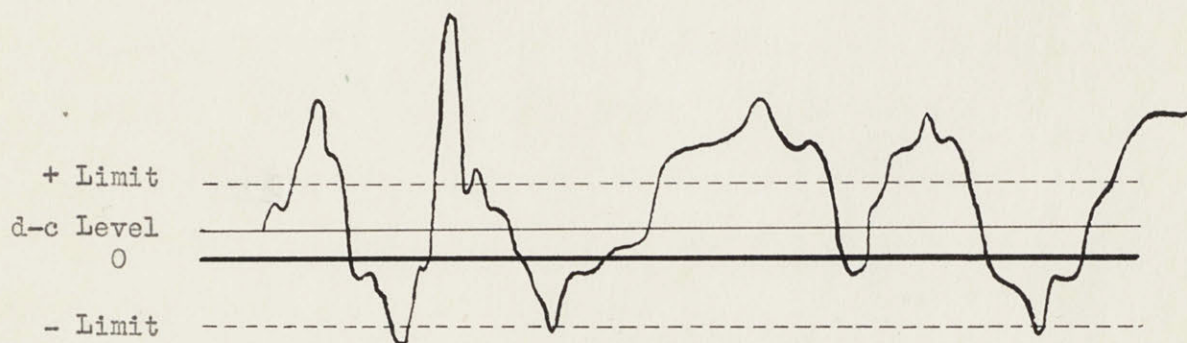


Fig. 5.9-1. Input Signal Plus Noise.

the presence of the limits markedly reduces the average value of the output signal. As the signal-to-noise ratio approaches zero, because of an increase in the noise, the average value of the output also approaches zero, even if the average value of signal component remains constant.

The best chance of success in designing a nonlinear filter which will yield the correct value for the signal, even though noise components in the input may call for outputs exceeding the unavoidable limits, apparently lies in utilizing that portion of the control signal which is lost in the limiting process. One nonlinear filter system which, in certain cases at least, gives an output of nearly the true

signal value, in spite of limiting, is shown in Fig. 5.9-2. The nonlinear filter consists of two channels operating in parallel. One channel consists of an auxiliary limiter which has a 1-to-1 response

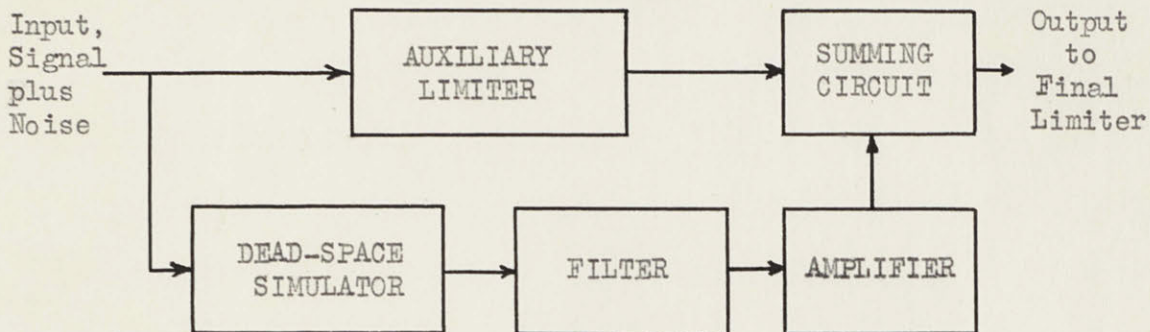


Fig. 5.9-2. Nonlinear Filter System.

below the limiting level but above limiting provides a constant output. The other channel consists of a dead-space simulator (an excess detector), a filter, and an amplifier. Limits in the auxiliary limiter and limits in the dead-space simulator are both set at the level of the limiting which unavoidably occurs later in the system. In this arrangement a signal below the limiting value passes through the auxiliary limiter with none of it transmitted by the shunt path through the dead-space simulator. For a larger signal, the excess above the limiting level passes through the dead-space simulator. The output of the dead-space simulator consists of those portions of the signals which exceed the limits. This output is filtered and added to the signal passed by the auxiliary limiter. When the resultant signal is limited again, the average obtained is closer to the d-c component of the input than the average of the output of the first limiter.

Two parameters which must be determined are: (1) the gain through the dead-space channel and, (2) the characteristics of the filter employed in the dead-space channel. Examination of two simple cases aids in establishing the optimum gain for this channel. In the first instance, a d-c signal of one half the limiting level is masked by a noise signal several times the limiting level, which for the convenience of illustration, is taken as a random square wave. Figure 5.9-3 illustrates the form of the signals appearing at various points in the system of Fig. 5.9-2. The average value of the output of the dead-space simulator is, as shown in Fig. 5.9-3c, equal to the level of the d-c signal in Fig. 5.9-3a. Figure 5.9-3d gives the signal obtained at the output of the summing circuit if the gain through the dead-space channel is made twice that through the auxiliary-limiter channel, and the time constant of the filter following the dead-space simulator is made very long compared with the significant noise frequencies. If this signal is next passed through a limiter and then a filter, the value of the limited and filtered output is equal to the d-c signal which originally appeared at the input to the system.

The second case to be considered occurs when a d-c signal equal to the limiting level appears at the input to the system along with a random-square-wave noise component having an amplitude equal to one half the limiting level. Here, three fourths of the d-c signal amplitude appears at the output of the auxiliary limiter and one fourth at the output of the filter in the dead-space channel. Again, if the gain in the excess channel is made twice that in the auxiliary-limiter channel, the signal finally obtained when the output signal from the

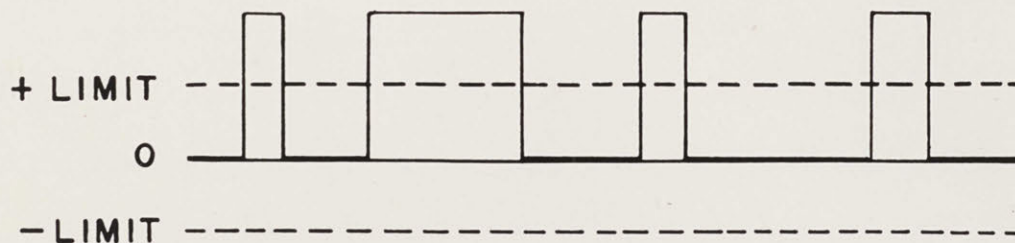
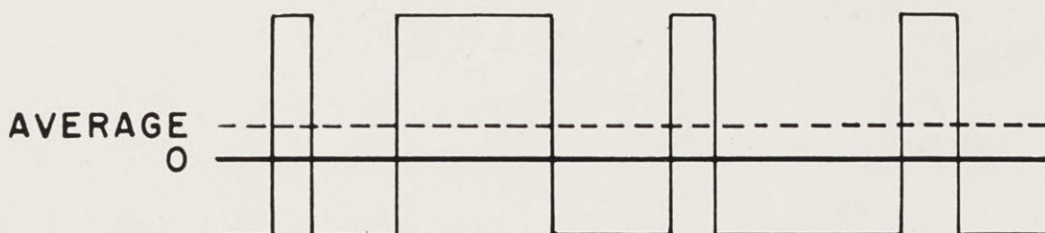
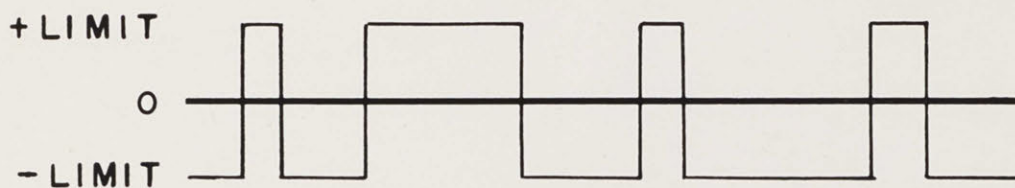
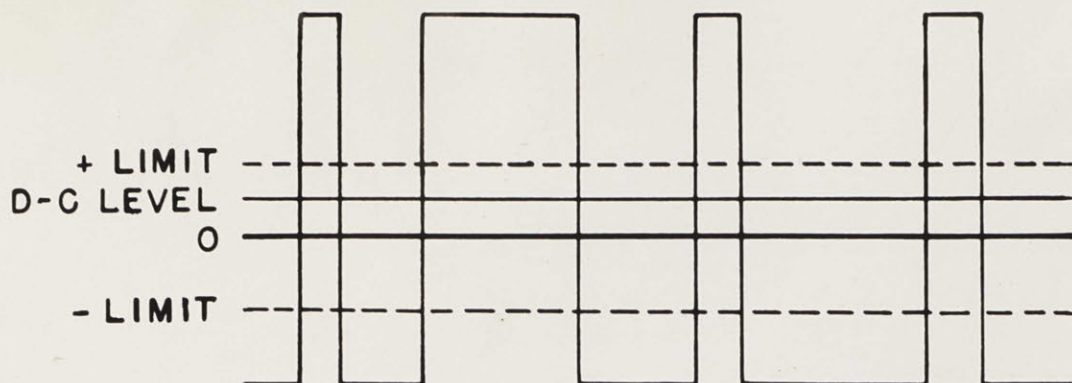


FIG. 5.9-3. FORM OF SIGNALS APPEARING AT VARIOUS POINTS IN THE NONLINEAR FILTER SYSTEM OF FIG. 5.9-2.

summing circuit of Fig. 5.9-2 is limited and filtered equals that obtained for the original d-c signal, if it had appeared at the input without any noise.

In the two preceding situations the scheme of Fig. 5.9-2 appears to provide faithful reproduction of the signal component of the input, in spite of the irremovable limits in the system. Furthermore, for signals below the limiting level no additional time lags have been introduced in the system. Nevertheless, a d-c signal and long filtering times in the dead-space channel have been assumed. The validity of these assumptions and, therefore, the effectiveness of such a scheme cannot be stated without further study.

The servo studies of Chap. 4 led to the contemplation of still another type of nonlinear control system. These studies indicated that possibly the optimum filter system for use in a missile should employ a filter in which the pass band is changed in such a fashion that the rms acceleration called for is constantly made equal to that available when the signals are large, or the maximum bandwidth is utilized while small signals are being received. Even if the elements used in the filter are themselves linear, the over-all system constitutes a nonlinear filter, because the parameters are varied in accordance with a characteristic of the input signal. A servo operating on a signal corresponding to the called-for acceleration would be required to regulate the bandwidth of the filter. Such a system probably could be built without undue complexity and might prove quite effective. As an alternative, the bandwidth of the filter might be adjusted in relation

to the signal-to-noise ratio of the input signal. Measurement of the signal-to-noise ratio is, of course, difficult without knowledge of the true signal, but possibly a satisfactory measure could be obtained by weighing the ratio of the output of the filter to its input in accordance with the bandwidth being used. Systems of this general type appear to lend considerable promise for improving the operation of either servos in general or the specific missile problems which have been considered.

No simulator studies have been made of nonlinear filter systems, but the investigation of such systems should receive attention in the future. Since the number of types of nonlinear filters possible is limited chiefly by the ingenuity of the investigator, a comprehensive study of these systems is a difficult task. Furthermore, the effectiveness of a nonlinear system depends to a large degree on the specific types of input signals and noise to be handled. In fact, Singleton<sup>27</sup> has shown that in the special case where a Gaussian signal is to be filtered from an input corrupted by Gaussian noise the minimum mean-square error results if a linear filter is employed. On the other hand, noise consisting of impulses may be removed more effectively from a Gaussian signal by passing the total input through a nonlinear system consisting of a limiter before any linear filtering is attempted.

#### 5.10. Some Comments on the Study of Homing-missile Systems.

A complete investigation of the homing-missile problem would require a prohibitively large amount of computer time. The value of a brute-force attack on the problem is questionable even if the required machine

time and capabilities were available. On the other hand, a general understanding of this problem may be obtained from the study of a few selected cases coupled with a careful interpretation and extrapolation of the results obtained. By way of illustration, several extensions which can be made to the work of this chapter are considered.

This investigation has been concerned primarily with head-on approaches because in this situation the effects of target maneuvers are most deleterious. For the beam approach, where target maneuvers make little difference, the miss obtained is determined mainly by the noise. For the tail approach, target maneuvers are again effective. All approaches are essentially the same, except for differences in the closing velocity, the radar noise, and the effective target maneuver normal to the line of sight. As noted in Chap. 3, the radar noise becomes most severe for beam approaches. On the other hand, the target can maneuver normal to the line of sight most effectively for head-on or tail approaches. Changes in the closing velocity with different approaches can be accounted for by varying  $(b + 1)$  in such a manner as to hold constant the quantity  $N$  of Eq. (1.4-18).<sup>\*</sup> This change can be partially accomplished by multiplying the  $(b + 1)$  obtained for the head-on case by a range-rate term. Such a modification should be included in the control system if a range-rate term can be obtained without undue complication. An exact duplication of results should be obtained for all approaches if the quantity  $N$ , the time of flight, the noise, and the target acceleration normal to the line of sight are all

<sup>\*</sup> The relation between the quantity  $N$  and range rate depends on the linearity of the kinematic equations but not on the linearity of the control equation. These comments are valid, therefore, even if acceleration limiting occurs.

held constant. For example, results obtained for head-on and tail approaches should be identical if, for the velocities used in this study, the  $(b + 1)$  used for the tail approach is made one third that used for the head-on approach and the initial range for the tail approach is made one third of that for the head-on approach.

If the noise has an rms value sufficiently low (as a result of having either a low power density or a narrow bandwidth) to require less than the limiting value of missile acceleration to be developed until very near the end of the flight, a simple-lag filter yields the smallest miss. The system here considered is essentially linear and, under this condition, Booton<sup>5</sup> showed that, even in the presence of white noise, a simple-lag filter system between  $\dot{\alpha}$  and  $\dot{\theta}$  is nearly optimum. Nevertheless, the acceleration called for by white noise becomes infinite. The acceleration capabilities of any physical system, on the other hand, are limited and a missile-control-system response should be selected which cuts off in such a manner as to keep the called-for acceleration of the missile within reasonable bounds. For noise which cuts off in a quadratic fashion, tests showed that, with the larger values of noise (such that with the optimum simple-lag filter the limiting value of acceleration is called for during a considerable portion of the flight) a quadratic system can be found which yields a smaller miss than the optimum simple-lag system. This result follows from the effects of limiting in the system and not because a quadratic system is the optimum based on linear theory. The study in Secs. 5.4, 5.5, and 5.6 was concerned with radar noise shaped by a quadratic filter. No particular

[REDACTED]

evidence exists to show that glint noise cuts off in a quadratic fashion. As noted in Chap. 3, this type of noise was selected because it is less demanding on the computing equipment than simple-lag noise. Likewise, a missile is less able to deal with simple-lag noise than with quadratic noise. Tests should be made to determine under what conditions the shape of the noise power spectrum is significant in determining the miss distance.

[REDACTED]

[REDACTED]

CHAPTER 6

CONCLUSIONS

6.1. Evaluation of the Ability of the D.A.C.L. Computer to Handle Trajectory Problems.

At the present time, the D.A.C.L. Computer appears to be capable of solving, with a fairly high degree of accuracy, the type of trajectory problems studied here, if use is made of all the available checking procedures before a study is begun, and if the parameters investigated are not too different from those used during the checking period. The accuracies to be expected are very difficult, if not impossible, to specify, but with the assumption that all checks have proved satisfactory, in no-noise studies of this type the miss distance probably will be correct to within plus or minus 5 feet, or 5 per cent, whichever is larger. In studies involving noise, the expected accuracy is poorer and, in some cases, results obtained at intervals of several months have been duplicated to within only about 30 per cent, although the agreement is usually better. For some studies this accuracy is acceptable, but in other studies such inaccuracies in the computer may overshadow the effect of large changes in the parameter being varied. Therefore, care must be taken when interpreting the results obtained from the machine and, where possible, every effort should be made to check the results analytically. Furthermore, extreme diligence must be exercised to guard against human errors which can invalidate the results obtained and, therefore, lead to erroneous conclusions.

[REDACTED]

██████████

A significant start toward an evaluation of the computer has been made in the work of this thesis. This evaluation program should be continued, and in future work the ability of the integrators to handle random input signals should be analyzed, the overload characteristics of the various computing components should be investigated, and the d-c equipment should be studied. Still more attention should be given to alternate ways of setting up problems in order to reduce the demands upon the computing equipment. Further effort should be devoted to determining the effect of errors in the system on the final answers so that a better insight may be acquired into the accuracies actually required of the various components.

As a better understanding of the capabilities of the computer is attained and as more operational experience is gained, both the reliability of the results obtained and the volume of the output should increase. At present, one of the most serious basic deficiencies appears to be the lack of a high-speed, high-accuracy position servo which can be used as a repeater or as an angle solver. Efforts are being made to outline a complete set of specifications for an acceptable servo and to evaluate various drives, such as magnetic clutches and hydraulic motors. The development of a truly satisfactory servo will require a long time. In the interim, the question of setting up problems so as to avoid overtaxing the limited capabilities of the present equipment must receive careful attention. With the proper care, however, the answers to a wide variety of extremely important problems can be obtained with the existing equipment.

██████████

6.2. Evaluation of the Probable Effectiveness of Missiles with Proportional-navigation Control Systems.

A complete evaluation of the probable effectiveness of homing-missiles with proportional-navigation control systems must include a number of factors which have been omitted here. The problem studied in this thesis has necessarily been a striking simplification of the actual homing-missile problem. The filtering and limiting occurring in the missile system have been idealized, with very little attention devoted to the exact position of the time lags or to the manner in which acceleration limiting occurs in the actual system. These considerations may or may not be important, but in any event, they should be investigated. The possibility of a difference between the heading of the missile and the direction of its velocity vector should be simulated, and the time lag which occurs between a change in the heading and a change in the direction of the velocity vector should be added as a separate quantity. Time lags occurring in the radar system should also be included. The presence of such additional time lags in the system will lead to definite limitations on the type of filtering which may be added and on the value of the navigation constant which may be employed if a stable system is to be maintained.<sup>28</sup>

A more extensive study should also include exactly how limiting takes place in the missile. For example, a system in which limiting results from restricting with mechanical stops the maximum deflection of the control surfaces does not provide limiting at a fixed acceleration which is independent of the rate at which the control surfaces

[REDACTED]

are moved back and forth. To provide a fixed limit on the actual acceleration (this is essential because of the structural limitations of the missile) the flap-deflection angle must be increased as the rate of change of the acceleration is increased. The actual system used for this purpose should be studied.

The effect of variable missile velocity should receive additional<sup>29</sup> attention, and gyro drift effects should be investigated. The results reported in this thesis were obtained with an assumed altitude of approximately 25,000 feet, but the study should be repeated for other altitudes up to the order of 60,000 feet. With the data presently available, a prediction of whether the misses caused by combined noise and target-maneuver effects at high altitude will be larger or smaller than those occurring at low altitude appears impossible. As the altitude increases, the acceleration capabilities of both the target and the missile are reduced and the speed of response of each is reduced. In the absence of noise, these changes may lead to approximately the same miss distances as achieved at lower altitudes, providing the target begins its maneuver at a somewhat greater range. Any marked change with altitude in the characteristics of the angular-scintillation noise appears unlikely. If the same filtering is used at all altitudes, the combination of the same noise and reduced acceleration capabilities could lead to considerably increased misses. Therefore, the filter characteristics should be varied with the altitude.

[REDACTED]

██████████

The final evaluation of a missile should be made from a three-dimensional study. Such an investigation requires considerably more computing equipment than is available at present and, in general, is a very much more difficult problem because of cross-coupling effects. Undoubtedly, the misses occurring in the three-dimensional case will be larger than those in a two-dimensional study. The important question which arises is, "How much larger will they be?" This must be answered by a study involving all the cross-coupling effects occurring in an actual missile system.

Another point which should not be overlooked in evaluating the effectiveness of a missile is its target-discrimination ability. Very rough calculations indicate that the acceleration required of the missile becomes fantastically large, unless the missile can distinguish between targets and, at a fairly large range, discriminate a particular aircraft in a formation. The same conditions which generate glint noise from a single target appear to be present when a radar is trained on a formation of planes. Measurements of the characteristics of this type of noise are even more difficult to obtain than for a single target and, as far as is known, no data are available on this subject.

The final evaluation of a missile should be concerned with the kill-probability of the missile rather than with the rms miss distance. The latter measure was chosen as a criterion because of the ease with which it may be calculated from the experimental data. The rms-miss distance is, however, a poor indication of the probability of kill,

██████████

[REDACTED]

which should also consider the deviation of the miss distances about their mean values, the characteristics of the warhead (including its fragmentation pattern), the profile presented by the target, and the vulnerability of various parts of the target.

As a result of the very limited amount of data which have been collected, a prediction of the effectiveness of any particular missile in actual tactical use is still impossible. An evaluation has been begun and enough experience has been gained to point out a number of the pitfalls arising in the simulator study of a problem. Further studies, therefore, should proceed more efficiently than this early one.

### 6.3. Comments on Oil Consumption and Drag.

Although the probability of kill is the final measure of the effectiveness of a missile, the designer must take into account such questions as the amount of oil required to move the control surfaces and the effects of drag in setting a maximum usable range for the missile. Each of these effects must be evaluated with regard to the noise which will be present in the system. Obviously, there is no possibility of optimizing the control-system parameters solely on the basis of minimum oil consumption and minimum drag because the oil consumption goes to zero merely by locking the control surfaces and the drag is minimized when the control surfaces are locked in the neutral position. An attempt, on the other hand, should be made to minimize the oil consumption and drag, while at the same time requiring that the miss distance or the probability of kill fall within prescribed

[REDACTED]

[REDACTED]

limits. The oil consumption and drag would be expected to drop as the order of the control equation is increased from a simple lag to a quadratic and to a cubic. Tests should be carried out to determine the importance of this dependence.

#### 6.4. General Conclusions Concerning Nonlinear Problems of the Type Studied.

The types of nonlinear systems which have been investigated constitute very important but very difficult classes of problems. Probably some time will elapse before anything approaching a general analytic solution to these problems will be available. In the meantime, simulators or computers can lend valuable assistance in obtaining solutions but these results must be carefully analyzed to ascertain that the desired problem and not the computing equipment is being studied. A thorough analysis of a few of the simple cases occurring in these problems will give more insight into the complete missile problem than a mass of data which are rendered worthless, or nearly so, by improper computer operation. In this respect, a better understanding of the effects of limiting in as simple a servo system as discussed in Chap. 4 should contribute much toward a better comprehension of the more complicated homing-missile system. For example, optimum missile operation may be achieved, if the control-system gain is continually adjusted so that the called-for acceleration is made nearly equal to the available acceleration. Such an arrangement is more difficult to instrument in a missile system involving time-varying coefficients than in a simple servo, but it may prove

[REDACTED]

practicable.

Both the missile and the simple servo have shown the very deleterious effects of acceleration limiting in the system. Other nonlinearities such as position, velocity, or voltage-amplitude limiting can be equally serious. Once limiting begins, the principle of superposition is no longer valid and experience has shown that, beyond this point, the errors arising in the system may increase very rapidly. These considerations lead to a skeptical attitude toward the use of nonlinear compensating schemes. Although these schemes may provide a marked improvement in the operation of a system for one type of input conditions, they may result in very poor operation for somewhat different inputs. A safer approach appears to be to operate the system close to the margin of unavoidably present nonlinearities but still attempt to keep it linear. Under these conditions a much better chance exists that the system can be handled analytically. Then half the battle may be won.

[REDACTED]

APPENDIX A. - GLOSSARY OF TERMS

A	- Missile time constant (sec).
$A_1, A_2, \dots$	- Constants.
a	- Acceleration at the output of a system.
$a_M$	- Missile acceleration.
$a_{max}$	- Maximum acceleration.
$a_t$	- Lateral acceleration of the target.
$a(\tau)$	- Missile step response.
$a_0, a_1, \dots, a_n$	- Constants.
$B_1, B_2, \dots$	- Constants.
$b + 1$	- Navigation constant in missile-control equation.
$b_0, b_1, \dots, b_n$	- Constants.
C, $C_1, C_2$	- Constants.
$c_p$	- Setting of coefficient potentiometer in integrator.
$c_1, \dots, c_n$	- Constants.
D( )	- Operator characterizing proportional-navigation system.
$d_1, \dots, d_n$	- Constants.
E	- Rms amplitude of a signal voltage.
$E_{out}, E_o$	- Output of a system.
$E_{rms}$	- Rms input to a system.
e	- Base of natural logarithms.
F(s)	- Transfer function.
f(t)	- Function of time.

$f(\tau)$	- Function of time.
$f_1(r, t)$	- Function of $r$ and $t$ .
$G(s)$	- Transfer function.
$\xi_1$	- $2\xi_{ss}/\omega_{ss}$ .
$\xi_2$	- $1/\omega_{ss}^2$ .
$H(s)$	- Transfer function.
$I(u, p)$	- Pearson's incomplete Gamma-function notation.
$I_1, I_2, \dots, I_8$	- Mean-square integrals.
$i$	- $\sqrt{-1}$ .
$j$	- Summation index.
$K$	- Gain of a system.
$K_N$	- Constant in expression for miss caused by noise.
$k$	- Twice the average zero-crossing rate of a random square wave.
$L$	- Linear operator.
$L_a$	- Length of aircraft.
$\mathcal{L}$	- Laplace transform.
$l$	- $\tau/A$ .
$l_1$	- $r_1/AV_R$ .
$M_N$	- Miss caused by radar noise.
$M_T$	- Miss caused by target maneuver.
$m_0, m_1, \dots, m_p$	- Minors of determinants which evaluate integral-squared error.
$N$	- Navigation constant times speed ratio, $\left[ (b + 1)V_M \cos \beta_0 \right] / V_R.$

$n$	- Number of solutions.
$P( )$	- Probability.
$p$	- Operator symbol $d/dt$ .
$R$	- Radius of sphere.
$R_1, R_2$	- $R_1^2 = n\sigma_1^2, R_2^2 = n\sigma_2^2$ .
$r$	- Missile-to-target range.
$r_0, r_1$	- Initial value of $r$ .
$S$	- Target wing span.
$S_n(R)$	- Range of integration.
$s$	- Complex frequency variable, Laplace transform variable.
$T$	- Time limit of integration.
$t$	- Time variable.
$t_f$	- Time of flight.
$u$	- As.
$u_1, u_2$	- Specific values of the argument $u$ appearing in Pearson's "Table of Incomplete $\Gamma$ -functions."
$V_M$	- Missile velocity (fps).
$V_R$	- Relative velocity (fps).
$V_T$	- Target velocity (fps).
$v$	- $1/Aw_{ss}$ .
$W$	- $R^2/2$ .
$w$	- $\chi^2/2$ .
$x$	- Abscissa of rectangular-coordinate system.

$x_M$	- Lateral movement of missile position from reference line.
$x_{M,\infty}$	- Rms value of miss caused by white noise.
$x_N$	- Lateral value of noise from reference line.
$x_T$	- Lateral movement of target position from reference line.
$x_n$	- Amplitude of a random square wave.
$x_1, \dots, x_n$	- Independent measurements of a normally distributed variable.
$x'$ and $x''$	- Rotated x coordinate.
$y$	- Ordinate of rectangular coordinate system.
$y'$ and $y''$	- Rotated y coordinate.
$\alpha$	- Missile-to-target line-of-sight angle.
$\alpha_A$	- Apparent value of $\alpha$ .
$\alpha_{At}$	- Transient value of $\alpha_A$ .
$\alpha_c$	- Angle through which output shaft of $\alpha$ servo has actually turned.
$\alpha_t$	- Transient value of $\alpha$ .
$\alpha_o$	- Initial value of $\alpha$ .
$\beta$	- Angle between missile heading and line of sight.
$\beta_o$	- Initial value of $\beta$ .
$\Gamma(n/2)$	- Incomplete Gamma-function.
$\gamma$	- Constant of integration.
$\Delta_k$	- Denominator in integral-squared-error formulas.
$\epsilon$	- Error of a system.

$\epsilon_0$	- Zero gain error of a system.
$\zeta_F$	- Damping ratio of missile-control-system filter.
$\zeta_{ss}$	- Damping ratio of a quadratic-system noise filter.
$\zeta_0$	- Damping ratio of y-locked simple-lag system.
$\eta$	- Normalizing factor.
$\theta$	- Missile velocity-vector angle.
$\theta_c$	- Called-for $\theta$ .
$\theta_{lim}$	- Limiting value of $\theta$ .
$\theta_t$	- Transient value of $\theta$ .
$M$	- $\mu^2/2\nu$ .
$\mu$	- $Ay/[V_M(b+1)]$ .
$N$	- $\mu/2$ .
$\nu$	- $y/[V_M(b+1)]$ .
$\rho$	- Per unit accuracy.
$\sigma_N$	- Rms value of miss caused by noise.
$\sigma_1, \sigma_2$	- Limits.
$\tau$	- Time variable of integration.
$\tau, \tau_1$	- Time constants.
$\Upsilon$	- $\frac{\chi^2 - n}{\sqrt{2n}}$ .
$\Phi_N$	- Spectral density of radar noise in $ft^2/\text{rad}/\text{sec}$ .
$\Phi'_N$	- Spectral density of noise in $\text{volts}^2/\text{rad}/\text{sec}$ .
$\Phi_{N,B}$	- Zero-frequency density of power return from beam of target.
$\Phi_{N,HO}$	- Zero-frequency density of power return from nose or tail of target.

$\Phi_{N,c}$	- Zero-frequency noise density, computer time.
$\Phi_{in}$	- Spectral density of input.
$\Phi_{out}$	- Spectral density of random signal at output of system.
$\Phi_{x,M}$	- Power spectrum of $x_M(t)$ .
$\Phi(\omega)$	- Spectral power density.
$\phi$	- Target velocity-vector angle.
$\phi_t$	- Transient value of $\phi$ .
$\phi_{x,M}(\tau)$	- Inverse Fourier transform of $\Phi_{x,M}$ .
$\phi(\tau)$	- Inverse Fourier transform of $\Phi(\omega)$ , autocorrelation function.
$\phi_0$	- Initial value of $\phi$ .
$\chi$	- $\sqrt{x_1^2 + x_2^2 + \dots + x_n^2}$ .
$\psi$	- $\tan^{-1} \left[ \frac{2a}{b} \left( \frac{1}{a} - \frac{b^2}{4a^2} \right) \right]^{1/2}$ .
$\omega$	- Frequency variable (rad/sec).
$\omega_F$	- Bandwidth of missile-control-system filter.
$\omega_{ss}$	- Single-sided bandwidth of quadratic noise filter.
$\omega_0$	- Natural frequency of y-locked simple-lag system.

[REDACTED]

APPENDIX B. - DESCRIPTION OF THE VARIABLE-TIME-SCALE SECTION OF  
THE M.I.T. FLIGHT SIMULATOR

The M.I.T. Flight Simulator<sup>6</sup> is divided into two main parts; a flight table section, which is designed to subject physical missile components to the angular motions which would occur in flight, and a generalized variable-time-scale section. In this thesis only the generalized computer was employed. The main features of this section are discussed briefly.

General Layout.

A general view of the new a-c portion of the generalized computer is shown in Fig. B-1. The portable table in front of the racks holds the recording equipment. Each of the first five racks from the left contains an electromechanical integrator unit complete with input and output amplifiers. The top of the second rack from the right contains six summing circuits. Immediately below these are the termination boards where all interconnections between units are made. The first rack on the right contains the overload-indication equipment at the top and, below this, fifteen coefficient amplifiers used for setting parameters into the problem. At the bottom of each rack is a power-regulator unit which receives plus 450 volts unregulated d.c. and delivers well-regulated plus 300 volts d.c.

Figure B-2 shows a general view of the d-c portion of the computer, where integrators are at the top of the left-hand rack. Below these are the summing circuits, then the termination board, and below that the modulators and demodulators. The middle rack contains the limiter

[REDACTED]

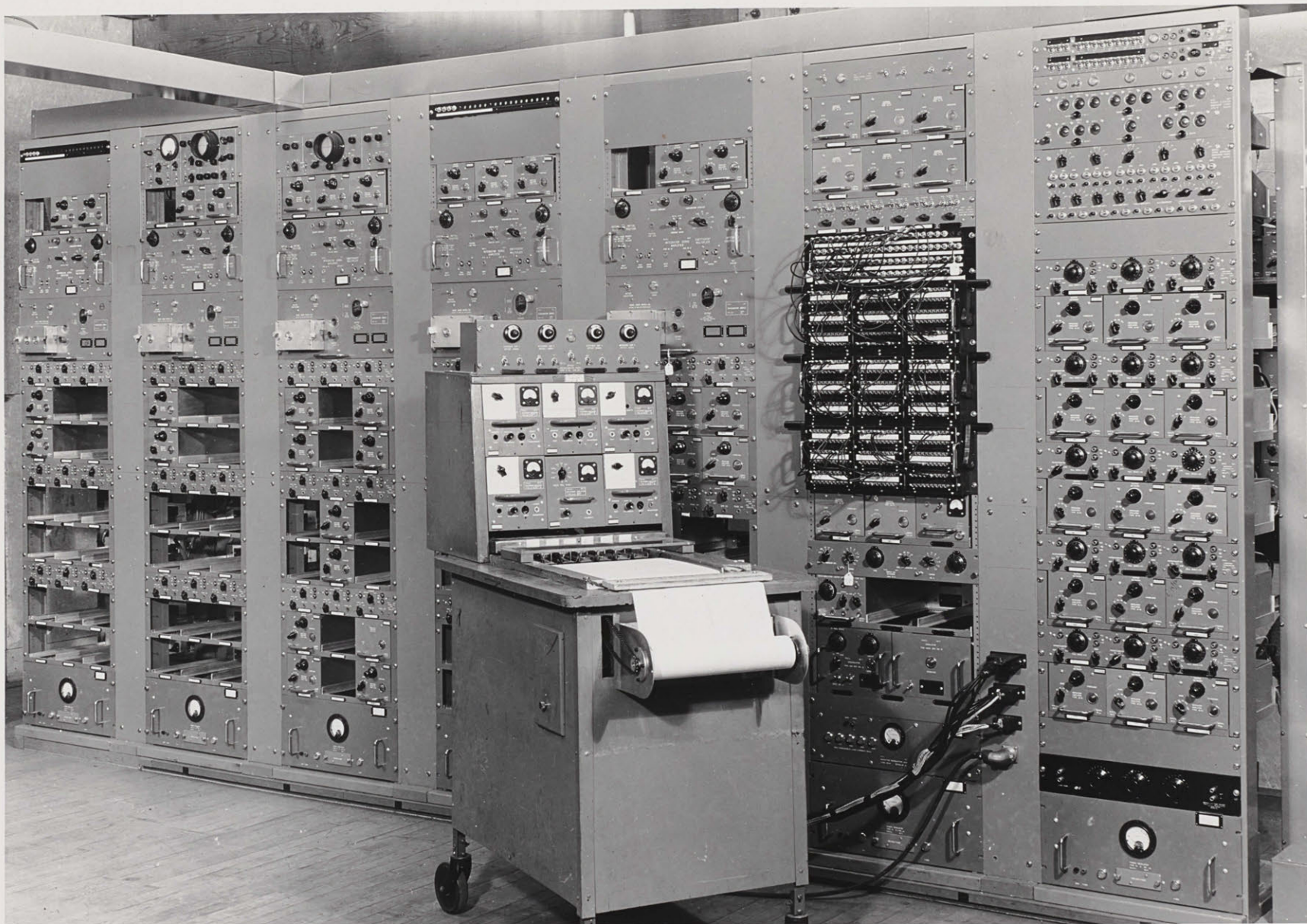


FIG. B-1. OVER-ALL VIEW OF THE GENERALIZED COMPUTER.

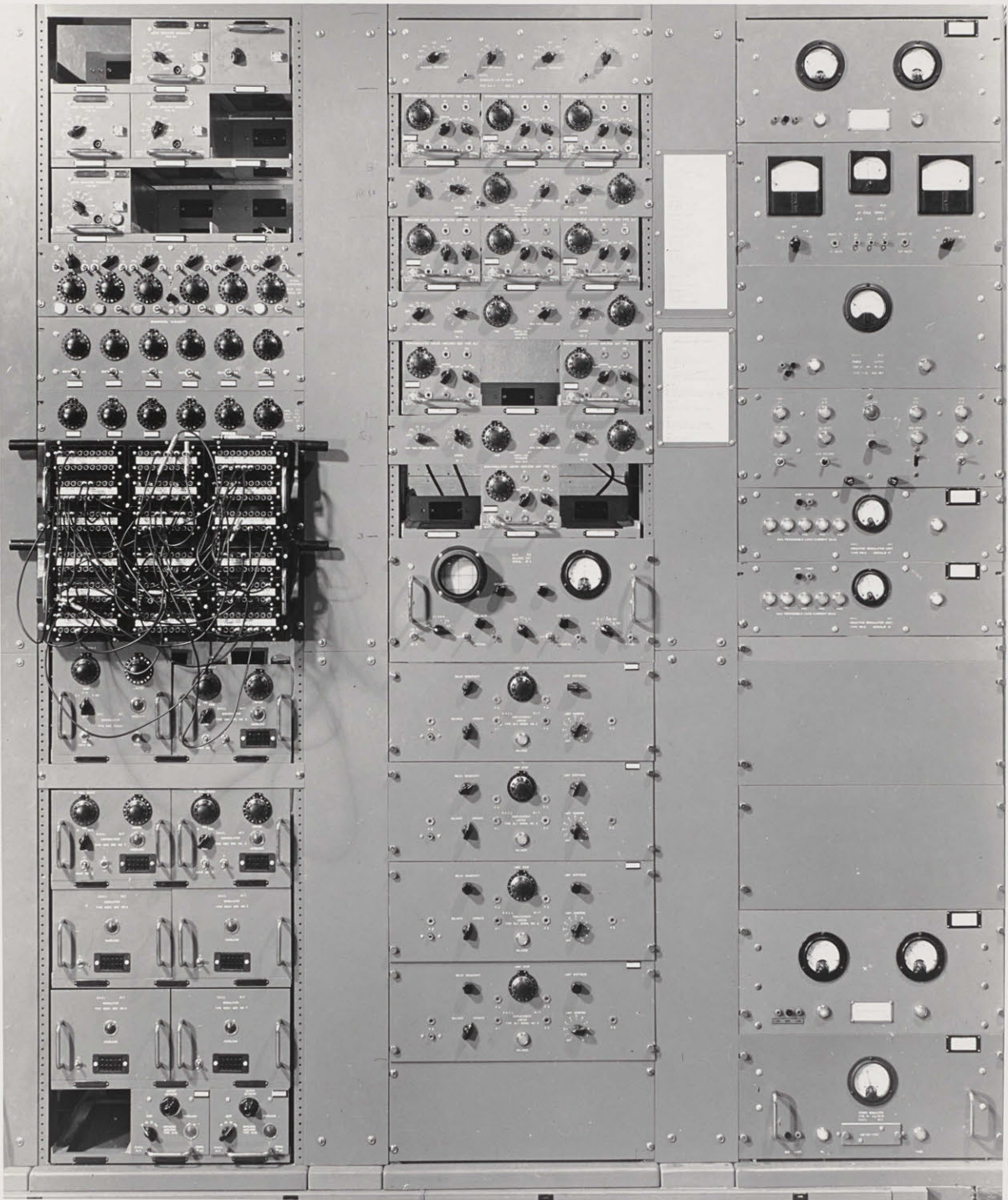


FIG. B-2. VIEW OF THE D-C PORTION OF THE COMPUTER.

amplifiers, time-constant networks, a balance unit used for testing purposes, and a group of displacement limiters. The right-hand rack contains all the power supplies for this group of equipment.

### Computing Components.

#### Integrators.

The electromechanical integrator<sup>7</sup> used in the computer employs a two-phase 400-cycle motor to drive a high-precision induction tachometer. A velocity servo is formed by feeding the tachometer output back to the input of the amplifier which feeds the motor. Such a servo yields an integration between the input voltage and the motor-shaft position. Provision is made for connecting a maximum of five output units (all potentiometers or all resolvers or a combination of the two) to the motor shaft through suitable gearing. The potentiometers make available signals proportional to the angle through which the motor shaft is turned while the resolvers give signals proportional to a linear combination of the sine and the cosine of the motor-shaft angle. A variable attenuator is provided in the input-signal channel and gearboxes of various ratios may be inserted between the motor and the output units so that the electrical and mechanical scale factors may be adjusted to operate the unit over its optimum range. Selection of the proper operating range is discussed in more detail in Sec. 2.2. These servos may also be used as position servos by closing a feedback loop around them with an appropriate error signal. The nominal steady-state accuracy of the integrator units is 0.1 per cent of full scale,\* but this accuracy may be seriously impaired by signals which call for

\* Accuracy is here based on the velocity of the motor shaft and 300 rad/sec represents full scale.

excessive angular rotation, velocity, or acceleration. The errors also may be increased by operating the servos over too small a range. Since the units are subject to the basic limitations on maximum available acceleration and velocity common to all electromechanical servos, these limitations must be considered in selecting the scale factors to be used and in deciding on the accuracy to be expected for the class of signals being handled. These considerations are discussed in some detail in Chap. 4.

An electrically operated clutch is provided in the gear train between the motor shaft and the output units in order to hold the output shaft at a fixed position while allowing the motor to turn at some desired velocity. This allows initial conditions, on position and velocity of the output shaft, to be set into the integrator.

In addition to the electromechanical integrators a group of all-electronic d-c integrators<sup>17</sup> is also available. Here integration is achieved by closing a feedback path around a high-gain d-c amplifier through a low-loss capacitor. Only one output, which is a negative constant times the integral of the input, is available from these units. Their nominal accuracy is only  $\pm 2$  per cent of full scale ( $\pm 100$  volts) but overloading difficulties are more easily avoided in these units than in the electromechanical integrators. This result follows since the amplitude of the signal imposes the only important limit on the system, with no limitation which is directly comparable to velocity or acceleration limiting in an electromechanical unit.

### Repeater Amplifiers.

The repeater amplifiers<sup>8, 9</sup> are general-purpose amplifiers employed as buffers, scale changers, drivers for potentiometers and resolvers, pickoff amplifiers following potentiometers and resolvers, and ground-isolation amplifiers. Type Ar-10 units have built-in attenuators providing fixed gains of times 1, 2, 5 and 10, while older Ar-6 and Ar-9 units have a fixed gain of times 10. A large amount of negative feedback ( $\mu\beta > 2000$ ) is employed in these amplifiers to give a high degree of gain stability. The nominal maximum output of these units is 50 volts, and the gain is initially set to  $\pm 0.02$  per cent of full output, while the noise level referred to the input is held below 50 microvolts.

### Coefficient Potentiometers.

Two styles of coefficient potentiometers are employed for setting fixed coefficients into a problem setup. The older units are adjusted at a test position with the aid of a standard attenuator and are then plugged into position in the computer. The newer units have direct-reading dials and are mounted permanently. Both types provide a resolution of approximately 0.1 per cent of full scale.

### Summing Circuits.

In the a-c portion of the computer, summing operations are performed with a resistive summing network followed by an amplifier. In the older arrangement the summing circuit was separate from the amplifier, while in the new equipment the summing network is built into the

amplifier unit. A maximum of eight summing channels is available in a single unit. Precision resistors are employed along with phase compensation, so that an over-all accuracy of  $\pm 0.05$  per cent is achieved for each channel with a maximum phase shift of 0.06 degree.

In the d-c portion of the computer, summing is also performed with resistive networks. These units provide an accuracy of  $\pm 0.1$  per cent if the requirements on source and load impedances are observed.

#### Demodulators and Modulators.

Demodulators and modulators<sup>17 \*</sup> are available for the purpose of converting 400-cycle suppressed-carrier signals to direct current and back again, as desired. These units may be employed for eliminating quadrature components from a signal, or for translating a 400-cycle signal to a d-c basis and back again.

The gain of the demodulators may be set, by means of a potentiometer, at any convenient gain from 0 to 100 while the gain of the modulators is fixed at times 1/2. The accuracy of these units is  $\pm 1/2$  per cent of full scale.

#### Limiter Amplifiers.

Amplitude limiting is one of the important nonlinear effects which it is advantageous to study on the computer.<sup>17 \*\*</sup> For example, it may be desirable to simulate the effect of limit stops in restricting the maximum deflection of a control surface. In the work which has been done to date, a sharp limit has been assumed. In order to achieve this

---

\*Johnson, op. cit., Secs. 3.3 and 3.6.

\*\*Johnson, op. cit., Sec. 3.4.

well-defined limit on the maximum amplitude of a signal, the limiting has been accomplished in the computer on a d-c basis. If a-c limiting is employed, the fundamental component of the signal continues to rise for some time after limiting of the peak first occurs. Since the integrators are sensitive only to the fundamental component of the signal, limiting of this type therefore does not occur at a well-defined level. If the peak amplitude of the input and the output signals is assumed to be 1.0 for the level at which limiting just begins, then the output continues to rise as the input is increased from 1.0. It reaches a value of 1.3 for an input of 2.0, and approaches a value of 1.57 for very large inputs. In addition, the output signal contains a large harmonic content while in the limiting range, and this may cause difficulty at other points in the computer. These difficulties are avoided by demodulating the signal, limiting it on a d-c basis, and then remodulating it. Some filtering must be employed following the demodulator, since the harmonics from its output result in poor modulator operation and a poorly defined limiting value for the same reason as in a-c limiter operation. The time constant of the filter fortunately can be made small enough that its effect cannot be noticed in the over-all operation. An RC filter with a time constant of 0.006 second was found to give satisfactory filtering. When this is used in a setup operating with an 8-to-1 time scale extension, it represents a time constant of only 0.75 millisecond. This lag is cascaded with the simulated filtering in the missile. Although this small increase appears to be negligible in the particular setup used, considerable

discretion must be exercised in adding such lags, since such additions may result in instability of the over-all system.

The limiter amplifiers provide gains of 1, 2, 5, and 10 times to an accuracy ranging between  $\pm 0.5$  and  $\pm 1.75$  per cent depending on the gain setting. In spite of the fact that these are d-c amplifiers, their drift rate is extremely low once they have been allowed to warm up. The nominal full-scale output is 100 volts across a 25,000-ohm load and the limiting level can be set directly at any value from approximately  $\pm 2$  volts to  $\pm 100$  volts, although limiting at levels below  $\pm 10$  volts should be avoided. Above 10 volts, the accuracy with which the limit can be set is only a few per cent since the d-c voltage used to set the limits is well regulated while the a-c signal source is unregulated.

Where limiters are employed, the problem of energy storage for signals greater than the limiting value should be considered. In the limiter amplifiers discussed here, two arrangements are possible. For one input, a series resistance of 510,000 ohms appears between the input to the limiter and the point where the voltage is actually limited. The operation obtained, therefore, depends upon whether the voltage to be limited appears in a purely resistive circuit, where no energy storage exists, or if it appears across a condenser. In the latter case, the voltage across the condenser can continue to build up and store more energy after the limits are reached; so that, if the source voltage later decreases, the excess energy must be dissipated before limiting ceases. An alternate input is automatically selected

when a limiter amplifier is used in what has been designated a limiter-amplifier resistance-capacitance filter position. This input provides a very low impedance for voltages above the limiting level and thus limits the stored energy.

#### High-speed Multiplier.

Figure B-3 shows a rack containing two complete high-speed multiplier<sup>18</sup> units. Each of these units employs four strain-gauge bridges driven in parallel by a loudspeaker-type electromechanical transducer. A fixed voltage is supplied to one of these bridges and a servo loop is closed around it. Therefore, the output from this channel and hence the strain applied to all the units, follows the input. The other three bridges may be fed from whatever voltages are desired. Thus, a single multiplier can be employed to raise a signal to the fourth power or to multiply three multiplicands by a common multiplier.

The nominal accuracy of the unit is 0.1 per cent of full scale if both the multiplier and multiplicand are kept within the allowable operating range. The full output range may be utilized at frequencies up to 65 cps and 50 per cent of full output at frequencies up to 100 cps. The phase shift at 30 cps is approximately 10 degrees.

#### Dividers.

A highly accurate divider could be set up by employing the multiplier just described as the feedback element in a closed-loop system. At the time a divider was required for this study, such operation had not been attempted; furthermore, the available multipliers were being

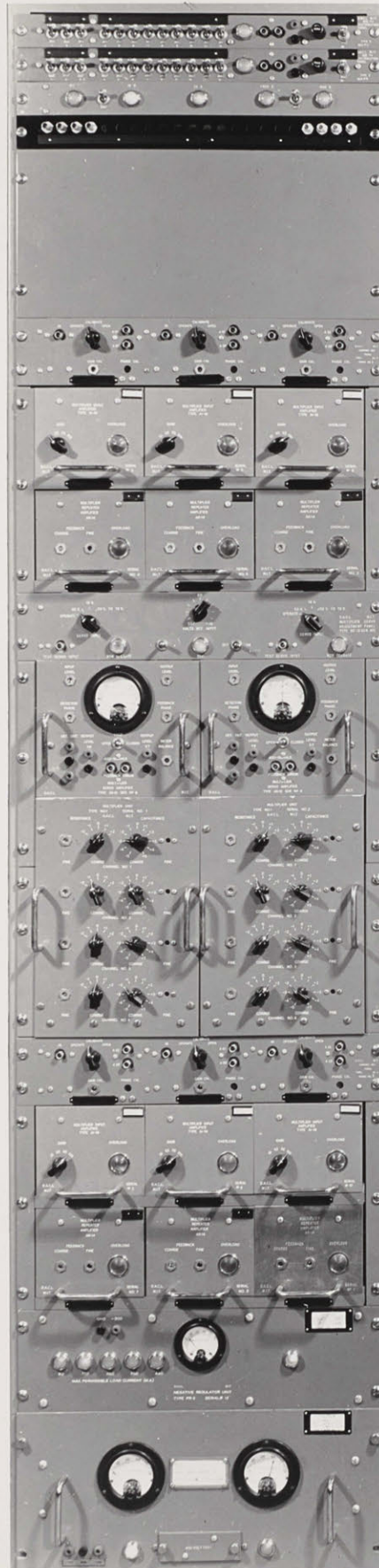


FIG. B-3. VIEW OF RACK CONTAINING HIGH-SPEED MULTIPLIER UNITS.

██████████

used as multipliers. On the other hand, it was a relatively easy matter to set up a conventional divider servo. This was done, and the unit served its intended purpose well, although it could hardly be called a precision computing element. Later, when a more accurate divider was required and standard integrator servo units were available, one of these units was connected as a divider.

#### Recording Equipment.

Output quantities are recorded on a 6-channel Brush recorder which uses galvanometer-type pen motors with direct-inking pens. Since the pens operate on direct current and the signals are 400-cycle voltages, special recorder-amplifier units are employed. These units provide a range of gains, so that signals can always be recorded to the best advantage. The output units in the amplifiers are electromechanical choppers which convert the incoming 400-cycle signal to direct current for operating the pens. For indicating the recording scale being used, a code marker is automatically applied to each of the six channels whenever the paper drive is started. This has been found extremely valuable during data analysis.

When frequently zeroed and calibrated, these recorder units are accurate to within approximately  $\pm 2$  per cent of full scale. Unfortunately both the zeros and the deflection sensitivities vary with time but the pens are calibrated frequently to maintain approximately the  $\pm 2$  per cent recording accuracy quoted above.

Toward the end of this investigation, a prototype plotting table which provides for recording two quantities on a 30-by-30-inch area,

██████████

was available for a short time.

#### Automatic-sequencing Equipment.

Soon after statistical studies were begun on the computer, it became evident to the author that the only practical way to use the machine for these studies would be to provide automatic operation. Therefore, an automatic-sequence-control unit was designed which performs the following sequence of operations:

1. Shuts off problem when the collision point is reached, and at the same time returns all recorder pens to zero, and turns off the recorder paper drive.
2. Returns all integrators to their initial positions and then clutches them. After this operation a time interval is provided to allow for parameter changes between successive solutions.
3. Starts the recorder drive motor to provide blank paper for binding purposes at the beginning of each solution.
4. Applies power to recorders and thereby records the scale markers for each channel.
5. Unclutches the integrators and starts the problem.

This equipment has proved of considerable help in all types of machine operation but is of most value in statistical studies where no parameters need to be changed between successive solutions. In such studies all the operator must do, once the machine has been checked out, is to code the solutions as they come out of the machine, see that the recorder does not run out of ink or paper, and watch for evidences

[REDACTED]

of poor machine operation. Under such conditions, proportional-  
navigation problems involving an initial range of 4000 feet may be  
solved, with an 8-to-1 time-scale-extension factor, at the rate of  
one solution approximately every 30 seconds.

[REDACTED]

[REDACTED]

APPENDIX C. - TABLE OF INTEGRALS

Integrals of the form

$$I_n = \frac{1}{2\pi i} \int_{-i\infty}^{i\infty} \left| \frac{c_{n-1}s^{n-1} + \dots + c_0}{d_n s^n + \dots + d_0} \right|^2 ds$$

may be evaluated with the following formulas. Tables of this type were given by James, Nichols, and Phillips.<sup>21</sup> The present tables, an extension of Phillips' work, were developed under the direction of R. C. Booton of the D.A.C.L. The details of the calculations were carried out by Misses V. D. Lee, J. M. Murphy, and B. L. White. Additional credit should be given to Miss J. M. Murphy for introducing the present factored form of the tables.

[REDACTED]

$$I_1 = \frac{c_0^2}{2d_0d_1}$$

$$I_2 = \frac{c_1^2d_0 + c_0^2d_2}{2d_0d_1d_2}$$

$$I_3 = \frac{c_2^2d_0d_1 + (c_1^2 - 2c_0c_2)d_0d_3 + c_0^2d_2d_3}{2d_0d_3(-d_0d_3 + d_1d_2)}$$

$$I_4 = \frac{c_3^2(-d_0^2d_3 + d_0d_1d_2) + (c_2^2 - 2c_1c_3)d_0d_1d_4 + (c_1^2 - 2c_0c_2)d_0d_3d_4 + c_0^2(-d_1d_4^2 + d_2d_3d_4)}{2d_0d_4(-d_0d_3^2 - d_1^2d_4 + d_1d_2d_3)}$$

$$I_5 = \frac{1}{2\Delta_5} \left[ c_4^2 m_0 + (c_3^2 - 2c_2c_4)m_1 + (c_2^2 - 2c_1c_3 + 2c_0c_4)m_2 + (c_1^2 - 2c_0c_2)m_3 + c_0^2 m_4 \right]$$

$$m_0 = \frac{1}{d_5} \left[ d_3 m_1 - d_1 m_2 \right]$$

$$m_1 = -d_0 d_3 + d_1 d_2$$

$$m_2 = d_0 d_5 + d_1 d_4$$

$$m_3 = \frac{1}{d_0} \left[ d_2 m_2 - d_4 m_1 \right]$$

$$m_4 = \frac{1}{d_0} \left[ d_2 m_3 - d_4 m_2 \right]$$

$$\Delta_5 = d_0 \left[ d_1 m_4 - d_3 m_3 + d_5 m_2 \right]$$

$$I_6 = \frac{1}{2\Delta_6} \left[ c_5^2 m_0 + (c_4^2 - 2c_3 c_5) m_1 + (c_3^2 - 2c_2 c_4 + 2c_1 c_5) m_2 + (c_2^2 - 2c_1 c_3 + 2c_0 c_4) m_3 \right. \\ \left. + (c_1^2 - 2c_0 c_2) m_4 + c_0^2 m_5 \right]$$

$$m_0 = \frac{1}{d_6} \left[ d_4 m_1 - d_2 m_2 + d_0 m_3 \right]$$

$$m_1 = d_0 d_1 d_5 + d_0 d_3^2 + d_1^2 d_4 - d_1 d_2 d_3$$

$$m_2 = d_0 d_3 d_5 + d_1^2 d_6 - d_1 d_2 d_5$$

$$m_3 = d_0 d_5^2 + d_1 d_3 d_6 - d_1 d_4 d_5$$

$$m_4 = \frac{1}{d_0} \left[ d_2 m_3 - d_4 m_2 + d_6 m_1 \right]$$

$$m_5 = \frac{1}{d_0} \left[ d_2 m_4 - d_4 m_3 + d_6 m_2 \right]$$

$$\Delta_6 = d_0 \left[ d_1 m_5 - d_3 m_4 + d_5 m_3 \right]$$

$$I_7 = \frac{1}{2\Delta_7} \left[ c_6^2 m_0 + (c_5^2 - 2c_4 c_6) m_1 + (c_4^2 - 2c_3 c_5 + 2c_2 c_6) m_2 + (c_3^2 - 2c_2 c_4 + 2c_1 c_5 - 2c_0 c_6) m_3 \right. \\ \left. + (c_2^2 - 2c_1 c_3 + 2c_0 c_4) m_4 + (c_1^2 - 2c_0 c_2) m_5 + c_0^2 m_6 \right]$$

$$m_0 = \frac{1}{d_7} \left[ d_5 m_1 - d_3 m_2 + d_1 m_3 \right]$$

$$m_1 = - (d_1 d_4 - d_0 d_5)^2 + (d_0 d_3 - d_1 d_2) (d_0 d_7 - d_1 d_6 + d_2 d_5 - d_3 d_4)$$

$$m_2 = (d_0 d_7 - d_1 d_6) (-d_0 d_5 + d_1 d_4) + (d_0 d_3 - d_1 d_2) (d_2 d_7 - d_3 d_6)$$

$$m_3 = (d_0 d_7 - d_1 d_6)^2 + (d_0 d_3 - d_1 d_2) (d_4 d_7 - d_5 d_6)$$

$$m_4 = \frac{1}{d_0} \left[ d_2 m_3 - d_4 m_2 + d_6 m_1 \right]$$

$$m_5 = \frac{1}{d_0} \left[ d_2 m_4 - d_4 m_3 + d_6 m_2 \right]$$

$$m_6 = \frac{1}{d_0} \left[ d_2 m_5 - d_4 m_4 + d_6 m_3 \right]$$

$$\Delta_7 = d_0 \left[ d_1 m_6 - d_3 m_5 + d_5 m_4 - d_7 m_3 \right]$$

$$I_8 = \frac{1}{2\Delta_8} \left[ c_7^2 m_0 + (c_6^2 - 2c_5c_7) m_1 + (c_5^2 - 2c_4c_6 + 2c_3c_7) m_2 + (c_4^2 - 2c_3c_5 + 2c_2c_6 - 2c_1c_7) m_3 \right. \\ \left. + (c_3^2 - 2c_2c_4 + 2c_1c_5 - 2c_0c_6) m_4 + (c_2^2 - 2c_1c_3 + 2c_0c_4) m_5 + (c_1^2 - 2c_0c_2) m_6 + c_0^2 m_7 \right]$$

$$m_0 = \frac{1}{d_8} \left[ d_6 m_1 - d_4 m_2 + d_2 m_3 - d_0 m_4 \right]$$

$$m_1 = (d_0 d_7 + d_2 d_5) (-d_0 d_1 d_7 + d_0 d_3 d_5 + 2d_1^2 d_6) + (d_3 d_7 - d_5^2) (d_0^2 d_5 + d_1 d_2^2) + d_1 d_3 d_8 (d_0 d_3 - d_1 d_2) \\ - d_1^2 d_8 (d_0 d_5 - d_1 d_4) + (-d_2 d_7 + d_3 d_6 - d_4 d_5) (d_0 d_3^2 + d_1^2 d_4) - d_1 d_6 (d_1^2 d_6 + 3d_0 d_3 d_5) \\ - d_1 d_2 d_3 (d_3 d_6 - d_4 d_5) + 2d_0 d_1 d_4 d_5^2$$

$$m_2 = (d_0 d_3 - d_1 d_2) (d_0 d_7^2 - d_1 d_5 d_8 - d_1 d_6 d_7 + d_2 d_5 d_7) + (d_3 d_8 - d_4 d_7) (-d_0 d_1 d_5 + d_0 d_3^2 - d_1 d_2 d_3 + d_1^2 d_4) \\ - d_0 d_5 d_7 (d_0 d_5 - d_1 d_4) + d_1^2 d_8 (d_0 d_7 - d_1 d_6)$$

$$m_3 = -d_1 (d_1 d_8 - d_2 d_7)^2 + (-d_5 d_8 + d_6 d_7) (d_0 d_1 d_5 - d_0 d_3^2 + d_1 d_2 d_3 - d_1^2 d_4) \\ + d_0 d_7^2 (-d_0 d_5 + d_1 d_4 + d_2 d_3) - 2d_0 d_1 d_3 d_7 d_8$$

$I_8$  (Continued)

$$m_4 = (-d_5d_8 + d_6d_7)(2d_0d_1d_7 - d_0d_3d_5 + d_1d_2d_5 - d_1^2d_6) + (-d_3d_8 + d_4d_7)(d_0d_3d_7 - d_1d_2d_7 + d_1^2d_8) - d_0^2d_7^3$$

$$m_5 = \frac{1}{d_0} \left[ d_2m_4 - d_4m_3 + d_6m_2 - d_8m_1 \right]$$

$$m_6 = \frac{1}{d_0} \left[ d_2m_5 - d_4m_4 + d_6m_3 - d_8m_2 \right]$$

$$m_7 = \frac{1}{d_0} \left[ d_2m_6 - d_4m_5 + d_6m_4 - d_8m_3 \right]$$

$$\Delta_8 = d_0 \left[ d_1m_7 - d_3m_6 + d_5m_5 - d_7m_4 \right]$$

[REDACTED]

APPENDIX D. - ACCURACY CONSIDERATIONS IN STATISTICAL STUDIES

by R. C. Booton, Jr.

Many of the important problems in the control field involve random (or statistical) variables. One such problem that has received much study is the effect of radar noise upon a guided-missile control system. An answer to a problem containing statistical variables must be derived from a number of solutions in which all conditions except the behavior of the statistical variable are the same. If, as is often the case, the solutions are obtained by numerical methods or from a computer, an important practical factor is the number of solutions required for a given accuracy. A complete answer concerning the required number of solutions is, in general, impossible, because it must involve a knowledge of the answer to the problem being studied. If, however, some simplifying assumptions are made, definite results can be stated. One especially important assumption is that the variable (answer) be normally distributed. The case where the variable is normally distributed with a zero mean value is discussed later in this paper.

Because of the statistical nature of the accuracy considerations, in general, no finite number of solutions can produce, with certainty, any value of accuracy. Theoretically, it is even possible for an infinite number of solutions to yield an inaccurate answer, but this possibility usually has zero probability. The only quantity that can be calculated is the probability of achieving a certain accuracy. For the zero-mean normally distributed case, the following paragraphs demonstrate the calculation of this probability. Figure D-1\* shows the

---

\* The original figure numbers have been changed to conform with the numbering system of this thesis.

[REDACTED]

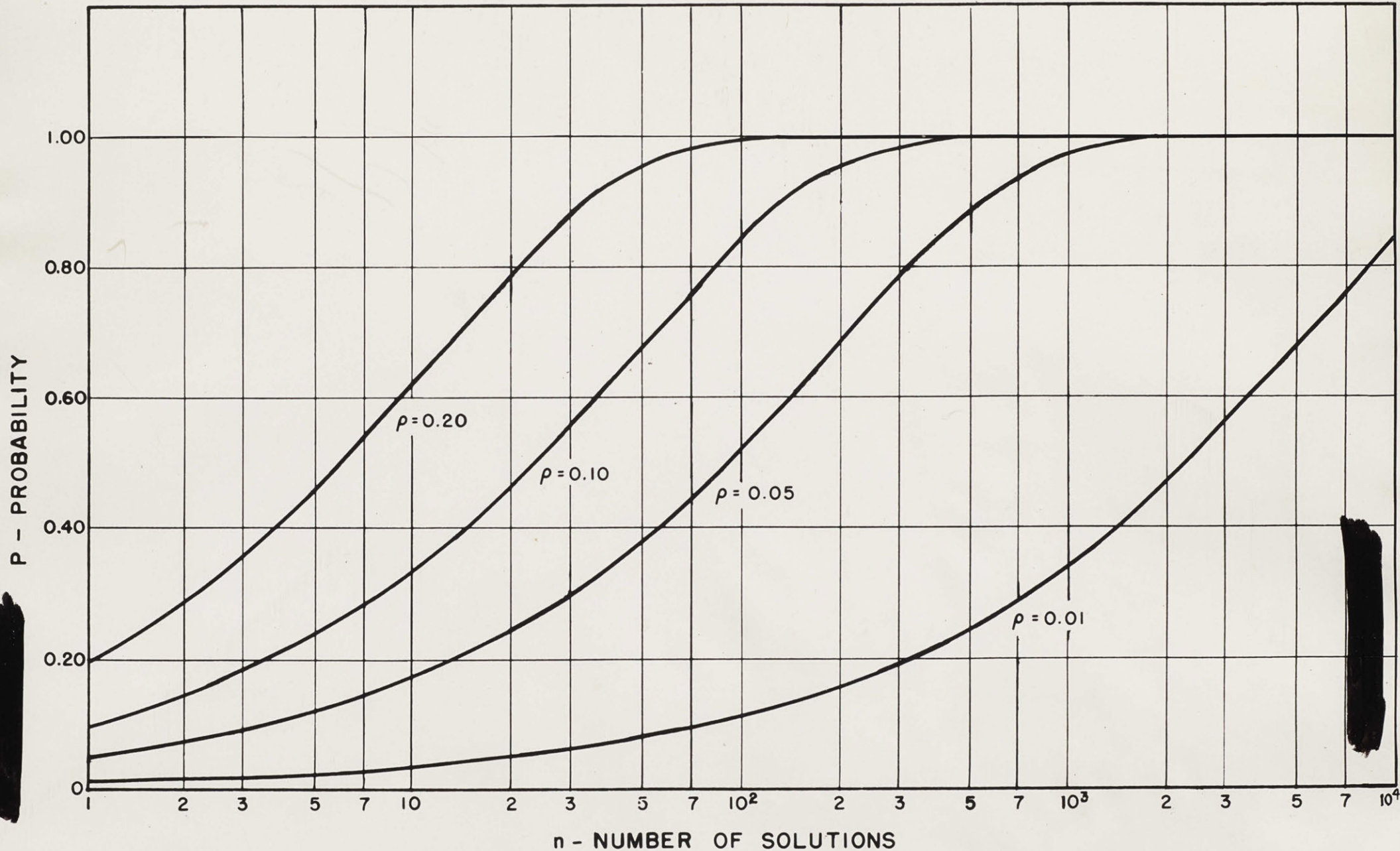


FIG. D-1. PROBABILITY OF ACHIEVING AN ACCURACY  $\rho$  (PER UNIT) AS A FUNCTION OF THE NUMBER OF SOLUTIONS.

probability of achieving certain accuracies as a function of the number of solutions.

For practical use, a value of accuracy that has a probability of over 0.95 can be regarded as almost certain. Figure D-2 shows the 0.95 probability accuracy as a function of the number of solutions required. This diagram reveals that an almost-certain accuracy of 5 per cent is achieved only with more than 800 solutions. Regardless of the source of the data, gathering this number of samples presents a formidable problem.

A more reasonable definition of accuracy can be taken as the accuracy that has 0.5 probability. This accuracy, which may be called the expected accuracy, is also plotted in Fig. D-2.

It should be pointed out that these calculations assume the independence of the samples. If the samples are taken from uncorrelated sources or if the times at which the samples are taken are sufficiently separated, the samples may be assumed independent. Since most computer solutions will probably be obtained with the successive use of a single random-variable source, the time interval that must be allowed between samplings to achieve independence should be investigated for the particular situation. An example of this type of calculation may be found in a doctoral thesis\* by W. W. Seifert.

The accuracy calculation given below should be extended to other cases. Other classical distributions, such as the nonzero-mean normal distribution and the Poisson distribution, seem to be reasonable cases to investigate. Experimental work has indicated that the accuracies

---

\* See p. 110.

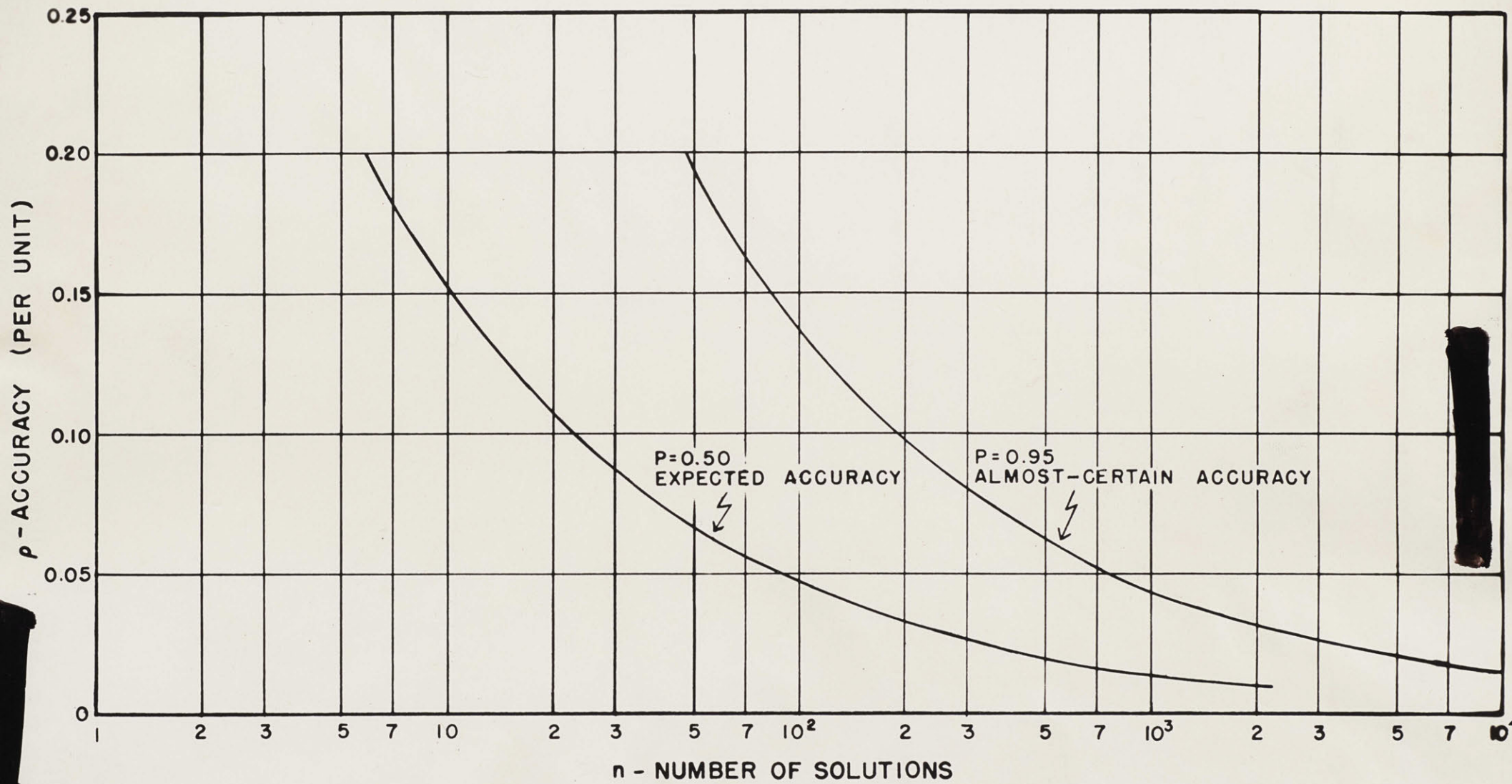


FIG. D-2. ALMOST-CERTAIN AND EXPECTED ACCURACY FROM n SOLUTIONS.

for many distributions only roughly approximating the normal and having a nonzero mean are not too far different from the accuracies plotted here.

The mathematical basis of the calculations for the curves presented in Figs. D-1 and D-2 will now be demonstrated. The values of the variable obtained from the various solutions (numerical or computer) will be treated as independent samples of a zero-mean normally distributed variable.

Suppose  $x_1, \dots, x_n$  are independent measurements of a normally distributed variable with mean of 0 and standard deviation of 1. The required result is the value of the probability that the rms value of the  $n$  measurements be between  $\sigma_1$  and  $\sigma_2$ . These limits will usually be taken as  $\sigma_1 = 1 - \rho$ ,  $\sigma_2 = 1 + \rho$ .

The rms value of  $x$  is defined as

$$x_{\text{rms}} = \sqrt{\frac{x_1^2 + x_2^2 + \dots + x_n^2}{n}}$$

Let

$$\chi^2 = x_1^2 + \dots + x_n^2.$$

Then  $\sigma_1 < x_{\text{rms}} < \sigma_2$  is equivalent to

$$R_1^2 = n\sigma_1^2 < \chi^2 < n\sigma_2^2 = R_2^2.$$

If  $P(\chi^2 < R^2)$  is the probability that  $\chi^2 < R^2$ ,

$$P(\chi^2 < R^2) = \int_{S_n(R)} \frac{1}{(2\pi)^{n/2}} e^{-\chi^2/2} dx_1 \dots dx_n,$$

where the range of integration  $S_n(R)$  is the  $n$ -dimensional sphere with center  $O$  and radius  $R$ ; that is,  $S_n(R)$  is the range of values of  $x_1, \dots, x_n$  for which  $x_1^2 + \dots + x_n^2 < R^2$ . By a change of variables and partial integration,

$$P(\chi^2 < R^2) = \frac{1}{2^{n/2} \Gamma(n/2)} \int_0^{R^2} (\chi^2)^{(n-2)/2} e^{-\chi^2/2} d\chi^2.$$

Letting

$$w = \chi^2/2, \quad W = R^2/2,$$

$$\begin{aligned} P(\chi^2 < R^2) &= \frac{1}{2^{n/2} \Gamma(n/2)} \int_0^W (2w)^{(n-2)/2} e^{-w} 2 dw \\ &= \frac{1}{\Gamma(n/2)} \int_0^W w^{n/2 - 1} e^{-w} dw \\ &= \frac{\Gamma_W(n/2)}{\Gamma(n/2)}, \end{aligned}$$

where  $\Gamma_W(n/2)$  is the incomplete gamma function. Pearson has tabulated\* the ratio of the incomplete gamma function to the complete gamma function. With the notation of these tables

$$P(\chi^2 < R^2) = I(u, p),$$

where

$$p = n/2 - 1$$

$$u = \frac{W}{\sqrt{n/2}} = \frac{R^2}{\sqrt{2n}}.$$

Then

$$P(\sigma_1 < x_{\text{rms}} < \sigma_2) = I(u_2, p) - I(u_1, p),$$

\* Pearson, Karl, Tables of the Incomplete  $\Gamma$ -function. London: His Majesty's Stationery Office, 1922.

where

$$p = n/2 - 1$$

$$u = \frac{W}{\sqrt{n/2}} = \frac{R^2}{\sqrt{2n}} :$$

Then

$$P(\sigma_1 < x_{\text{rms}} < \sigma_2) = I(u_2, p) - I(u_1, p),$$

where

$$p = n/2 - 1$$

$$u_2 = \sigma_2^2 \sqrt{n/2}$$

$$u_1 = \sigma_1^2 \sqrt{n/2} .$$

Since Pearson's tables contain values of  $I(u, p)$  up to 50 only, it is necessary to use an approximation for values of  $n$  greater than 100. It can be shown that for large  $n$ ,  $\chi^2$  is approximately normally distributed with a mean of  $n$ , and deviation of  $\sqrt{2n}$ .

Thus

$$T = \frac{\chi^2 - n}{\sqrt{2n}} = \sqrt{n/2} (x_{\text{rms}}^2 - 1)$$

is approximately normal (0,1).

Then

$$P(\sigma_1 < x_{\text{rms}} < \sigma_2) = \frac{1}{\sqrt{2\pi}} \int_{\sqrt{n/2} (\sigma_1^2 - 1)}^{\sqrt{n/2} (\sigma_2^2 - 1)} e^{-T^2/2} dT.$$

If, as before,

$$\sigma_1^2 = (1 - \rho)^2 = 1 - 2\rho + \rho^2$$

and

$$\sigma_2^2 = (1 + \rho)^2 = 1 + 2\rho + \rho^2,$$

then

$$\begin{aligned} P(\sigma_1 < x_{\text{rms}} < \sigma_2) &= \frac{1}{\sqrt{2\pi}} \int_{\sqrt{n/2}(-2\rho + \rho^2)}^{\sqrt{n/2}(2\rho + \rho^2)} e^{-T^2/2} dT \\ &= \frac{1}{\sqrt{2\pi}} \int_{-\rho\sqrt{2n}}^{\rho\sqrt{2n}} e^{-T^2/2} dT, \text{ approximately.} \end{aligned}$$

This approximation is accurate for values of  $n$  greater than about 30.

## APPENDIX E. - SOLUTION CODING AND DATA RECORDING TECHNIQUES

The problem of maintaining adequate records of the exact manner in which any large-scale computer is set up assumes considerable importance. Unless the problem being run is completely specified and records are kept of the parameter values used for each solution and of the scale factors used at various points within the computer and at the output recorders, the problem of analyzing the data obtained from the machine becomes a hopeless task. A few comments on the operating techniques which have been developed at D.A.C.L. will be given as a possible aid to others faced with similar problems.

After a basic setup diagram such as shown in Fig. 5.2-4 is decided upon, detailed setup sheets are drawn for each servo, showing the electrical gains, the gearbox ratio, and the arrangement of output units required. Details are drawn up for the setup of any special equipment such as the limiter and the noise equipment and a schedule of amplifier positions and gains is made along with a listing of the cable trunks required. Furthermore, a pair of code sheets such as shown in Figs. E-1 and E-2 are drawn up, listing the parameters which are varied and the parameters which are held constant during a particular study. In so far as possible, the schedule of runs to be made in a particular study is established before machine operation begins and each run to be made is given a twelve-letter code and assigned a number. As the solutions are obtained from the machine each is stamped with the code, a number, and the date, to assist in later analysis and filing. In addition, a data sheet (Fig. E-3) is kept for each set of noise runs and on this sheet

are listed the miss for each run of the group and the average value of the noise-monitor output for that run. The two values are read directly as the data are obtained from the machine and the rms value of the miss and the value of the noise power density are computed as soon as possible after the conclusion of a set of runs.

CODE POSITION	1	2	3	4	5	6	7	8	9	10	11	12
Parameter Code Letter												
A	✓		-90	2000	0	0	4	✓	✓	✓	1/4	.707
B			-60	4000	10	0.597	6				1/16	.353
C		✓	-30	6000	20	1.38	8				1/36	.236
D			0	8000	30	2.8	10				1/64	.177
E			+ 30	10,000	40	3.45					1/100	.141
F			+ 60	12,000		6.9						0.4
G			+ 90	14,000		13.5						0.2
H						24.2						0.133
I												0.1
J												0.08
K												
L												
M												
N												
O												
P												
Q												
R												
S												
T												
U												
V												
W												
X												
Y												
Z												

FIG. B-1. AC CODE SHEET.

PROBLEM: Proportional navigation with quadratic filter.

Missile dynamics neglected.

Limiting on  $\dot{\theta}$ . Input to filter not limited.

$V_T = 1000$  ft/sec.

$a_T = 4g$  constant turn beginning at  $r_1$ .

$V_M = 2000$  ft/sec.

$a_{M,max} = 10g$ .

Initial-heading error,  $E = 0$ .

$\dot{\theta}_0 = 0$ .

$\theta_0 = 0$ .

Noise power spectrum shaped by passing white noise  
through a quadratic filter with a damping  $\zeta_{ss} = 0.7$ .

SPECIAL COMPUTER SETUP:

1/y servo in place of  $\alpha$  servo.

8:1 time-scale extension.

FIG. E-2. LIST OF PARAMETERS HELD CONSTANT FOR ALL CODE AC STUDIES.

D.A.C.L. DATA SHEET

<u>DATE</u> _____	<u>RANGE</u> _____	<u>CHANNEL</u>	<u>QUANTITY</u>	<u>SCALE</u>
<u>CODE</u> _____	<u>LIMITING</u> _____	1.	_____	_____
	<u>ASPECT ANGLE <math>\phi</math></u> _____	2.	_____	_____
	<u>b + 1</u> _____	3.	_____	_____
	<u>A</u> _____	4.	_____	_____
		5.	_____	_____
		6.	_____	_____

1.			26.			51.			76.		
2.			27.			52.			77.		
3.			28.			53.			78.		
4.			29.			54.			79.		
5.			30.			55.			80.		
6.			31.			56.			81.		
7.			32.			57.			82.		
8.			33.			58.			83.		
9.			34.			59.			84.		
10.			35.			60.			85.		
11.			36.			61.			86.		
12.			37.			62.			87.		
13.			38.			63.			88.		
14.			39.			64.			89.		
15.			40.			65.			90.		
16.			41.			66.			91.		
17.			42.			67.			92.		
18.			43.			68.			93.		
19.			44.			69.			94.		
20.			45.			70.			95.		
21.			46.			71.			96.		
22.			47.			72.			97.		
23.			48.			73.			98.		
24.			49.			74.			99.		
25.			50.			75.			100.		

FIG. E-3. TYPICAL DATA SHEET

[REDACTED]

APPENDIX F. - BIBLIOGRAPHY

1. Clymer, A. B., Proportional Navigation Trajectories, Meteor Report No. 24. Cambridge, Mass.: Mass. Inst. of Tech., June 30, 1949 (Secret).
  2. Steeg, C. W., Jr., Trajectory Analyses and Stability Criteria, Meteor Report No. 27. Cambridge, Mass.: Mass. Inst. of Tech., December 31, 1948 (Secret).
  3. Jones, T. F., Jr., R. C. Booton, Jr., and G. H. Hart, The Effect of Time Lag on Proportional Navigation Trajectories, Meteor Report No. 38. Cambridge, Mass.: Mass. Inst. of Tech., July, 1949 (Confidential).
  4. Booton, R. C., Jr., Effect of Circular Target Maneuvers on Homing Missile Trajectories, Meteor Report No. 47. Cambridge, Mass.: Mass. Inst. of Tech., November, 1949 (Secret).
  5. Booton, R. C., Jr., Optimum Design and Miss Distributions of Homing Missiles, Meteor Report No. 50. Cambridge, Mass.: Mass. Inst. of Tech., March 31, 1950 (Secret).
  6. Hall, A. C., "A Generalized Analogue Computer for Flight Simulation," Transactions of the American Institute of Electrical Engineers, Vol. 69, Part I: pp. 308-320, 1950.
  7. Fuchs, A. M., Trajectory Plotting Equipment. Thesis (S.M.) E. E. Dept., Massachusetts Institute of Technology, June, 1950.
  8. Weiss, M. T., A 400-Cycle Multiple-Loop Feedback Amplifier. Thesis (S.M.) E. E. Dept., Massachusetts Institute of Technology, September, 1947.
- [REDACTED]

- [REDACTED]
9. Nowell, J. C., Redesign of a 400-Cycle Multiple-Loop Feedback Amplifier. Thesis (S.B.) E. E. Dept., Massachusetts Institute of Technology, June, 1948.
  10. Wiener, N., "Generalized Harmonic Analysis," Acta Mathematica, Vol. 55: pp. 117-258, 1930.
  11. Hastings, A. E., and J. E. Meade, Improvement of Radar Tracking, NRL Report No. R-3424. Washington, D. C.: Naval Research Laboratory, February 24, 1949 (Confidential).
  12. Crout, P. D., and F. E. Bothwell, A Theoretical Treatment of Radar Target Return, Report No. 719. Cambridge, Mass.: Mass. Inst. of Tech., Radiation Laboratory, August 31, 1945 (Restricted).
  13. Budenbom, H. T., "Monopulse Radar Noise," Symposium on Noise Reduction, February 10, 11 and 12, 1949, Report AL-930, Part I. Los Angeles, Calif.: North American Aviation, Inc., November, 1949 (Confidential).
  14. Burlingame, J. F., Characteristics of Target Generated Noise in Gun Laying Radar, AN/APG-25(XN-2), Engineering Report No. R49A0329. Schenectady, N. Y.: General Electric Company, December 31, 1949 (Confidential).
  15. Meade, J. E., A. E. Hastings, and H. L. Gerwin, Noise in Tracking Radars, NRL Report No. 3759. Washington, D. C.: Naval Research Laboratory, November 15, 1950 (Confidential).
  16. Interim Progress Report of the Meteor Project, Meteor Report No. 66. Cambridge, Mass.: Mass. Inst. of Tech., March, 1951 (Secret). Pp. 55-58.
- [REDACTED]

17. Johnson, E. C., An Electronic Simulator for Nonlinear Servomechanisms. Thesis (S.M.) E. E. Dept., Massachusetts Institute of Technology, June, 1949.
18. Woods, C. H., The Dynamical Design of an Electromechanical Multiplier. Thesis (S.M.) E. E. Dept., Massachusetts Institute of Technology, September, 1948.
19. Hall, A. C., The Analysis and Synthesis of Linear Servomechanisms. Thesis (Sc.D.) E. E. Dept., Massachusetts Institute of Technology, June, 1943.
20. Wiener, N., "Harmonic Analysis of Irregular Motion," Journal of Mathematics and Physics, Vol. 5: pp. 99-121, 158-189, 1926.
21. Wiener, N., Extrapolation, Interpolation, and Smoothing of Stationary Time Series with Engineering Applications. Published jointly by The Technology Press of the Massachusetts Institute of Technology and John Wiley and Sons, Inc., New York, 1949.
22. Lee, Y. W., Optimum Linear Systems, Class notes for Mass. Inst. of Tech., E. E. Dept., Course 6.563. Unpublished.
23. James, H. M., N. B. Nichols, and R. S. Phillips, Theory of Servomechanisms, Vol. 25, Radiation Laboratory Series. New York: McGraw-Hill Book Company, Inc., 1947. Chaps. 6-8.
24. Newton, G. C., Jr., A Compensating Network Theory for Feedback-Control Systems Subject to Saturation. Thesis (Sc.D.) E. E. Dept., Massachusetts Institute of Technology, June, 1950.

25. Fuchs, A. M., a Servo Employing Output Resolver Connected Directly to Motor Shaft, Memorandum No. M-4.8-12. Cambridge, Mass.: Mass. Inst. of Tech., Dynamic Analysis and Control Laboratory, August 22, 1950.
26. Patterson, W. P., and E. M. Graham, Jr., Effect of Control Surface Limitations on Missile Performance. Thesis (S.M.) E. E. Dept., Massachusetts Institute of Technology, June, 1950 (Secret).
27. Singleton, H. E., Theory of Nonlinear Transducers, Technical Report No. 160. Cambridge, Mass.: Mass. Inst. of Tech., Research Laboratory of Electronics, August 12, 1950.
28. Booton, R. C., Jr., Results of Simulator Study of Basic Guidance Considerations of Interferometer Homing Systems, Memorandum No. M-2.7-22. Cambridge, Mass.: Mass. Inst. of Tech., Dynamic Analysis and Control Laboratory, January 17, 1951 (Secret).
29. Frailey, J. H., P. Horton, and B. B. Crocker, Performance of Air-to-Air Homing Missiles, Part I - Boost Glide, Meteor Report No. 41. Cambridge, Mass.: Mass. Inst. of Tech., June, 1949 (Confidential).

[REDACTED]

APPENDIX G. - BIOGRAPHICAL NOTE ON THE AUTHOR

William Walther Seifert was born in Troy, N.Y. on February 22, 1920. He attended the public schools of Troy and was graduated from Rensselaer Polytechnic Institute with a B.E.E. degree in 1941. He was then appointed as an Instructor in Electrical Engineering at R.P.I. and held this position, teaching and conducting research, until April 1944. The results of this research, which was a basic study of means of shielding electromagnetic radiations, appear in a report\* entitled "Shielding for Diathermy." He then accepted a position at a field station maintained by M.I.T. at the Bureau of Standards in Washington, D.C. There his work related chiefly to radar receivers used in the early guided missiles, "Pelican" and "Bat." In December 1945 he transferred to Cambridge to accept a position in the Dynamic Analysis and Control Laboratory, which was then being formed at M.I.T. In March 1946 he was appointed a Research Assistant in Electrical Engineering at M.I.T. and began his graduate studies. A year later he was promoted to the rank of Research Associate. In September 1947 he received his S.M. degree in Electrical Engineering and then continued his graduate studies. During 1949 and 1950 he combined his research work with teaching courses in elementary network theory and engineering electronics.

He is a member of Sigma Xi and an associate member of the Institute of Radio Engineers.

---

Stoker, W.C., and W. W. Seifert, Shielding for Diathermy, Rensselaer Polytechnic Institute Engineering and Science Series Bulletin No. 59. Troy, New York: Rensselaer Polytechnic Institute, June 1949.

[REDACTED]